METAL COMPLEX FACILITATED TRANSPORT AND
ACTIVATION OF MOLECULAR OXYGEN

By

KENNETH JOHN BALKUS, JR.

A DISSERTATION TO THE GRADUATE SCHOOL
OF THE UNIVERSITY OF FLORIDA IN
PARTIAL FULFILLMENT OF THE REQUIREMENTS FOR
THE DEGREE OF DOCTOR OF PHILOSOPHY

UNIVERSITY OF FLORIDA

1986

To Ken and Brenda, my parents

ACKNOWLEDGEMENTS

First and foremost, I would like to thank my family, my parents Ken and Brenda, brothers David, Michael and Chris, and sister, Lisa for their encouragement and support over the years.

During my stay at Florida, I crossed paths with so many people, who in one way or another, have influenced my life. Whether for the better or worse, I feel the richer for it. I certainly owe the most to Dr. Russell Drago, not only for his wisdom and support but for teaching me what it takes to be successful in the world of academia. I would also like to thank his charming wife, Ruth, who on many occasions made Florida seem like a home away from home.

I would also like to thank some of my predecessors, including Dr. Dorth Hamilton, Dr. Dave "Go Michigan" Pribich, and Dr. Carl Bilgrien, whose inspiration and friendship will last a long time. Additionally, I would like to thank the dynamic personalities of the Drago group for making my stay at Florida quite interesting, especially the lunch club, including Andy Griffis, Jerry Grunewald, Bobby Taylor, and Rich "Repo" Riley. I would also like to acknowledge Dr. Iwona Bresinska, Jeff Clark and Andy Kortz for their helpful discussions. Maribel Lisk deserves a special nod for her continuous help and also for sharing her private drawers. I would also like to thank Dr. Nicholas Kildahl for originally instilling in me a love for chemistry.

iii

Outside the realm of chemistry, I need to thank Chuck Iandoli, and Thelva Jimenez for remaining close friends throughout this ordeal. Finally, I would like to extend a special thank you to Ann Balke who has become a very positive force in my life. Without her love and patience, this dissertation might not have been possible.

TABLE OF CONTENTS

LIST OF TABLES

LIST OF FIGURES

LIST OF FIGURES (continued)

Abstract of Dissertation Presented to the Graduate School
of the University of Florida in Partial Fulfillment of the
Requirements for the Degree of Doctor of Philosophy

METAL COMPLEX FACILITATED TRANSPORT AND
ACTIVATION OF MOLECULAR OXYGEN

By

Kenneth John Balkus, Jr.

December 1986

Chairman: Professor Russell S. Drago
Major Department: Chemistry

The research reported in Chapters I-IV involves the synthesis

and spectroscopic characterization of synthetic O_2 and CO carriers,

improvement of the stability and reversibility of these metal

dioxygen and carbonyl complexes by varying the supports and ligand

environment, and the incorporation of these complexes in

polystyrene membranes as part of a novel gas separation process.

Bis(salicylidene-γ-iminopropyl)methylaminocobalt(II) and

derivations thereof, supported on both polystyrene and silica which

bind O_2 reversibly in the solid state, are described in detail.

The characterization of a novel zeolite encapsulated anionic

complex is also reported. This compound, proposed to be

$Co(CN)_4^{2-}$-Y, binds dioxygen reversibly, at least 400 cycles and is

stable to moisture. Several new Cu(II) complexes supported on

polystyrene were prepared and their reversible interaction with

carbon monoxide was investigated.

A new method for the separation of oxygen from air is

presented. The system involves the incorporation of supported

transition metal complexes that reversibly bind dioxygen into

polystyrene membranes in order to facilitate the transport of O_2.

These films, subsequently employed in a closed volume experiment, exhibited enhanced O_2 permselectivity. The permeation apparatus, experimental procedure and membrane characterization are presented in detail. A mechanism of transport which involves a site to site interaction between metal centers is discussed.

The work in Chapter V focuses on employing lacunary heteropolyanions (HPAs) as oxidatively resistant ligands for catalytically active metal ions. The reactivity in organic solvents of $[XMW_{11}O_{39}]^{n-}$, where M = Co(II), Mn(II) and Fe(III), was investigated. In the presence of alkyl peroxide or iodosylbenzene, these HPAs were found to catalyze the oxidation of several organic substrates. This research led to the discovery of a dirhodium heteropolytungstate catalyst. This polyoxometallate is proposed to be a metal-metal bonded Rh_2^{4+} substituted Keggin ion. The preparation and characterization of this compound are described in detail. The RhHPA was found to be an effective catalyst for the allylic oxidation of cyclic olefins by molecular O_2. Unusual selectivity for the production of the $\alpha,\beta-$ unsaturated carbonyl was observed. A consideration of the general features of this reaction led to a proposed mechanism which involves an ion free radical decomposition of insitu generated peroxides.

CHAPTER I
GENERAL INTRODUCTION

Understanding the binding and activation of molecular oxygen by transition metals is of paramount importance to the scientific community. When one considers all the life forms which respire in some manner as well as all the chemical processes that depend on oxygen, the magnitude of this task becomes clear. As we improve our general knowledge of oxygen fixation there is an increase in the number of applications for O_2. Since oxygen comprises only 21% of the earth's atmosphere, there is a need for inexpensive processes for the production of pure oxygen and oxygen enriched air. Part one of this dissertation addresses this problem and presents a novel method for the enrichment of oxygen from air. This method involves the incorporation of supported metal complexes that reversibly bind O_2 into flat polymer membranes. By applying a partial pressure differential across the membrane, the metal complexes facilitate the transport of oxygen which enhances the ability of the polymer itself to transport O_2. Chapter II describes the preparation of these oxygen binding metal complexes. Chapter III considers metal complexes that reversibly bind other gases such as carbon monoxide. The results for the metal complex containing membrane based gas separations as well as a mechanistic model to describe this mode of O_2 transport are detailed in Chapter IV.

The utilization of molecular oxygen to effect a variety of chemical transformations most often requires a transition metal catalyst. A goal of researchers in this area is to develop catalysts that impart a high degree of both selectivity and activity to the reaction. Typically the most selective oxidation catalysts suffer instability or conversely the most active catalysts are generally the least selective. Part two describes an effort to employ polyoxometalates as homogeneous oxidation catalysts. Soluble metal oxides, more specifically heteropolytungstates, were employed as oxidatively resistant ligands and substituted with a catalytically active metal center(s). The preparation, characterization and reactivity of a rhodium heteropolytungstate are described in Chapter V.

Each chapter is preceded by a brief introduction which provides the necessary background information to allow a better understanding of the chapter material as well as the progression of topics presented in this general introduction.

CHAPTER II
THE PREPARATION OF METAL COMPLEXES
THAT REVERSIBLY BIND DIOXYGEN

Introduction

The reversible fixation of dioxygen by metal complexes has
attracted the interest of many not only because of the biological
implications but also for a more practical reason, namely the
separation of O_2 from gas mixtures. Since the first synthetic
dioxygen complex, $(NH_3)_5CoO_2Co(NH_3)_5$, was characterized in 1898,[1]
many oxygen carriers and metal-O_2 complexes have been reported.
The term oxygen carrier can be defined as a metal complex which can
reversibly fixate or bind O_2. Reversible in this case means the
oxygen can be bound and released upon a change in pressure or
temperature. This also implies that the oxygenation and
deoxygenation can be carried out numerous times or cycled
continuously without a change to the metal complex. In developing
effective synthetic oxygen carriers one must first have an
understanding of those factors which determine the nature of the
metal bound dioxygen. Molecular oxygen or the free O_2 molecule has
a triplet, $^3\Sigma_g^-$ ground state with the two unpaired electrons in the
π^* orbitals as shown in the molecular orbital diagram below.
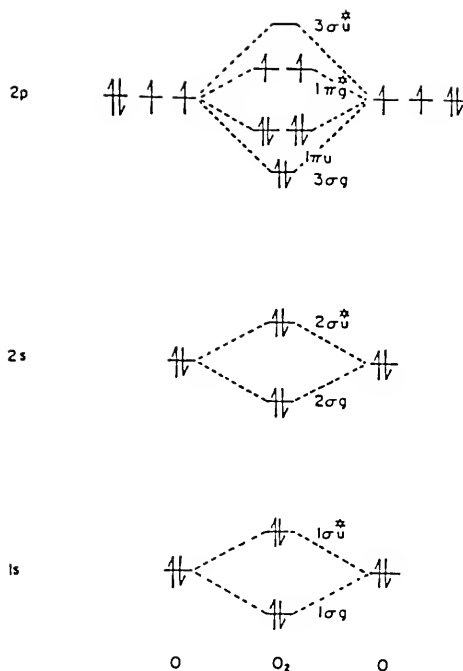
As a result of the triplet ground state, molecular oxygen is generally unreactive towards diamagnetic molecules since a change in spin is kinetically unfavorable. The formation of oxygen adducts with transition metals is often favorable owing in part to spin orbit coupling which can serve to relax the restrictions to spin pairing. The exact nature of the metal bound oxygen has been the subject of much controversy. Drago's spin pairing model has become a widely accepted description of this metal O_2 bonding.[2] This essentially involves pairing of one or both of the unpaired electrons of oxygen with unpaired electrons on the metal. This is best illustrated by a molecular orbital diagram for an oxygen adduct of Co(II) shown below. EPR experiments have established
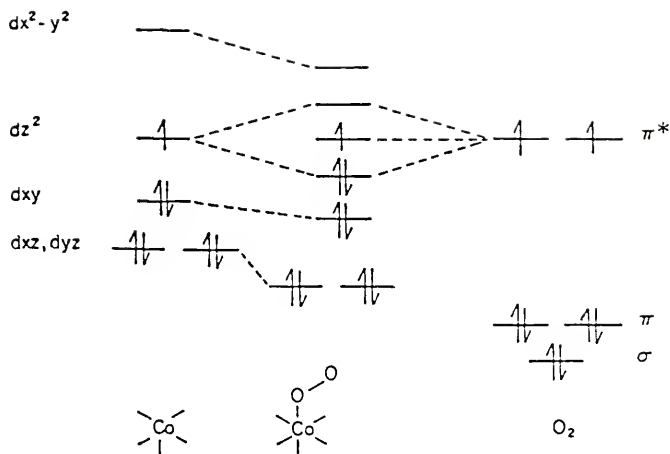
that the unpaired electron is in an essentially oxygen based orbital. Therefore, the degree to which oxygen is reduced depends upon the electron distribution in the σ molecular orbital formed from the d_z^2 and π^* orbitals. By varying the ligand field strength around the cobalt center the contribution of the d_z^2 to the σ bonding orbital will change and therefore the degree of electron transfer to the oxygen will vary accordingly. Since the difference between $Co^{2+}-O_2^{\circ}$ and $Co^{3+}-O_2^-$ is only relative to the electron distribution in the σ MO, no distinction will be made between neutral oxygen and any of its reduced forms when referring to metal dioxygen complexes that are reversible oxygen carriers.

Generally, oxygen will ligate to metals in one of three different geometries: end on bonded (A), bridged (B), or ring bonded (C) as shown below. Specific examples of the different

M - O
O

O - O
M

M
O
O
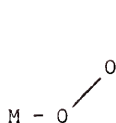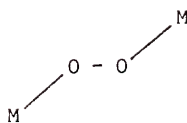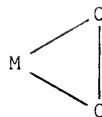
A   B   C

structural types as well as some of the chemistry associated with these complexes can be found in several recent reviews and will not be presented here.[3-5] Suffice to say that most of the metal dioxygen complexes to be discussed in this chapter will be of the type A or end on variety.

The first example of reversible oxygen adduct formation was reported in 1938 by Tsumaki.[6] The complex was N,N' -bis(salicylidene)ethylenediamine cobalt(II) or Co(II)SALEN shown below. Cobalt(II) Schiff base complexes of this type were studied
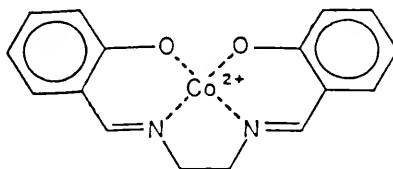
extensively as reversible oxygen carriers with the hope of developing a light weight oxygen storage system. The U.S. Air Force, currently employs liquid oxygen storage systems on military

aircraft, developed an O_2 generating system based on a fluorinated derivative of Co(SALEN).[7] Unfortunately the oxygen carrying capacity for complexes of this type was greatly diminished after a number of cycles.[8] The deactivation of oxygen carriers is usually the result of either irreversible oxidation of the metal center, such as μ-peroxodimer formation, or degradation of the ligand by O_2. Most of the efforts to enhance the stability of these complexes, i.e. their resistance to irreversible oxidation, have been in either one of two directions, namely supporting the metal complexes or the preparation of sterically hindered chelate complexes. Examples of the later are Collman's "picket fence" porphyrin complexes[9] and Busch's lacunar macrobycylic ligands.[10] Supported metal complexes will be the focus of much of the work in this chapter.

In general, there are relatively few metal complexes that reversibly bind molecular oxygen in the solid state. Dioxygen binding in the solid state requires a crystal lattice with pores or channels such that O_2 can diffuse freely through the solid.[11] The restraints of the crystal lattice often render potential oxygen carriers unreactive towards O_2. For those complexes that do bind dioxygen in the solid state, determination of those thermodynamic parameters associated with oxygen binding can be very complicated. For example, phase changes or changes in the crystal structure will have an effect on equilibrium measurements. Solid state equilibria are often described by Langmuir kinetics such as

$$\frac{X}{1 - X} = KP_{O_2} = \frac{P_{O_2}}{P_{\frac{1}{2}}}$$

where X = mole fraction of oxygenated sites, 1-X = mole fraction of unoxygenated sites, K = the dioxygen binding constant, P_{O_2} = the partial pressure of O_2 in the gas phase, and $P_{\frac{1}{2}}$ = the partial pressure of O_2 required to oxygenate half of the metal complexes. Unusual solid state O_2 binding properties are best illustrated by the Fe(II) picket fence porphyrins. When a sterically constrained axial base such as 2-methyl-imdazole was coordinated to the Fe(II) picket fence porphyrin (Figure 2-1), the absorption of oxygen did not display a simple langmuir isotherm.[12,13] In other words, the oxygen affinity of the metal complex did not remain constant with a change in oxygen pressure but rather showed two distinct reversible forms. This type of behavior has been compared to the cooperative oxygen binding of hemoglobin. Apparently, the initial oxygenation of some of the Fe(II) sites induces a reversible change in the crystal lattice creating Fe(II) sites that have a higher affinity for O_2.

In light of the crystal lattice restrictions in solid state oxygen absorption, a logical solution would be to attatch the metal complex to the surface of a solid. The purpose of the support is threefold: 1) the individual complexes can be bound to the support eliminating crystal packing effects and either through high surface area or a porous solid more of the complex per unit mass can be exposed to oxygen; 2) in separating the metal complexes on the support, irreversible oxidation that is multiordered in metal complex may be prevented; and 3) various supports such as polymers may influence the binding of oxygen by providing a hydrophobic environment analogous to the solvation effects observed with natural oxygen carriers such as myoglobin.

Figure 2-1. Oxygen adduct of 2-methylimidazole meso-tetra
            (α, α, α, α - o-pivalamidophenyl) porphyrin iron(II).
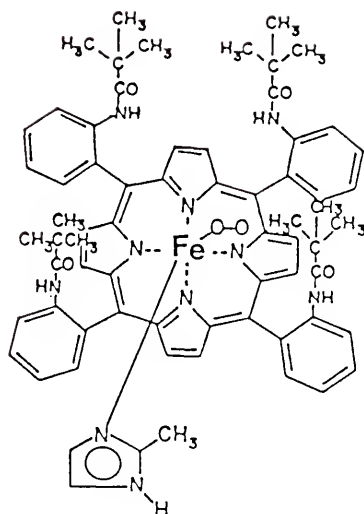
Metal complexes can be supported on polymers in a number of ways. For example, a polymer with a basic functionality such as polypyridine or a polymer that has a monodentate ligand covalently attached, such as polystyrene functionalized with imidazole, provides an axial base for many metal complexes that require such a ligand to bind oxygen. Chelate complexes such as Co(TPP),[14] Fe(TPP)[15] (TPP = tetraphenylporphyrin), Co(DPGB)$_2$,[16] (DPGB = diphenylglyoximatodifluoroborate, and Co(SALEN),[17] have been supported in this fashion. This mode of attachment suffers in that there can be dissociation of the axial ligand or coordination of two proximal bases rendering the metal coordinately saturated. An alternative is to covalently attatch the chelate ligand directly to the polymer. To this end, many polymer bound bidentate, tridentate, and tetradentate ligands have been prepared.[18,19] Most noteworthy was the report of synthetic procedure for attaching multidentate amines to organic polymers.[20,21] Such amines form the basic building blocks for many chelate ligands. Of particular interest is the preparation of polymer bound pentadentate Schiff base ligands, such as polystyrene supported bis(3-(salicylideneamino)propyl)methylamine or [P]-SDPT as shown below. Polymer supported CoSDPT reversibly binds oxygen in the solid state as compared with CoSDPT in solution which has a $\Delta H = -9.8$ kcal;[22] this translates into $\Delta G = +1.28$ kcal and a $P_{1/2} = 6.7 \times 10^3$ torr! The oxygen binding ability of many covalently or coordinatively attached metal chelate complexes has been investigated,[23] especially in relation to their catalytic oxidizing potential.[21,24] Polystyrene supported CoSDPT (21% substituted) was studied as a solid state oxygen absorbent.[25] It was estimated that
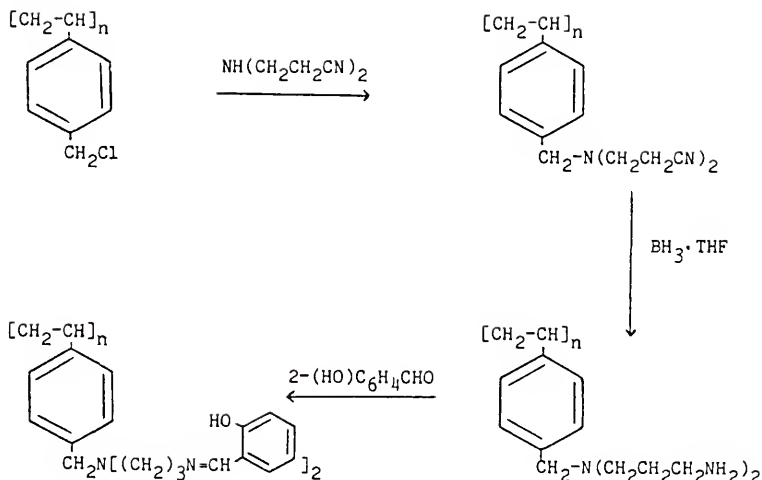
this system could be economically competitive with cryogenic or
pressure-swing absorption oxygen separation process. However, the
capacity of [P]-CoSDPT to uptake oxygen decreased with an
increasing number of capture/release cycles. By virtue of most
polymers being flexible in nature, it is a rather difficult task to
achieve site isolation of supported metal complexes.

A more ridgid support, such as an inorganic oxide, can hinder
the motions of the attached metal complexes providing a more
effective site separation. Silica, SiO_2, has a surface covered
with hydroxyl groups which can be modified in a large number of
ways with organo-silanes. For example, silica gel has been
functionalized with imidazole then used to stabilize Fe(II)TPP.[26]
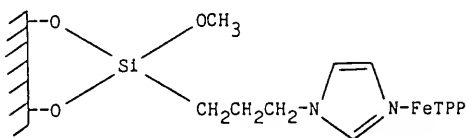
The [SG]-FeTPP reversibly binds oxygen (at 0°C $P_{1/2}$ = 230 torr) compared with [P]-FeTPP which irreversibly oxidizes with formation of a μ-peroxodimer. Cobalt(II) phthalocyanine has been supported on silica functionalized with pyridine and also shown to reversibly bind O_2.[27] Site isolation on silica gel can be achieved in two ways either by having a dilute concentration of functionalized sites or by a new method which involves cofunctionalization of the support with alkylsilanes.[28] It is thought that organosilanes can migrate across the surface of silica by exchanging protons with adjacent silanol groups. This results in aggregation and deactivation of the metal complexes. Alkylation of the surface prevents this migration and allows a higher loading of metal complexes. There are few examples of covalent attatchment of metal complexes to silica gel. There is a recent report of a cobalt(II) hematoporphyrin complex immobilized via a peptide bond to silica.[29] However, the cobalt is irreversibly oxidized in air. CoSDPT has been covalently supported on silica gel and shown to be an effective oxygen carrier.[30] To date this is probably the most effective means for stabilizing such a complex on the surface of a solid support. This chapter will describe the preparation of such complexes.

Alternative supports gaining considerable attention are zeolites or molecular sieves. The absorbative properties of zeolites are well known and many commercial gas separation or purification processes are based on these properties.[31] In particular, both oxygen and nitrogen are produced on a commercial scale by pressure-swing adsorption (PSA) based on molecular

sieves. As a solid support, zeolites have many unique features.
The structures of zeolites include a variety of pores, channels and
cavities of fixed dimensions. The framework has both strong Lewis
acid and Bronsted acid sites. The ionic nature of the cavities can
be varied with the Si/Al ratio and a whole host of cations can be
exchanged into these cages. Therefore, the steric constraints
coupled with the electrostatic environment within the zeolite cages
create a unique solid support. There are relatively few examples
of oxygen binding metal complexes that have been encapsulated in
zeolites. A number of cobalt(II) amine complexes in X and Y
zeolites have been prepared.[32-35] There is also a report of oxygen
binding by Cr^{2+} on an A zeolite[36] and a $Ru^{3+}O_2$ adduct in a Y
zeolite.[37] More recently a $[Co(bipy)(terpy)]^{2+}$ complex was
prepared in a Y zeolite and found to reversibly bind O_2.[38] This
was subsequently employed to separate oxygen from air with a
separation factor (O_2/N_2) $\alpha = 12.3$.[39] However, this complex was
extremely moisture sensitive, precluding any practical
application. Generally the approach to preparing these complexes
has been to use ligands that the cage will readily accommodate
resulting in cationic or neutral complexes. Ideally a metal
complex which is indifferent to water and possesses oxidatively
resistant ligands would be best suited for zeolite encapsulation.
Such a complex is $[Co(CN)_5]^{3-}$ first reported by Adamson[40] and the
oxygen adduct later characterized by Raymond and Brown.[41,42] This
complex has been incorporated in both A and Y zeolites by Dr. Iwona
Bresinska and found to be a very stable oxygen carrier, the details
of which will be discussed in this chapter. This is a very

significant result, especially in light of the popular misconception that anionic complexes cannot be prepared in the zeolite cavities.[32]

The supported metal complexes to be discussed here hold promise as solid state oxygen absorbents and their application to facilitated transport in membranes is even more exciting.

Experimental

Solvents and Reagents

Dimethylformamide (DMF) was distilled over BaO, freeze pump thawed and stored under nitrogen. Dioxane and tetrahydrofuran (THF) were distilled over CaH_2. All other solvents and reagents were stored over 4A molecular sieves and used without further purification.

Spectral Studies

Infrared spectra were recorded on a Nicolet 5DXB Fourier transform infrared spectrophotometer using NaCl discs for nujol mulls. Electronic spectra were obtained with a Perkin-Elmer 330 spectrometer. Solid state spectra were recorded as nujol mulls on Whatman No. 1 qualitative filter paper. X-band ESR spectra were obtained with a Bruker ER 200D-SRC spectrometer.

[P]-DPT

Chloromethylated (90%), divinylbenzene crosslinked (4%) polystyrene beads were obtained as a gift from Sybron Corporation. Polystyrene bound dipropylenetriamine, [P]-DPT, was prepared according to the literature.[21]

[P]-SDPT, -3,5Br$_2$SDPT and -3FSDPT

The polymer bound pentadentate ligand, [P]-SDPT, was prepared according to the literature.[21] The 3,5-dibromo and the 3-fluoro substituted salicylaldehyde derivatives were prepared in a similar manner. For example, a large excess of 3,5-dibromosalicylaldehyde was slurried with [P]-DPT in benzene at reflux overnight. The water of condensation was collected in a Dean-Stark trap. The functionalized resin was suction filtered and dried under a vacuum at 80 °C. The 3-fluorosalicylaldehyde was obtained as a gift from Olin Corporation.

[P]-CoSDPT, -3,5Br$_2$SDPT and -3FSDPT

Cobalt(II) was incorporated into the SDPT ligands by slurrying excess cobalt(II) acetate with the resins in DMF under argon at room temperature for two days. The polymer supported cobalt complexes were suction filtered, washed with DMF, and dried under a vacuum at 80 °C.

[SG]-DPT

Silica bound dipropylenetriamine was prepared according to the method previously described.[30]

[SG]-CoSDPT, -3,5Br$_2$SDPT and -FSDPT

The silica supported Cobalt(II)SDPT complexes were prepared from [SG]-DPT in the same way as described above for the polystyrene bound analogues.

Zeolite Complexes

The zeolite work described below was part of a joint research effort by myself and Dr. Iwona Bresinska. Dr. Bresinska synthesized the metal complex containing zeolites and determined the elemental composition. The major contribution on my part was the characterization of these complexes.

The notation employed to describe the zeolite encapsulated metal complexes follows the general formula, Co(MCN)-Y-1 where the Co represents a cobalt(II) exchaged zeolite, MCN represents the alkali metal cyanide salt used in the complex preparation (note: M is not necessarily the cation for the original zeolite starting material), and Y is the type of zeolite and the final digit represents a specific preparation.

The general preparatory procedure followed for the compounds listed in Table 2-2 was as follows. The cobalt(II) exchanged zeolite was slurried with an alkali metal cyanide salt in an appropriate deoxygenated solvent, most often methanol, for a designated time period. All syntheses were carried out at room temperature. The complex containing sieves were then suction filtered and washed with solvent until the filtrate tested negative for cyanide ion. The cyanide solutions were disposed of by treating with an $FeCl_2$/NaCl methanol/water solution to generate the innocuous iron cyano complex. The zeolite was dried under vacuum and stored in a dessicator. Elemental determinations were performed by the microanalysis service of the University of Florida. Cobalt content was determined with a Perkin-Elmer Plasma II emission spectrometer.

Results and Discussion

The polymer and silica supported Co(II)SDPT complex and its derivatives did not exhibit an ESR signal as could be expected for high spin Co(II). The liquid N_2 temperature ESR for the oxygen adduct of [P]-CoSDPT, shown in Figure 2-2, has approximate g values of 2.06, 2.02 and 1.99. This compares well with those g values previously reported (g_z = 2.08, g_y = 2.016, and g_x = 1.99).[21] The other polystyrene supported complexes are very similar. For example, [P]-Co3FSDPT (Figure 2-3) has g_z ~ 2.08, g_y ~ 2.03 and g_x ~ 1.86. The [P]-CoSDPT was prepared with electron withdrawing substituents on the salicylidene portion of the ligand in an effort to enhance the reversibility of dioxygen binding. In other words, by reducing the electron density at the cobalt center the $P_{\frac{1}{2}}$ for the complex should increase as predicted by the spin pairing model.[2] This was demonstrated by the fact that a solid [P]-CoSDPT sample only needed to be exposed to air in order to observe a Co-O_2 ESR signal whereas [P]-Co3FSDPT required at least 20 psig O_2 to oxygenate the sample. This effect is also manifested in the fact that the 3,5-dibromo and 3-flouro derivatives facilitated the transport of O_2 to a higher partial pressure of O_2 than [P]-CoSDPT (vide infra).

The silica supported complexes were prepared with a loading of either 0.1 mmoles Co complex/gram of silica gel or 0.5 mmoles/gram. In some cases the surface was alkylated. The ESR for a 0.1mmoles/gram SG loading and methylated surface for [SG]-CoSDPT and [SG]-Co3,5Br$_2$SDPT are shown in Figures 2-4 and 2-5. The g values are similar to the polymer supported complexes (g_z ~ 2.08,

Figure 2-2. X-band ESR of [P]-CoSDPTO$_2$ at 80 °K, $g_z \sim 2.06$, $g_y \sim 2.02$ and $g_x \sim 1.99$.
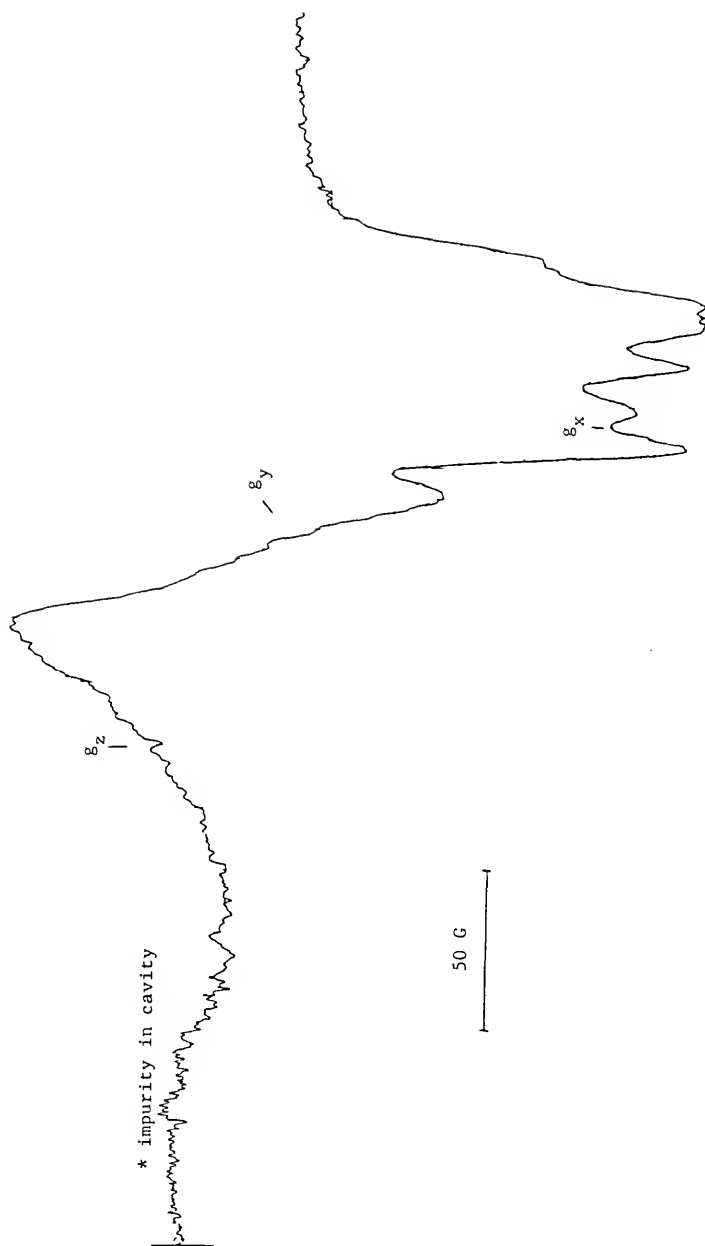
Figure 2-3. X-band ESR of [P]-Co3FSDPTO$_2$ at 96 °K, $g_z \sim 2.08$, $g_y \sim 2.03$ and $g_x \sim 1.86$.

g_z

g_y

g_x

50 G
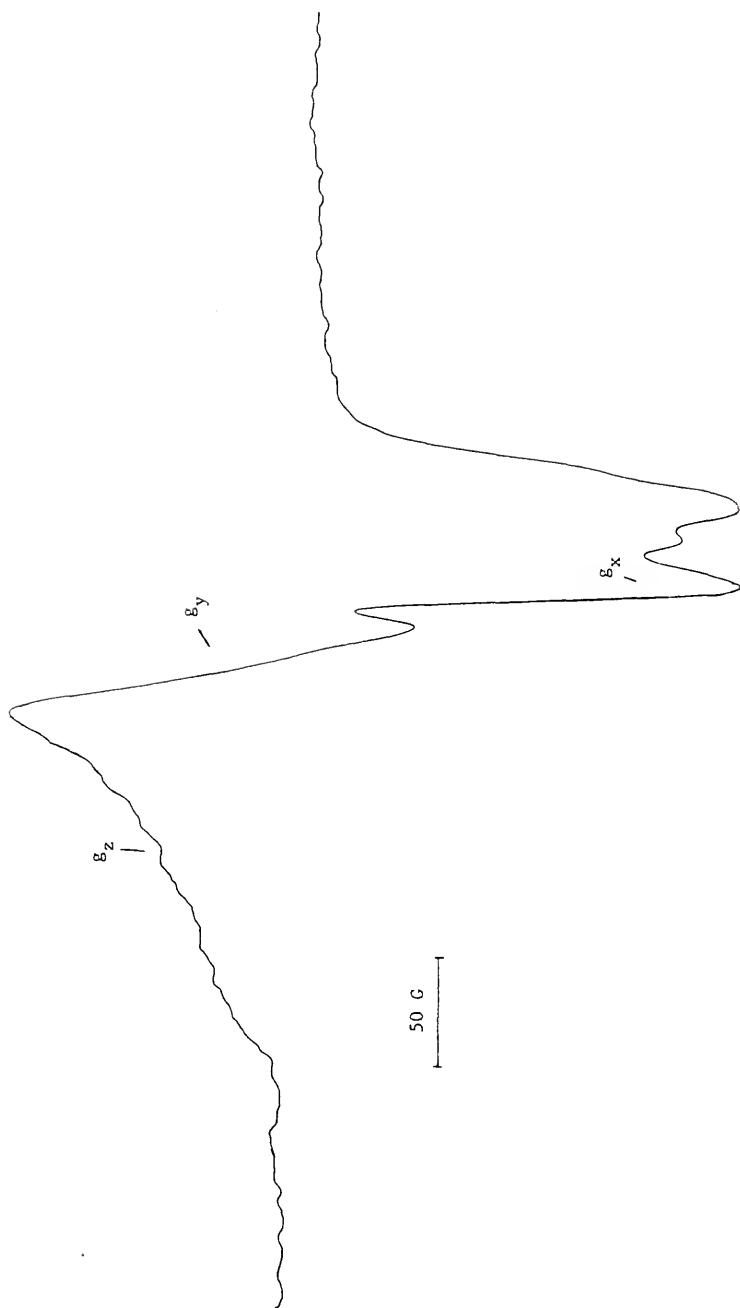
Figure 2-4. X-band ESR of [SG]-CoSDPTO$_2$ (0.1 mm/gm SG, methylated) at 80 °K, $g_z \sim 2.08$, $g_y \sim 2.02$ and $g_x \sim 1.99$.

g_z

g_y

g_x

50 G
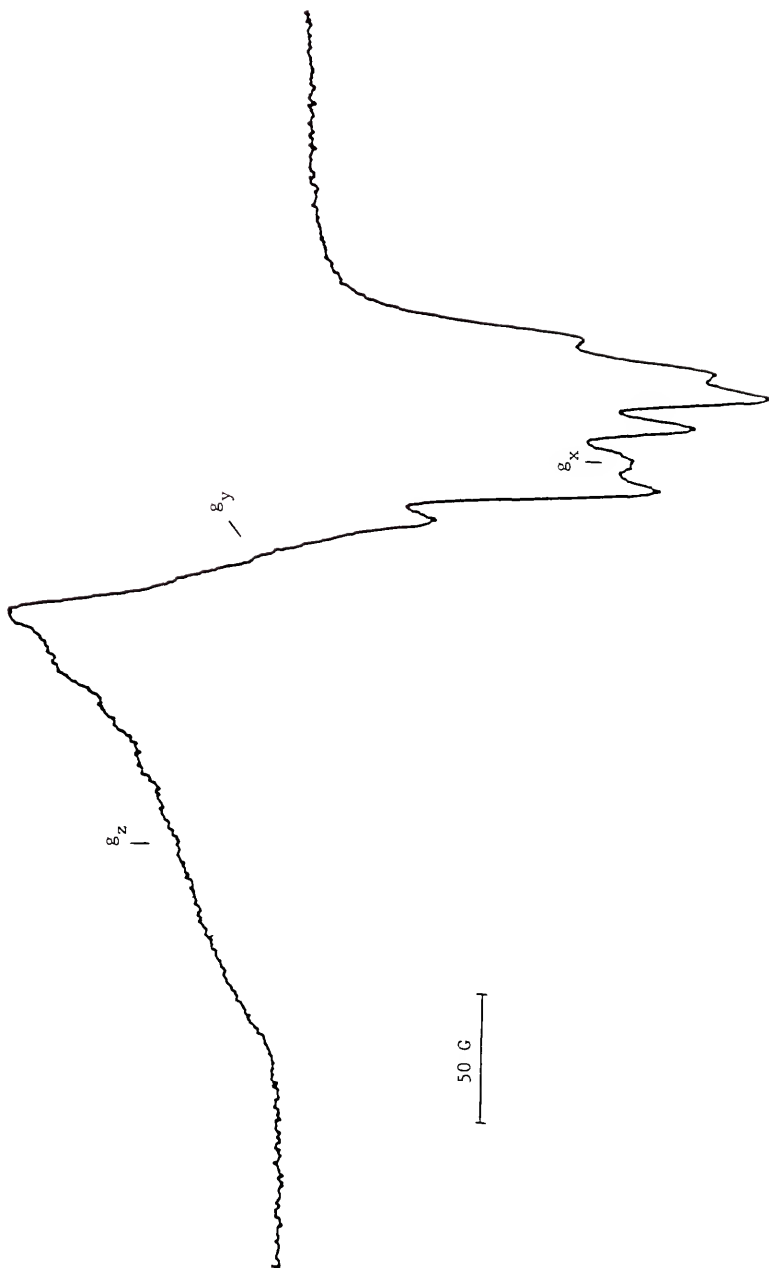
Figure 2-5. X-band ESR of [SG]-Co3,5Br$_2$SDPT (0.1 mm/gm SG, methylated) at 80 °K, g_z ~ 2.09, g_y ~ 2.00 and g_x ~ 1.99.

g_z

g_y

g_x

50 G
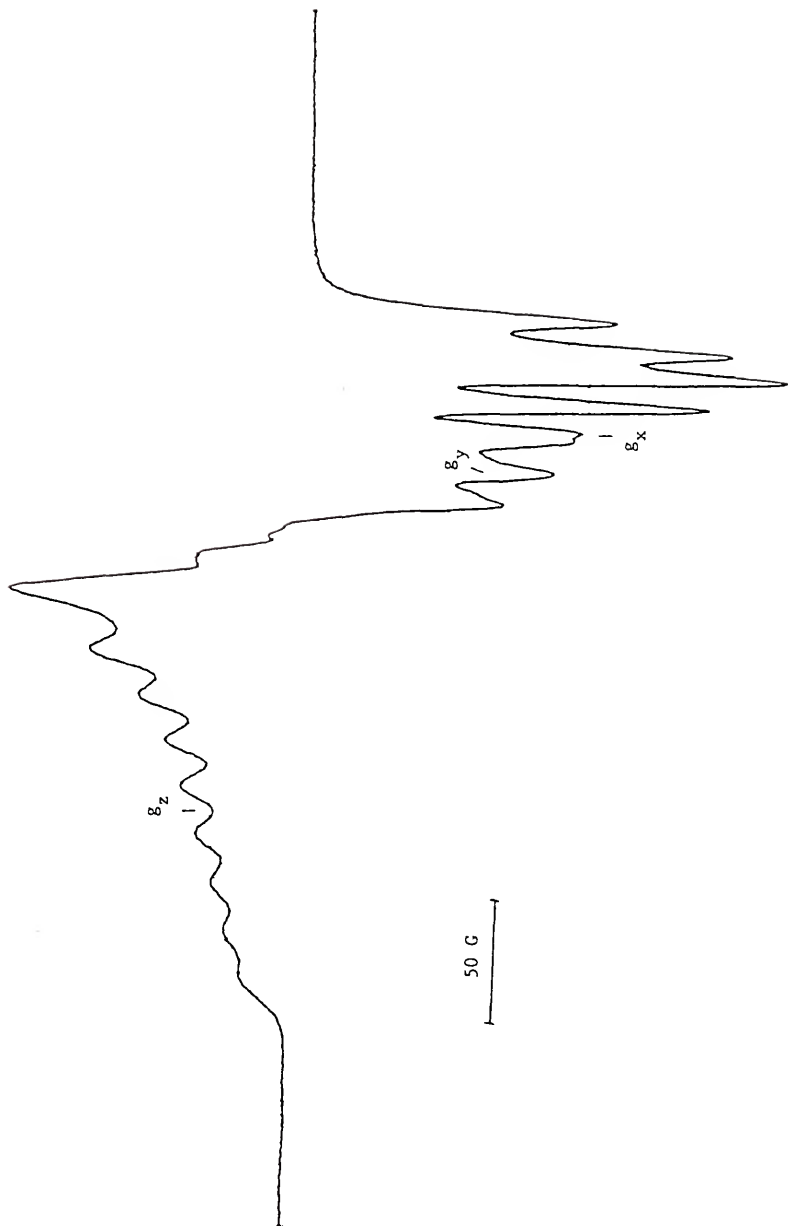
$g_y \sim 2.02$. $g_x \sim 1.99$ and $g_z \sim 2.09$, $g_y \sim 2.00$, $g_x \sim 1.99$). A 0.5 loading sample does not display the cobalt hyperfine splitting observed in these spectra of more dilute samples which suggests these samples are magnetically dilute. In other words, the cobalt centers are well isolated. Site separation of the complexes should enhance their stability in the presence of O_2 provided irreversible oxidation is a second order process. At this point, the only measures of stability are a shelf life of at least two years and irreversible oxidation of the SG support material has not been observed in the polymer membranes.

The two types of zeolite supports studied were of the A and Y variety as shown below. These zeolites are characterized by the
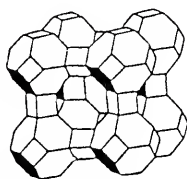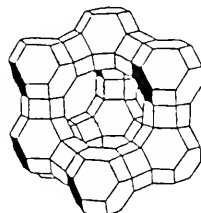
A   Y

parameters in Table 2-1.

Table 2-1

Composition of A and Y Zeolites

Zeolite	Unit Cell Composition	Pore Diameter	Supercage Diameter
A	$Na_{12}(Al)_2)_{12}(SiO_2)_{12}$	4.2 A	11.4 A
Y	$Na_{56}(AlO_2)_{56}SiO_2)_{136}$	7.4 A	13.0 A

The A zeolite is composed of octahederal sodalite units connected
by cubes whereas hexagonal prisms connect the sodalite cages in the
Y zeolites. The Y zeolite, which has the larger cavity, has been
the focus of this research. There are several cation sites in the
faujasite (Y) framework. Of particular interest are those
positions commonly referred to as SII sites, which are located in
the hexagonal face of the sodalite cage extending into the
supercage. Cobalt(II) at these positions could form complexes
within the large cage taking advantage of the steric constraints
imposed by this site. This approach has proved successful in
preparing otherwise unstable metal complexes in zeolites. However,
up to this point only cationic and neutral complexes have been
isolated. Owing to the electrostatics of the cage, the generation
of an anionic complex inside the zeolite was deemed unlikely. It
was gratifying to prove the contrary by preparing $Co(CN)_x^{n-}$
complexes in the zeolites. Additionally, these complexes are quite
effective oxygen carriers (vide infra). The cyanide ion itself
could not be incorporated into the zeolite. This was evidenced by
the fact that slurrying NaCN with Na-Y zeolite in methanol for 15
hours results in no CN^- incorporation. This means that any CN^-
detected in the Co-Y zeolites must be attributed to complex
formation with the cobalt. Generally, cyanide ion promotes the
formation of transition metal complexes with high coordination
numbers. For Co(II), the pentacoordinate anion $Co(CN)_5^{3-}$ is the
most stable. Except for polymeric materials the only other
isolable cyano cobaltate complex reported is $(PNP)_2Co(CN)_4$, where
PNP = bis(triphenylphosphine)iminium cation.[43] This complex was

characterized by x-ray crystallography and found to be square planer. There is evidence for the existence of cobalt(II) complexes with from 1 to 5 cyanide ligands in solution.[44,45] Characterization of the zeolite encapsulated $Co(CN)_x^{n-}$ complexes was complicated by the strong affinity of these complexes for molecular oxygen. Therefore, the spectral studies reported herein are for the oxygen adducts.

The Co(II) in the Co-Y zeolite is probably coordinated to at least two lattice oxygens. Upon complexation with cyanide, this interaction is believed to be partially retained when four or less cyanides are coordinated. As can be seen from Table 2-2 the extent of complexation depends upon the amount of cyanide used, the solvent and the reaction time. The N/Co ratio does not necessarily represent the empirical formula of a cobalt complex, since not all of the cobalt may be complexed. Additionally, some of the exchanged cobalt could get washed out during the reaction with NaCN, whereas the N/Co ratio in Table 2-2 is relative to the initial concentration of cobalt.

The IR spectra of these zeolites provide a good handle to the degree of complexation under various conditions. The data in Table 2-3 summarizes the infrared bands observed in the CN stretching region. These frequencies are similar to those reported for Co(II) cyano complexes (2094-2134 cm^{-1}).[46] For example, $[(C_2H_5)_4N]_3[Co(CN)_5]$ has a $\nu CN = 2080$ cm^{-1}, whereas the oxygen adduct shows a $\nu CN = 2120$ cm^{-1}. At low N/Co ratios a higher frequency band is observed and may be attributed to a lower number of cyanides coordinated to cobalt. Increasing the CN^-

Table 2-2

Conditions for the Preparation of $Co(CN)_x^{n-}$ Containing Zeolite

Compound	Solvent[a]	Time (hours)	[Co] (mmole/gm)	[CN][b] (mmole/gm)	N/Co[c]
Co(NaCN)-Y-1	CH_3OH	18	1.0	4.0	0.76
Co(NaCN)-Y-2	CH_3OH	164	1.0	20.0	1.32
Co(NaCN)-Y-3	CH_3OH	96	0.94	22.0	4.29
Co(NaCN)-Y-4	CH_3OH	120	0.94	20.0	3.0
Co(NaCN)-Y-5	H_2O	120	0.94	20.0	0.99
Co(NaCN)-Y-6	H_2O	120	1.27	40.0	0.72
Co(NaCN)-Y-7	CH_3OH	120	1.27	40.0	2.09
Co(NaCN)-Y-8	DMF	237	0.94	24.0	2.63
Co(NaCN)-Y-9	CH_3OH	139	1.27	88.0	2.34
Co(NaCN)-Y-10	H_2O	117	1.10	90.9	1.60
Co(NaCN)-Y-11	H_2O	100	1.27	144.0	0.75
Co(KCN)-Y-1	CH_3OH	120	0.94	14.2	3.02
Co(LiCN)-Y-1	DMF	237	0.94	25	2.29
Co(NaCN)-A-3	CH_3OH	188	1.88	18.0	0.94

a solvent for CN^- incorporation
b concentration of CN^- used in the reaction
c ratio of nitrogen in the product to the initial
    cobalt condentration

Table 2-3

Infrared $Co(CN)_x$ - Zeolite[a]

Compound	CN frequencies (cm^{-1})
Co(NaCN)-Y-1	2176.9(m), 2138(m)
Co(NaCN)-Y-2	2178.8(m-w), 2137(m-s)
Co(NaCN)-Y-3	2217(w), 2131.7(s), 2090(w)
Co(NaCN)-Y-4	2209(w), 2130.9(s)
Co(NaCN)-Y-5	2130.7(s)
Co(NaCN)-Y-6	2131.2(s)
Co(NaCN)-Y-7	2201(w), 2131(s)
Co(NaCN)-Y-8	2163(sh), 2133.5(w), 2090.2(m-w)
Co(NaCN)-Y-9	2205(m-w), 2131.8(s), 2097.9(w)
Co(NaCN)-Y-10	2197.9(sh), 2130.4(s)
Co(NaCN)-Y-11	2130.5(s)
Co(LiCN)-Y-1	2163(vw)
Co(KCN)-Y-1	2124(s)
Co(NaCN)-A-3	2135.7(s), 2108(vw), 2095(vw)
NaCN	2090.7

a   exposed to oxygen

concentration generates the band at 2131 cm^{-1}, as illustrated in Figure 2-6. Spectrum C shows three bands as might be expected for a complex of C_{4v} symmetry but compounds 5, 6 and 11 show only a single band which would be consistent with D_{4h} symmetry. The band at 2090 cm^{-1} may coincide with the unoxygenated complex. This would be in line with acetonitrile solutions having CN/Co ratios of 3 and 4 which display major peaks at 2096 and 2090 cm^{-1} respectively.[45]

The counterion has been shown to have a profound effect on complex formation. The CN stretching frequency has been observed to increase with the probability of contact ion pairing.[45] This increase in νCN is thought to result from kinimatic coupling.[47] This would be consistent with Co(NaCN)-Y (2131 cm^{-1}) and Co(KCN)-Y (2124 cm^{-1}).

In order to better define the nature of the zeolite encapsulated complexes, the electronic spectra were recorded by placing a nujol/zeolite paste on a piece of filter paper in the instrument sample light path. Likewise, a piece of paper with only nujol was placed in the reference beam. The visible spectra obtained in this fashion displayed broad and possibly overlapping bands with low signal to noise ratios. Therefore, the assignments of band maxima are tentative. The results for a series of Co(II) cyano complexes are shown in Table 2-3. It should be pointed out that $Co(CN)_5{}^{3-}$ exhibits only very weak absorptions in the 400 to 800 region and was excluded from Table 2-4. Although the maxima have not been reported for the electronic spectrum of $Co(CN)_5O_2{}^{3-}$, the distinctive features appear below 500 nm. Additionally, the

Figure 2-6. FT-IR (nujol mull) for
A. Co(NaCN)-Y-1
        2176.9 cm^{-1}
        2138.0 cm^{-1}
B. Co(NaCN)-Y-2
        2178.8 cm^{-1}
        2137.0 cm^{-1}
C. Co(NaCN)-Y-3
        2217.0 cm^{-1}
        2131.7 cm^{-1}
        2090.0 cm^{-1}
D. Co(NaCN)-Y-5
        2130.7 cm^{-1}.
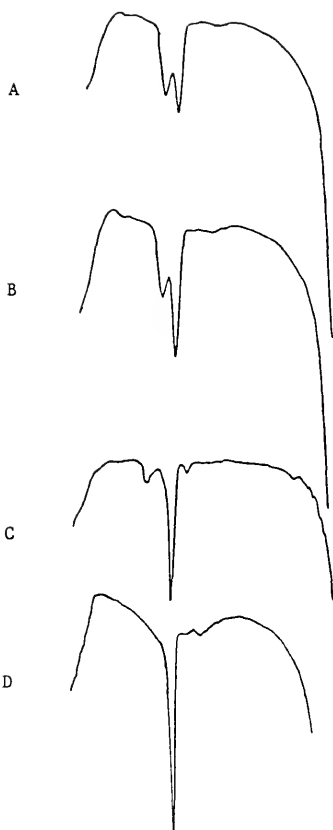
Table 2-4

Electronic Spectra for Cobalt(II) Cyano Complexes

Complex	Bands (nm)
Co(NaCN)-Y-1[c]	514
Co(NaCN)-Y-2[c]	514(sh), 648(sh)
Co(NaCN)-Y-3[c]	514(sh), 560, 665
Co(NaCN)-Y-6[c]	520(sh), 583(sh), 650(sh)
Co(KCN)-Y-1[c]	555(sh), 668(sh), 690(sh)
Co-Y	430, 530, 570, 624(sh)
$[Co(CN)_2(CH_3CN)_2]$	605[a], 625[b], 690(sh)[b]
$[Co(CN)_3(CH_3CN)]^-$	590[a], 602[b]
$[Co(CN)_4]^{2-}/CH_2Cl_2$	563(sh)[b], 594[b]
$[Co(CN)_4]^{2-}/CH_3CN)$	581(sh)[b], 598(sh)[b], 617[b]

a. reference 44
b. reference 45
c. oxygen adduct

other cobalt(II) cyano complexes listed in Table 2-4 have not been reported as being reactive toward oxygen. The electronic spectrum for Co(II) exchanged Y zeolite is shown in Figure 2-7. A violet product is obtained after heating the pink hexaaquo complex under a vacuum. The complex producing the violet color probably consists of Co(II) bound to two lattice oxygens and two waters. Usually tetrahedral complexes are characterized by intense low energy transitions. Unfortunately, because of the solid state techniques involved, the extinction coefficients were not accessible. All of the spectra for the zeolite encapsulated $Co(CN)_x^{n-}$ complexes were characterized by large charge transfer bands with a number of low energy transitions. Cobalt(NaCN)-Y-1 (Figure 2-8) is also violet in color and has a single band at ~ 514 nm. This zeolite shows a very weak CoO_2 ESR signal indicating a very low concentration of those complexes capable of binding O_2. In comparison with Co(NaCN)-Y-2 (Figure 2-9) and Co(NaCN)-Y-3 (Figure 2-10), the band at 514 nm is reduced in intensity and a lower energy band grows in. Cobalt(NaCN)-Y-3 is gray in color and is a very effective oxygen absorbent. No discernable color change is observed during oxygenation or deoxygenation. It should also be noted that $Co(CN)_5^{3-}$ is yellow or pale green and the oxygen adduct is red-brown.

The ESR of the oxygenated Co(NaCN)-Y-3 is shown in Figure 2-11. This is a typical CoO_2 signal with $g\perp$~2.01 and $g\parallel$~2.07. Evacuating the sample to below 10^{-4} torr produces the spectrum in Figure 2-12 with $g\perp$~2.25 and $g\parallel$~1.95. The sample has not been completely deoxygenated as evidenced by the weak O_2 signal at the

Figure 2-7. Electronic Spectrum for Co-Y Zeolite (nujol mull, 0-1 scale, 60 nm/min).
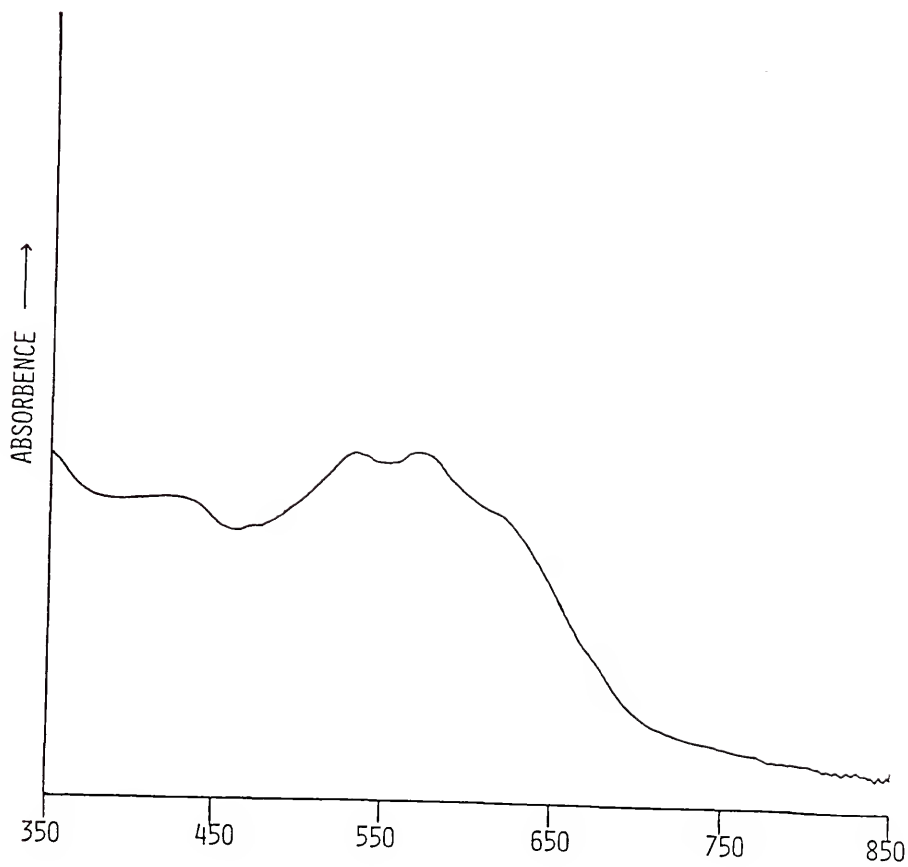
Figure 2-8. Electronic Spectrum for Co(NaCN)-Y-1 (nujol mull, 0-1 scale, 60 nm/min).
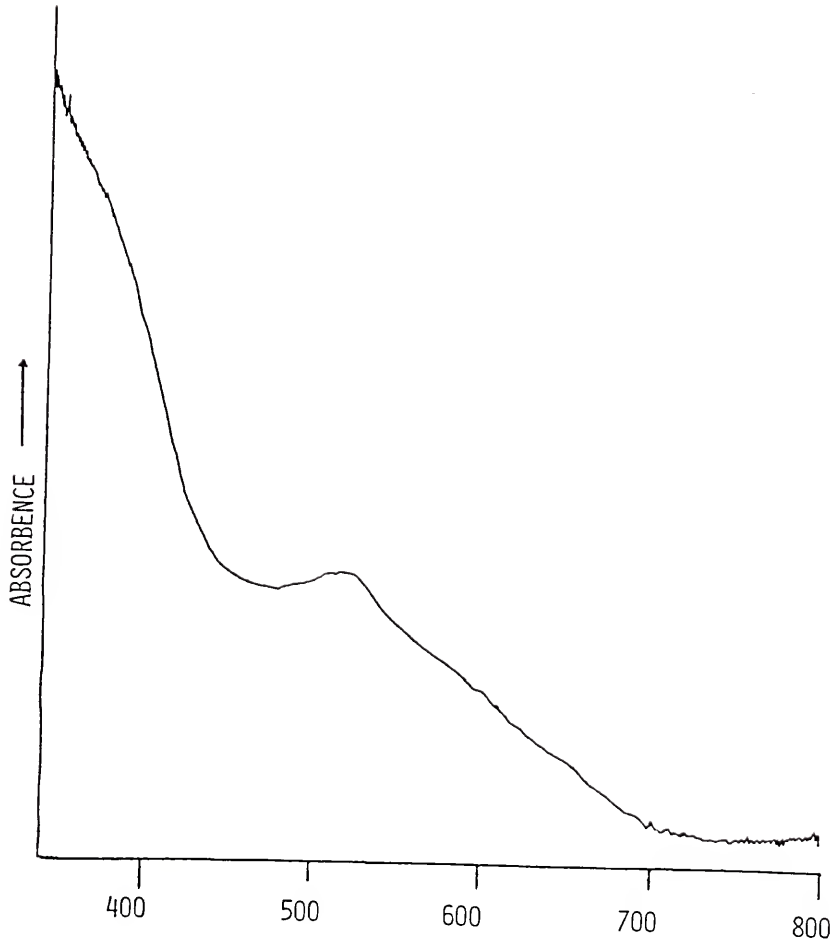
Figure 2-9. Electronic Spectrum for Co-(NaCN)-Y-2 (nujol mull, 0-1 scale, 60 nm/min).
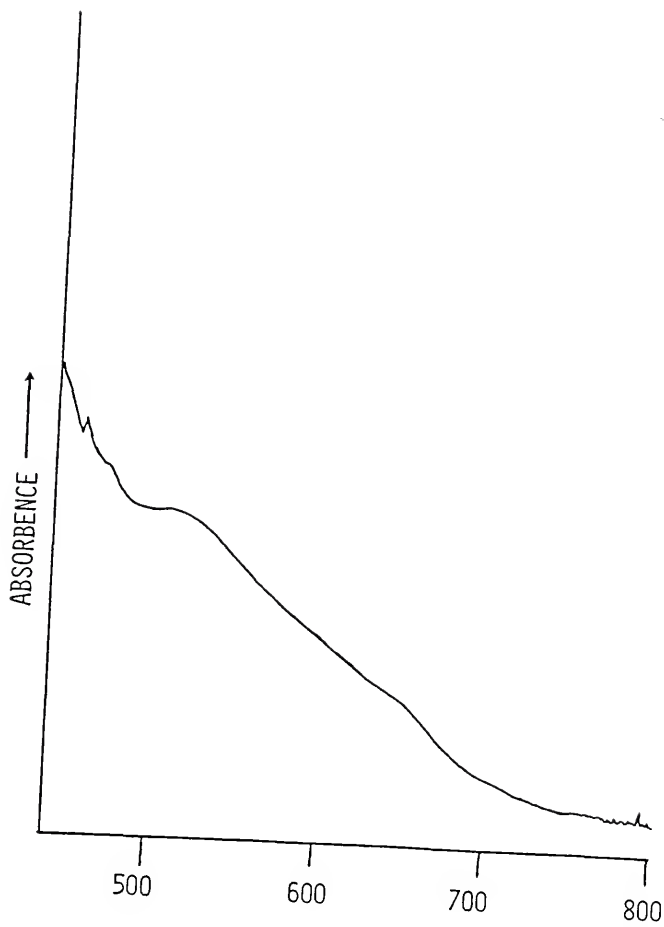
Figure 2-10. Electronic Spectrum for Co(NaCN)-Y-3 (nujol mull, 0-1 scale, 60 nm/min).

Figure 2-11. X-band ESR of Co(NaCN)-Y-3 + O_2 after 50 oxygenation/deoxygenation cycles (83 °K), $g_\perp \sim 2.07$ and $g_\parallel \sim 2.01$.
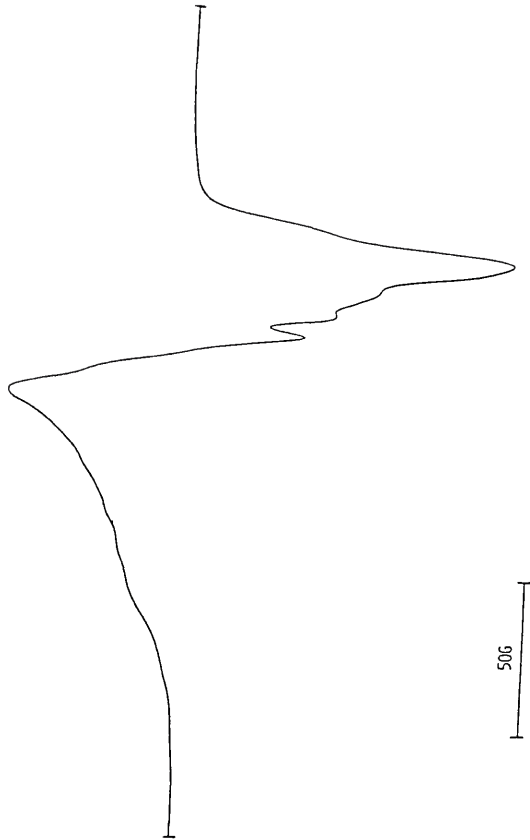
506

Figure 2-12. X-band ESR of Co(NaCN)-Y-3 after 50 oxygenation/deoxygenation cycles (83 °K), $g_\perp \sim 2.25$ and $g_\parallel \sim 1.95$.

200G
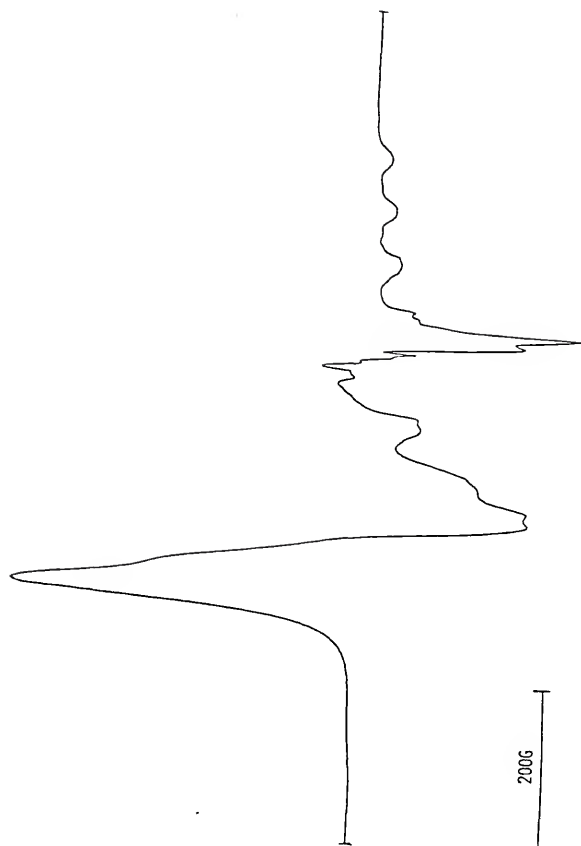
center of the spectrum. The relatively large anisotropy in the g

tensor supports the contention that the complex is not $Co(CN)_5^{3-}$

but rather $Co(CN)_4^{2-}$ with the axial position occupied by a lattice

oxygen as shown below. Additionally, for an acetonitrile solution
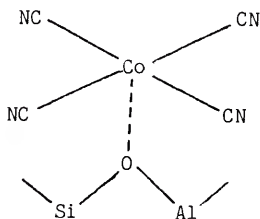
containing a 5:1 mixture of cyanide and Co(II) the $g_\perp \sim 2.18$ and

$g_\| \sim 2.00$,[44] whereas a solution containing a 3:1 mixture of cyanide

and Co(II) produces an ESR spectrum with $g_\perp \sim 2.28$ and $g_\| \sim 2.00$.

The oxygenation of the zeolite containing Co(II) complexes is

reversible and can be cycled at least 400 times. In fact, the

spectra shown in Figures 2-11 and 2-12 were taken after 50

cycles. However, the $P_{1/2}$ for this complex must by very small since

reducing the pressure to below 10^{-4} torr did not completely

deoxygenate the sample. In terms of commercial applications as a

pressure swing adsorption catalyst, good reversibility is important

as well as the oxygen carrying capacity and the stability. The

ideal absorbent should have the capacity to absorb at least 10 mL

of oxygen per gram of catalyst. Such an absorbent would find

greater utility for large scale gas operations. On a smaller

scale, such as for a breathing apparatus which would require a

minimum of 30 liters of oxygen per minute, the O_2 binding capacity

of the absorbent would have to be even greater. In a crude vacuum line experiment, one gram of Co(NaCN)-Y-3 was placed in a tube of known volume then degassed under less than 10^{-4} torr pressure. The sample after exposure to 4 torr of O_2, absorbed nearly 1 mL of oxygen. This compares well with [Co(bipy)(terpy)]Li-Y which absorbs 0.47 mL of O_2 per gram of zeolite under 15 torr of O_2.[39]

A good PSA catalyst should be stable in the presence of H_2O, CO_2, and SO_2. The cyanocobaltate complexes are stable to moisture since they can even be prepared in water (Co(NaCN)-Y-5,6). In the absence of moisture, CO_2 and SO_2 have no effect on the O_2 binding properties of the complexes. However, if water was present, a radical species was generated with SO_2, probably $SO_2^{\cdot -}$ or $SO_2^{\cdot -}$, and the capacity to bind oxygen was lost. Similar radicals are formed with wet NaY zeolite itself under the same conditions.

In conclusion, stable cobalt(II) complexes have been supported on polystyrene, silica gel, and zeolites. These complexes have been demonstrated to be effective oxygen carriers. This property has been exploited in Chapter IV, where these supported complexes were employed as additives in polymer membranes to facilitate the transport of oxygen.

The studies presented above were extended to include complexes that reversibly bind carbon monoxide which are discussed in Chapter III. Many of the complexes that bind O_2 also react with CO, forming complexes that are often more stable and less reactive than the O_2 complexes. Therefore, the CO carriers may provide good models for the O_2 carriers in the metal complex facilitated membrane gas separations.

CHAPTER III
THE PREPARATION AND CHARACTERIZATION OF
Cu(I) COMPLEXES THAT REVERSIBLY BIND CARBON MONOXIDE

Introduction

The reversible fixation of carbon monoxide has been an area of considerable interest for nearly a century. Some of the impetus behind recent advances in CO chemistry has been a need for efficient gas separation processes which is discussed in more detail in Chapter IV. A primary application is the recovery of CO from industrial byproduct gas streams which can then be used in chemical production. Often the synthesis gas, CO/H_2, used in chemical production is obtained from steam reforming of natural gas. However, this energy intensive process could be avoided and our limited natural gas supply could be conserved if CO could be supplied from byproduct gas streams. There are many liquid absorbtion processes for the separation of carbon monoxide from gas mixtures, most of which are based on copper(I) chemistry. The most notable commercial development, known as the COSORB process, involves a $CuAlCl_4$ complex in an aromatic base.[48,49] In comparison with cryogenic separation, the COSORB process can produce 100.0 million pounds of CO per year versus 87.3 million with a purity of 99.83% versus 99.38% for nearly half the cost. It would appear that the development of selective absorption processes could be a profitable venture. The direction of current research efforts has focused on solid absorbents and membrane separation which will be

51

discussed in Chapter IV. There are numerous metal complexes that reversibly bind carbon monoxide in solution such as $CH_3Mn(CO)_5$,[50] Vaska's complex $IrCl(CO)(PPh_3)_2$,[51] the metal-metal bonded bis-μ-(bisdiphenylphosphinomethane)dihalodipalladium(II),[52] phthalocyanatoiron(II),[53] and the biologically significant metal porphyrin complexes.[54] A recent study of supported complexes for the separation of gas mixture describes the attempt to support on polystyrene $Pd_2(dmp)_2Cl_2$, which rapidly binds CO in solution at 25 °C.[55] This complex could not be supported nor did the crystalline complex bind CO, probably the result of lattice constraints. As described in Chapter II, polymeric supports are practical from the standpoint that they are easy to functionalize. Site isolation of metal complexes is not important for the fixation of carbon monoxide unlike the oxygen carriers. Therefore, relatively simple systems can be investigated without the elaborate synthetic procedures used in the preparation of oxygen carriers to insure stability. For example, simple

$$-(CH_2)-\left(\begin{array}{cc} -C & -C \\ \| & \| \\ HON & NO \end{array}\right)\left(\begin{array}{c} -C \\ \| \\ O \end{array}\right)-$$
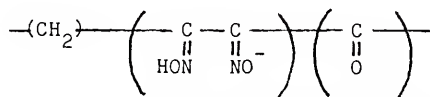
polyoximes of the general formula impregnated with Fe(II) and Cu(I) salts reversibly bind CO.[56-58] These functionalized polymers were subsequently employed in an unsuccessful attempt to facilitate the transport of CO through a polymer membrane.[59]

Other supports recently investigated include zeolites and carbon. Zeolitic molecular sieves containing Cu(I) cations were found to have a high affinity for CO, even in the presence of

water.[60] Unfortunately, small amounts of CO were absorbed because of low exchange of copper in the zeolite. A serious drawback of using $CuAlCl_4$ in facilitated transport is that it is extremely moisture sensitive and forms HCl in the presence of water. The COSORB process requires less than 1 ppm of H_2O in the feed gas. The active component of the COSORB process, $CuAlCl_4$, was recently supported on active carbon.[61,62] Also stable in the presence of moisture, this complex is an effective absorbent for CO. It was proposed that the $CuAlCl_4$ complex was located in polar micropores of the active carbon, where the walls composed of condensed aromatic rings interact with the Cu(I). This support apparently inhibits the aggregation of the metal complexes since these micropores are so small. As a result even Copper(I) chloride has been supported on carbon and found to be an effective CO carrier.[63] At 20 °C, the carbon supported $CuAlCl_4$ complex adsorbs slightly more than a 1:1 molar ratio of CO. Low pressure (0.4 mmHg) and high temperature (180 °C) is required to desorb nearly all of the CO. The influence of the aromatic rings of the carbon in stabilizing the Cu^+ complex is not unique but seemingly an integrable part of a number of separation processes (ex. COSORB process-aromatic base). Along these same lines, $CuAlCl_4$ was observed to reversibly bind CO in a polystyrene/toluene solution.[64,65] In the absence of polystyrene, the $CuAlCl_4$ solution displays a marked decrease in CO binding ability, especially in the presence of water. It was proposed that polystyrene forms a stronger charge transfer complex by virtue of a chelate effect where two aromatic rings interact with the $CuAlCl_4$ complex.

Seemingly there is little need for the aromatic solvent and indeed it was very recently reported $CuAlCl_4$ supported on macroreticular crosslinked polystyrene reversibly adsorbs CO.[66] Linear or gel type crosslinked polystyrene supported $CuAlCl_4$ are far less active, which probably can be attributed to diffusional problems. These functionalized polystyrene beads can adsorb as much as 69 mL CO per gram at STP. The effects of the polymer support must be twofold: 1) provide a hydrophobic environment and 2) form a weak complex with the Cu(I).

The $CuAlCl_4$ complex supported on a macroreticular resin was reported subsequent to the completion of the work described in this chapter. The original goal of this research was to prepare polymer supported ligands that would bind and stabilize copper(I) which could effectively act as a CO carrier. Numerous copper(I) complexes reversibly bind CO.[67,68] Since the copper(I) prefers to be four coordinate, a bidentate or tridentated ligand would be advantagous. Several CO carrying copper(I) complexes with bi and tridentate ligands have been reported, all of which contain one or more unsaturated amines.[69-74] Complexes with saturated amines are far less stable and readily undergo a disproportionation.[75]

Herein the synthesis and reactivity of polystyrene supported copper(I) chloride, dimethylamine copper(I) chloride and dicyanoethylamine copper(I) chloride are described in detail as well as attempts to prepare homogeneous solution analogues.

Experimental

All reagents were used as received unless otherwise specified.

Copper(I) iodide. Copper(I) iodide (Aldrich Chemical Co.) was dissolved in acetonitrile and precipitated with deionized water. The white solid was dried in a vacuum at 60 °C then stored in a dry inert atmosphere box unexposed to light.

Copper(I) chloride. Copper(I) chloride was prepared according to the literature procedure[76] and stored in a dry inert atmosphere box sealed from light.

[P]-CH$_2$Cl. The chloromethylated linear polystyrene as well as the 4% divinylbenzene crosslinked, 90% chloromethylated polystyrene beads were provided by Sybron Corporation.

[P]-DCEA. Bis(2-cyanoethyl)amine, (DCEA) supported on crosslinked polystyrene beads was prepared as previously described.

The linear polystyrene supported DCEA was prepared as follows. Ten grams of the [P]-CH$_2$Cl was dissolved in 150 mL of dioxane in a 500 mL round bottom flask equipped with a reflux condenser. Into the solution was stirred 30 mL of 3,3'-iminodiproprionitrile for 30 minutes at room temperature then at low heat for two days. The solution was filtered and methanol added to the filtrate until a gelatinous precipitate formed. The solid was redissolved in CH$_2$Cl$_2$, filtered and methanol added to the filtrate until a white precipitate formed. The isolated [P]-DCEA was dried in vacuo. Calculated for 90% Substitution: C, 81.2; H, 7.67; N, 11.2. Found: C, 73.8; H, 6.8; N, 7.0 which corresponds to 81% substitution.

[P]-DCEACuX. Excess copper(I) halide dissolved in dry acetonitrile was slurried with one gram [P]-DCEA for twelve hours at room temperature in an inert atmosphere box. The resin was suction filtered and washed with CH_3CN then dried under N_2. For $X = I^-$ calculated: C, 41.4; H, 3.9; N, 9.1. Found: C, 68.7; H, 6.6; N, 11.00 which corresponds to 42% complexation, taking into account one coordinated CH_3CN per copper ion.

For $X = Cl^-$ calculated: C, 53.0; H, 5.0; N, 11.6. Found: C, 65.1; H, 6.2; N, 10.5 which corresponds to 67% complexation assuming one molecule of solvation.

[P]-DCEACuCl (linear). In a dry inert atmosphere box 1 gram of [P]-DCEA was stirred with 1 gram (XS)CuCl in 80 mL of acetonitrile at room temperature for 24 hours. The now sticky orange resin was suction filtered and dried in vacuo.

BenzylDCEA. The 3,3'-benzyliminodiproprionitrile was prepared according to the published procedure.[21]

[P]-N(CH_3)_2. Polystyrene bound dimethylamine was prepared as follows. Twenty grams [P]-CH_2Cl were slurried with 50 grams of anhydrous dimethylamine under argon at room temperature for 20 hours. The resin was suction filtered, washed with dioxane, 50/50 dioxane/H_2O, H_2O, 50/50 H_2O/THF, and dried in vacuo at 80 °C.

[P]-N(CH_3)_2CuCl. In an inert atmosphere box 2 grams of [P]-N(CH_3)_2 were slurried with excess CuCl in 50 mL of acetonitrile for 5 hours. The pale yellow resin was suction filtered, washed with CH_3CN and dried under N_2.

[P]-CH$_2$ClCuCl.   In an inert atmosphere box 1 gram of [P]-CH$_2$Cl
was slurried with excess CuCl in 50 mL of acetonitrile for 24 hours
at room temperature. The resin was suction filtered, washed with
acetonitrile and dried under nitrogen.

[Cu(DCEA)$_2$]Cl$_2$.   Was prepared according to the published
procedure.[77]

Results and Discussion

The potentially tridentate ligand HN(CH$_2$CH$_2$CN)$_2$, DCEA, forms a
2:1 complex with CuCl$_2$ in the manner shown below. The nitrile-

copper bond is relatively weak as evidenced by a bond length of
2.70 Å and a single weak νCN stretch in the IR at 2258 cm^{-1} (free
ligand 2250 cm^{-1}). The shift in frequency to a higher value is
indicative of the nitrile being N bound rather than π bonded. The
amine-copper bond is somewhat stronger (2.10 Å) with the νNH
stretch at 3202 cm^{-1} shifted to a lower value than the free ligand
(3335 cm^{-1}).[77] When copper(I) salts were reacted with DCEA in
acetonitrile under nitrogen, either rapid disporportionation
occurred as evidenced by the formation of a copper mirror on the
reaction vessel or a green solid was formed. The green compound
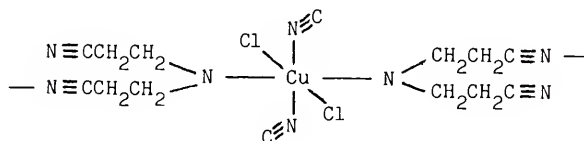
was a Cu^{2+} complex as evidenced by an ESR. The IR showed no shift in the νCN but the νNH shifted to 3296 cm^{-1}. The $Cu(DCEA)_2Cl_2$ was a bright purple color. The green solid obtained from the Cu^+ reactions is probably an amine complex of some sort. Covalent attatchment of the DCEA ligand to a solid polymeric support would inhibit formation of complexes of the type formed with copper(II) and also reduce the basicity of the amine functionality. When [P]-DCEA is reacted with $CuCl_2$ in boiling ethanol, a yellow resin results with the ESR shown in Figure 3-1 and a CN stretch at 2248 cm^{-1}. For the linear [P]-DCEA and $CuCl_2$ in boiling acetonitrile, a yellow resin was recovered with the ESR shown in Figure 3-2. The IR shows a νCN = 2257 cm^{-1} providing some evidence for bound nitriles. When CuI or CuCl is reacted with [P]-DCEA, the resulting resin shows no notable IR shifts in the nitrile region. Placing the resin in ammonia solution turns it blue indicating the presence of $Cu(N_2H_3)_4^{2+}$, which is evidence for the incorporation of copper. The [P]-DCEA has complexed Cu^+ since no ESR signal is observed and it should be further noted that the functionalized polymer remains ESR silent even upon exposure to air. This resin which has only been dried under nitrogen, is unreactive towards carbon monoxide. However, if the polymer beads are placed under a vacuum then exposed to a CO atmosphere, CO binding is observed. It is postulated that the Cu(I) complex is solvated prior to evacuation rendering the Cu^+ coordinatively saturated and inert towards CO. Copper(I) forms complexes of the type $[Cu(CH_3CN)_n]^+$, where n = 1-3 depending upon the anion.[78,79] The copper(I) halides form 1:1 complexes with acetonitrile. Such complexes are very air

Figure 3-1. X-band ESR of [P]-DCEACuCl$_2$, g ~ 2.13 (93 °K).

300 G
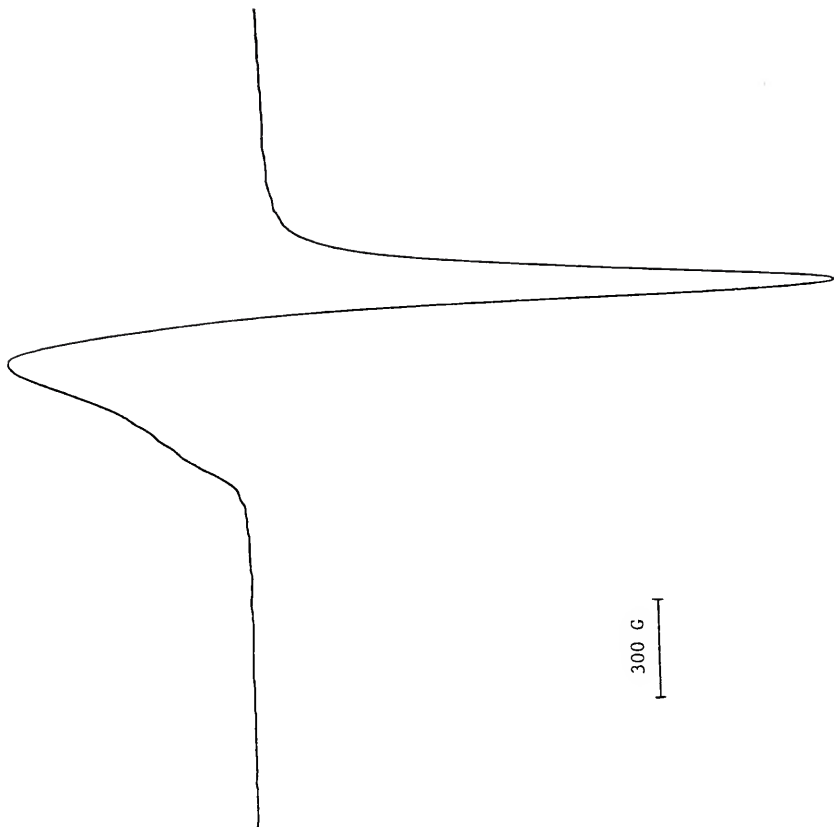
Figure 3-2. X-band ESR of [P]-DCEACuCl$_2$ (linear), g ~ 2.14 (90 °K).

300 G
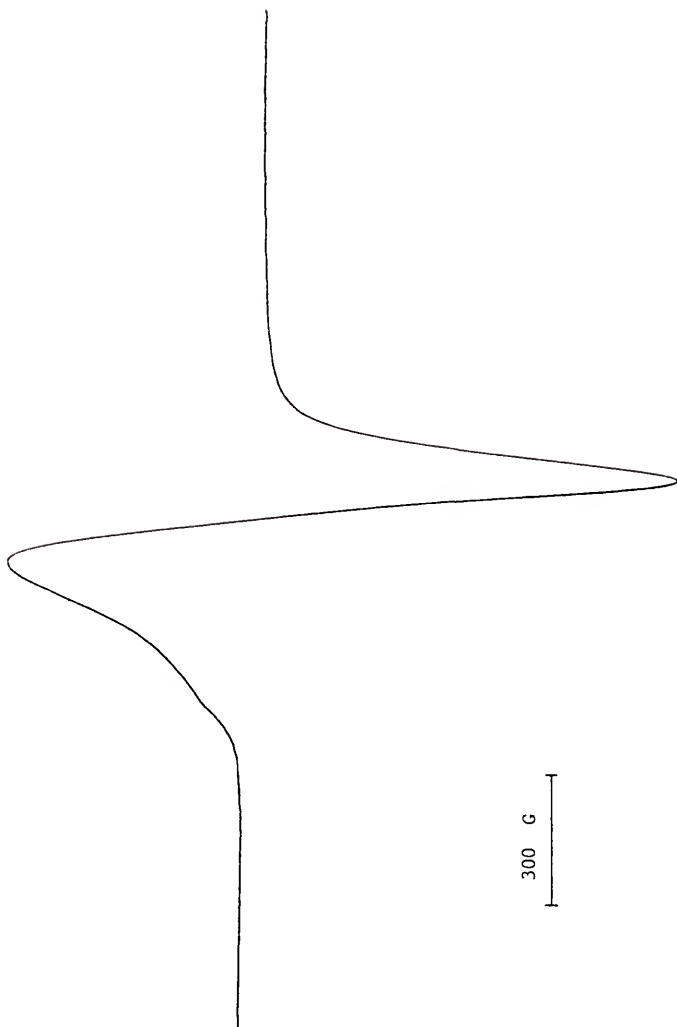
sensitive and the nitrile is easily lost. It is postulated that the product of the acetonitrile synthesis is [P]-DCEACuX·S as shown below. The CuI complex binds carbon monoxide with $\nu CO = 2091$ cm^{-1}.

$$[P] \longrightarrow N \quad \substack{CN \\ CuX \cdot CH_3CN \\ CN}$$
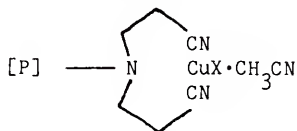
Under similar conditions the CuCl complex also binds CO reversibly with $\nu CO = 2100$ cm^{-1}. The reversibility was demonstrated by placing the resin in the apparatus described in Figure 5-3, applying a vacuum of less than 1 mmHg, then exposing the polymer beads to 15 psig CO. The CO could then be removed by again reducing the pressure to less than 1 mmHg. A typical cycle is shown in Figure 3-3. The absorption/desorption of CO can be cycled at least five times without a loss in activity. Upon exposing the resin to air after evacuation, the ability of the complex to fixate CO was greatly diminished. Pumping on the air exposed sample partially restores the ability to bind CO. The minimum conditions necessary to absorb and desorb CO have not been determined but it is known that at higher CO pressure the concentration of carbonylated complexes increases. This is reflected in the IR spectra where the CO streching band is noticeably more intense. Figure 3-4 shows the IR for a [P]-DCEACuCl sample after exposure to 25 psig CO ($\nu CO = 2094$ cm^{-1}). This can be compared to the spectra in Figure 3-3. This suggests that complete complexation throughout the crosslinked beads is a permeation controlled process. In other words, at the higher pressure more CO will permeate through the polymer faster and more Cu-CO adducts will be formed. This is also

Figure 3-3. FT-IR of [P]-DCEACuCl (nujol mull)
A. After evacuation
B. After exposure to 15 psig CO,
  * indicates CO strech at 2100 cm^{-1}
C. After evacuation.
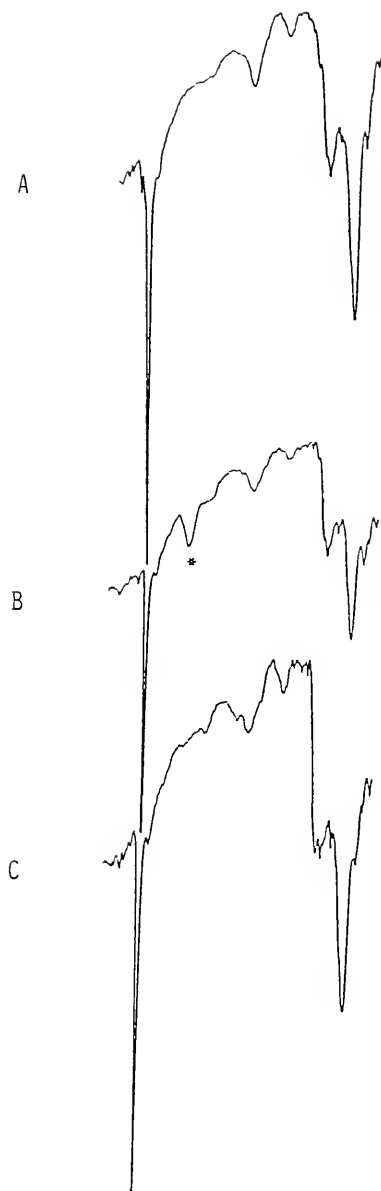
Figure 3-4. FT-IR of [P]-DCEACuCl (nujol mull) after exposure to 25 psig CO (the arrow indicates the CO strech at 2093 cm^{-1}).

% TRANSMITTANCE

WAVENUMBERS CM^{-1}

2200   1800
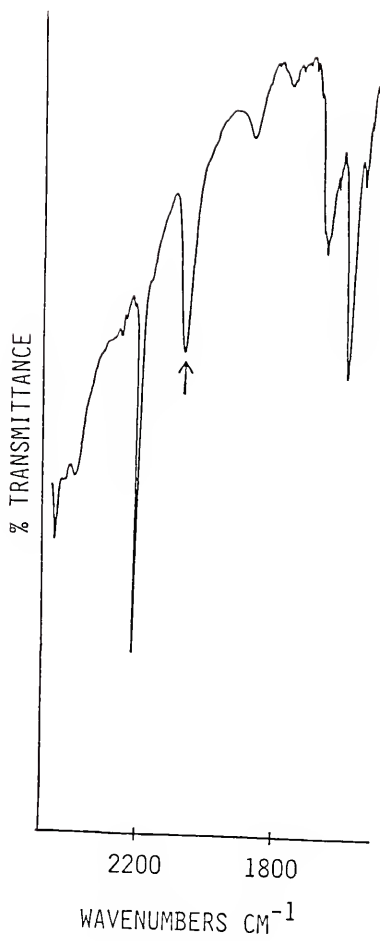
supported by the fact that the linear [P]-DCEACuX did not bind CO under the same conditions. The porous nature of the macroreticular resin provides diffusion pathways for the CO while the CO must permeate through the amorphous regions of the linear polymer. The importance of the nature of the polymeric support was further demonstrated in an attempt to prepare a silica bound DCEACuX complex. Even with careful preparative techniques, the Cu^+ was oxidized. This may attest to the importance of a hydrophobic environment.

In order to discern the nature of the bound species in [P]-DCEACuX the preparation of a solution analogue was attempted. The ligand $C_6H_5-N(CH_2CH_2CN)_2$, phenylDCEA, was unreactive towards Cu^{2+} which was not surprising since it was later learned that phenylDCEA is synthesized using a copper catalyst consisting of a mixture of CuCl and Cu° powder.[80] Additionally, it could be expected that the aniline type amine would be less basic than a benzylamine. Acetonitrile solutions of CuCl and benzylDCEA are unreactive towards CO at room temperature. However, at 0 °C two CO stretches are observed in the IR at 2025 cm^{-1} and 1994 cm^{-1} indicative of a strongly bound terminal CO and possibly a bridging CO. Unfortunately an acetonitrile solution containing only CuCl behaves in the same fashion. It is well known that copper(I) halides absorb CO in organic solvents at room temperature (CH_3OH, 2070 cm^{-1}; THF, 2085 cm^{-1})[81] but apparently the acetonitrile complex behaves in an unusual fashion. It is sufficient to say that the polymer supported complexes react in a manner unlike that of similar species generated in solution.

The weak interaction of the nitriles in complex formation, as indicated by the infrared spectra, leads one to believe they may not be necessary in order to stabilize the CO carrier. Keeping this in mind, dimethylamine was supported on the crosslinked polystyrene beads. The complex $[P]-N(CH_3)_2CuCl$ CH_3CN binds CO ($\nu CO = 2065$ cm^{-1}) much more strongly than $[P]-DCEACuCl$ but is just as reversible. A typical CO absorption/desorption cycle is shown in Figure 3-5. It should be noted that CO is bound when the complex is still solvated and the subsequent loss of the CN stretch with repeated cycles appears to have no effect on the binding ability of the complex. Exposing the tan colored resin to air instantly changes the color to orange, resulting in the ESR spectrum shown in Figure 3-6. The orange resin shows a very weak peak at 2066 cm^{-1} upon exposure to CO. Pumping on the orange resin at 10^{-4} mmHg for 5 hours reduces the intensity of the ESR signal. If the orange resin is allowed to stand in air for several days it will change to an olive green color accompanied by an increase in intensity of the ESR signal but no changes occur in the general features of the spectrum. The nature and reactivity of $[P]-N(CH_3)_2CuCl$ are clearly different than that observed for $[P]-DCEACuCl$. However, as a further control CuCl was simply adsorbed onto the polystyrene beads from an acetonitrile solution and screened for its CO binding capacity. Keeping in mind that solid copper(I) chloride binds CO only under extreme conditions and that in the presence of moisture it is both light and air sensitive, it came as somewhat of a surprise that $[P]-CH_2ClCuCl\cdot CH_3CN$ reversibly binds CO at room temperature. A typical cycle is shown in Figure 3-7. The CO is bound weakly

Figure 3-5. FT-IR of [P]-N(CH$_3$)$_2$CuCl
A. solitated complex after exposures to
   25 psig CO (νCO = 2065 cm^{-1})
B. after evacuated
C. after exposure of 25 psig CO
D. after evacuated, exposure to air,
   then 25 psig CO.
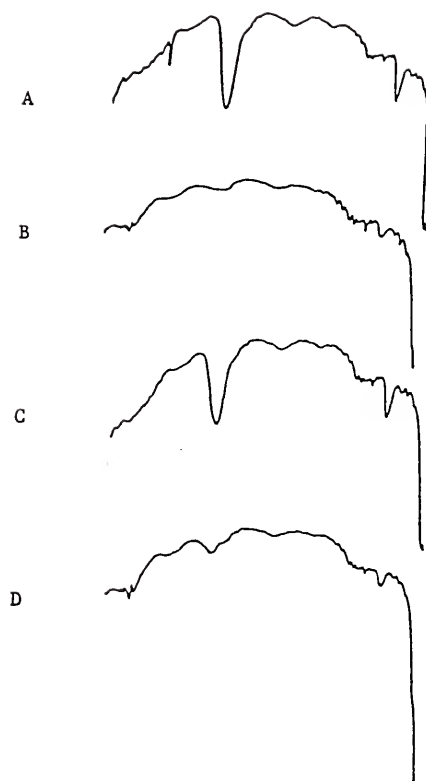
Figure 3-6. X-band ESR of [P]-N(CH$_3$)$_2$CuCl$_2$ (orange) after exposure to air, g$\perp$ ~ 2.09 and g$\parallel$ ~ 2.28 (room temperature).

300 G
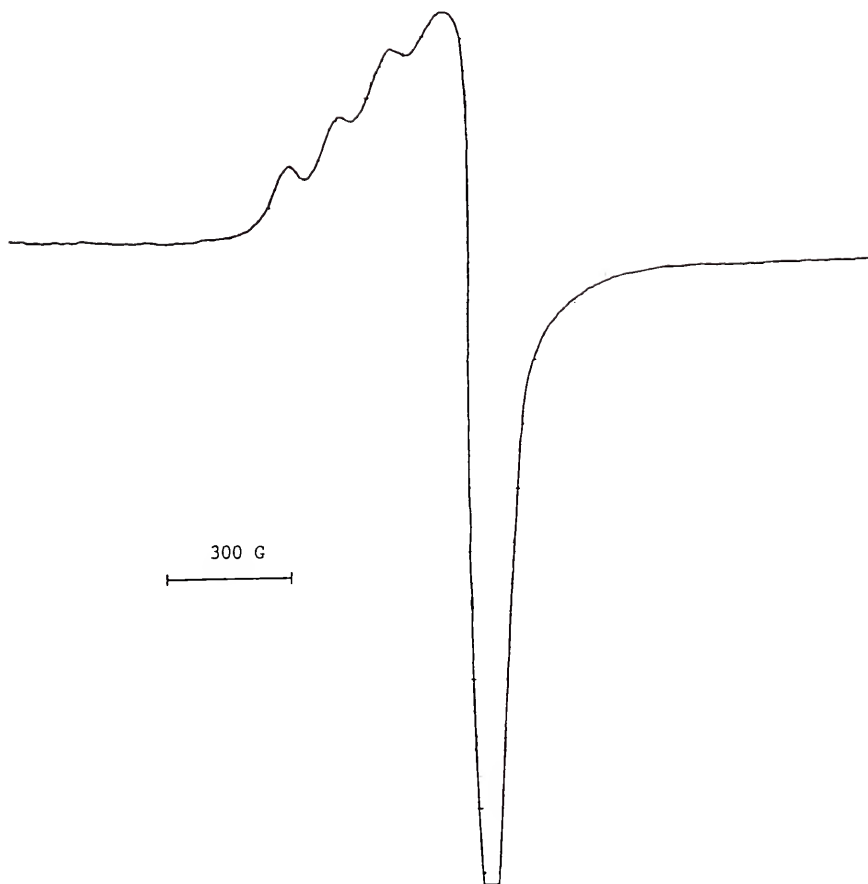
Figure 3-7. FT-IR of [P]-DCEACuCl·CH$_3$CN

       A. After preparation

       B. After exposure to 25 psig CO,
          νCO = 2096 cm^{-1}

       C. After evacuation

       D. After exposure to CO

       E. After evacuation, exposure to air,
          then exposure to CO.
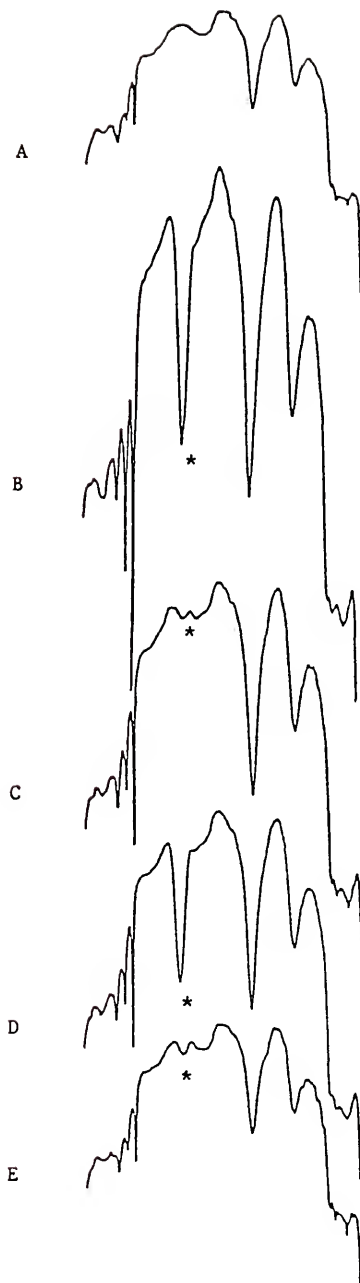
(νCO = 2096 cm^{-1}) and is not completely removed upon exposure to reduced pressure. Interestingly enough, the CN stretch does not decrease in intensity even after repeated cycling. The acetonitrile is still weakly bound (νCN = 2252 cm^{-1}) but apparently stronger than for either [P]-DCEACuX·CH$_3$CN or [P]-N(CH$_3$)$_2$CuCl·CH$_3$CN. Even though the IR does not dictate a stronger interaction one might rationalize these results as follows. If the Cu(CH$_3$CN)$_x$Cl forms a charge transfer complex with the aromatic rings of polystyrene which would donate electron density to the metal center, then there could be π backbonding from the metal d orbitals to the π^* orbitals of the nitrile. This would lower the frequency of the CN stretch. In the presence of air, the ability of [P]-CH$_2$ClCuCl·CH$_3$CN to bind CO is drastically reduced and an ESR signal is observed.

In conclusion it has been demonstrated that three different copper(I) halide complexes supported on polystyrene are reversible CO carriers. In comparing [P]-DCEACuCl and [P]-N(CH$_3$)$_2$CuCl it appears that the nitrile groups of DCEA play a major role in stabilizing the complex. The fact that the polymer supported copper(I) acetonitrile complex binds CO leads to a study of the unusual properties of metal complexes in polymer matricies which will be developed in Chapter IV. The developments described above directly relate to the goals outlined in Chapter II, namely the preparation and characterization of supported metal complexes that reversibly bind O$_2$. Although the reactivity of the supported copper(I) halide complexes with O$_2$ was not firmly established, the reversible binding of CO by these complexes was a significant

discovery. Eventually, inclusion of such complexes in the membrane gas separations discussed in Chapter IV may provide important mechanistic details related to the facilitated transport of O_2, especially in light of the wider range of physical methods available to study CO complexes.

CHAPTER IV
METAL COMPLEX FACILITATED TRANSPORT OF
GASES IN POLYMER MEMBRANES

Introduction

Gaseous oxygen constitutes 20.946% of the earth's atmosphere and is essential to nearly all living creatures. Additionally, many industries rely on O_2, especially those which involve combustion processes such as in primary metals manufacture (ex. steel) and chemical production (ex. ethylene oxide). Oxygen production in 1986 is expected to exceed 380 billion cubic feet to the tune of over two billion dollars.[82] Likewise the demand for nitrogen is high at nearly 660 billion cubic feet or 3.3 billion dollars worth. Many industries do not require high purity oxygen but can get by with oxygen enriched air. This market is continually growing and already includes waste water treatment facilities, the pulp and paper industry, fermentation processes, fish farming and fire flooding of oil reservoirs as well as numerous applications in the medical industry. The large scale production of oxygen is achieved by a cryogenic air separation process or increasingly more often by pressure swing adsorption which essentially involves N_2 adsorption from air by zeolites. An alternative separation method which has received considerable attention as of late involves selective gas permeation through a polymer membrane.

78

The separation of gases by polymer membranes is based on the principle that different gases permeate differently where permeability refers to the overall mass transport of a gas through a membrane, as opposed to diffusion which only relates movement of the gas inside the membrane. This was first noted in 1831 by Mitchell, the inventor of the toy rubber balloon, who observed that his balloons would deflate at different rates depending upon the gas inside.[83] It was not until 1866 that an understanding of this process was advanced by Thomas Graham, who is credited as being the father of gas separations. Graham proposed a solution-diffusion model to describe the selective permeation of gases in polymer membranes.[84] He also showed by employing a rubber membrane that one could exploit the relative differences in permeabilities between gases and separate a gas mixture by applying a partial pressure differential across the membrane. Specifically, Graham was able to produce a gas mixture containing 41% oxygen from air. In 1879 von Wroblewoski quanitified Graham's work by adapting Fick's law of diffusion to the permeation process[85] as shown below

$$J = D\ S\Delta p/l$$

where J is the flux of air flow as a mass quantity per unit time, D is the diffusion coefficient, S is the solubility, Δp is the partial pressure differential and l is the membrane thickness. What this implies is that the gas dissolved at the surface of a rubbery polymer obeys Henry's law, $C = Sp$, and diffusion of the gas obeys Fick's law where flux is proportional to the concentration

gradient or pressure differential. With the advent of World War I came a resurgence in membrane research as it related to balloon and airship fabrics. In 1918, Shakespear was able to show that the permeability of a gas is independent of the presence of other gases.[86] He also developed the Kathrometer or thermal conductivity detector (TCD) as part of a permeability tester.[87] An enormous amount of research was conducted up through the 1950's and 1960's on the permeation properties of polymers which was prompted by the use of plastics in the packaging industry. A considerable amount of the engineering was developed during this period even though the use of membranes in gas separations was commercially unfeasable at the time.[88] A more complete historical perspective as well as the current status of membrane technology can be found in several recent reviews.[89-94] In general, the simple solution-diffusion model holds for nonswollen rubbery polymers. However, a vast amount of literature is devoted to deviations from this model. It will become evident in the following pages that simple changes in a polymer membrane can result in large variations in the permeation properties. The permeability of a gas is essentially a rate measurement for movement of that gas through a polymer of thickness l, with an applied pressure differential Δp. The permeability coefficient $\overline{P}$, is usually reported in units of $cm^3(STP)$ $cm/cm^2 sec$ $cmHg$ or $mmHg$. The separation factor or the ability of a polymer to separate two gases is given as α, where $\alpha = \overline{P}_1/\overline{P}_2$. Since $\overline{P} = D \cdot S$, it is reasonable to assume those molecules with a small molecular diameter (ex. He) would have high permeabilities because of a high diffusion coefficient and those

molecules that are easily condensed (ex. CO_2) would also have high permeabilities because of a high sorption coefficient. Molecules such as O_2 and N_2 which both have low diffusion and sorption coefficients have low permeabilities and are particularily difficult to separate. The ideal membrane material would exhibit high selectivity and high flux as well as good mechanical strength. Generally, the most selective membranes are the least permeable and vice versa. Since nearly every polymer that can be cast into a membrane has been evaluated for gas permeation properties, the focus of many research efforts has been to enhance the separability of polymer membranes. There has been an effort in the area of module design in order to develop membrane systems which provide high surface area and flux to polymers that are selective but generally have low permeabilities. Another area which is growing in interest involves the incorporation of additives to modify the permeation properties. This approach has been directed towards membranes that are highly permeable and poorly selective.

There are essentially four types of membrane configurations, namely the tube, flat, hollow fiber and liquid membranes. The tube membrane finds little or no application in gas separations, but is most often used in liquid filtration where there is a high concentration of particulates.

The flat membrane can be packaged in a variety of ways. The oldest and most commonly used module type in small scale gas separations simply involves a flat plate or disc which may be unsupported (i.e. the polymer itself), reinforced (i.e. the polymer

may contain a mesh screen for support), or a composite (i.e. either one or both surfaces of the membrane may be attached to a support material such as another polymer, paper or similar material). These flat membranes can be secured in a gas separation cell manifolded to a vacuum pump, then placed in a series of cascades or stages to achieve a desired separation. Several oxygen enrichment systems based on this type of membrane have been patented.[95-99] The application of such systems is for the small scale production of oxygen enriched air. A major end use is in respiratory care. A typical oxygen enrichment unit produces an air mixture containing 30-40% O_2, depending upon the polymer employed, at a flow rate of 6 liters/minute.[100] Because flat membranes of this type must be relatively thick to be structurally stable to the applied partial pressure differential, a low flow rate is obtained. In order to obtain large flow rates a membrane must be extremely thin which is incompatable with the need for thicker films to maintain structural integrity. Much thinner flat films and subsequently higher flow rates can be obtained with a spiral-wound element. This membrane module consists of two retangular sheets of polymer membrane (200-5000 A thick) separated by sheets of a porous supporting material (100 μ thick). This arrangement is a composite membrane. The membranes are separated by a mesh channel spacer and wrapped around a perforated hollow plastic tube. This high pressure feed gas is directed through the end of this spiral and the product gas permeates through the membranes and exits through the hollow tube. Several oxygen enrichment plants based on this technology have recently gone on line.[101,102] Such plants have the

capacity to produce 200 ft^3 per minute of air containing 29-30% oxygen. Commercial units are now being offered that can supply as much as 2000 ft^3 per minute of oxygen enriched air. A single 8 inch spiral-wound element can produce nearly 177 liters per minute of O_2 enriched air compared with the thick flat membranes at 6 liters per minute.

Another type of membrane which has achieved commercial success is the hollow fiber membrane. The hollow fibers are usually less than 300 μ in diameter which is finer than human hair. These membranes are typically on the order of 1 μ thick. The hollow fibers suffer from the same problems as the ultra thin flat membranes, a high flux but poor selectivity. This is because the thin membranes are more likely to have micropores or pinholes. This is a problem when one considers all a membrane needs is a channel of 5-10 Å in diameter to have most gas molecules of interest flow through rather easily. This was resolved with the development of composite hollow fiber membranes.[103, 104] The hollow fibers were lamenated with a thin layer (~ 1 μ) of a rubbery polymer to plug the pinholes. Monsanto first commercialized these membranes, known as PRISM separators, for the recovery of H_2 and CO_2 in methanol synthesis.[105] This technology was recently applied to air separation by Dow Chemical.[106] This hollow fiber membrane system has the capacity to produce over 2000 ft^3 per minute of 35% oxygen enriched air. The advantage of hollow fibers over flat spiral-wound membranes is that a higher separation surface area per unit volume can be achieved. For example, for flat membranes the area to volume ratio is typically on the order of a few

hundred ft^{-1} where as for the hollow fibers the ratio is several thousand ft^{-1}.

Although the thin composite hollow fiber and flat membranes can generate industrially acceptable fluxes the selectivities are poor. The O_2/N_2 separation factor for polymers is generally less than 3. A recent approach to enhancing the transport of a specific gas through a membrane involves the encapsulation of a metal complex containing solution into a porous polymer membrane. The metal complex serves to facilitate the transport of a gas from one boundary layer of the solution to the other. This type of membrane is known as an immobilized liquid membrane, the primary advantage of which is unsurpassed permselectivity.[107-110] This system differs from solvent extraction in that the facilitated transport depends on the chemical reaction rate, diffusion rates in the solution and the permeability in the polymer. Some of the early efforts in this area employed simple metal salts of Cu^+ and Ag^+ to separate aliphatic and unsaturated hydrocarbons.[111-113] This was extended to ion exchange membranes containing Ag^+ which reacted reversibly with ethylene under 90% humidity.[114] Transition metal complexes with organic ligands, especially multidentate ligands, offer a wider variation of equalibrium and rate constants for selectively binding a permeate gas. More than twenty years ago, hemoglobin was observed to facilitate the transport of oxygen across wet filter paper.[115,116] However, it was not until very recently that this concept was applied to the separation of oxygen from air. Bend Research, Inc. has obtained patent coverage on a ligand membrane based oxygen enrichment process which involves a

metal chelate complex, solvent, axial base and membrane support.[117] The examples cited include; 1) Co(II) macrocyclic amine complexes in DMSO with 1-methylimidazole as the axial base and 2) Co(II) Schiff base complexes in DMSO and α-butyrolactone. The best results were obtained with N,N'-bis(salcylideneimino)di-n-propylamine cobalt(II) or CoSDPT in 1:1 DMSO and α-butyrolactone encapsulated in 130 μ thick microporous nylon 6,6 membrane. At 25 °C, an air mixture containing 88% oxygen was produced in a single pass through this membrane which corresponds to an O_2/N_2 selectivity of 30. This process is depicted below. Although the

High Pressure Side   CoSDPT   Low Pressure Side

160 mmHg   2 mmHg

O_2 O_2

N_2 CoSDPT-O_2

DMSO/α-butyrolactone
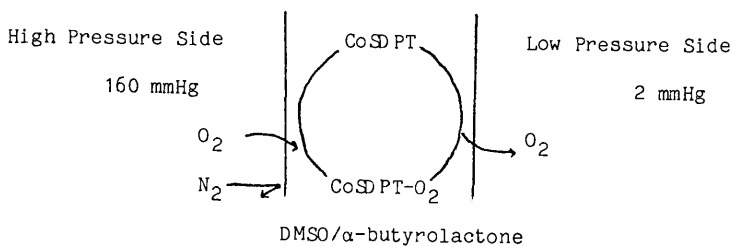
permselectivity of these membranes is quite remarkable there are several features which may hinder its commercial development, such as the need for a solvent and axial base. The mechanism of facilitated transport in the liquid membrane involves diffusion of the complexes, therefore, the solvent is a critical element to this system. One positive aspect of the Bend patent claim is that it was demonstrated that the incorporation of solutions containing oxygen carriers in a polymer membrane enhances the permeation of oxygen.

The results to be presented in this chapter represent a new approach to enhancing the permeation properties of polymer membranes and involves a novel method and mechanism of transport. The goal of this work was to incorporate supported metal complexes that reversibly bind dioxygen into solid nonporous polymer membranes in order to enhance the selective permeation of O_2 by a mechanism unlike that in isotropic polymers or liquid membranes. This could generally apply to any metal complex-polymer system in which the complex has an affinity for a particular gas for which there is a desired permselectivity. This was demonstrated by using a flat polystyrene film containing a dispersion of supported Co(II) Shiff base complex discribed in Chapter II.[118] These metal complex containing membranes show enhanced oxygen permeation relative to an appropriate blank. This membrane system differs from the liquid membrane in that the metal complexes are fixed and previously known to bind O_2 in the solid state. Only very recently has there been a few reports of facilitated transport with oxygen carriers in membranes. A cobalt porphyrin complex and 1-methylimidazole was dispersed in a poly(butylmethylacrylate) film and found to separate oxygen from nitrogen with a selectivity greater than ten.[119] Similarly, CoSALEN and pyridine have been incorporated in a polysulfone membrane to separate air.[120] In both these cases the metal complex is unsupported and can be viewed as being dissolved in the polymer. Also, CoSALEN was dissolved in a poly(octylmethylacrylate-Co-4-vinylpyridine) film and was observed to facilitate the transport of O_2.[121] All of these results, including the Bend patent, were reported subsequent to the start of

work reported here. Even though the various approaches taken to enhance membrane separations with oxygen carriers are not strictly analgous to the incorporation of the supported complexes described herein, they do represent examples of facilitated transport which serve to exemplify the importance of this work in the area of membrane separation.

The concept of supported metal complex facilitated transport of O_2 polymer membranes depends upon the developments in Chapters II and III. The ability of a supported metal complex to reversibly bind O_2 or CO in the solid state is an important consideration in preparing the membranes for these experiments. The supported CoSDPT complexes described in Chapter II were the complexes of choice for demonstrating this novel method of membrane based gas separation.

The results to be discussed include an evaluation of the permeation experimental procedure, polystyrene as a membrane material and metal complex containing membranes, including permeation as well as structural properties. Additionally, a transport mechanism will be discussed in light of these results.

<div align="center">Experimental</div>

Permeation Apparatus

The design and construction of the permeation cell was accomplished without knowledge of the prior art. During the course of this research the apparatus underwent a series of revisions which followed a progression of difficulties in the permeation experiments. The evolution of the currently employed permeation

cell is worth recounting even if just to relate the complexities involved in experiments of this type.

The function of the permeation cell was to support a membrane under closed volume permeation experimental conditions. In other words, the apparatus was designed so an initial vacuum could be applied to the lower interface of the membrane while a constant pressure was applied to the upper interface. Then as the penetrant gas permeated through the membrane into the envacuated chamber the pressure change could be monitored. The original prototype is shown in Figure 4-1 with exception that the first model had only one o-ring located in the lower chamber. It was soon realized that in order to achieve a proper seal, a slightly greased o-ring was needed on both the top and bottom of the membrane. Given the relatively large area of the film that is exposed to reduced pressure (3.14 cm^2), nearly all the films tried collapsed under a vacuum. Therefore, the chamber was filled with glass beads and a fine mesh screen was secured over the beads as pictured below. The
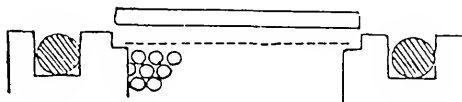
membrane rested on top of the brass ring and screen. However, the sharp edge of the brass ring would continuously cut the membrane, so it was beveled as pictured below. This alleviated some of the

Figure 4-1. This is a vertical crossectional view of the gas
separation apparatus. The two cylindrical elements
which enclose the two chambers are of brass
construction and separated by the metal complex
containing membrane and a set of o-rings. The two
chambers are sealed together over the o-rings and
membrane by six bolts equally spaced around the
periphery of the brass cylinder. Air or a gas mixture
is continuously supplied through the top chamber in
the direction indicated by the arrows. The lower
chamber is filled with glass beads to support the
membrane or alternatively a porous plate or disc of a
material unreactive towards O_2 may be interposed
between the two chambers for thin membranes which
require additional suppport. The lower chamber is
connected to a pump through a needle valve and may be
evacuated to form a vaccum therein. Gas permeating
through the membrane into the lower chamber may be
sampled through the ball valve.

3"

$\frac{1}{2}$"

Polymer
Membrane

Rubber O-rings

Ball
Valve

Needle Valve

2"

$\frac{1}{2}$"

$\frac{1}{4}$"

Glass
Beads

Sintered S.S. Plate
0·12 cm thick
5 micron pore size
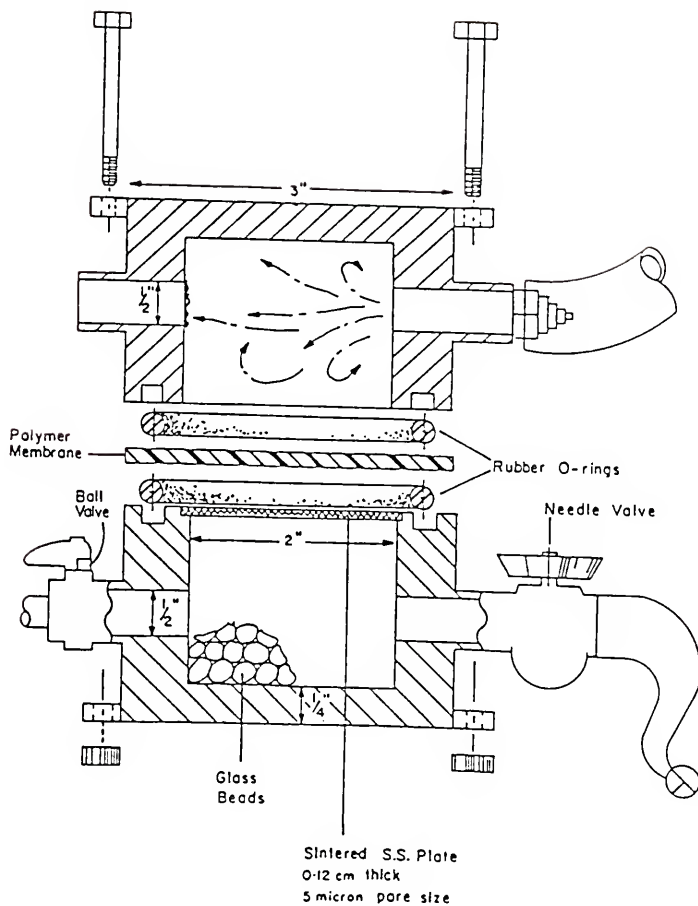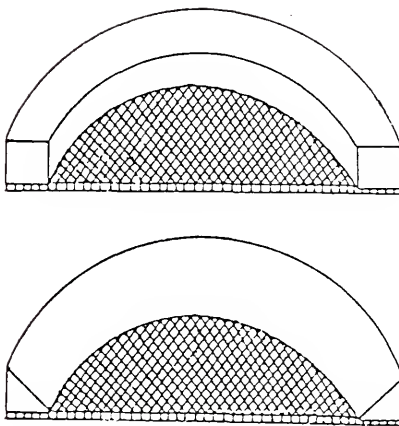
stress around the edges but the films were still sucked down a
millimeter or so toward the screen. Additionally, the screen
contorted to the shape of the top layer of the beads. Therefore,
the irregular surface of the screen provided additional areas of
stress to the membrane. All these problems were rectified with a
rigid support consisting of a porous (5 micron pore size) stainless
steel disc. The sintered metal plate was machined so that it would
rest on the same ledge as the screen but be thick enough to fit
flush with the surface of the chamber. At best the widest gap
between the metal disc and the edge of the chamber is less than
0.5 mm. Satisfactory permeation data were obtained with this
version of the apparatus. However, problems with membrane stress
cracking were still recurring. By virtue of the membrane material,
polystyrene, being a glassy polymer, brittleness was unavoidable
without employing a plasticizing agent. A logical approach to this
problem was to reduce the surface area of the membrane exposed to a

vacuum. This lead to a total redesign of the permeation cell. The apparatus in Figure 4-2 has a much smaller surface area that is exposed to reduced pressure. Although stress cracking was still prevalent using this set up, the permeation data were much more consistent.

A schematic representation of the entire permeation experimental set up is shown in Figure 4-3. The top chamber was connected to a plexiglass wind tunnel containing a squirrel cage fan. This provided a continuous stream of air blowing through the top chamber and over the surface of the membrane. The lower chamber was connected to a vacuum pump and a mercury manometer with rubber hoses. The lower chamber was exposed to a vacuum through a needle valve, then the applied vacuum was removed and the permeation of gases monitored manometrically. Samples were taken by opening the ball valve and inserting a syringe needle into the rubber septum capped exit port. By modern standards this apparatus may be considered crude but consistent results were obtained and the principle of facilitated transport of gases through polystyrene with supported metal complexes was demonstrated.

Permeation Procedure

The typical permeation experiment was conducted as follows. A polymer membrane was secured between the two chambers of the apparatus, as shown in Figure 4-2. This was done by centering the film between the lightly greased o-rings and then clamping the two halves together, being careful to keep the two chambers centered. Generally, the membrane was allowed to stand in this manner for a period of time before applying a vacuum. It was thought that since

Figure 4-2. This is a vertical, crossectional view of the revised
gas separation apparatus.

- 1.21 cm.
- 3.8 cm.
- 0.6 cm.
- 1.3 cm
- 1.1 cm.
- BRASS

Polymer Membrane →

SINTERED STAINLESS STEEL PLATE
0.12 cm. thick
5 micron pore size

- 1.28 cm.
- 3.18 cm.
- 1.1 cm
- 1.3 cm.
- VACUUM
- 7.63 cm.
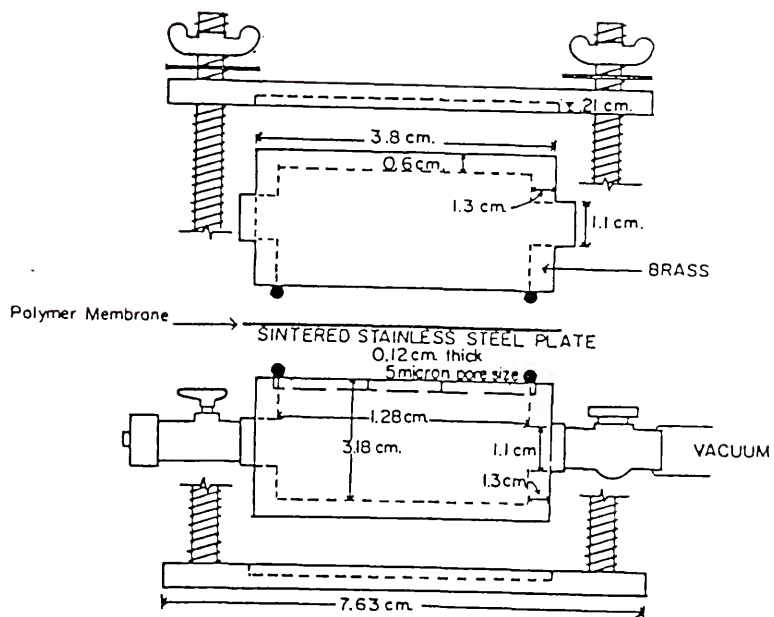
Figure 4-3. Schematic diagram of the gas permeation experimental set up.
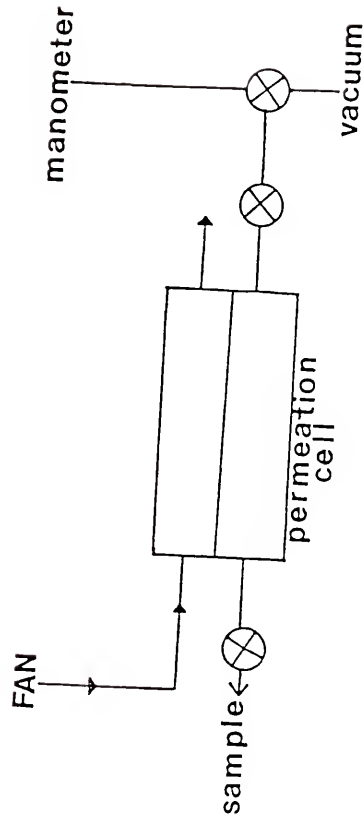
the polymer responds to the applied stress from the o-rings by molding itself around the rings then it may be beneficial to allow the polymer sufficient time to reorient itself before applying additional stress. Undoubtably some cracking occurs when the membrane is clamped in place but this effect may by minimized if the additional stress from a vacuum is not applied immediately. When the vacuum is applied, the lower chamber is typically pumped for a period of one half hour preceding the experiment. This is done in order to remove any excess solvent that may have been trapped in the film during its preparation. The membranes employed would not be described as pliable but rather as flexible only because of their thinness. Even though the films appear dry, some solvent is trapped as evidenced by a weight loss during the experiment and the desorbing solvent has been detected by the GC in a related study.[122] So after the lower chamber has been evacuated for a period of time, the vacuum is removed and an initial pressure reading is taken. The membranes studied were relatively thick, therefore, permeation was slow and readings were only taken every few hours. During pressure reading, gas samples were taken from the lower chamber with a 100 µL gas tight syringe. Using this sample size the residual gases in air, such as argon, neon and water, which can be separated from O_2 and N_2 on the GC were not detected. Even if these gases were present in integratable amounts, they would not have effected the ratio of O_2 to N_2. These samples were then analyzed by a Varian 3700 gas chromatograph equipped with a thermal conductivity detector. The column employed was an 8 foot, 1/8 inch O.D., stainless steel column containing 5A

molecular sieves. The gas samples were analized with the oven at
30 °C and 75 °C. The injector and detecter were at 200 °C. Helium
was the carrier gas with a flow rate of 30 mL/min. Since the
sample is at a reduced pressure it is diluted with air as it is
withdrawn from the sampling port. The standard deviation between
samples was typically on the order of 0.1 %. From the percent
oxygen in the injected sample determined by the GC, the actual
percent oxygen in the lower chamber can be determined as the
following example illustrates.

$$40x + (720)(21.00 \pm .02) = (760)(21.5 \pm 0.2)$$

That is (total pressure in lower chamber, in mmHg)x + (pressure of
air which dilutes the sample)(percent oxygen in air) = (atmospheric
pressure, assumed to be 760 mmHg)(percent oxygen in sample as
determined by GC). From this equation the solution x = 30.5%,
representing the percent oxygen in the lower chamber, is
obtained. This represents a 9.5% oxygen enrichment of air.

Membrane Preparation

The permeation properties of a membrane depend not only on the
choice of the polymer but also on the physical structure. The
structure in turn is directly related to the preparatory procedure,
especially the thermal history of the membrane. The membranes
employed in this study were prepared using a solution casting
technique. Polystyrene was dissolved in an appropriate nonpolar
solvent, most often toluene or methylene chloride. The polymer
solution was stired until viscous then poured onto a leveled glass

plate or dish as shown in Figure 4-4. Great care must be taken to avoid the entrapment of air bubbles in the film. It seems the more viscous the casting solution the more likely air pockets will form in the membrane. Critical to obtaining meaningful permeation data for a membrane is the need to have a fairly uniform thickness. Metal plates were prepared that were notched for a particular thickness. These could be dragged across the glass plate containing the casting solution in an effort to control the thickness of the membrane. However, after evaporation, there were variances in the thickness even if the plates were used. So for the most part, the polymer solutions were allowed to dry as they were cast. The evaporation of solvent was done at room temperature, so it might take several days before the film could be dry enough to handle. The slow evaporation was preferable to heating or reducing pressure which seemed to promote the formation of pores and bubbles. The films were removed from the glass plates by simply peeling them off or in some cases submersing the plates in water. Care must be taken not to crease the membrane when peeling it off the glass.

The membranes containing the supported metal complexes were prepared in much the same way. The solid supported complexes were ground to a fine powder then sprinkled into the polymer solution. It is important that the polymer solution is not too viscous otherwise the supported complexes will not be wetted by the polymer. This should result in clumping of the additive and an uneven distribution throughout the film. The amount of supported complex incorporated into the membrane is determined after the

Figure 4-4. Glass plate for membrane preparation.

SIDE VIEW

5"

~2"

~1"

Plate Glass

3/8" Threaded Rod

1/2" O.D. Threaded Sleeve so the plate can be leveled.

TOP VIEW

5"

5"
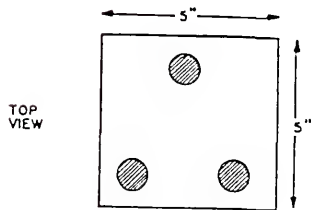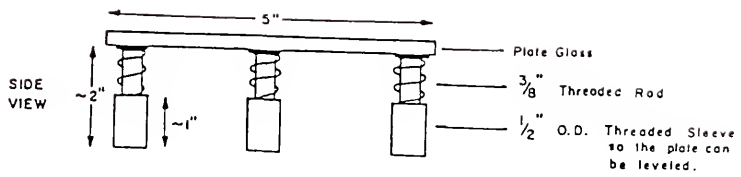
membrane has been evaluated and then by dissolving the film and
filtering off the solid.

Membrane Characterization

The membrane thickness was determined with a caliper to the
nearest hundreth of a millimeter. Scanning electron microscopy
(SEM) was performed on a number of membranes with a University of
Florida materials science departmental instrument.

Membrane Evaluation

The evaluation of the complex containing membranes was based
on a comparison of experimental permeation data with that
calculated for an appropriate blank. The permeation data for two
typical PS/[SG] blank membranes are shown in Table 4-1. The
percent oxygen was calculated as previously described and the
percent enrichment is the difference between the percent oxygen in
the lower chamber and air, as determined by GC. Then the partial
pressure and natural log of the partial pressure difference between
the high and low pressure sides at time, t for O_2 and N_2 were
calculated and tabulated as shown in Table 4-2. With this data at
hand a first order kinetic treatment was applied in order to
determine the permeability coefficients for O_2 and N_2.

$$\frac{dP}{dt} = \frac{RTA}{22414V_{cell}} \frac{\overline{P}(P_H - P_L)}{1}$$

$$\int \frac{dP}{P_H - P_L} = \frac{RTA}{22414V_{cell}} \int \frac{\overline{P}}{1} \, dt$$

Table 4-1

Permeation Data for Two PS/[SG] Films

time (hours)	total pressure (mmHg)	flux (mmHg/hr)	%oxygen	%enrichment
		A		
0	<1	----	----	----
2	11	5.50	27.204	6.425
4	23	5.75	30.573	9.847
6	31	5.17	30.405	9.586
10	43	4.30	31.619	10.728
13	51	3.92	33.075	12.205
24	76	3.17	34.147	13.300
30	101	3.37	33.524	12.657
		B		
0	<1	----	----	----
2	19	9.15	23.032	2.240
6	35	5.83	24.854	4.039
9.5	48	5.05	27.219	6.951
12.5	56	4.48	28.206	7.451
24	115	4.79	25.568	4.818

Table 4-2

Partial Pressures of O_2 and N_2 for Two PS/[SG] Films

time	P_{O_2}	P_{N_2}	$\ln \Delta P_{O_2}$	$\ln \Delta P_{N_2}$
		A		
0	<.21	<.79	5.071	6.396
2	3.02	7.98	5.053	6.384
4	7.10	15.90	5.027	6.371
6	9.48	21.52	5.011	6.361
10	13.64	29.36	4.983	6.347
13	16.93	34.07	4.960	6.339
24	26.07	49.93	4.894	6.311
30	33.99	67.01	4.833	6.279
		B		
0	<.21	<.79	5.027	6.396
2	4.42	14.58	5.044	6.373
6	8.76	26.24	5.016	6.353
9.5	13.42	34.58	4.985	6.338
12.5	15.93	46.07	4.967	6.328
24	29.69	85.31	4.867	6.244

with P_H constant

$$d(P_H - P_L) = -dP$$

$$\ln(P_H - P_L) = \frac{-RTA}{22414 V_{cell}} \frac{\overline{P}}{l} t + const$$

Where $\overline{P}$ = permeability coefficient (cm^3(STP)cm/cm^2sec mmHg),
l = film thickness (cm), A = film area (cm^3), $(P_H - P_L)$ = partial
pressure differential across the membrane (mmHg), R = gas constant
(6.24×10^4 cm^3mmHg/molK), and T = temperature (K). The const. or
intercept represents the $\ln(P_H - P_L)$ at t = 0. For a perfect
vacuum the intercept would be 5.0726 but for calculating a
theoretical P_{O_2} versus time curve a value of 5.071 was employed
(vide infra). Determining the permeability of a polymer involves
measuring the rate of transmission for particular permeant.
Therefore, the permeability coefficient is a rate constant which
has been expressed with several different units throughout the
literature. One of the more popular units for the permeability
coefficient is cm^3(STP)cm/cm^2sec mmHg which was used in this
study. However, it should be pointed out that the units chosen in
this study are of little consequence in the final evaluation of the
metal complex containing membranes since the metal promoted O_2
enrichment are only relative to the blanks. For example, any area,
temperature, and cell volume could have been used in the
calculations as long as they were the same for the blanks and
complex containing films. The goal of the study in this chapter
was to demonstrate oxygen enrichment by metal complex containing
membranes relative to blank membranes. Therefore, it was only

important to obtain consistant values for the O_2 permeability of
the blank membranes rather than the absolute numbers.

Plots of ln $(P_H - P_L)$ for O_2 vs. time for two PS/[SG] are
shown in Figure 4-5. Generaly such plots yield a straight lines,
indicating first order processes. The slope of these lines are
equal to $(-RTA/22414V_{cell}$ l) $\overline{P}$. Multiplying the slope by a
constant $(-22414V_{cell}$ l/RTA) produces the permeability
coefficient $\overline{P}$. For oxygen in example A above, the
slope = -7.517×10^{-3} and the constant is given as

$$- \frac{(22414)(4.09)(0.0518)}{(6.24 \times 10^{4})(298)(1.287)} \quad \times \quad \frac{1 \text{ hour}}{3600 \text{ sec}} \quad = \quad - 5.51 \times 10^{-8}$$

and the $\overline{P}_{O_2}$ = (slope)(const) = 4.14×10^{-10} and the calculated
$\overline{P}_{N_2}$ = 1.96×10^{-10}. The slope was calculated using a linear
regression analysis. For blank membrane B the $\overline{P}_{O_2}$ = 4.52×10^{-10}
and the $\overline{P}_{N_2}$ = 3.27×10^{-10}. The correlation values for plots A and
B in Figure 4-5 are -0.996 and -0.998 respectively. Not all blank
films exhibited linearity. This in part is due to changes in the
morphology of the membranes. Both loss of solvent and cracking
would change the permeability of a membrane. Many glassy polymers
exhibit this anomolous behavior and models have been developed to
describe the permeability which employ ϕ, a steady-state permeation
rate in the calculation.[123] Often the mass of penetrant is plotted
against time and ϕ is the slope of the of the resulting asymptotic
line. This produces what is known as a time lag. For our system,
treating the data in this manner would neglect a time period when
metal-dioxygen binding is most facile. In our case, using a first

Figure 4-5. A plot of $\ln(P_H - P_L)$ vs. time for two polystyrene
membranes containing [SG]
A) 1 = 0.518 ± .040 mm, 26.2 % by wt.
B) 1 = 0.514 ± .036 mm, 44.7 % by wt.
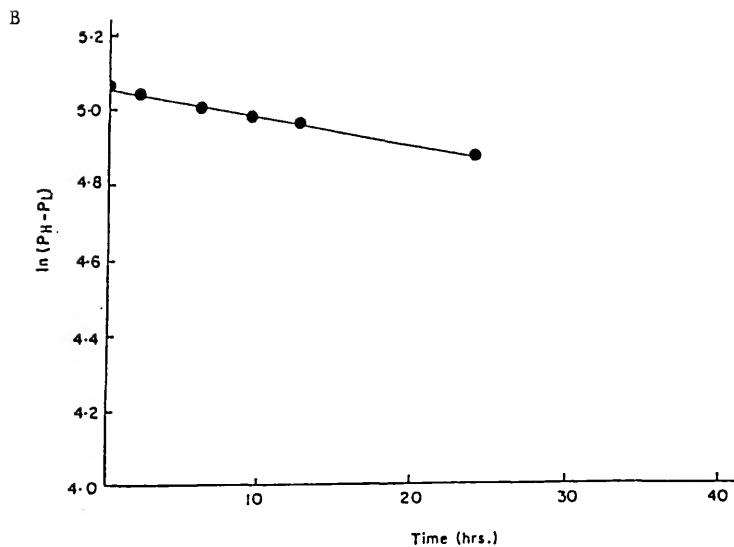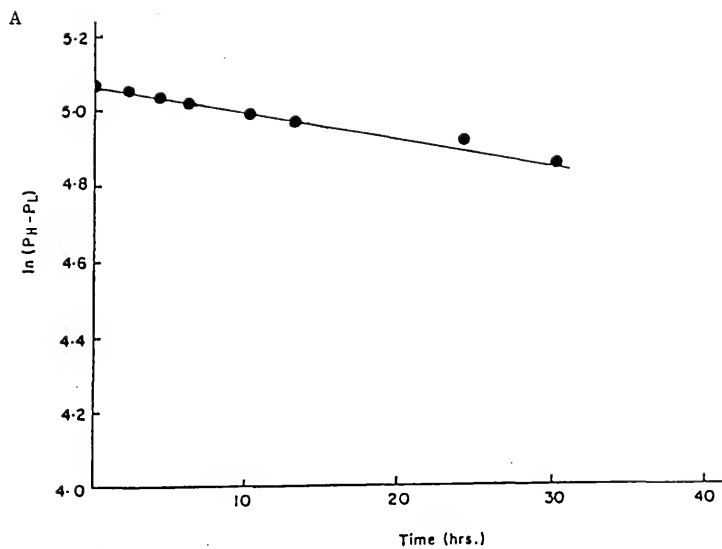
order approximation allows us to analyze data from time = 0. This approach does not model the mechanism of transport but rather it provides the simple means for comparing the complex containing membranes with the blanks.

The average permeability coefficient was determined for a series of blank films containing a support, for the examples above, this was silica and the $\overline{P}_{blank}$ was found to be 4.2×10^{-10} (vide infra). Using this $\overline{P}$, the partial pressure of oxygen at a given time can be back calculated for a blank film of thickness l. Now consider a membrane containing [SG]-CoSDPT with l = 0.533 ± .097 mm, the following partial pressures for oxygen were recorded and the P_{O_2}'s for a blank calculated. This is shown in Table 4-3. The

Table 4-3

O_2 Enrichment Results for a PS/[SG]-CoSDPT Film

time (hrs)	total P_{O_2} (mmHg)	calc. or blank P_{O_2} (mmHg)	P_{O_2} from metal promoted enrichment (mmHg)
2	6.19	2.61	3.58
4	10.15	4.92	5.23
6	13.88	7.19	6.69
8	16.63	9.43	7.20
11	19.83	12.73	7.10
24	31.37	26.21	5.16
30	37.35	32.01	5.34

difference between the observed partial pressure and that calculated for a blank is attributed to metal promoted enrichment. This is shown graphically in Figure 4-6 where the experimental partial pressure of oxygen versus time curve was compared with the calculated curve. This plot shows the metal promoted enhanced permeation of oxygen under approximately 16 mmHg of O_2. As the pressure of O_2 is increased, we approach the $P_{\frac{1}{2}}$ for the complex and the cobalt is no longer effective for facilitating the transport of oxygen. Above this pressure, the experimental curve parallels and then begins to approach the calculated curve because of the loss in free volume associated with the completely oxygenated complexes. Appendix I contains the permeation data for the metal complex containing membranes and the blanks.

Results and Discussion

Blank Polymer Membranes

In order to test the permeation apparatus, a series of eleven polystyrene membranes was tested and a mean permeability coefficient of 2.6 x 10^{-10} cm^3(STP)cm/(cm^2 s mmHg) with a standard deviation of ± 0.9 x 10^{-10} was determined. This value is approximately one order of magnitude greater than most of the reported literature values (1.2 - 2.6 x 10^{-11}).[124-128] This disparity can be rationalized in a number of ways. There are many inherent disadvantages associated with polystyrene as a membrane material by virtue of it being a glassy polymer. The glass transition temperature, T_g, signals a rather ill defined change in the space between molecules or free volume. Below this temperature

Figure 4-6. A plot of P_{O_2} vs. time for a polystyrene
membrane containing [SG]-CoSMDPT. ▲ calculated for
a film without cobalt, ● experimental.
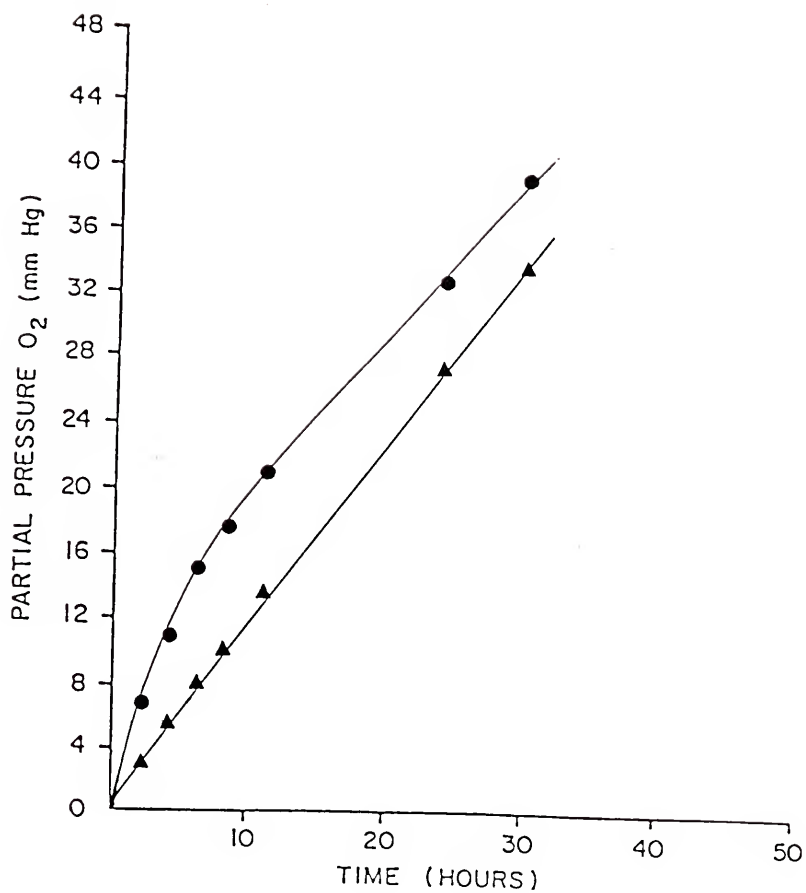
segmental motion of the polymer chains is very slow or nonexistent and motion of the side groups become limited. The atactic polystyrene employed in this study has a T_g = 100 °C. Most of the discrepancy in permeation data found in the literature pertain to glassy polymers. Most often the disagreement in experimental results can be traced back to the manner in which the membrane was fabricated. The morphology of a glassy polymer membrane depends a great deal on the way it was prepared, making some results difficult to reproduce.[129] For example, films cast directly from latex dispersions have higher permeabilities than those cast from polymer solutions.[130] Those films cast from solutions tend to have voids that will affect the permeation results. Additionally, these voids can result in pores and thin spots. The pores would then allow free flow of gases across the membrane, resulting in poor selectivity. The thin spots would result in an inflated permeability because the calculated permeability coefficient is based on the overall thickness of the membrane which excludes any spaces inside the membrane. In general, glassy polymers can be very brittle and crack under pressure. It has been shown that the shear strength of thin polystyrene films depend a great deal upon the method of preparation.[131] Usually under an applied stress, glassy polymers fracture cleanly and suddenly. However, for any stress below the failure stress, elastic behavior is observed, i.e. deformations formed in the polymer matrix are reversible. This is generally true for short periods of time because this stress involves the movement of nonbonded atoms or separatation of entangled polymer chains. Over a long enough time period the

polymer chains will untangle themselves irreversibly. For example, over a 24 hour period, a polystyrene membrane that was clamped into the permeation cell, irreversibly molded itself to the set of o-rings which held it in place. Therefore, when a vacuum is applied to one side of a polystyrene membrane, stress cracking occurs and as pressure increases the polymer does not relax back to its original state. This results in formation of pores and thin spots leading to poor separation. This inelastic response to the strain imposed by a vacuum is further complicated by the presence of additives such as the supported metal complexes. As the polymer chains untangle themselves, the fillers can occupy this space as shown below. Such problems are what led to the development of thin

UNSTRAINED   STRAINED   W/ FILLERS
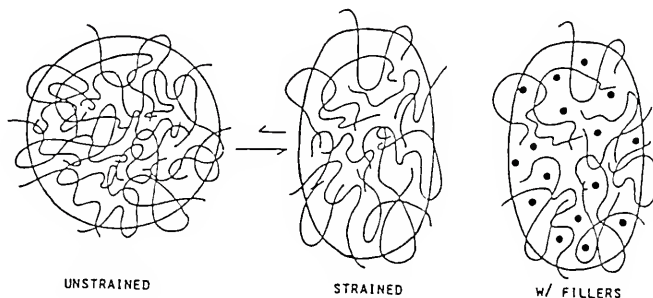
composite membranes previously described. At the onset of this project, the choice of polystyrene as the membrane material was rather arbitrary. The fact that polystyrene readily dissolves and can be easily cast into flat films coupled with an abundant supply of Styrofoam coffee cups first led to its use in this work. Even

though, stress cracking is a problem, consistent $\bar{P}$ values were obtained for polystyrene membranes. This allowed the metal complex containing membranes to be compared with appropriate blanks and the difference in O_2 enrichment could then be attributed to metal facilitated transport. Polystyrene itself is not an appropriate blank since it has been shown that the incorporation of additives or fillers effect the permeation properties of a membrane.[132-135] Generally, polymer membranes containing fillers exhibit lower permeabilites. Filler particles affect the packing of the polymer chains and they can form aggregates that contain spaces or free volume that are inaccessable to the polymer segments. Additionally, impermeable additives lower the flux because the diffusion path will not always be normal to the membrane surface. Very few additives could be described as totally inert. Fillers which can immobilize a penetrant by adsorption have a small effect on the steady state permeation rate but show a large increase in the so called time lag (vide supra). Fillers are often added as powders to increase the hardness of rubbery polymers but with glassy polymers the films become brittle. This could result in stress cracking during the permeation experiment.

Polystyrene membranes containing a dispersion of [P]-DPT were prepared as blanks for the polymer supported metal complex containing membranes. Polymer bound DPT was used in place of the supported Shiff base ligand so that if the salicylidene portion of the ligand was substituted then a new series of blanks would not have to be determined. The mean permeability coefficient for oxygen was also determined for polystyrene membranes containing

silica gel and NaY zeolites. These results are shown in
Table 4-4. Within experimental error the blank PS films containing

Table 4-4

Blank Films

Membrane	$\overline{P}_{O_2}$ x 10^{10} ($\dfrac{cm^3 \text{ (STP) cm}}{cm \text{ sec mmHg}}$)
PS/[P]—D PT	5.0 ± 0.2
PS/[SG]	4.2 ± 1.4
PS/Na-Y	5.9 ± 0.9

the solid supports exhibit nearly the same permeability.
Intuitively one might expect the membranes containing the
impermeable solids, silica and Na-Y zeolits, to have the lowest
permeability. However, these blanks are also the least
reproducible suggesting a higher degree of cracking. All of these
additives produce membranes with permeabilities greater than
polystyrene itself. This may be the result of stress cracking and
creep that would be expected for a filled glassy polymer under
stress (vacuum). Another factor which influences the permeation
properties is the presence of solvent. The solvent in most cases
was toluene which swells polystyrene. To this end, toluene may
serve as a plasticizing agent and depress the glass transition
temperature.[136] This would increase the permeabilities of O_2 and
N_2. Most of the membranes in this study exhibited a weight loss
after the permeation experiment, typically from 1-2% by weight.

This may be attributed to a solvent that the membranes containing additives were more effective for retaining. The DVB crosslinked polystyrene beads are expected to have a T_g only slightly higher than PS itself.[137] Therefore, the PS and PS/[P]-DPT membranes would be expected to have similar permeabilities. However, the macroreticular resin, [P]-DPT would swell more than the linear polystyrene retaining more solvent in the membrane and rendering it more permeable. One would expect silica gel and zeolites to be very weakly attracted to a nonpolar solvent. So solvent may only be trapped in the interstices of silica or zeolite aggregates and not strongly absorbed.

Regardless of what exactly caused the higher permeabilities of the additive containing membranes compared with PS itself, consistent $\overline{P}_{O_2}$ values were obtained. These membranes were subsequently used as blanks for the cobalt containing membranes. It should also be pointed out that since absolute permeabilities were not obtained, the separation factors are not relevant. The measured $\overline{P}_{O_2}$ for the blanks was the only source of comparison for the metal complex containing membranes.

PS/[P]-CoSDPT Membranes

Covalently bound CoSDPT to DVB crosslinked polystyrene beads (Figure 4-7) was previously described in Chapter II as an effective oxygen carrier in the solid state and therefore, was chosen as a model compound to demonstrate our concept of facilitated transport in solid polymer membranes. A typical polystyrene membrane containing 16.7% by weight of the polymer beads functionalized with CoSDPT is shown in Figure 4-8 and shows metal complex promoted

Figure 4-7. Polystyrene supported CoSDPT.
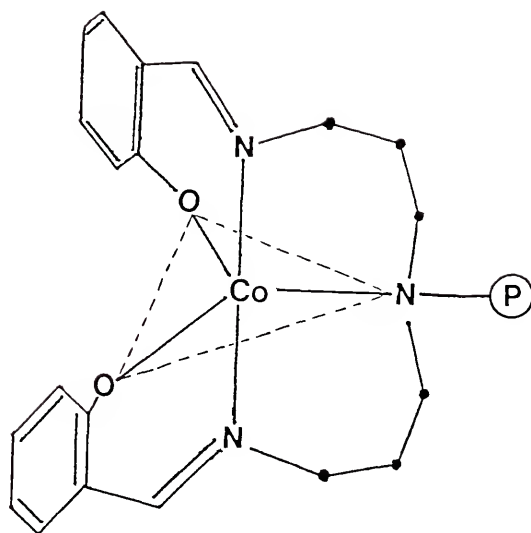
Figure 4-8.   Plot of partial pressure O_2 vs. time for a
              polystyrene/ [P] - CoSMDPT film (16.4% by wt of
              functionalized beads); ● experimental; ▲ calculated
              for film without cobalt.
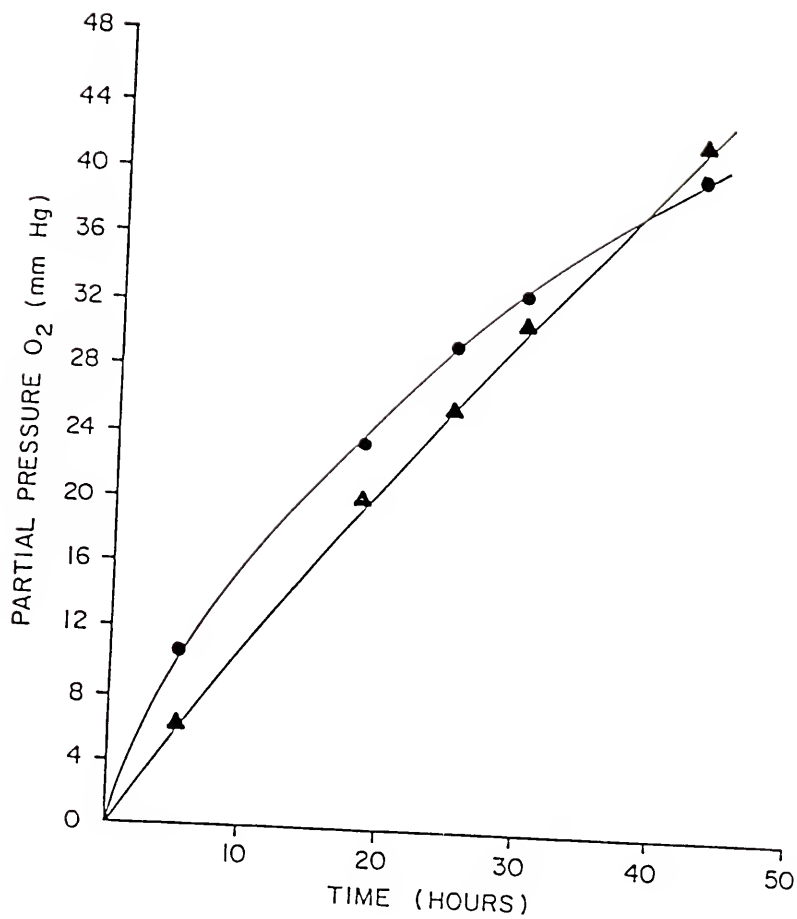
oxygen enrichment below approximately 16 mmHg O_2. Above this
pressure, the cobalt complexes are almost completely oxygenated and
begin to inhibit permeation by blocking diffusion pathways. This
is better illustrated in Figure 4-9 which shows a plot of the
difference between the experimental partial pressure of O_2 versus
time curve and the calculated curve. As the [P]-CoSDPT facilitates
the transport of O_2, the difference between the curves increases.
As the increasing O_2 partial pressure approaches the $P_{1/2}$ for the
complex, the stable $Co-O_2$ adducts begin to remove free volume
resulting in a decrease in permeability. Generally, free volume
theory is used to describe molecular diffusion in
polymers.[138,139] In simple terms, the theory states that within a
polymer membrane there is a volume occupied by the polymer
molecules and there is a volume associated with the space
surrounding these molecules. This space or free volume is
continuously redistributed by movements of the polymer chains. For
molecular diffusion to occur, free volume must appear adjacent to
the gas molecule and then by motions of the polymer chains the
penetrant is displaced from one hole to the next. The concept of
free volume in glassy polymers is complicated by the fact that many
of the holes become immobilized[140] and are a variety of sizes.[141]
This makes the free volume difficult to measure and even more
difficult to reproduce between samples. The presence of fillers
can have an obstructive effect on the transport of gases as well as
the immobilization of polymer chains.[142] The completely oxygenated
cobalt complex occupies a volume in the PS membrane which is
greater than that for the [P]-DPT used in the blank film as shown
below. Therefore, if [P]-CoSDPT-O_2 is viewed as an obstructive

Figure 4-9.   Plot of the difference in partial pressure of O_2 between the calculated curve and experimental curve in figure 4-7 vs. time.
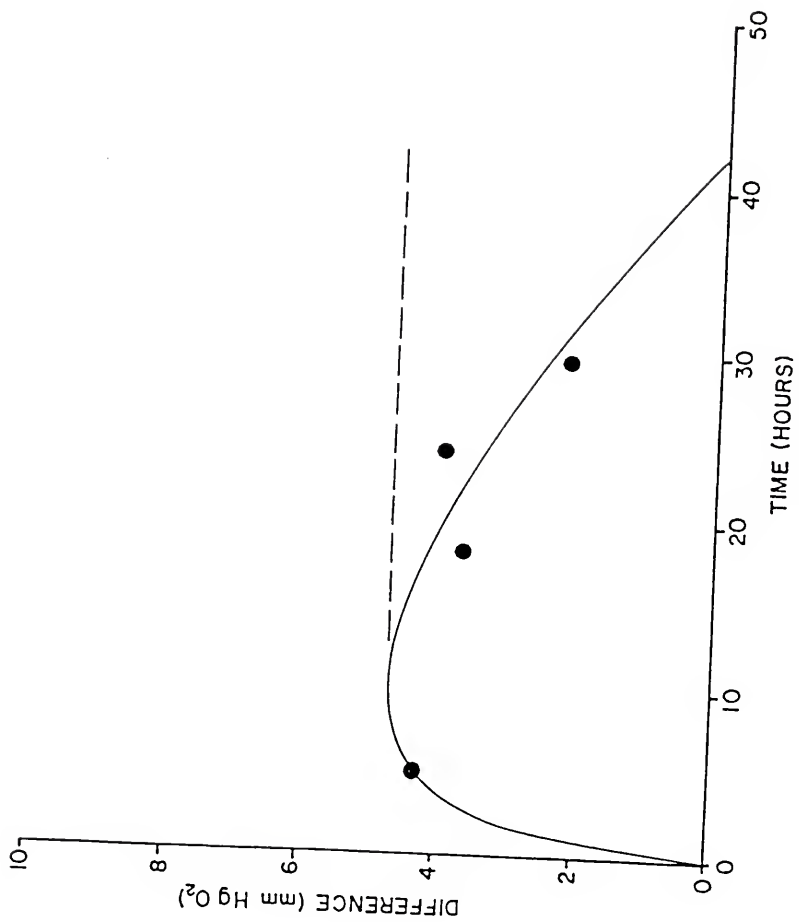
filler, then a membrane containing [P]-CoSDPT-O_2 would be expected to have a lower permeability than a membrane containing [P]-DPT. This further implies that a membrane containing [P]-NiSDPT should also have a lower permeability than for a [P]-DPT containing film and that if the PS/[P]-CoSDPT permeation data were calculated against a PS/[P]-NiSDPT blank then even higher Co(II) facilitated oxygen enrichments would be observed.

PS/[P]-CoBr$_2$SDPT, -3FSDPT Membranes

Both [P]-CoBr$_2$SDPT and [P]-Co3FSDPT were perpared, as described in Chapter II, in order to incorporate into the polystyrene membranes an oxygen carrier with a higher $P_{1/2}$ than [P]-CoSDPT. This would allow the supported metal complex facilitated transport of O_2 to occur up to a higher partial pressure of O_2. The results for a PS membrane containing 18% by weight [P]-CoBr$_2$SDPT are shown in Figure 4-10. The cobalt complex promoted oxygen enrichment is observed below approximately 24 mmHg of O_2. This is higher than what was observed for the PS/[P]-CoSDPT membrane in Figure 4-8. The greater oxygen enrichment is further illustrated by the difference curve in Figure 4-11 which can also be compared with Figure 4-9. As the partial pressure of O_2 increases, the difference curve should level off then begin to decrease. The curve in Figure 4-11 reaches a maximum then begins to fall off but the data point at 48 hours indicates the permeation

Figure 4-10. Plot of partial pressure O_2 vs. time for a polystyrene/ [P]-CoBr$_2$SDPT film (18.4% by wt of functionalized beads); ● experimental; ▲ calculated for film without cobalt.
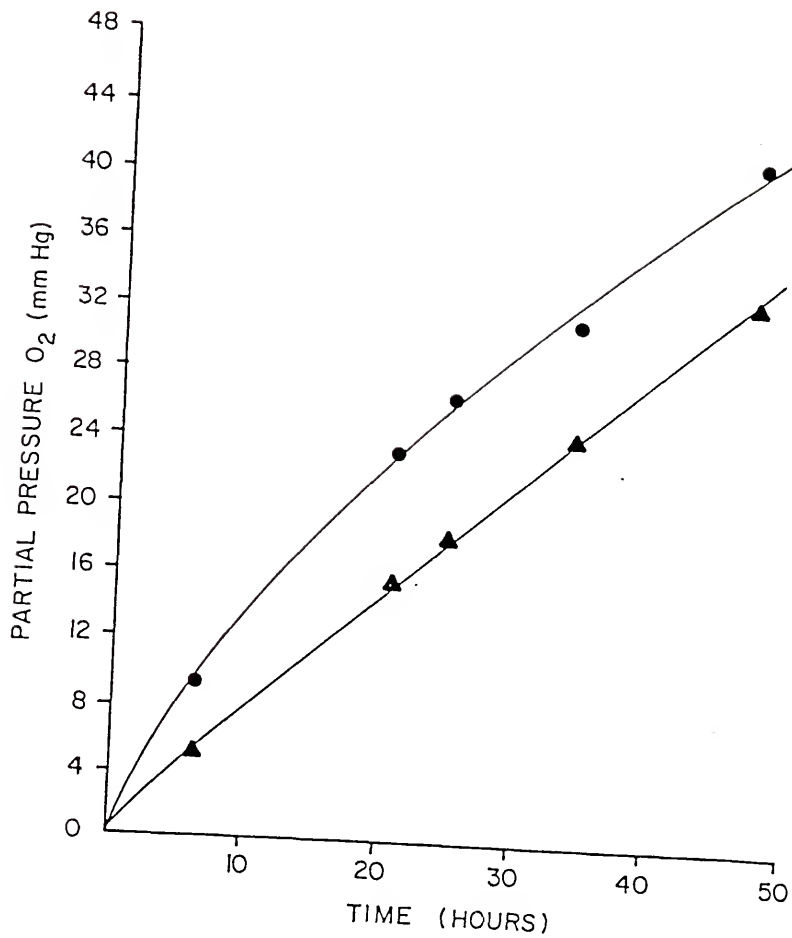
Figure 4-11.   Plot of the difference in partial pressure of O_2 between the calculated curve and experimental curve in figure 4-10 vs. time.
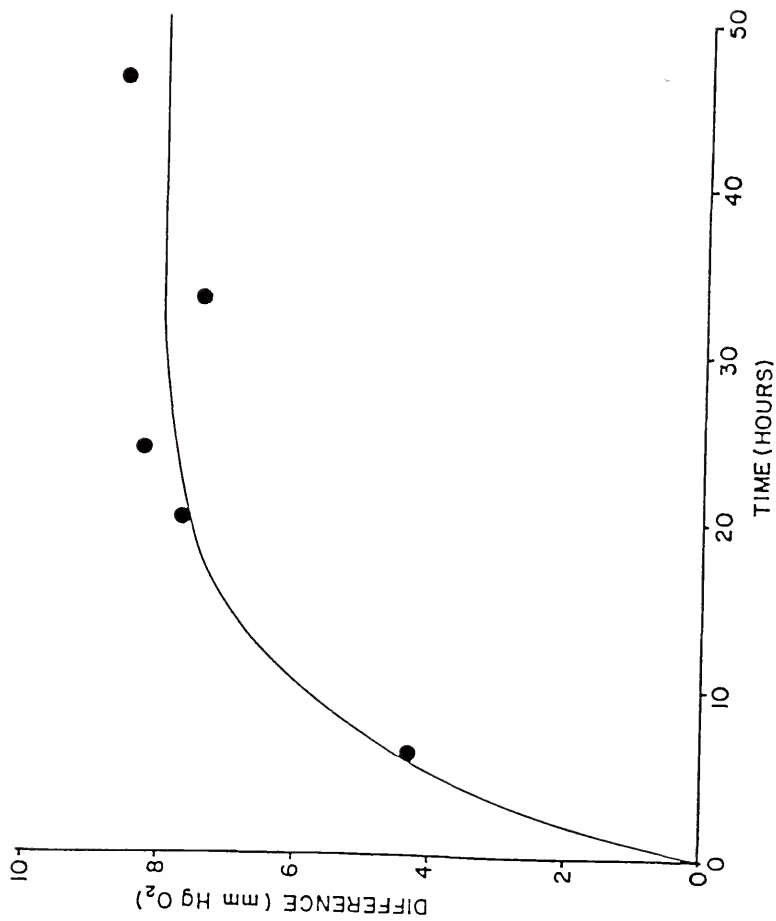
of O_2 has increased slightly. Within the time frame for this experiment, a substantial amount of stress cracking probably has occured by the 48 hour mark which would result in an increase in the permeation of O_2. Therefore, those data points obtained in the later stages of the experiment are less reliable than the initial data but were included unless they were grossly inconsistent.

The maximum partial pressure of O_2 from metal promoted enrichment observed for a series of representative polystyrene membranes containing [P]-CoSDPT, [P]-CoBr$_2$SDPT and [P]-Co3FSDPT is summarized in Table 4-5. As expected, the films containing polymer [P]-CoBr$_2$SDPT showed higher enrichments than for [P]-CoSDPT. The 3-flouro derivative produced lower enrichments relative to the blanks because they were thin and produced lower fluxes which means the films were structurely more sound.

Cycling Experiments

If the supported cobalt complexes are stable with respect to oxidation and form reversible O_2 adducts, then one might expect a polystyrene/[P]-CoSDPT film could be cycled without a loss in the observed metal promoted oxygen enrichment. However, this is not the case as shown in Figure 4-12. After 48 hours, the film in Figure 4-12 was evacuated a second time and then the permeation of O_2 and N_2 was remeasured. As Figure 4-12 shows, there is a marked decrease in the O_2 permeation attributed to the supported cobalt complexes. This decrease in O_2 enrichment can be rationalized in a number of ways. A major problem in reproducing permeation results in polystyrene membranes involves stress cracking. The glass PS membranes lose their structural integrity with time as internal

Table 4-5

O_2 Enrichment for Various Co(II) Containing Films

Membrane	Additive % by weight	Time (hrs)	Partial pressure(mmHg) O_2 from metal promoted enrichment
PS/[P]-CoSDPT	12.5	11.0	5.23
PS/[P]-CoSDPT	13.8	23.5	12.95
PS/[P]-CoSDPT	17.2	10.0	8.48
PS/[P]-CoSDPT[a]	16.4	24.0	5.40
PS/[P]-CoBr$_2$SDPT	6.8	24.0	6.58
PS/[P]-CoBr$_2$SDPT	14.5	24.0	11.09
PS/[P]-CoBr$_2$SDPT	18.0	24.0	11.57
PS/[P]-CoBr$_2$SDPT	21.7	24.0	10.91
PS/[P]-Co3FSDPT	6.3	6.0	5.23
PS/[P]-Co3FSDPT	6.8	6.0	6.67
PS/[P]-Co3FSDPT	14.7	6.0	6.04
PS/[P]-Co3FSDPT	16.5	4.0	3.87

a. data obtained with large volume apparatus in
    Figure 4.1

Figure 4-12. Plot of partial pressure O_2 vs. time for a
PS/[P]-CoSDPT film (17.2% by wt of functionalized
beads); ● experimental - 1st run; ○ experimental -
2nd run; ▲ calculated for a film without cobalt.
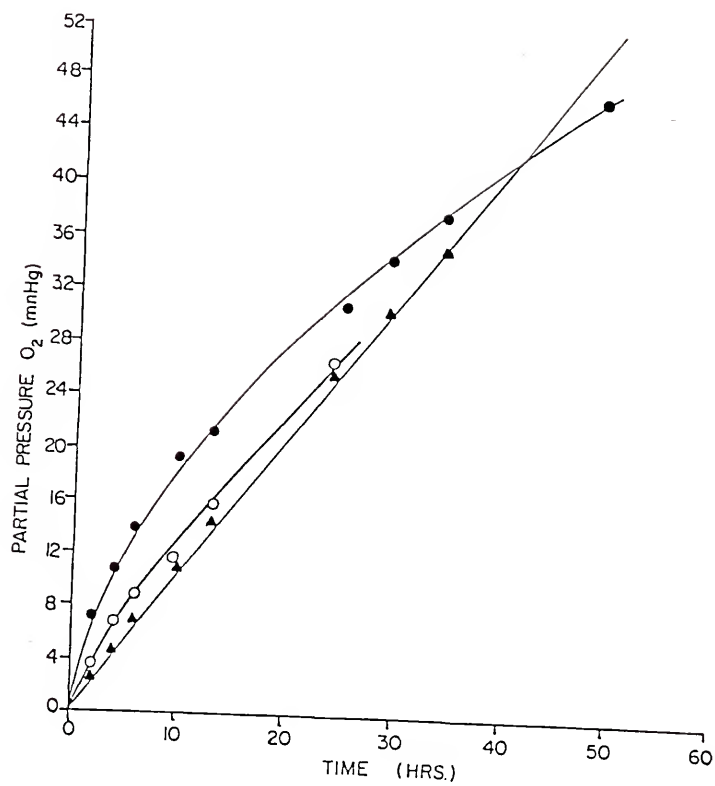
fractures occur. This results in pathways for air to flow through and is reflected in a loss of permselectivity for the membrane. An additional factor contributing to the loss of enrichment stems from the solvent content of the film. As mentioned previously, the solvent serves to plasticize the polymer thereby increasing its permeability. As solvent is withdrawn, the permeability should decrease. This implies that the blanks used to calculate the P_{O_2} vs. time curve for the second cycle are inappropriate because they were for only a single cycle. A loss in O_2 enrichment for a second cycle was observed for all the films tested. However, the PS membranes cycled a second time are structurally different than the original films, therefore, the permeation properties would be expected to change.

An additional contribution to the loss in O_2 enrichment is from irreversible oxidation of the cobalt complexes. This was evidenced by a loss in the Co-O_2 ESR signal. The ESR spectra for the supported cobalt dioxygen complex in a polystyrene matrix were generally broad and weak. In most cases, cobalt hyperfine was not resolved and there was often evidence for additional paramagnetic species. A typical ESR spectrum for PS/[P]-CoBr$_2$SDPT is shown in Figure 4-13. There appear to be two signals in this spectrum, the source of which is unknown. Similarly, the ESR for a PS/[SG]-CoSDPT film is shown in Figure 4-14. In this case, the CoO$_2$ signal is stronger but the existence of other species is still evident. It has been shown that the incorporation of a metal complex into a polymer matrix can drasically reduce the $P_{1/2}$ for O_2 complexation.[143] Therefore, it is possible that small impurities

Figure 4-13. X-band ESR of PS/[P]-CoBr$_2$SDPT at 82 °K.

300 G
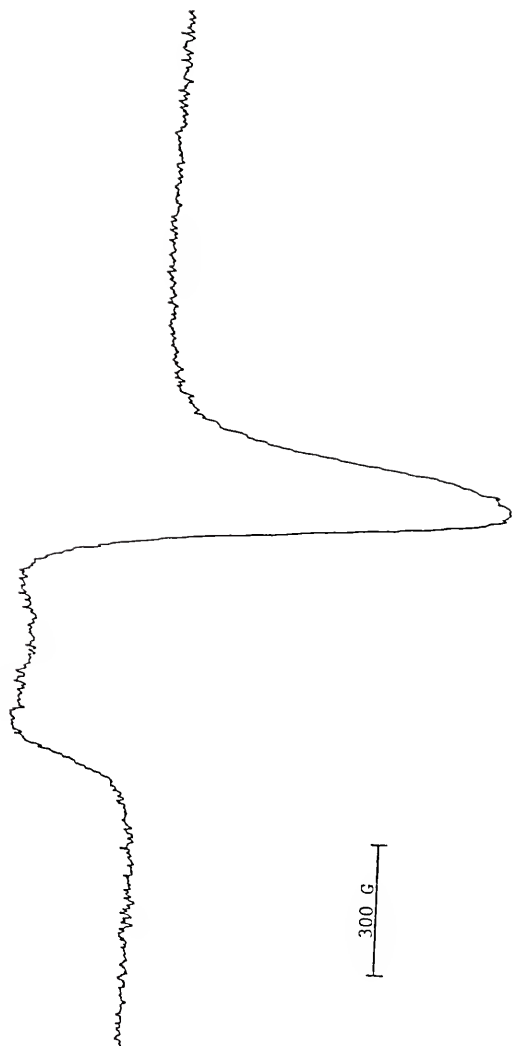
Figure 4-14. X-band ESR of PS/[SG]-CoSDPT (0.5 mmole/gram SG) at 88 °K.

200 G
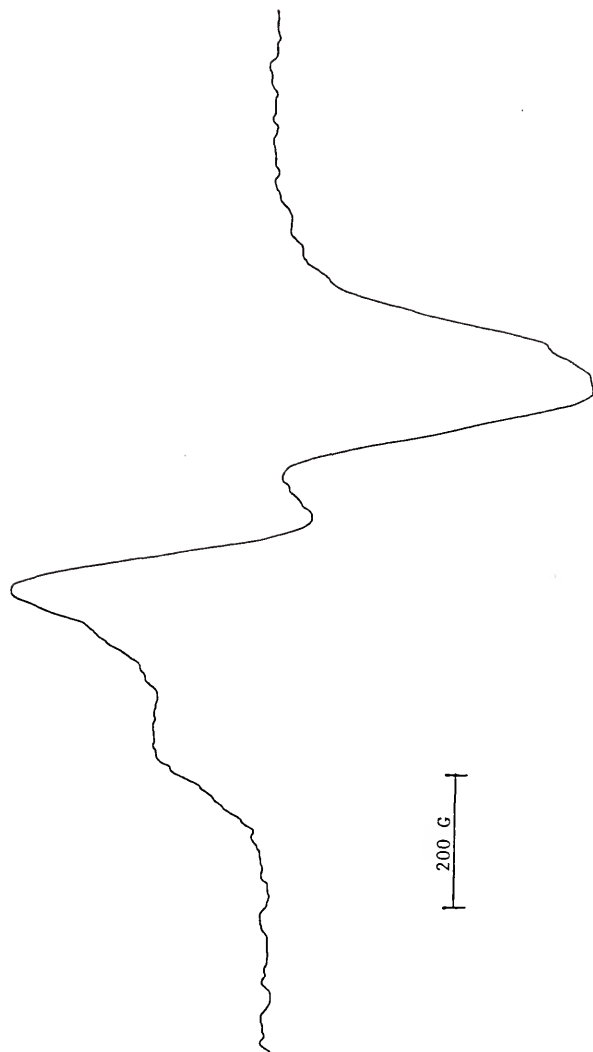
of other cobalt complexes contaminating the CoSDPT complexes may
bind O_2 when in a polymer matrix.

PS/[SG]-CoSDPT Membranes

The results for a series of PS/[SG]-CoSDPT membranes are shown
in Table 4-6. As a support, the silica is impermeable which is
reflected in the observed enrichments as a function of loading. As
the amount of [SG]-CoSDPT incorporated into the film is increased
the enrichment increases but then begins to decrease. A similar
trend can be noted in Table 4-5. As the weight percent of

Table 4-6

O_2 Enrichment for PS/[SG]-CoSDPT Films

Additives % by weight	Time (hrs)	Partial pressure (mmHg) O_2 from metal promoted enrichment
2.0	12	6.4
4.6	14	6.8
6.5	12	8.6
10.0	13	8.0
13.1	9	13.2
14.9	8	7.2

supported complex in the membrane increases, the likelyhood of
forming clumps or aggregates also increases. The clumps may not be
wetted by the polystyrene and become a structural weakness within
the membrane. In order to get a better handle on this problem,

scanning electron micrographs (SEMs) were taken for a variety of films. Figure 4-15 shows the surface view of a high loading (14.2%) and low loading (4.6%) PS/[SG]-CoSDPT membrane. The difference is striking. The low loading sample has a relatively smooth surface with some clump formation. The particle size is or pores. However, the possibility still exists for micropores since the SEM will only view down to 50 angstroms. On the other hand, the surface of the high loading sample is obviously disrupted and there may be some visible pores. A crossectional view is shown in Figure 4-16. The smearing effect is the result of the fracturing technique at 77 °K. The low loading sample shows no visible clumps or pores whereas the high loading sample displays areas of complex aggregation.

These results suggest that the membrane loading is quite limited, especially for the inorganic supports. Smaller particle size and better dispersion may alleviate some of this problem.

PS/Co(NaCN)-Y and Co(bipy)(terpy)-Y Membranes

The zeolite containing complexes described in Chapter II were also incorporated into polystyrene membranes (Table 4-7). The

Table 4-7

O_2 Enrichment for Cobalt Zeolite Films

membrane	% by weight	time	enrichment
PS/Co(NaCN)-Y-3	12.4	24	11.95
PS/Co(NaCN)-Y-3	12.5	14	5.33
PS/Co(NaCN)-Y-3	15.6	14	6.64
PS/Co(bipy)(terpy)	19.8	24	13.55

Figure 4-15. Scanning Electron Micrograph, surface view
            A. PS/[SG]-CoSDPT 14.2% by wt (high loading)
            B. PS/[SG]-CoSDPT 4.6% by wt (low loading).

A. 10KV X10000 0202 1.0U UFMSE

B. 10KV X10000 0302 1.0U UFMSE
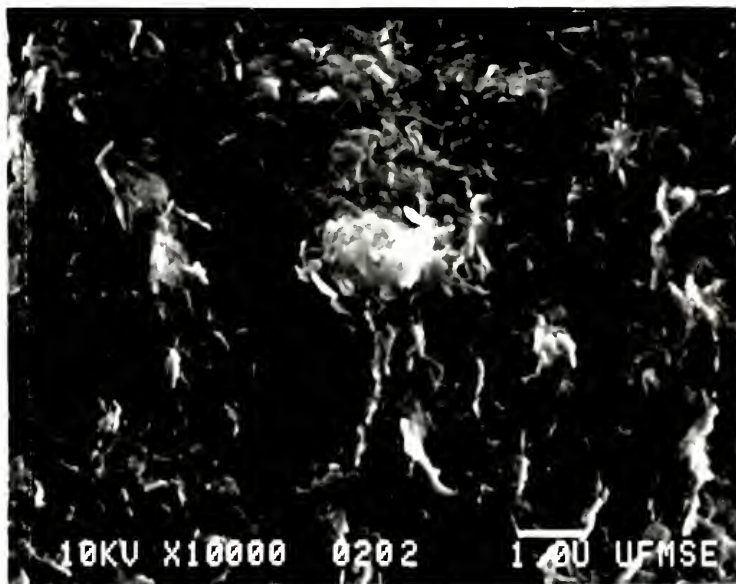
Figure 4-16. Scanning Electon Micrograph, crossectional view
             A. PS/[SG]-CoSDPT 14.2% by wt (high loading)
             B. PS/[SG]-CoSDPT 4.6% by wt (low loading).

Co(NaCN)-Y-3 complex apparently forms a stronger adduct with O_2 than the supported CoSDPT complexes as evidenced by a strong ESR signal shown in Figure 4-17. Some cobalt hyperfine is apparent but there is also an additional broad peak in the perpendicular region. It is more likely in this case than with CoSDPT that another $Co(CN)_x^{n-}$ complex is binding O_2 when embedded in the polymer. Although the Co(NaCN)-Y complexes may bind O_2 too strongly for practical application in membrane separations, they have served to further demonstrate the supported metal complex enhanced permeation of O_2 through a PS membrane. The Co(bipy)(terpy)-Y is not as stable as the cyano complexes but in the hydrophobic polymer matrix it is quite effective for facilitating the transport of O_2.

Mechanism

The mechanism of O_2 transport involved in the membranes described above is unlike that in liquid membranes or rubbery polymers. In the supported metal complex facilitated transport of O_2 in solid polymer membranes, there are at least five basic processes to consider as listed in Figure 4-18, sorption into the polymer, O_2 binding to the metal complex, diffusion within the polymer, desorption from the polymer and deoxygenation of the metal complex. The attainment of solution equilibrium at the polymer interfaces is essentially instantaneous and invariably an exothermic process, as is the dioxygen binding to the metal complex. The importance of the metal centers in the diffusion process is much more complex. It is postulated that the cobalt complexes transport O_2 via a site to site interaction, i.e. by a bucket brigade type movement as shown below. This would require a

Figure 4-17. X-band ESR of PS/Co(NaCN)-Y-3 at 105 °K.

200 G
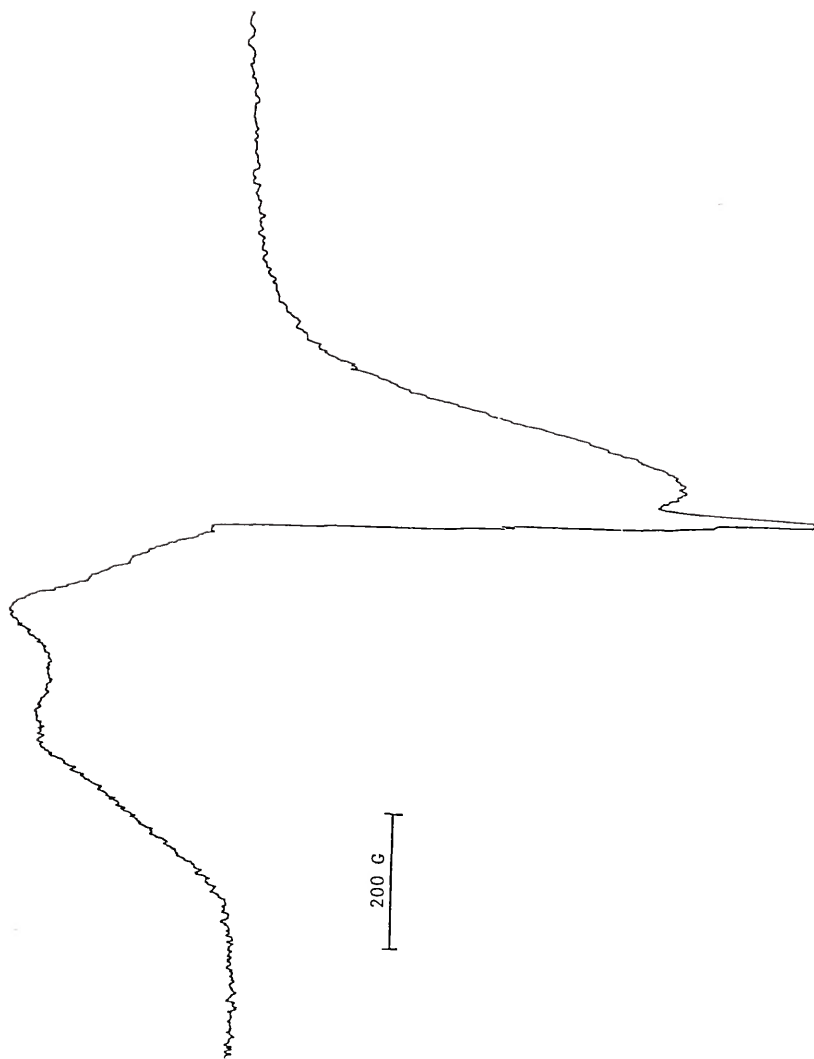
Figure 4-18 Contributions to O_2 permeation in supported metal complex containing polystyrene membranes.

SORPTION INTO POLYMER

O_2 BINDING TO METAL COMPLEX

DIFFUSION

DESORPTION FROM POLYMER

DEOXYGENATION OF METAL COMPLEX
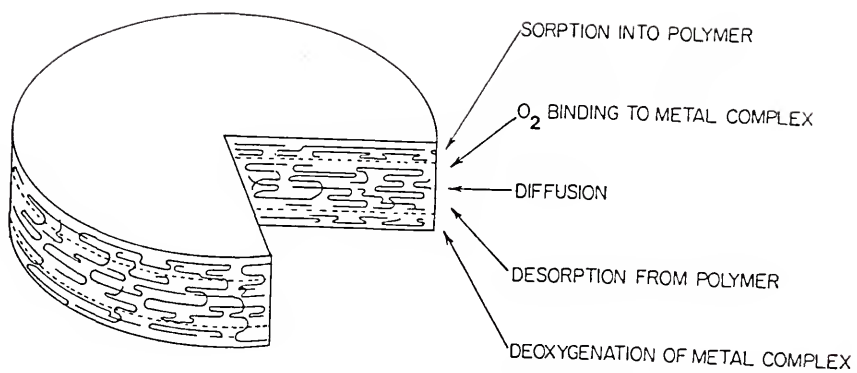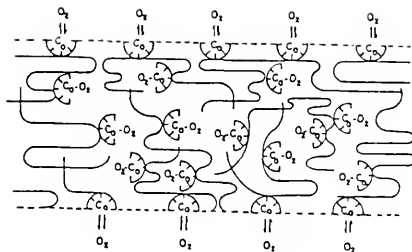
fairly homogeneous dispersion of the oxygen carriers throughout the membrane. This is confirmed by the fact that PS membranes containing [SG]-CoSDPT only on the lower interface showed no O_2 enrichment and membranes with [SG]-CoSDPT only on the high pressure side showed very small enrichment (3.4 mmHg). Therefore, the supported complexes need to be dispersed throughout the film in order to observe substantial enrichment.

During the permeation experiment the lower interface is initially degassed. However, to confirm the fact that the observed enrichment was not only due to desorption of O_2 from the complexes within the membrane without further interactions the amount of O_2 that would be desorbed was calculated and compared with the observed enrichment. For example, the partial pressure O_2 vs. time curve for a PS/[P]-CoBr$_2$SDPT membrane is shown in Figure 4-19. The film contains 14.5% by weight of the supported complex or 0.134 grams. This translates to 0.146 mmoles of CoBr$_2$SDPT but only 11% of the total area is exposed to a vaccum which would mean deoxygenation of 0.016 mmoles. Using the ideal gas law and the volume for the entire system (70.78 mL), a pressure of 4.3 mmHg O_2 would be the maximum that could be attributed to desorption from the complexes. ·The maximum enrichment observed was 11.09 mmHg O_2

Figure 4-19.   Plot of partial pressure O_2 vs. time for a
PS/[P]-CoBr$_2$SDPT film (14.5% by wt),
● experimental; ▲ calculated.
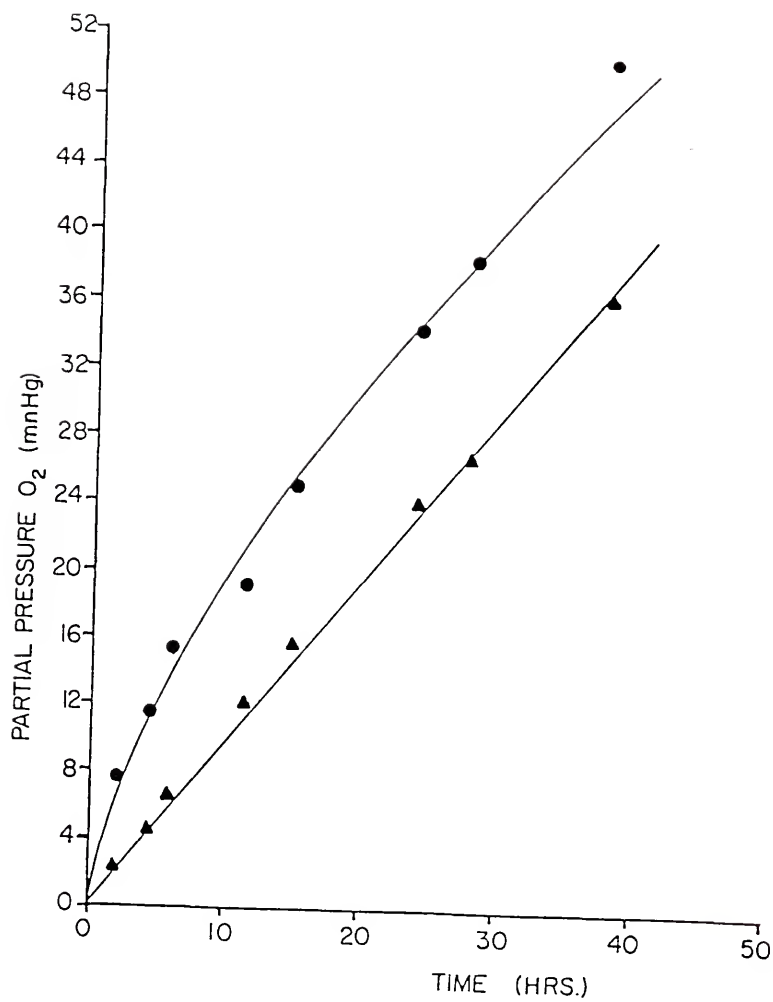
which means the cobalt complexes are reversibly binding O_2. In fact the 4.3 mmHg value is unrealistic since the complexes at the high pressure interface remain essentially completely oxygenated.

The nature of the bound O_2 is also an important point to consider. It has been suggested that the higher affinity of CoTPP for O_2 when bound to polystyrene results from solvation effects.[144] It is possible that the bound O_2 in the CoSDPT/Polystyrene films may interact with the aromatic rings. Additionally, dioxygen has been found to form charge transfer complexes with organic molecules,[145] in particular with polystyrene.[146] Considering in some cases the irreversible oxidation of cobalt(II) and the unusual ESR spectra, it is unlikely that oxygen exists solely in its ground state molecular form with these membranes. At this point, the manner in which this influences the permeation of O_2 is uncertain.

In conclusion, the evidence presented above supports the claim that supported cobalt complexes incorporated into a polystyrene membrane enhance the permeation of dioxygen. In order to fully develop this discovery, a wide range of polymeric membrane materials needs to be tested and the proper engineering applied so the full separating potential of these systems can be realized. Additionally, it is acknowlegded that the methodology for demonstrating the cobalt(II) facilitated transport of O_2 needs further improvement. The varient nature of the membranes employed in this study and possibly in future studies may necessitate the need for an internal standard. The permeation of N_2 may serve in this capacity. In this way, the ambiguities in the permeation data

which were proposed to arise from such things as stress cracking or simply changes in the morphology of the film, may be accurately accounted for. At the same time, it will be interesting to evaluate the effects of membrane aging on the permeation properties which is something the current method of data analysis cannot accommodate. At this juncture, it is reasonable to assume the pioneering work that has been presented here provides the ground work for future developments in this novel area of facilitated transport.

CHAPTER V
THE PREPARATION, CHARACTERIZATION AND
CATALYTIC PROPERTIES OF HETEROPOLYANIONS

Introduction

Some of the early transition metals form a class of heteropolyanions having the general formula $[X_x M_m O_y]^{n-}$ where M is either molybdinum, tungsten, vanadium, niobium or tantalum in their highest oxidation state (+6 or +5). The heteroatom X, may be from virtually any group in the periodic table except for the rare gases and there appears to be even less limitations on size and charge. One can envision literally thousands of different complexes as the result of all the possible heteroatoms and structural conformations. This subject has been well reviewed. [147-150] However, over the past few years there has been a resurgence of interest in poloxometalate chemistry and there are constantly reports with regard to catalysis. In order to be concise yet provide an ample background, only those heteropolyanions (HPAs) which have a direct bearing on this chapter will be discussed.

By far the most studied heteropolyanion has the general formula $[XM_{12}O_{40}]^{n-}$ (M = Mo, W), commonly known as the Keggin ion, named after the man who first determined the structure of $H_3[PW_{12}O_{40}] \cdot 5H_2O$. [151] The Keggin structure, shown in Figure 5-1, consists of a central or primary heteroatom linked to four groups of three edge sharing MO_6 octahedra which in turn are connected to

155

Figure 5-1. The Keggin Ion, $[PW_{12}O_{40}]^{3-}$.
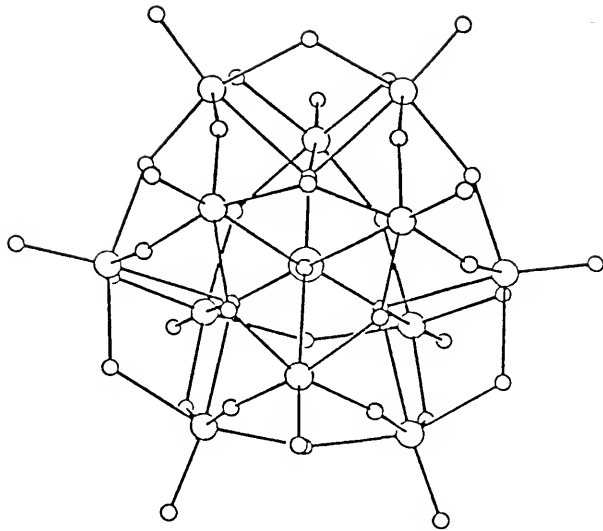
each other by corner sharing oxygens. The Keggin ion has overall tetrahedral symmetry.

In addition to the central heteroatom, these HPAs may incorporate one or more peripheral or secondary heteroatoms. For heteropolytungstates of the Keggin structure, an adenda $W=O$ unit can be removed by addition of base to produce stable and isolable lacunary or defect polyanions of the general formula $XW_{11}O_{39}^{7-}$. Alternatively, such HPAs can be prepared by stoicheometrically acidifying a mixture of the components. These lacunary heteropolyanions may be considered pentadentate ligands. Numerous 1:1 complexes[151-160] and in some cases 2:1 complexes[161] have been reported for transition metals and other elements. Additionally, a variety of organometallic moieties can be incorporated into the polyanion framework. Examples include $[(\pi-C_5H_5)Ti(PW_{11}O_{39})]^{4-}$,[162] $[(RM)SiW_{11}O_{39}]^{n-}$ (M = Sn, Ge, As; R = CH_3, C_2H_5, C_3H_5, C_6H_5, CH_2CH_2COOH, etc.)[163], $[(RSi)_2W_{11}SiO_{40}]^{n-}$ (R = C_2H_5, C_6H_5, $NC(CH_2)_3$, C_3H_5)[161] and some unusual metal-metal bonded derivatives $[LM-SnW_{11}O_{39}]^{n-}$ (LM = $(\pi-C_5H_5)(CO)_2Fe$, $(C_7H_8)_2Rh$, $(\pi-FC_6H_4)((C_2H_5)_3P)_2Pt$, $(\pi-C_5H_5)(CO)_3W$, $((C_6H_5)_3P)_2(CO)H_2Ir$, $((C_6H_5)_3P)(NO)(CO)_2Fe$),[164] $[LM(SnW_{11}SiO_{39})]^{11-}$ (LM = $(CO)_3Co$, $(\pi-C_3H_5)Pd$, $(CO)_3(NO)Fe$).[164] These organometallic derivatives are especially interesting for they represent soluble analogues of solid oxide supported catalysts. The nature of surface bound species on heterogeneous catalysts are difficult to characterize while similar species bound to soluble heteropolyanions may provide considerable information regarding those factors which influence their catalytic activity. An alternative approach to coordinating

organometallic catalysts or catalyst precursors to heteropolyanions is to replace several Mo^{VI} or W^{VI} adenda atoms with Ti^{IV}, V^V, Nb^V thereby creating an oxide surface with more negative charge density and therefore more attractive to the metal complexes. A variety of organometallic complexes have been supported on the surface of heteropolyanions in this manner.[165-172] For example $[(\pi-C_5Me_5)Rh(CH_3CN)_3]^{2+}$ was reacted with $[SiW_9Nb_3O_{40}]^{7-}$ to form $[(\pi-C_5Me_5)RhSiW_9Nb_3O_{40}]^{5-}$ as shown in Figure 5-2.[172] Coordination occurs at the bridging oxygen. The O-alkylation of $[PM_{12}O_{40}]^{3-}$ (M = Mo, W) also shows the preferred alkylation site to be a bridging oxygen not the terminal oxygen.[173] Although, it has not been demonstrated yet that such complexes can perform any catalysis, they are significant from the standpoint that the incorporation of heteroatoms into the heteropolytungstate greatly affects its reactivity. Simple HPAs such as $[PMo_{12}O_{40}]^{3-}$ or $[PMo_{12}O_{40}]^{4-}$ have less surface charge density than ClO_4^-.[174] The substitution of low valent transition metals into the heteropolyanion can also effect the surface charge density. 1-Brucine does not bind to $[PW_{12}O_{40}]^{3-}$ however, there is an association of brucine with $[PFeW_{11}O_{40}H_2]^{4-}$ in a ratio of more than 5:1.[175] Such results suggest that with the proper heteroatoms one may fine tune these polyanions to achieve a variety of desired properties, especially in relation to catalysis. A theorerical study has shown a correlation between the structure of heteropolyanions and the experimental results for oxidation reactions and acid catalyzed processes.[176]

Figure 5-2. $[(\pi-C_5Me_5)RhSiW_9Nb_3O_{40}]^{5-}$.   The organometallic moiety
is bound to two Nb-O-W and one W-O-W edge sharing
oxygens.
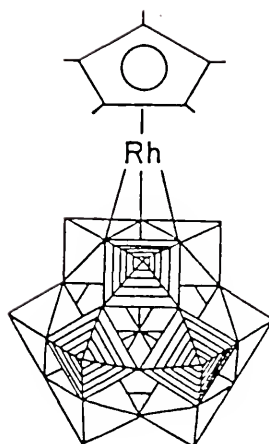
The systematic study of heteropolyanions in catalysis is considered to be a new field. The dual functions of both strong acidity and strong oxidizing ability of HPAs makes them very attractive catalysts. Much of the work in this area has been heterogeneous catalysis such as the conversion of methanol to hydrocarbons[177-180] and the production of methacrylic acid either by oxidative dehydrogenation of isobutyric acid [181-183] or directly form methacrolein.[184] The acid-base properties of heteropolyanions have been exploited in selective heterogeneous oxidation[185,186] while the availability of multiple oxidation states has led to the development of homogeneous catalysts.[187] The HPA $[PMo_6W_6O_{40}]^{3-}$ has been employed as an oxidant in place of $CuCl_2$ in the palladium catalyzed Wacker oxidation of olefins.[188,189] Heteropolyanions can undergo multi-electron reductions to generate what are commonly known as "heteropolyblues". This can be facilitated by chemical, electrochemical, or photochemical means. The photosensitivity of heteropolyanions has long been known but only recently exploited to dehydrogenate organic substrates.[190] An exciting development in this area is the recent report of the homogeneous catalytic photochemical functionalization of alkanes by HPAs.[191] The alkane C-H bond activation proceeds by an unusual mechanism with the formation of unprecidented products. Additionally, heteropolyanions are oxidatively stable compared with other alkane activation catalysts, such as metalloporphyrins.

Until very recently, catalytic studies with heteropolyanions have centered around their bulk properties while the catalytic activity of various heteroatoms has gone virtually unexplored. If

one considers lacunary anions as oxidatively resistant ligands,
then the incorporation of reactive metal centers into these
polyoxoanions may result in unusually stable homogeneous
catalysts. In general, very little is known regarding the
reactivity of heteroatoms, especially in nonaqueous solvents. For
most transition metal heteroatoms, the terminal ligand is usually a
water molecule or less protonated species depending upon the M.

$$
\begin{array}{c}
H_2O \\
\vdots \\
W-O \qquad O-W \\
\diagdown \quad \diagup \\
M \\
\diagup \quad \diagdown \\
W-O \qquad O-W \\
\vdots \\
O \\
| \\
X
\end{array}
$$
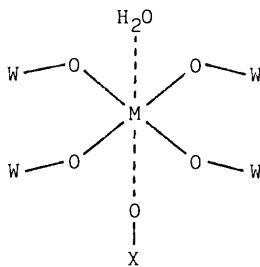
In many cases the water can be replaced by other
ligands.[152,156,192,193] However, these studies were conducted in
protic media and the equilibrium for the aqua ligand exchange was
generally close to that for aqueous Co^{2+} and not particularly
favorable. In 1984, Pope reported unusual reactivities for some
heteropolyanions in anhydrous nonpolar solvents.[194] A variety of
Co^{2+} and Mn^{2+} heteropolytungstates were phase transferred to
nonpolar solvents with large chain alkyl ammonium salts leading to
a loss of the terminal aquo ligand and generation of a coordinately
unstaturated species. The anhydrous HPAs react with numerous donor
ligands. The most exciting discovery was the reversible binding of
dioxygen by the manganese complexes. These polyoxometalates may

represent the first examples of oxygen carriers without organic ligands.

$$[XMn(H_2)W_{11}O_{39}]_{(aq)} \xrightarrow[\text{Toluene}]{R_4N^+} [XMnW_{11}O_{39}]^{n-} \xrightarrow{O_2} [XMn(O_2)W_{11}O_{39}]^{n-}$$
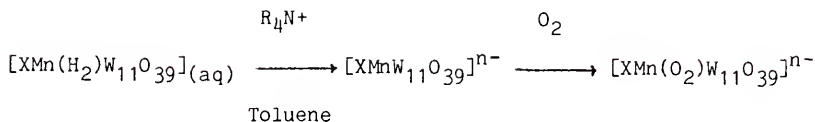
Keeping in mind the general theme of binding and activation of small inorganic molecules developed in Chapters II-IV, such HPAs present some attractive possibilities as oxidation catalysts. A program of study aimed at screening heteropolyanions as catalysts for the oxidation of organic substrates with molecular oxygen in nonaqueous solvents was initiated and the preliminary results discussed herein. This chapter begins with the results for $[XMW_{11}O_{39}]^{n-}$ (M = Co^{2+}, Mn^{2+}, Fe^{3+}) catalyzed oxidations with molecular oxygen as well as other oxygen sources such as peroxides and idosylbenzene. Subsequent to the start of this work, Hill reported the epoxidation of olefins by iodosylbenzene or pentaflouroiodosylbenzene catalyzed by $(PMW_{11}O_{39})^{5-}$ (M = Co^{2+}, Mn^{2+}) in acetonitrile.[195] In comparison with metalloporphyrins or metal triflates under similar conditions, the HPAs were for more active and selective for the conversion of olefins to epoxides. Additionally, the lifetimes of the HPA catalysts was far longer than the corresponding metalloporphyrins or metal salts owing to the oxidative stability of the lacunary anion.

The remainder of the chapter is devoted to the rather serendipitous discovery of what is proposed to be a Rh_2^{4+} containing heteropolytungstate. The characterization of this compound as well as its reactivity in non-aqueous solvents will be discussed. In particular, the RhHPA was found to catalyze the selective oxidation of cyclic olefins to the corresponding allylic ketone. The reaction appears to proceed by an unusual free radical but not free radical chain mechanism, the details of which will be discussed below.

Experimental

Solvents and reagents

Acetonitrile was predried over CaH_2, distilled from P_2O_5, then stored over 4A molecular sieves. All other solvents and reagents were stored over 4A molecular sieves and used without further purification. Olefin substrates were passed through a nuetral alumina column prior to use in order to remove trace peroxides. Hydrogen peroxide was used as a 30% aqueous solution and tert-butylhydroperoxide as 70% aqueous and 3.0 M toluene solutions. Cyclohexenyl peroxide was prepared by slurrying cyclohexene and 2,2'-azobis(2-methylpropionitrile) at 70 °C under oxygen for two hours, then at room temperature overnight. The volatiles were separated by vacuum transfer and the purity ascertained by GC. All peroxides were standardized by iodometric titration. Iodosylbenzene was prepared according to the literature[197] and refrigerated.

Spectral studies

Infared spectra were recorded on a Nicolet 5DXB Fourier transform infrared spectrophotometer using NaCl discs either as nujol mull or neat for the liquid metal complexes. Ultraviolet-visible spectra were obtained on a Perkin-Elmer 330 spectrophotometer with matched quartz 1.0 cm cells. EPR spectra were recorded on a Bruker ER 200D-SRC X-band spectrometer.

Gas chromatograms were obtained with a Varian 3700 GC equipped with a flame ionization detector and a Hewlett-Packard 3390A intergrator. Products were separated on either an eight foot 1/8 inch O.D. stainless steel column packed with 5% diethylene glycol adipate supported on 80/100 mesh chromasorb P, an eight foot 1/8 inch O.D. stainless steel column packed with 15% diethylene glycol succinate supported on 80/100 mesh chromasorb W-AW or a six foot 1/8 inch O.D. stainless steel column packed with 10% carbowax supported on 80/100 mesh chromasorb W-HP.

C^{13} and W^{183} NMR spectra were obtained on a Nicolet NT-300 spectrometer. Tungsten samples were prepared as 10 mL saturated solutions in 20 mm NMR tubes. The probe frequency was 12.5 MHz. The samples were referenced to a 1 M Na_2WO_4/D_2O solution.

Fast atom bombardment mass spectral determinations were carried out at the Middle Atlantic Mass Spectrometry Laboratory, National Science Foundation shared instrumentation facility located at Johns Hopkins University. All spectra were aquired with a KRATOS MS-50 equipped with a RF magnet. The MS-50 operated at an accelerating voltage of 8kV. The samples were bombarded with Xenon at 8kV. The matrix used was thioglycerol.

Electrochemical measurements were conducted with a PAR model 173 Potentiostat/Galvanostat equipped with a PAR model 175 universal programmer. A standard electrochemical cell was employed using a Pt auxillary electrode, a Pt button working electrode and a Ag/AgCl reference electrode. The supporting electrolyte was tetrabutylammoniumtetraflouroborate (0.1 M acetonitrile).

Ozonolysis was conducted with a Welsback model T-408 Laboratory Ozonator.

Elemental analyses were performed by Galbraith Laboratories or the microanalysis service of the University of Florida.

Oxidation Apparatus

The oxidation experiments were carried out in 250 mL Parr pressure bottles and secured in the stainless steel pressure set up detailed in Figure 5-3. Pressure was monitored with a Autoclave Engineers model AEC1 pressure transducer. The oxidations were performed in a constant temperature oil bath equipped with a Frowi FW-21G temperature controller. Samples were taken by syringe (12 inch, 20 gauge needle). Oxidations conducted under inert atmosphere were done in a 50 mL round bottom flask with rubber septa.

Oxidation Procedure

For the oxidation experiments carried out above atomspheric pressure the typical procedure is as follows. The catalyst was weighed into a 250 mL Parr pressure bottle followed by the addition of a stir bar and 50 mL of solvent. Then 1 mL of internal standard was syringed into the solution. The olefin substrate was passed through a neutral alumina column into a 5 mL volumetric flask. The

Figure 5-3. Pressure set up for the oxidation of organic
substrates. The reaction solution is placed in the
250 mL Parr pressure bottle with a magnetic stir
bar. The bottle is sealed with a silicon stopper and
clamped by the wing nuts and shielded inside the
aluminum frame. All the values and fittings are
stainless steel and of Swagelock construction. Saftey
features include an adjustable pressure release valve
and a solid sheild. The bottle may be filled with gas
through the inlet. The three valves allow for easy
flushing of the system. The gas pressure is
constantly monitored with an Autoclave pressure
transdium. Samples can be withdrawn without a loss in
pressure by inserting the 12 inch needle through the
rubber septem and open ball valve.
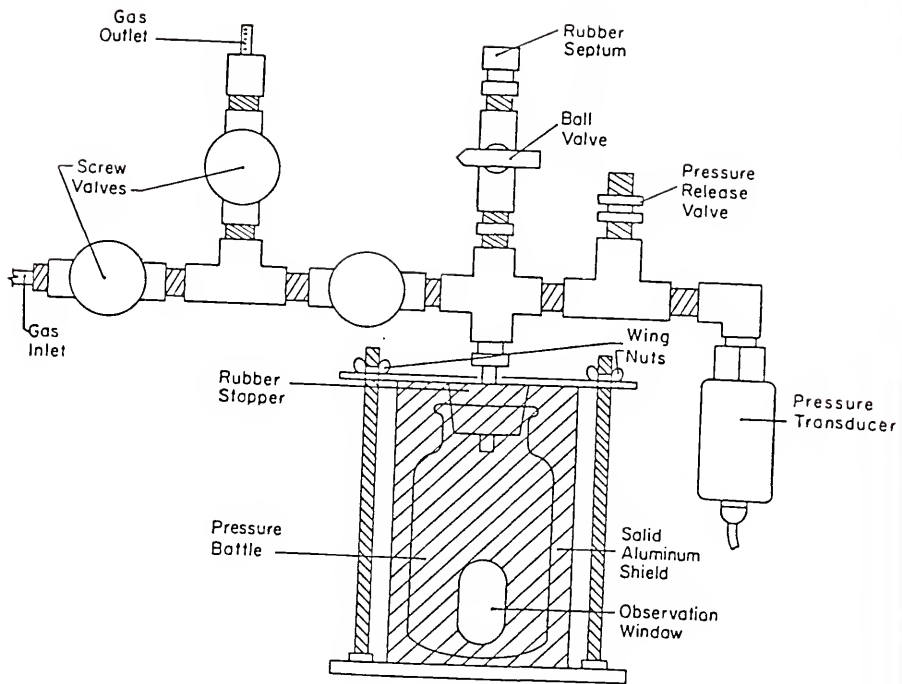
substrate was then transfered to the reaction vessel. An initial aliquot was taken then the high pressure apparatus in Figure 5-3 was assembled and immersed in a constant temperature bath. The bottle and pressure head were then purged with oxygen at least five times and filled to an initial pressure.

For a typical run the conditions were as follows: 0.3 grams RhHPA, 50 mL dry acetonitrile, 1 mL 2-octanone (internal standard), 5 mL cyclohexene (peroxide free), 50 °C oil bath and 40 psig oxygen.

During the course of the reaction, samples were withdrawn by syringe and transfered to a 0.5 dram vial. Then approximately 0.2 µl samples were injected into the GC for analysis. Since the concentration of 2-octanone remains constant, the GC response for a series of samples containing known concentrations of product can be measured and the ratio of peak area for the products/peak area for the standard versus moles of product/moles of standard can be plotted. From this calibration curve, the number of moles of product(s) formed during the reaction can be calculated.

Oxidations with peroxide or iodosylbenzene were carried out in a 50 mL round bottom flask. The reaction solutions were prepared in the same manner as the high pressure O_2 oxidations described above. The flask was purged with argon or nitrogen prior to the addition of the oxidant. The products were quantified in the same way as described above.

Several heteropolyanions were only water soluble and required a phase transfer catalyst to be organic soluble. The general procedure was to dissolve a weighed amount of HPA in distilled

water in an erlenmyer flask. The aqueous phase was covered with a nonpolar solvent such as toluene and a large excess of tetraheptylammonium bromide was added as the phase transfer catalyst. The large chain alkyl ammonium cation draws the heteropolyanion into the organic phase. This is evidenced by the transfer of color from the lower aqueous phase to the toluene layer. The organic solvent containing the HPA can then be used for the catalysis experiments.

Catalyst Preparation

$K_6[GeM(H_2O)W_{11}O_{39}]$ (M = Co(II), Mn(II), Fe(III)). This preparation is an adaptation of a method described by Weakly.[153] Details of the manganese(II) derivative are outlined below. In a 250 mL round bottom flask, 0.5 grams of GeO_2 was stirred in 10 mL of a 5% NaOH solution. To this, 17 grams of $Na_2WO_4 \cdot 2H_2O$ dissolved in 40 mL of distilled H_2O were added. This mixture was then stirred at 90 °C. Slowly, 10 mL of 12 M HCl was added dropwise and the solution was stirred for one hour. The solution was then cooled to room temperature and 20 mL of ether was added. With stirring, 10 mL of 12 M HCl was added dropwise in order to form the etherate of the lacunary anion $[GeW_{11}O_{39}]^{8-}$. Three layers may be evident, the lower etherate, middle aqueous layer and the top unprotonated ether layer. The lower layer is extracted with a separatory funnel and returned to a 250 mL round bottom flask with 40-50 mL of water. The solution was then warmed at 70 °C for one half hour to remove the ether. Then add 1.23 grams $Mn(CH_3CO_2)_2 \cdot 4H_2O$ dissolved in 5 mL of water. The solution was allowed to stir for one half hour. Potassuim acetate (21 grams)

was dissolved in 25 mL of hot water containing 2 mL of glacial acetic acid. This was then added to the stirring HPA solution. The mixture was gravity filtered hot then cooled to 0 °C. A yellow precipitate formed and was isolated by suction filtration, the complex was recrystalized from hot water, washed with a 1:1 ethanol/water solution, and dried in vacuo.

$[(n-C_4H_9)_4N]_6[GeMn(H_2O)W_{11}O_{39}]$. This catalyst was prepared in the same manner as above.

$[(n-C_4H_9)_4N]_6[SiMn(H_2O)W_{11}O_{39}]$. In a 250 mL round bottom flask, 18.2 grams of $Na_2WO_4 \cdot 2H_2O$ and 1.1 grams of $Na_2SiO_3 \cdot 9H_2O$ were stirred in 25 mL of water at 90 °C. Slowly, 5 mL of 12 M HCl was added dropwise and allowed to stir for one hour. Then 1 gram of manganese acetate dissolved in 5 mL water was added and stirred for one hour. The solution was filtered and excess solid $(n-C_4H_9)_4NBr$ added. The orange solution was suction filtered and the filtrate was reduced to an orange solid with a rotovap. The solid was recrystalized from hot water and dried in vacuo at 100 °C.

$K_8[GeW_{11}O_{39}]$. This preparation follows the suggestion of Tourne that simple addition of a calculated amount of strong acid to a solution of sodium tungstate and germanium dioxide followed by excess solid KCl results in formation of the GeW_{11} salt in a considerably pure state.[154] In 40 mL of water, 18.0 grams of $Na_2WO_4 \cdot 2H_2O$ and 0.5 grams of GeO_2 were stirred at 90 °C. Then 5.8 mL of 12 M HCl were added dropwise and the solution was stirred for one hour. A large excess (7 grams) of KCl was added to the solution and stirred for one half hour. The solution was cooled. A white precipitate formed and was isolated by suction filtration.

[$(C_8H_{17})_3CH_3N$]$_8$[$GeW_{11}O_{39}$]. The procedure for the preparation of [$GeM(H_2O)W_{11}O_{39}$]$^{n-}$ is followed up to the part of adding the secondary heteroatom. At this point, 18 grams of trioctylmethylammonium bromide in 30 mL of hot water is added to the stirring HPA solution and allowed to stir for one half hour. The reaction mixture is cooled to room temperature and a brown oil forms which is subsequently filtered and redissolved in acetonitrile. This yellow solution is filtered and evaporated to dryness to leave an orange brown oil.

[$(n-C_4H_9)_4N$]$_5$[$GeRh(H_2O)W_{11}O_{39}$]. The same procedure as for [$GeM(H_2O)W_{11}O_{39}$]$^{n-}$ was followed up to the point of secondary heteroatom addition. To the lacunary ion solution, 1.3 grams of $RhCl_3 \cdot 3H_2O$ dissolved in 10 mL of water was added and stirred for one hour. Then, 10 grams of tetrabutylammonium bromide dissolved in 30 mL of water is slowly added to the solution. The red-brown preceptate formed is isolated by suction filtration, washed with ethanol and dried in vacuo.

[$(n-C_4H_9)_4N$]$_{6-2x}$[$GeRh_2(H_2O)_2W_{10+x}O_{38+x}$]. Method 1. The procedure for preparation of [$GeRh(H_2O)W_{11}O_{39}$]$^{5-}$ was followed to the point of addition of the alkylammonium salt. If instead of slowly adding an aqueous solution of $(n-C_4H_9)_4NBr$, the salt was added in bulk and an olive green precipitate forms. The solid was isolated by suction filtration, washed with ethanol and dried in vacuo.

Method 2. [$(n-C_4H_9)_4N$]$_5$[$GeRh(H_2O)W_{11}O_{39}$] was prepared as above, then slurried in ethanol or isopropanol with moderate heating. After several hours the red-brown solid turns an olive

green color. The solid was isolated by suction filtration, washed with ethanol and dried in vacuo.

$[(C_8H_{17})_3CH_3N]_{6-2x}[GeRh_2(H_2O)_2W_{10+x}O_{38+x}]$. The preparation follows that for $[GeM(H_2O)W_{11}O_{39}]^{n-}$ up to the addition of the secondary heteroatom. To the solution of the lacunary ion was added 1.32 grams of rhodiumtrichloride in 10 mL of water and the mixture was allowed to stir for one hour. Trioctylmethylammonium bromide (13.5 grams), in 40 mL hot water, was added to the solution. A green oil forms upon addition of the alkylammonium salt and is isolated by suction filtration. The green oil is redissolved in acetonitrile, filtered then evaporated to an oil, and dried in vacuo at 100 °C.

$Rh_2(O_2CCH_3)_4$. Tetrakis(acetato)dirhodium(II) was prepared according to the published procedure.[198]

Results and Discussion

Reactivity in Non-Aqueous Solvent

$[XM(H_2O)W_{11}O_{39}]^{n-}$ (X = Ge(IV), Si(IV); M = Co(II), Mn(II), Fe(II)). Upon transfer of the $[XM(H_2O)W_{11}O_{39}]^{n-}$ complexes to toluene, the colors in Table 5-1 were observed in agreement with Pope.[194] For the GeMW$_{11}$ complexes, it was necessary to store the HPA toluene solutions over over 4A molecular sieve to remove the gas ligand. Upon removal of the terminal water, the Mn(II) HPAs were very air sensitive with irreversible oxidation occuring rapidly. Pope mentions irreversible oxidation does not occur in the presence of water or pyridine. Keeping this in mind, the catalyzed oxidation of 1-hexene in toluene and benzene (65 °C) with

Table 5-1

HPA Colors in Toluene

I	$[GeCo(H_2O)W_{11}O_{39}]^{6-}$	pink
II	$[GeCoW_{11}O_{39}]^{6-}$	green
III	$[GeMn(H_2O)W_{11}O_{39}]^{6-}$	yellow[a]
IV	$[GeMn(O_2)W_{11}O_{39}]^{6-}$	purple(-15 °C); green(25 °C)
V	$[GeMnW_{11}O_{39}]^{5-}$	red
VI	$[SiMn((H_2O)W_{11}O_{39}]^{6-}$	yellow[a]
VII	$[SiMn(O_2)W_{11}O_{39}]^{6-}$	purple-red
VIII	$[SiMnW_{11}O_{39}]^{5-}$	red
IX	$[GeFe(H_2O)W_{11}O_{39}]^{5-}$	yellow[a,b]

a   no observable color change upon loss of
      aqua ligand
b   this work

molecular oxygen (80 psig) was attempted in the presence of HPAs I, II and III. No oxidation products were observed. However, the yellow HPA III solution turned purple overnight. The purple color is indicative of the O_2 adduct, interpreted as a Mn^{IV} - peroxo species. Pope reported an ESR spectrum for the yellow $[GeMnW_{11}O_{39}]^{6-}$, with g ~ 4.3 and A = 86.3 G, and an ESR for the purple O_2 adduct with a similar g but with A = 88.5. He later contradicted this report by stating the purple HPA is ESR silent.[198] The yellow $[GeMnW_{11}O_{39}]^{6-}$ prepared above in toluene has the ESR shown in Figure 5-4. There exists two sets of six lines with g values that are fairly close (g ~ 4.3 for the more intense

Figure 5-4. X-band ESR of $[GeMn(H_2O)W_{11}O_{39}]^{6-}$ in Toluene (97 °K).

200 G
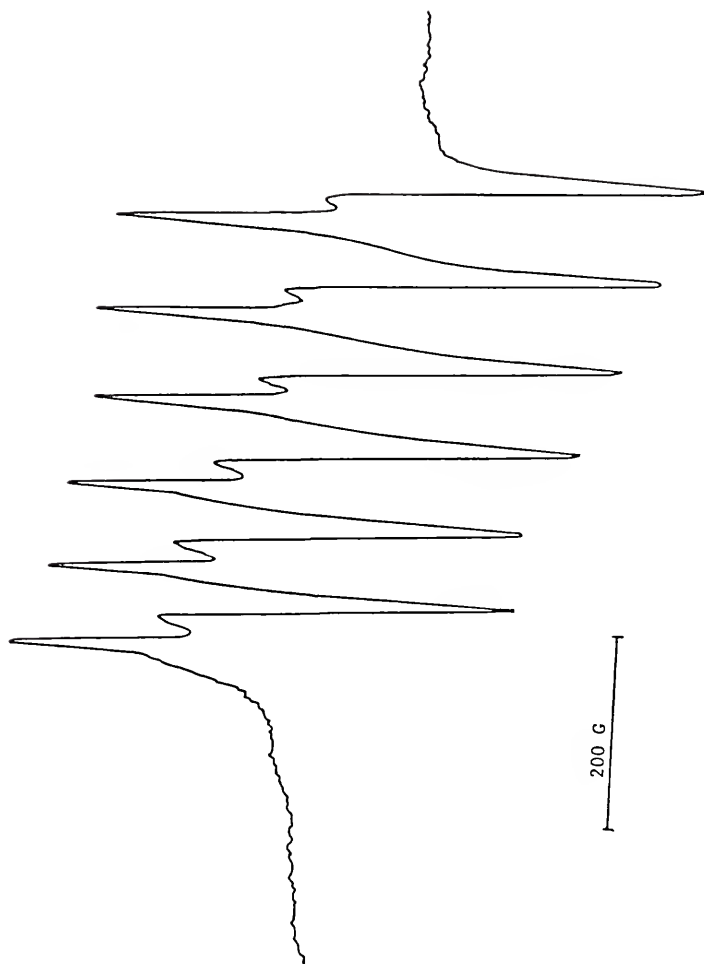
lines and g ~ 4.26 for the less intense signals). The A values are also similar, 88.9 G and 87.9 G respectively. In the spectra reported by Pope, the field width was large and there appeared to be shoulders on some of the peaks. Therefore, there may have been two superimposed sextets in his $[GeMnW_{11}O_{39}]^{6-}$ sample as well. It appears there are two species in solution, possibly from the same chemical entity but in equalibrium. Water is still present in the yellow toluene solution and is probably forming an adduct with a portion of the Mn HPAs, giving rise to two seperate ESR spectra. The signal is still observed in the presence of the purple, ESR silent O_2 adduct. This ESR signal that is observed for the purple solution was initially interperted by Pope as being for the O_2 adduct. The purple solution which was obtained in the oxidation experimental discribed above shows a very weak ESR spectrum similar to the yellow solution which indicates a portion of the HPA has been oxygenated producing a decrease in intensity for the ESR signal. What is interesting is that the purple solution was stable at room temperature, in fact, it was generated at 60 °C. This is in contrast to Pope's report that the purple solution persists only below 0 °C, above that it irreversibly oxidizes to the red Mn(III) species. Apparently, the excess water in the solution stabilizes the Mn(IV). This is further supported by the observation that placing the yellow $[GeMnW_{11}O_{39}]^{6-}$ in a toluene solution over 4A molecular sieves to rigorously remove water, results in a very air unstable yellow solution that rapidly changes to the red Mn(III) color upon exposure to air. In the presence of tert-butylhydroperoxide (tBHP), the yellow germanium centered Mn(II) HPA

solution instantly turns purple and has the ESR as shown in Figure 5-5. The addition of excess tBHP results in a complete loss of the low field signal and resolution of a signal at g ~ 2.03 shown in Figure 5-6. This new signal may be a Mn(IV) species such as an oxo complex. One might argue that a Mn(IV) ESR might be difficult to observe from spin-orbit coupling considerations and the ESR in Figure 5-6 is an organic free radical arising from decomposition of the peroxide. However, at room temperature the signal nearly disappears which is uncharacteristic for an organic free radical. Analagous behavior is observed with the $[GeCo(H_2O)W_{11}O_{39}]^{6-}$ anion in toluene with excess tBHP. The pink Co^{2+} solution is ESR silent and changes to an orange solution with the ESR shown in Figure 5-7 upon the addition of peroxide. The ESR for the Co HPA, although much broader, is similar in apperance to the Mn HPA and likewise disappears at room temperature. This paramagnetic species might correspond to a Co(IV) ion. The generation of these high valent Mn and Co complexes with peroxides provides some good oxidizing agents.

The oxidation of cylcohexene and 1-hexene catalyzed by Co(II), Mn(II), and Fe(III) heteropolytungstates was investigated using a variety of oxidents. The results for a series of experiments are summarized in Table 5-2. Although some activity was noted, in only one instance were turnovers measured and that was for the FeHPA which oxidized cyclohexene to primarily the allylic ketone product with approximately 23 turnovers in 24 hours. All other peroxide oxidations produced only trace quanities of what would be considered the autoxidation products. In most cases, some solvent

Figure 5-5. X-band ESR of $[GeMnW_{11}O_{39}]^{6-}$ + tBHP in toluene (115 °K), $g \sim 4.3$, $A \sim 89.5$ and $g \sim 2.01$.

200 G
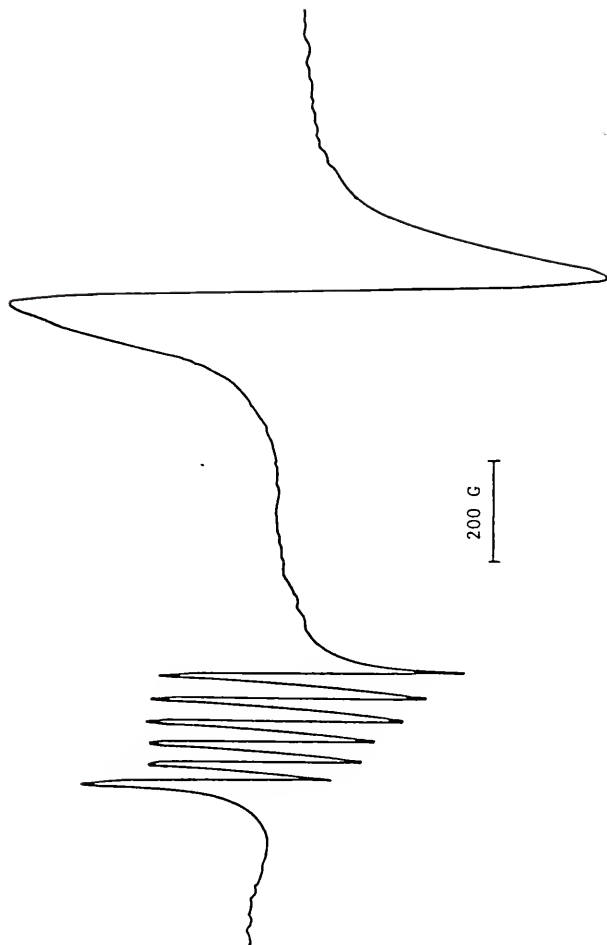
Figure 5-6. X-band ESR of $[GeMnW_{11}O_{39}]^{6-}$ + (xs)tBHP in toluene (87 °K), g ≃ 2.03.

20 G
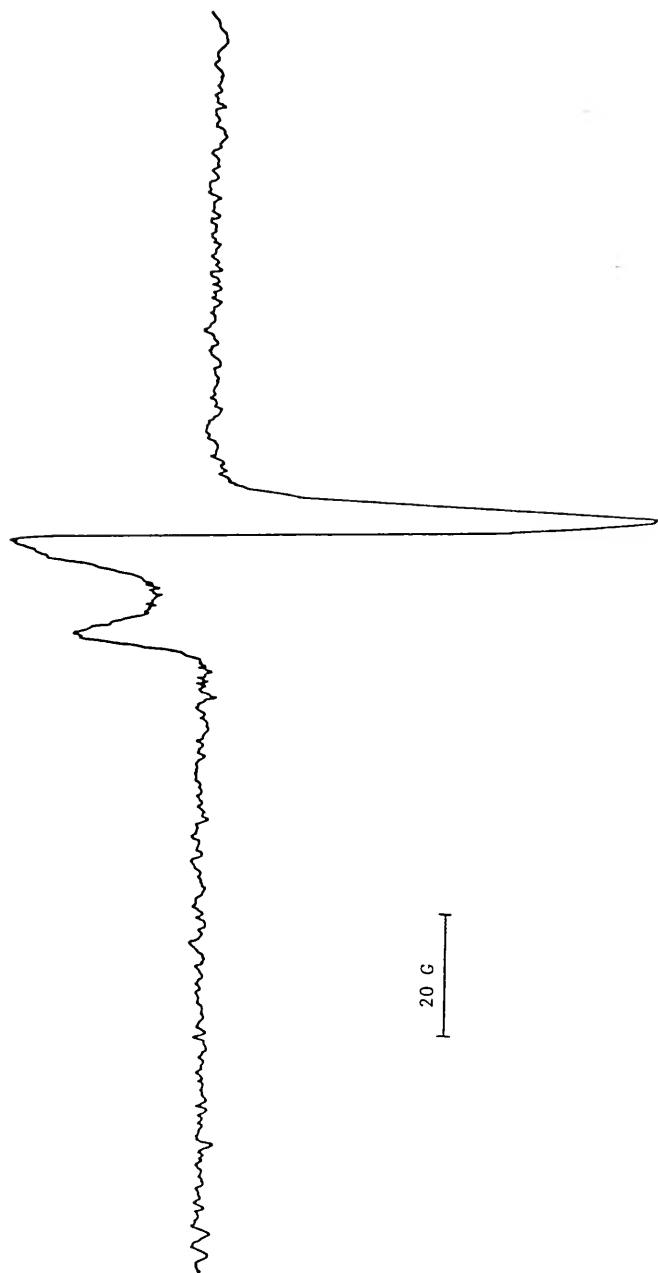
Figure 5-7. X-band ESR of $[GeCo(H_2O)W_{11}O_{39}]^{6-}$ + (xs)tBHP in toluene (78 °K), g ~ 2.02.

20 G
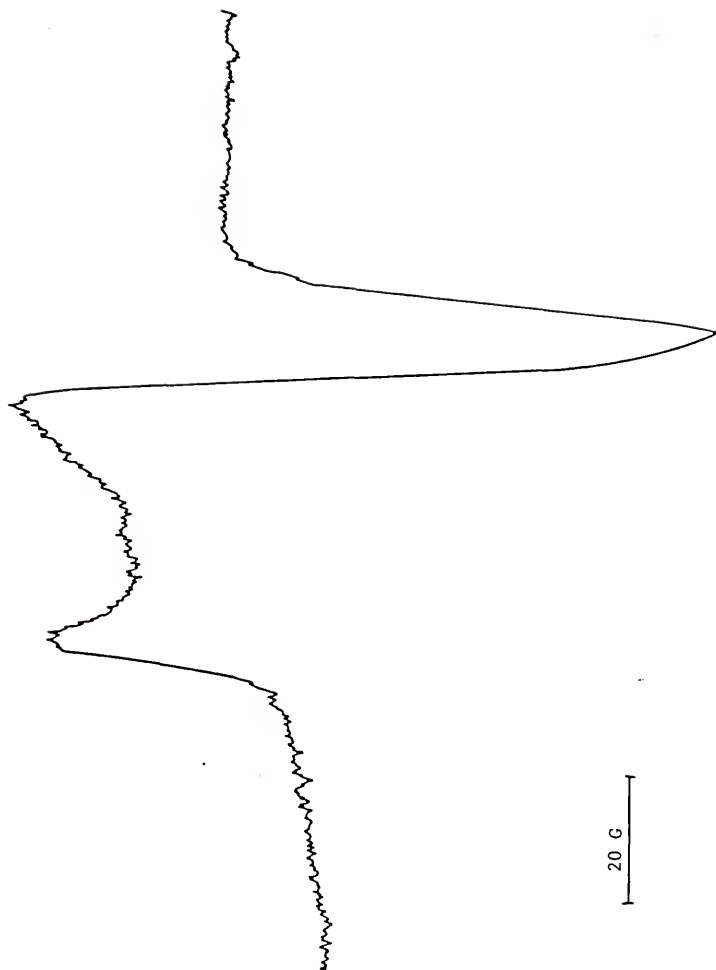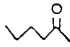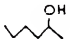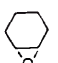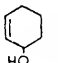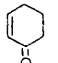
Table 5-2

$(XMW_{11}O_{39})^{n-}$ Catalyzed Oxidation of Olefins After 24 Hours

A.   cyclohexene

HPA	Oxident	T (°C)	$\overset{O}{\diagup\hspace{-0.3em}\diagdown}$	OH	$\diagdown\hspace{-0.3em}\diagup^{O}$	other products
GeMnW$_{11}$[a]	tBHP	60	trace	--	-	benzaldehyde(trace)
CeFeW$_{11}$[a]	tBHP	30	1.16	trace	--	benzaldehyde(0.62)[d]
GeCoW$_{11}$[a]	H$_2$O$_2$	25	trace	trace	trace	benzaldehyde(trace)
GeMnW$_{11}$[b]	IOAr	25	--	--	trace	--

B.   1-hexene

HPA	Oxident	T (°C)	epoxide	HO	O	other products
GeMnW$_{11}$[a]	tBHP	25	--	--	--	benzaldehde(trace)
GeMnW$_{11}$[b]	H$_2$O$_2$	25	trace	trace	--	--
GeCoW$_{11}$[a]	H$_2$O$_2$	25	--	trace	--	--
GeMnW$_{11}$[b]	IOAr	25	trace	--	trace	--
GeCoW$_{11}$[b]	IOAr	25	--	--	trace	--
GeCoW$_{11}$[a]	IOAr	25	--	--	trace	benzaldehyde(trace)
GeCoW$_{11}$[a,c]	IOAr	25	--	--	--	benzaldehyde(trace)
SiMnW$_{11}$[a]	IOAr	27	--	--	trace	benzaldehyde(trace)

a.   toluene solvent   c.   solution rigorously dried
b.   benzene solvent   d.   in the absence of olefin,
                                        0.55 mmmole were produced

oxidation was noted as well. The oxidations with iodosylbenzene (IOAr) are far more interesting since only the epoxides were observed as trace products. Oxygen atom transfer from iodosylbenzene has been shown to be catalyzed by metalloporphyrins,[199-204] Shiff base complexes,[202] and even simple metal salts.[203,204] Hill recently reported $(PMW_{11}O_{39})^{n-}$, (M = Co(II), Mn(II), Fe(III)) epoxidized olefins with iodosylbenzene in acetonitrile solvent.[196] Since this system is analygous to those in Table 5-2, the solvent must play a significant role in the reactivity of the HPAs. The low product yield in tolulene or benzene discuraged further investigation of these systems.

$[GeRh_2(H_2O)_2W_{10+x}O_{38+x}]^{(6-2x)-}$. There are two reports in the literature of rhodium(III) substituted heteropolytungstate of the Keggin structure,[158,205] the later being refuted as a simple ion pair. The procedure of Tourne (below) involves stirring a

$$K_6GeW_{11}O_{39} + RhCl_3 \xrightarrow[H_2O]{90\ ^\circ C} K_5GeRh(H_2O)W_{11}O_{39}$$
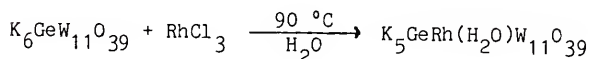
hot solution of the lacunary anion and rhodiumtrichloride for 30 minutes, followed by cooling, and precipitation of $K_5GeRh(H_2O)W_{11}O_{39}$ with ethanol or methanol. Since the lacunary anion can be prepared in solution relatively free from contamination by metatungstates (vide supra), it was thought that the tetrabutylammonium salt could be prepared according to the following sequence. Slow addition of an aqueous solution of the

$$11WO_4^{2-} + GeO_2 + 14H^+ \xrightarrow[H_2O]{90\ ^\circ C} GeW_{11}O_{39}^{8-} + 7H_2O$$

$$GeW_{11}O_{39}^{8-} \xrightarrow[ether]{H^+} \text{"Etherate"}$$

$$\text{"Etherate"} \xrightarrow[H_2O]{70\ ^\circ C} GeW_{11}O_{39}^{8-}$$

$$GeW_{11}O_{39}^{8-} + RhCl_3 \xrightarrow[H_2O]{70\ ^\circ C} GeRh(H_2O)W_{11}O_{39}^{5-}$$

$$GeRh(H_2O)W_{11}O_{39}^{5-} \xrightarrow[H_2O]{t\text{-butyl}_4NBr} [n\text{-butyl}_4N]_5[GeRh(H_2O)W_{11}O_{39}]$$
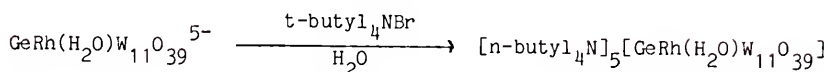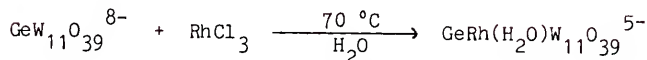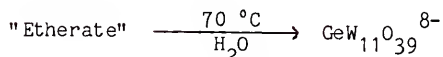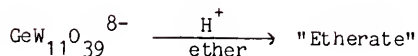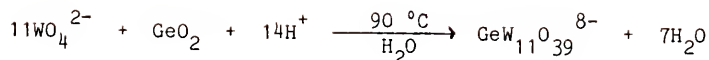
tetrabutylammonium bromide resulted in formation of a red-brown precipatate, proposed to be the Rh(II) HPA. However, if the alkylammonium salt is added in bulk a green precipitate is formed. The green color is reminiscent of rhodium(II) such as with the rhodium(II) carboxylate dimers. The green RhHPA is not paramagnetic as evidenced by the lack of an ESR signal. Additionally, the W^{183} NMR shows no line broadening or shifts indicative of the presence of a paramagnetic center. This can be rationalized in terms of antiferromagnetic coupling as a result of a Rh_2^{4+} species. This is plausible as far as Rh(II) chemistry is concerned since most of the stable Rh(II) compounds are dimers.[206] Heteropolyanions containing a homonuclear transition metal-metal bonded species is unprecedented in the literature. Generally Rh(III) complexes are fairly easy to reduce, for example, rhodium(II) acetate is prepared by simply refluxing $RhCl_3$ in a 50/50 mixture of acetic acid and ethanol.[206] If the red-brown

$[(n-C_4H_9)_4N]_5[GeRh(H_2O)W_{11}O_{39}]$ is slurried in warm ethanol or isopropanol the green RhHPA is obtained. Therefore, either a mildly reducing solvent or the bulk addition of the alkylammonium bromide results in formation of the Rh_2^{4+} moiety.

In pursuing the reactivity of heteropolyanions in non-aqueous solvents, it was desirable to employ a cation that would impart maximum solubility properties. The cation, trioctylmethylammonium ion, has been used prevously to this end and results in the formation of highly soluble metal complexes.[207] The addition of hot water containing $(C_8H_{17})_3CH_3NBr$ to a solution of $[GeW_{11}O_{39}]^{8-}$ and $RhCl_3$ results in the immediate formation of a green liquid metal complex i.e. an oil. It is speculated that the Rh(III) may oxidize the Br^- to give the Rh_2^{4+} species. The trioctylmethylammonium salt, as expected, has a high degree of solubility ranging from non-polar solvents such as benzene or toluene to more polar solvents such as chloroform, dimethylsulfoxide, dimethylformamide, etc.. Therefore, the majority of the invesigations with the RhHPA were conducted with the trioctylmethylammonium salt.

The incorporation of Rh_2^{4+} into the heteropolytungstate is not terribly surprising owing to the propensity of the lacunary anions to accommodate a variety of heteroatoms. However, the isolation of the RhHPA is exciting from the standpoint that it is the first example of a substituted Keggin ion containing a homonuclear metal-metal bonded species which may be part of a whole new class of HPAs. This is particularly interesting from a catalytic standpoint, since this RhHPA was found to have unusual catalytic

properties (vide infra). The incorporation of other multimetallic catalysts into HPAs presents some atractive possibilities.

Until recently, the characterization of heteropolyanions has been very difficult owing to the complexity of these metal oxide systems. Generally, a number of different experimental techniques is required to be reasonably certain about the polyoxometalate structure. The characterization of the RhHPA has proven to be quite challenging and this effort will be described in the following pages.

In order to discern the nature of the Rh_2^{4+} substitution in the tungstate framework, it must first be confirmed that the Rh_2^{4+} is covalently bound and simply not present as an ion pair. This was accomplished by passing an acetonitrile solution of the RhHPA through a column containing a cation exchange resin ($RSO_3^-Na^+$). No decolorization of the solution was observed as one might have expected if the Rh_2^{4+} was present as part of an ion pair. Alternatively, passing the RhHPA acetontrile solution through an anion exchange resin ($RN(CH_3)_3^+Cl^-$) results in nearly complete decolorization of the solution leaving a colored band at the top of the column. This supports the assumption that the Rh_2^{4+} is covalently attached to the HPA giving a species with a negative charge.

By far the most widely used spectroscopic technique in this area is vibrational spectroscopy. The metal-oxygen streching vibrations can be observed in the region from approximately 1200 to 50 cm^{-1}. Often the band positions, shapes and intensities can be fairly diagnostic for a particular polyoxoanion structure. The

infrared spectrum for $[(C_8H_{17})_3CH_3N]_8[GeW_{11}O_{39}]$ is shown in Figure 5-8 and is typical for the XM_{11} lacunary ligands. Since it has been demonstrated that substitution into the Keggin structure results only in relativity small frequency shifts, the IR for the RhHPA is interpreted in light of the extensive analysis of the vibrational spectra already reported for analagous HPAs.[208] The band at 968 cm^{-1} is attributed to a terminal W=O stretch. The band at 896 cm^{-1} is associated with a Ge-O stretch. The bands at 832, 782 and 725 cm^{-1} involve skeletal deformations of the anion resulting in asymmetric W-O-W stretches for the corner sharing and edge sharing oxygens respectively. The lowest frequency bands involve those bridges closest to the peripheral heteroatom. In general, from the complete Keggin ion XW_{12} to the lacunary ligand XW_{11} there is a decrease in the stretching frequencies as a result of a weakening of W-O bonds in the lacunary ligand. Upon substitution, the stretching frequencies increased because the W-O bonding is more cohesive. However, the frequencies for XMW_{11} always remain lower than the frequencies for the complete XW_{12} unit. Table 5-3 shows the infrared data for a series of HPAs. From the IR data, it is reasonable to assume that the RhHPA has some semblance of the Keggin structure. Unfortunately, this does not provide a handle to the nature of the substitution. This insensitivity of the infrared to substitution is best illustrated by the spectra for the red-brown Rh^{3+}HPA in Figure 5-9, and the green Rh_2^{4+}HPA in Figure 5-10 which are nearly identical.

Figure 5-8. FT-IR of $[(C_8H_{17})_3CH_3N]_8[GeW_{11}O_{39}]$, neat.

WAVENUMBERS (cm⁻¹)
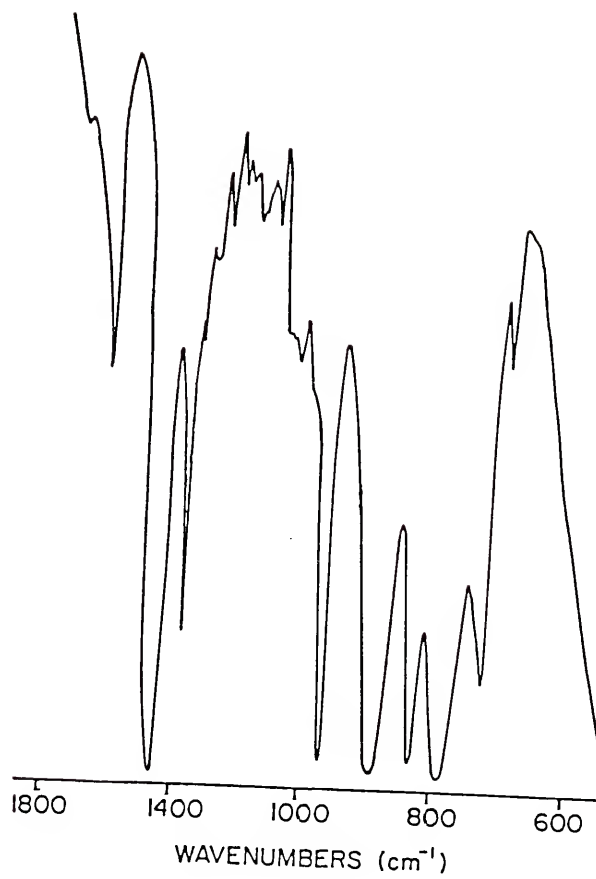
Figure 5-9. FT-IR of red-brown [butyl$_4$N]$_5$[GeRh(H$_2$O)W$_{11}$O$_{39}$], nujal mull.

% TRANSMITTANCE

WAVENUMBERS (cm⁻¹)
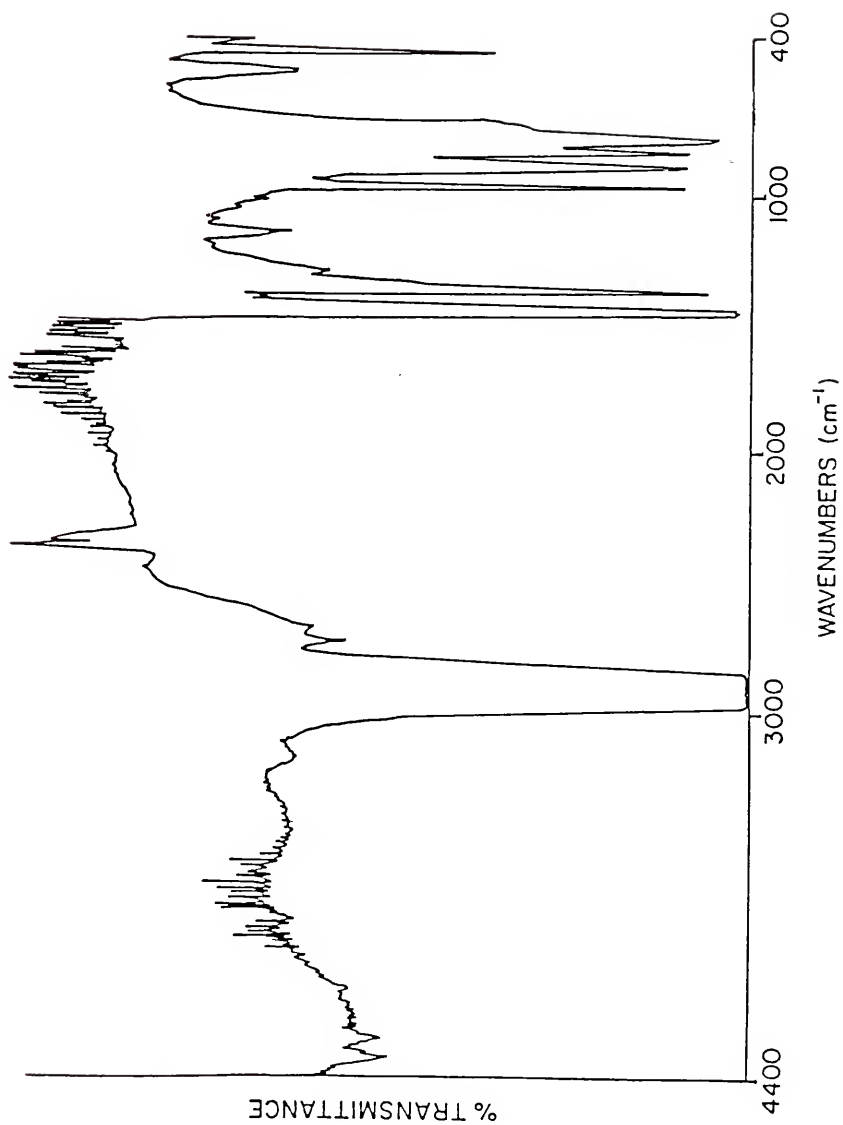
Figure 5-10. FT-IR of green [butyl$_4$N]$_{6-2x}$[GeRh$_2$(H$_2$O)$_2$W$_{10+x}$O$_{38+x}$], nujal mull.
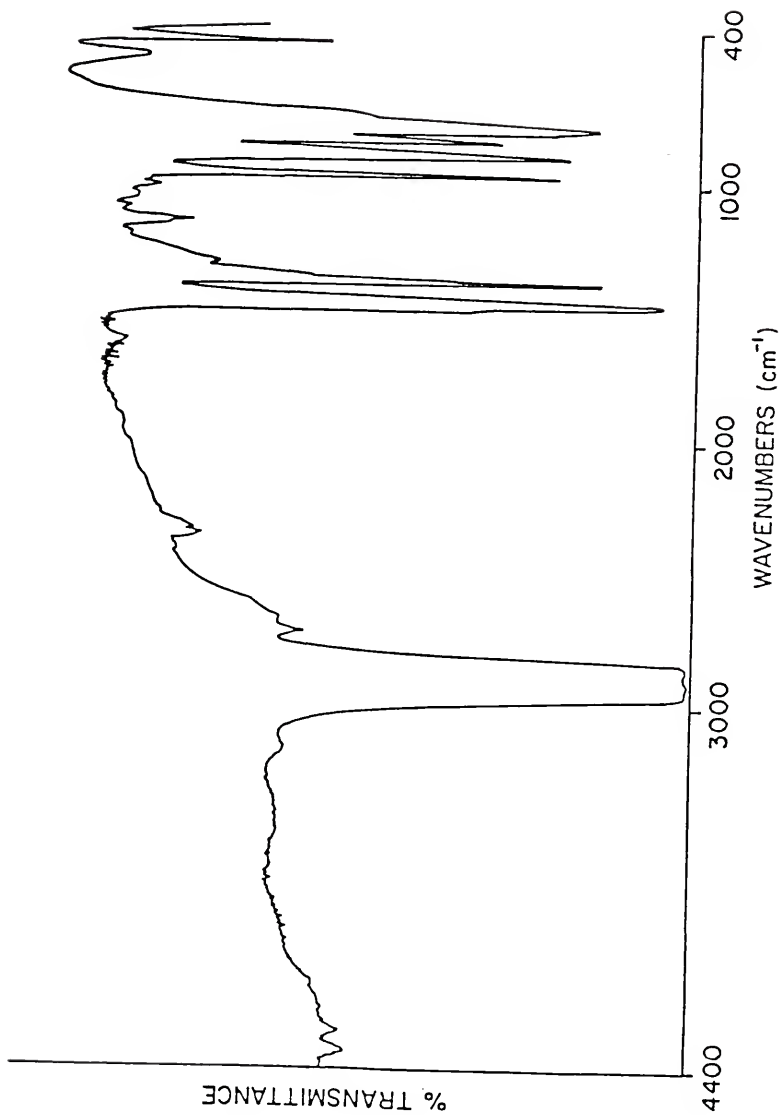
Table 5-3

HPA Infrared Results

HPA	frequency (cm^{-1})				
$K_6[GeMn(H_2O)W_{11}O_{39}]$	952	878	811	768	722
$K_6[GeCo(H_2O)W_{11}O_{39}]$	957	890	814	771	722
$K_5[GeFe(H_2O)W_{11}O_{39}]$	952	887	803	781	722
$(butyl_4N)_6[GeMn(H_2O)W_{11}O_{39}]$	946	890	809	772	722
$(butyl_4N)_5[GeRh(H_2O)W_{11}O_{39}]$	963	888	833	788	738
$(butyl_4N)_{6-2x}[GeRh(H_2O)_2W_{10+x}O_{38+x}]$	963	887	833	787	734
$[(C_8H_{17})_3CH_3N]_8(GeW_{11}O_{39})$	968	889	833	785	724
$[(C_8H_{17})_3CH_3N]_{6-2x}[GeRh_2(H_2O)_2W_{10+x}O_{38+x}]$	969	896	832	782	725

A relatively new analytical technique for the characterization
of heteropolyanions involves multinuclear NMR. The use of W^{183} NMR
for the structural characterization of heteropolytungstates was
first reported by Baker in 1979.[209] Since that time, numerous
papers have appeared involving tungsten-183 NMR in structural
determinations of HPAs.[167,172,209-224] Additionally, a recent
review of multinuclear NMR for Cr^{53}, $Mo^{95,97}$ and W^{183} has
appeared.[218] The prior development of W^{183} NMR was hindered
because of its low sensitivity which can be attributed to a
combination of low receptivity and low resonance frequency. The
receptivity or signal intensity is proportional to

$$\gamma^3 NI(I + 1)$$

where γ is the magnetogyric ratio, N is the natural abundance of

the isotope and I is the nuclear spin quantum number, (for W^{183} $I = \frac{1}{2}$, $N = 14.40$ atom%, $\gamma = 1.120 \times 10^7$ radT^{-1}s^{-1}). The sensitivity is only 1.06×10^{-5} that of the proton. The resonance frequency is at 4.166388 MHz in a magnetic field where the protons of TMS resonate at exactly 100 MHz. This is at the lower limit of most commerically available probes. Additionally, the aquisition of quality spectra can be time comsuming. For example, the T_1 for $W(CO)_6$ is greater than 80 seconds.[225] The relaxation times for polyoxoanions have not been reported but are probably on the order of 5 seconds. A redeeming factor is that observed line widths are extremely narrow allowing for the resolution of spin-spin coupling with other magnetic nuclei. Also, there is only one isotope of tungsten to contend with.

For the complete Keggin ions, $[XW_{12}O_{40}]^{n-}$, of Td symmetry, all twelve tungsten atoms are symmetrically equivalent and a single sharp resonance is observed. For example, the resonance for $[GeW_{12}O_{40}]^{4-}$ in D_2O has a chemical shift at -81.9 ppm relative to WO_4^{2-} in D_2O.[207] Removal of a W=O unit to produce the lacunary ion $[XW_{11}O_{39}]^{2-}$ reduces the symmetry to the C_s point group. This results in one unique tungsten atom and five inequivalent pairs of tungsten atoms represented by six resonances in the ratio of 2:2:2:2:2:1. For example, $[SiW_{11}O_{39}]^{8-}$ in D_2O has resonances at -100.9, -116.1, -121.3, -127.9, -143.2, and -176.2 ppm.[218] A disubstituted Keggin ion can have five different structural isomers, including C_1, C_2, C_{2v}, and two with C_s symmetry. $[Ti_2PW_{10}O_{40}]^{7-}$ in D_2O (C_2 point group) has five resonances of equal intensity at -73.7, -112.5, -125.5, -127.0 and -143.0 ppm.[218] Two

dimensional W^{183} NMR has been used to unequivocally assign the spectra of heteropolytungstates.[211,212] However, the simple integrated intensities of the resonances are most often used to determine the anion symmetry. The W^{183} spectra for $[(n-butyl)_4N]_{6-2x}[GeRh_2(CH_3CN)_2W_{10+x}O_{38+x}]$ in 1:1 CD_3CN/CH_3CN is shown in Figure 5-11. The four signals at -69.3, -79.2, -81.4 and -93.3 ppm are in a ratio of 3.1:2.5:1.0:1.2. It is reasonable to assume an error of ±20% when using the observed intensities and the 10 or 11 tungstens could then be accounted for. The fact that there are only four resonances suggests that two or more peaks may be overlapping. Normally for polyoxotungstates line widths are on the order of less than 1 Hz. The line widths measured in Figure 5-11 are on the order of 5-8 Hz and it is reasonable to assume measuring errors of ±5 Hz.[218] Since there is a strong dependence on both solvent and concentration (±1 ppm) for the observed chemical shifts (vide infra), a change in solvent might resolve additional peaks. Tungsten-183 NMR spectra for the same sample of $[(C_8H_{17})_3CH_3N]_{6-2x}$ $[GeRh_2L_2W_{10+x}O_{38+x}]$ (L = H_2O or CH_3CN) were recorded in 1:1 CD_3CN/CH_3CN (Figure 5-12), $CDCl_3:CHCl_3$ (Figure 5-13), and toluene-D_8/toluene (Figure 5-14). The chemical shifts and integrated intensities (parentheses) are shown in Table 5-4. In non-polar toluene only three peaks are observed upon going to a more polar solvent like chloroform the peak a -76 ppm splits into two signals approximately 1 ppm apart. In a stronger donor solvent, such as acetonitrile, there is a general upfield shift for all the resonances. The peak that was at -75.6 ppm in choloroform shifts almost 4 ppm upfield in acetonitrile. The line widths are

Figure 5-11. W^{183} NMR of $[(n\text{-butyl})_4N]_{6-2x}$ $[GeRh_2(CH_3CN)_nW_{10+x}O_{38+x}]$ in 1:1 CD_3CN/CH_3CN.
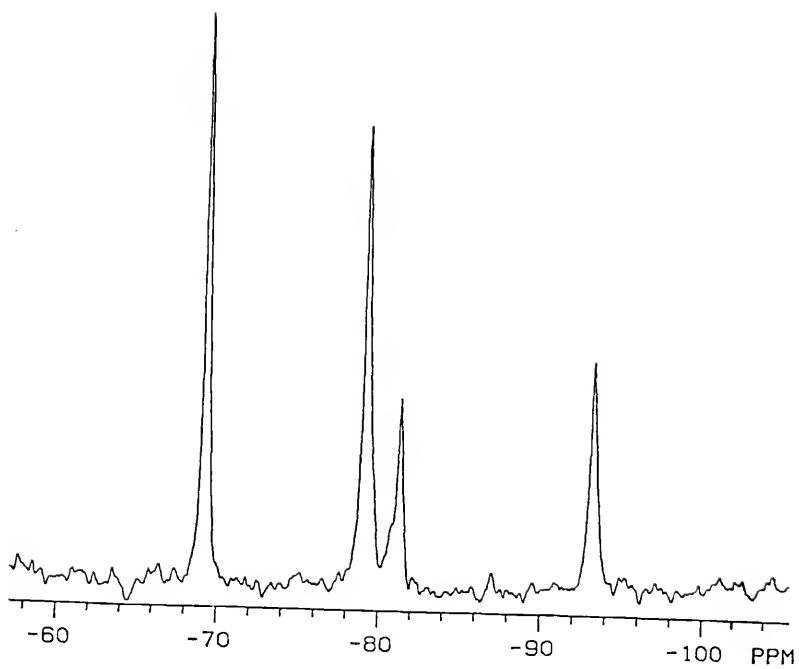
Figure 5-12. W^{183} NMR of $[(C_8H_{17})_3CH_3N]_{6-2x}[GeRh_2L_nW_{10+x}O_{38+x}]$ in 1:1 CD_3CN/CH_3CN.
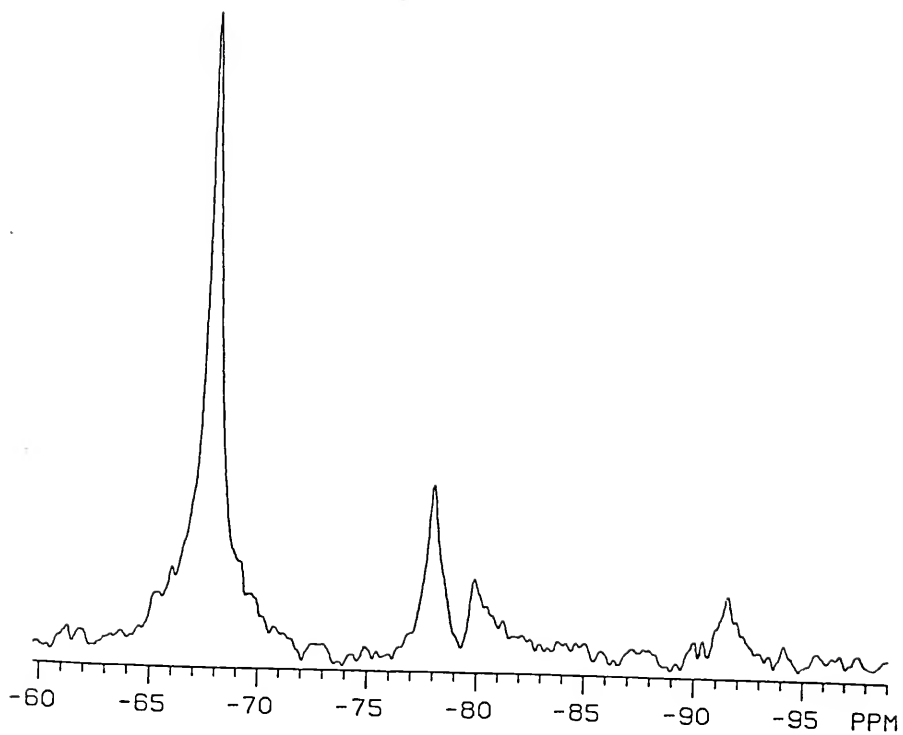
Figure 5-13. W^{183} NMR of $[(C_8H_{17})_3CH_3N]_{6-2x}[GeRh_2L_nW_{10+x}O_{38+x}]$ in 1:1 CD_3Cl_3/CH_3Cl_3.
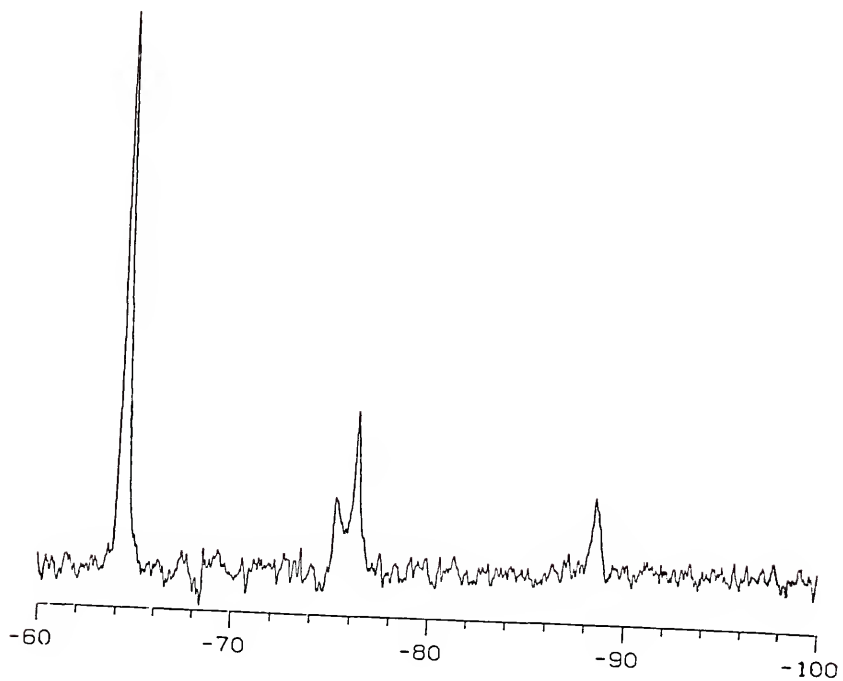
Figure 5-14. W^{183} NMR of $[(C_8H_{17})_3CH_3N]_{6-2x}[GeRh_2L_nW_{10+x}O_{38+x}]$ in 1:1 toluene-D_8/toluene.
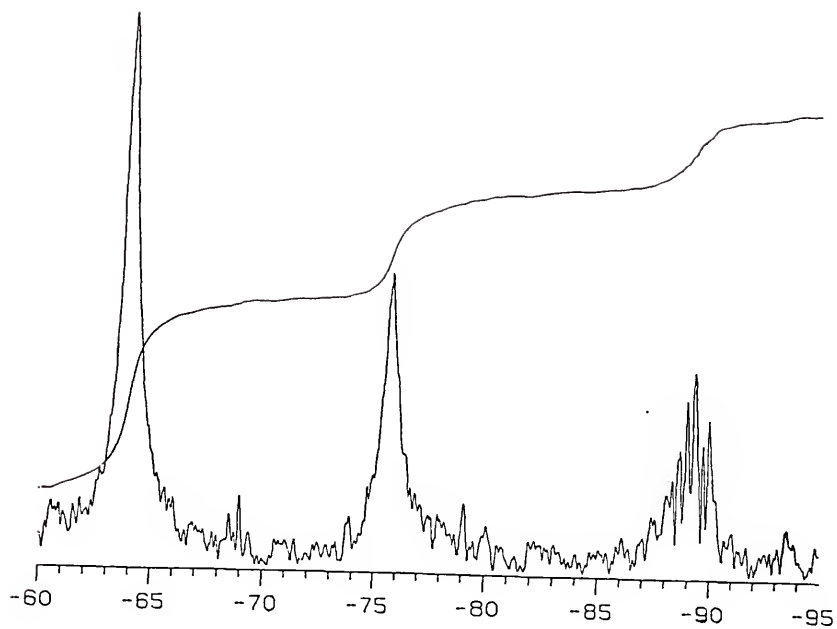
Table 5-4

W^{183} δ data for $[(C_8H_{17})_3CH_3N]_{6-2x}[GeRh_2L_2W_{10+x}O_{38+x}]$

Solvent	Chemical Shifts (ppm)			
CD_3CN/CH_3CN	-67.8(8.5)	-78.0(2.5)	-79.9(1.0)	-91.6(1.0)
	-67.0(7.9)	-77.4(2.3)	-79.1(1.0)	-90.9(1.2)[a]
$CDCl_3/CHCl_3$	-64.5(7.0)	-75.6(1.0)	-76.5(2.1)	-88.8(1.2)
	-64.2(6.6)	-75.6(1.2)	-76.6(2.2)	-88.7(1.0)[a]
Toluene/D_8	-64.0(2.7)	-75.8(1.5)	-89.4(1.0)[b]	
	-64.4(2.0)	-76.2(1.5)	-89.5(1.0)[a,b]	

a   spectra not shown
b   resonance split by noise peaks

such (toluene, 25-30 Hz; $CHCl_3$, 12-25Hz) that resolution of all
signals still may not be observed. It should be pointed out that
the samples are not spinning. Additionally, the signal to noise
ratio in some samples is low making interpretation difficult. The
chemical shifts between samples is fairly constant, within
±1 ppm. Of concern is the inconsistancy of the relative peak
intensities between samples and solvents. The first thing that
comes to mind is the cycle time, i.e. was there a long enough time
between pulses to allow the tungstens to relax? The cycle time
employed in the previous experiments was 2.39 seconds. It has been

suggested that the relaxation times in heteropolytungstates may be five seconds or greater.[225] Therefore, an experiment was conducted to see how the cycle time effected the observed signal intensities. The cycle time was varied from 0.256, 2.04, and 8.20 seconds for the RhHPA in chloroform and the results are shown in Table 5-5. The cycletime of 0.256 is probably less than T_1,

Table 5-5

Results Cycletime Experiment

cycletime	δ (ppm)[a]			
0.256	-64.0(9.1)	-74.9(1.0)	-76.1(1.7)	-88.3(1.3)
2.04	-64.2(8.2)	-75.1(1.1)	-76.3(2.2)	-88.5(1.0)
8.20	-64.2(7.9)	-75.1(1.1)	-76.3(2.0)	-88.5(1.0)

a   intensity ratio in parentheses

while 8.2 seconds is an unneccessarily long time. The digital resolution for a cycle time of 2.04 seconds seems adequate but maybe borderline. It would appear that the cycle time of 2.39 seconds employed in previous experiments was reasonable. In chloroform, the average intensity ratio of a 7:1:2:1 was observed when the cycle time was 2.39 seconds and a 8:1:2:1 at 8.20 seconds. Assuming an error of ±20%, a structure consisting of

10 or 11 tungstens is plausible. An ion pair $[Rh_2]^{4+}$ $[GeW_{12}O_{40}]^{4-}$ structure is unlikely based on IR results and experiments with the ion exchange resins. Additionally, $[GeW_{12}O_{40}]^{4-}$ would exhibit a single resonance (-81.9, D_2O). There is an isolable isomer of $[GeW_{12}O_{40}]^{4-}$ known as the β isomer which has C_{3v} symmetry and exhibits three resonances in the ratio 1:2:1 (-89.5, -91.6 and -104.4 ppm-D_2O). However, the β isomer rapidly converts to the primary or α form above room temperature[226] and since the RhHPA was prepared at 95 °C the formation of the β isomer was precluded.

The above NMR results are consistent with neither a "Rh_2W_{10}" nor a "Rh_2W_{11}" structure. Poor resolution may account for not observing the expected spectra. The W^{188} NMR for the trioctylmethylammonium salt of $GeW_{11}O_{39}^{8-}$ in acetonitrile should support or rule out the "Rh_2W_{11}" structure depending upon the observed spectrum.

Fast atom bombardment mass spectroscopy (FABMS) is an ideal technique for determining the molecular weights of large, polar, nonvolatile molecules. FABMS has recently been used successfully to establish the molecular formulas of heteropolyanions.[227,228] The positive ion FAB mass spectra and expansions for three different samples of the RhHPA prepared in the same way are shown in Figures 5-15 to 5-20. The spectra were obtained over a range of 2210 to 5590 m/z and no ions were detected above 5200 m/z. The three RhHPA samples, designated as A, B and C, all have protonated molecular ions around 4700 m/z. This represents the most abundant ion and not necessarily the average molecular weight. This value also differs from the wide scan range to the expansion, as shown in Table 5-6. The values in parentheses represent the next highest

Figure 5-15.   Positive ion FABMS of RhHPA sample A.
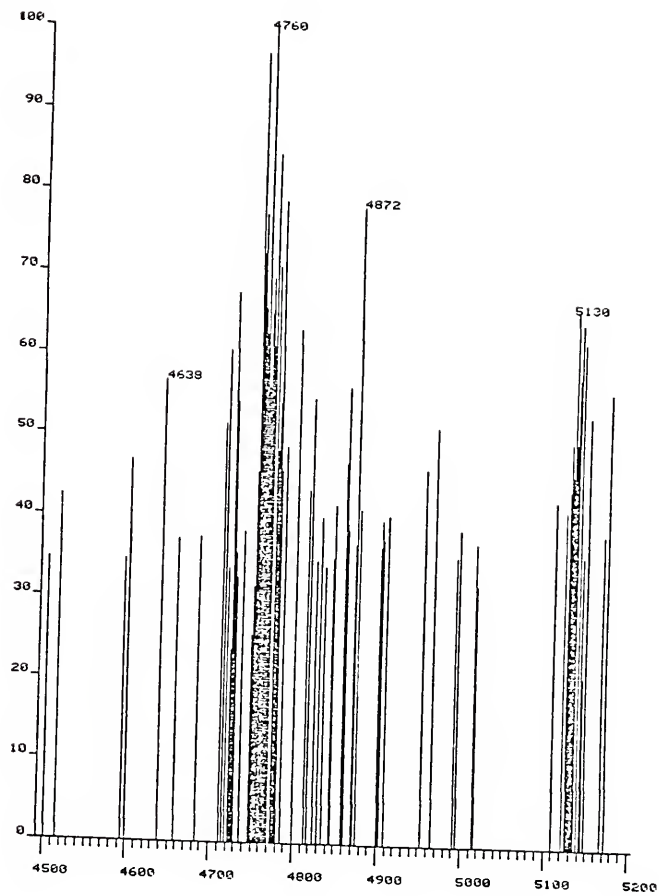
Figure 5-16. Expansion of positive ion FABMS of RhHPA sample A.
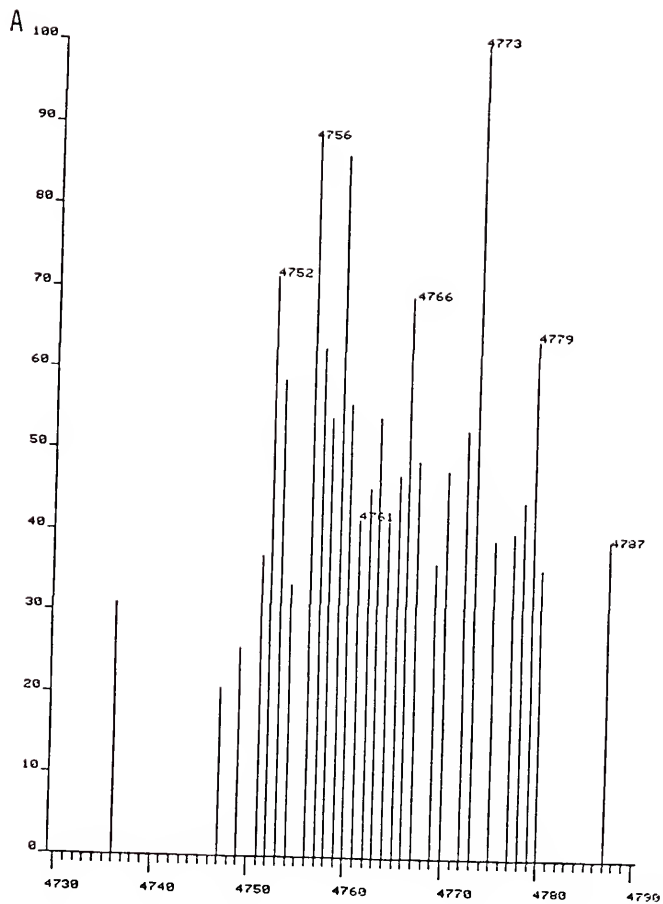
Figure 5-17. Positive ion FABMS of RhHPA sample B.
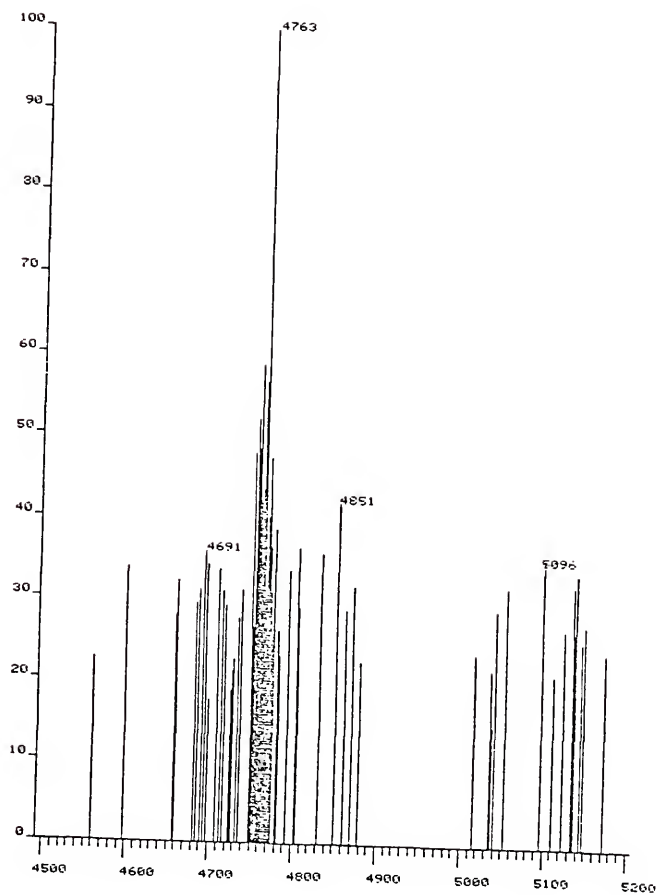
Figure 5-18. Expansion of positive ion FABMS of RhHPA sample B.
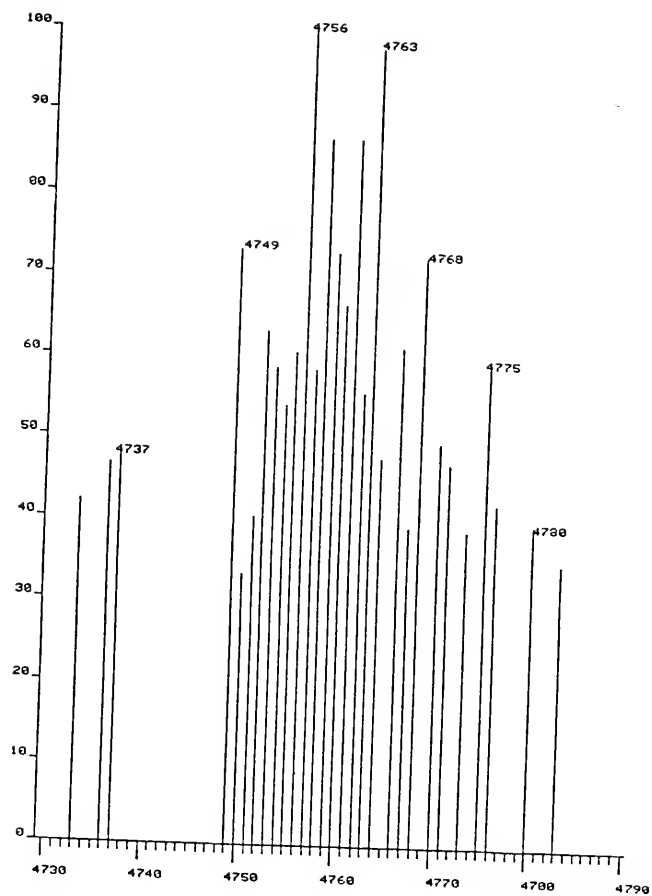
Figure 5-19. Positive ion FABMS of RhHPA sample C.
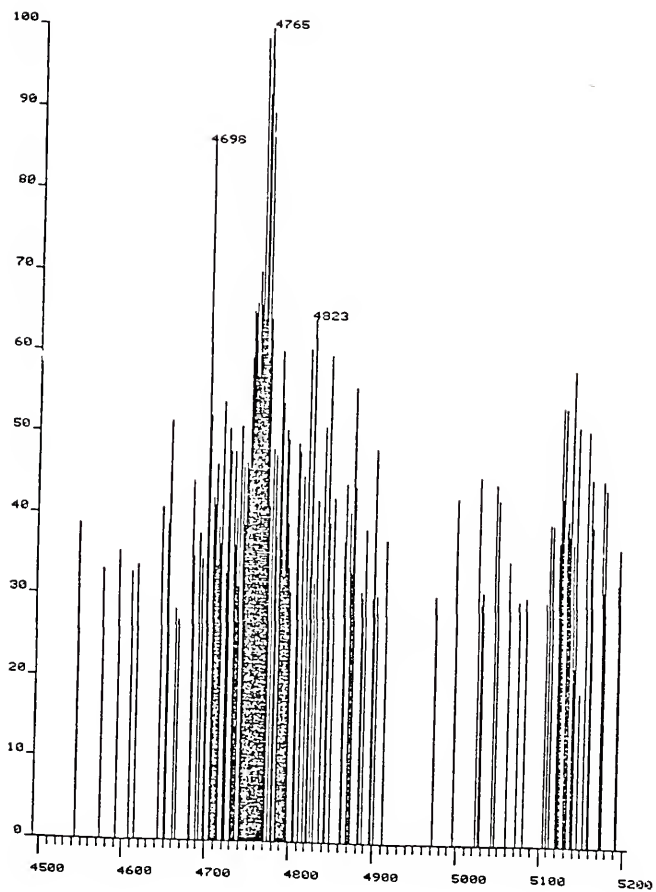
Figure 5-20. Expansion of positive ion FABMS of RhHPA sample C.
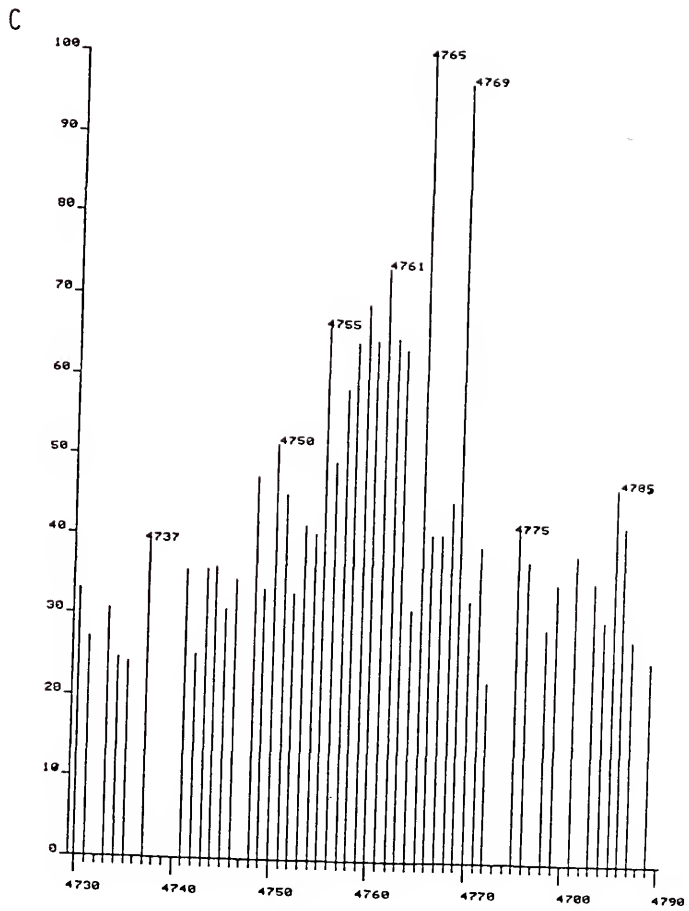
Table 5-6

FABMS Results

RhHPA	m/z	m/z (expansion)
A	4760	4773(4756)
B	4763	4756(4763)
C	4765	4765(4769)

peak. The nominal mass for a few different possible formulas for the RhHPA are shown below. There is usually a disparity between

$$[(C_8H_{17})_3CH_3N]_4[GeRh_2W_{11}O_{39}] \qquad 4399$$

$$[(C_8H_{17})_3CH_3N]_4[GeRh_2(H_2O)_8W_{11}O_{39}] \qquad 4543$$

$$[(C_8H_{17})_3CH_3N]_8[GeRh_2W_{10}O_{38}] \qquad 5671$$

$$[(C_8H_{17})_3CH_3N]_6[GeRh_2W_{10}O_{37}] \qquad 4919$$

$$Rh_2[GeW_{12}O_{40}] \qquad 3127$$

the most abundant mass ion and the calculated nominal mass, monoisotopic mass or average mass. In order to accurately interpret these results a computer simulation was done, but this only indicated that the scan range for these spectra was too large. The FABMS for these samples need to be recorded under a smaller range mass to be properly simulated and an effort in this regard is now being made. However, a few general obsservations can be made. For example, these results support the claim that Rh_2^{4+} is not present as simply an ion pair because the molecular masses

for such a such a species would be far too small. Secondly, it
would appear that the disubstituted anions may have molecular
masses greater than what is observed. If the waters are bound
tightly and can be calculated into the mass, then an HPA of the
formula $[(C_8H_{17})_3CH_3N]_4[GeRh_2(H_2O)_8W_{11}O_{39}]\cdot12H_2O$ would have a
nominal mass of 4760 as found in sample A.

The RhHPA is highly hydrated as evidenced by a strong OH
stretch in the IR where the Rh_2^{4+} heteroatoms presumably have
terminal aqua ligands. In poor donor solvents such as toluene,
benzene, methylene chloride, chloroform or carbontetrachloride the
green color is maintained with retention of the associated
waters. In stronger donor solvents such as acetonitrile, pyridine,
or methylimidazole the color changes from green to red-orange or
yellow. If an acetonitrile solution of the RhHPA is evaporated to
a reddish oil and allowed to stand in air, actually moist air given
the Florida humidity, the oil changes back to a green color. If
this process is monitored by infrared spectroscopy, the nitrile
stretch for associated acetonitrile gradually disappears and the OH
stretch grows back in. Within the limits of resolution of the IR
spectrometer, the frequency of νCN is the same as that for free
acetonitrile. The very weak coordination of CH_3CN will be of
importance for catalysis (vide infra). Such behavior is
reminisecnt of the trans influence exerted by the Rh-Rh bond in the
carboxylates which gives rise to weak Rh-axial ligand bonds. Some
of the color changes noted above parallel the behavior of
rhodium(II) carboxylates in various solvents or with different
bases. Generally, the rhodium(II) acetate are green or blue but

with π acids they are red-brown. Such changes have been studied
extensively by electronic spectroscopy in an effort to resolve the
controversial nature of the axial metal-ligand bond.[229-231] The
electronic spectra of heteropolyanions is usually dominated by
oxygen to metal charge transfer bands and provide little or no
structural information. However, for various heteroatoms their
ligand field spectra can provide information regarding the nature
of coordination. The tetrabutylammonium salt of the RhHPA was
soluble in acetonitrile but appeared to decompose when attempts
were made to recover it from solution. Therefore, all studies were
conducted with the trioctylmethylammonium salt. As previously
mentioned, the RhHPA in acetonitrile gradually changes from green
to red-orange. This exchange was monitored by UV-VIS spectroscopy
and shown in Figure 5-21. The hydrated RhHPA displays a broad band
at 575 nm and a shoulder at 475 nm. Over a span of 90 minutes, the
acetonitrile adduct is formed which produces two isobestic points
with a broad band at 490 mn. At very dilute concentrations, a $W \leftarrow O$
charge transfer band can be resolved at 270 mn which does not shift
upon changing solvents from toluene to acetonitrile. In toluene, a
very weak shoulder at 358 mn which possibly could be assigned to a
$Rh \leftarrow O$ CT. However, in acetonitrile this band could not be
resolved. The RhHPA was examined in a variety of solvents and the
results, shown in Table 5-7, are compared with some rhodium(II)
carboxylates. Much in the same manner as the rhodium(II)
carboxylates the RhHPA is reactive towards carbon monoxide. A
saturated carbon tetrachloride solution of the RhHPA exposed to
10 psig CO at room temperature for several hours displays a CO

Figure 5-21. The electronic spectrum of
$[C_8H_{17})_3CH_3N]_{6-2x}[GeRh_2(H_2O)_nW_{10+x}O_{38+x}]$ in acetonitrile.
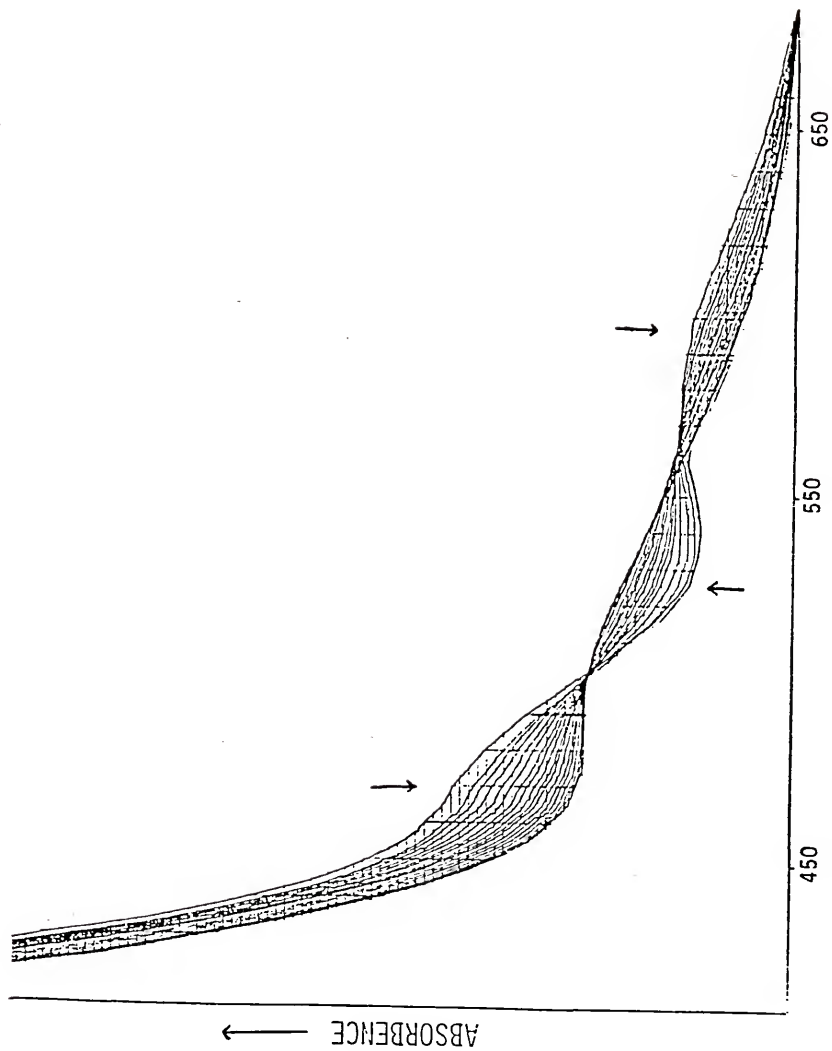
Table 5-7

Bands in Rh_2^{4+} Electronic Spectra

Rh_2^{4+}	Solvent	λ(mn)	
RhHPA	Toluene[a]	575, 470(sh)	
	CH_3CN	490	
	py	438, 490(sh)	
	1-MeIM	480	
	DMSO	490(sh)	
$Rh_2(OAc)_4$	H_2O	587, 447[b]	584, 441[c]
	CH_3CN	552, 437[b]	---
	DMSO	500[b]	497[c]
	py	---	514[c]
$Rh_2(But)_4$	CH_3CN	556[d]	
	py	518[d]	
	1-MeIM	527[d]	
Rh(III)HPA	H_2O	384(sh), 454(sh)[e]	

a H_2O adduct
b reference 229
c reference 230, solid state diffuse reflectance
d reference 231, 2:1 adducts in CH_2Cl_2
e reference 158

stretch in the infrared at 2134.8 cm^{-1}, shown in Figure 5-22. The CO adduct of rhodium(II) perflourobutyrate was reported as 2134.8 cm^{-1} (free CO 2143 cm^{-1}).[232] The RhHPA that did not dissolve in CCl_4 was redissolved in acetonitrile then evaporated to dryness the IR shows two weak bands at 2068.7 and 2073.2 cm^{-1}. The RhHPA recovered from the CCl_4 solution has a weak broad band in the same location. Taking the solid RhHPA freshly recovered from acetonitrile and exposing it to CO pressure results in two weak bands at 2968.3 and 2071.1 cm^{-1}. The nature of this much stronger CO adduct is uncertain but possibly the CO has reduced a small amount of Rh^{2+} to Rh^{+} which would bind the CO stronger. However, Rh_2^{3+} is very unstable and disruption of the Rh-Rh bond would be likely to occur.

The spectroscopic results described above support the existence of a Rh_2^{4+} species. However, the manner in which this moiety is substituted into the tungsten framework is less conclusive. The present results tend to favor a monosubstituted anion, as shown below. The infrared spectrum of the $GeW_{11}O_{39}^{8-}$
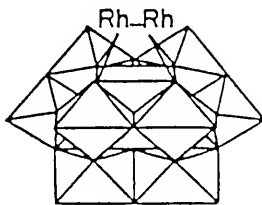
lacunary ligand is similar to the RhHPA. One might expect a more drastic shift in vibrational frequencies if an additional tungsten were removed upon coordination of Rh_2^{4+}, especially if one

Figure 5-22.   FT-IR of RhHPA + CO in CCl_4
A.   Before exposure to CO
B.   After exposure to CO, νCO = 2134.8 cm^{-1}.
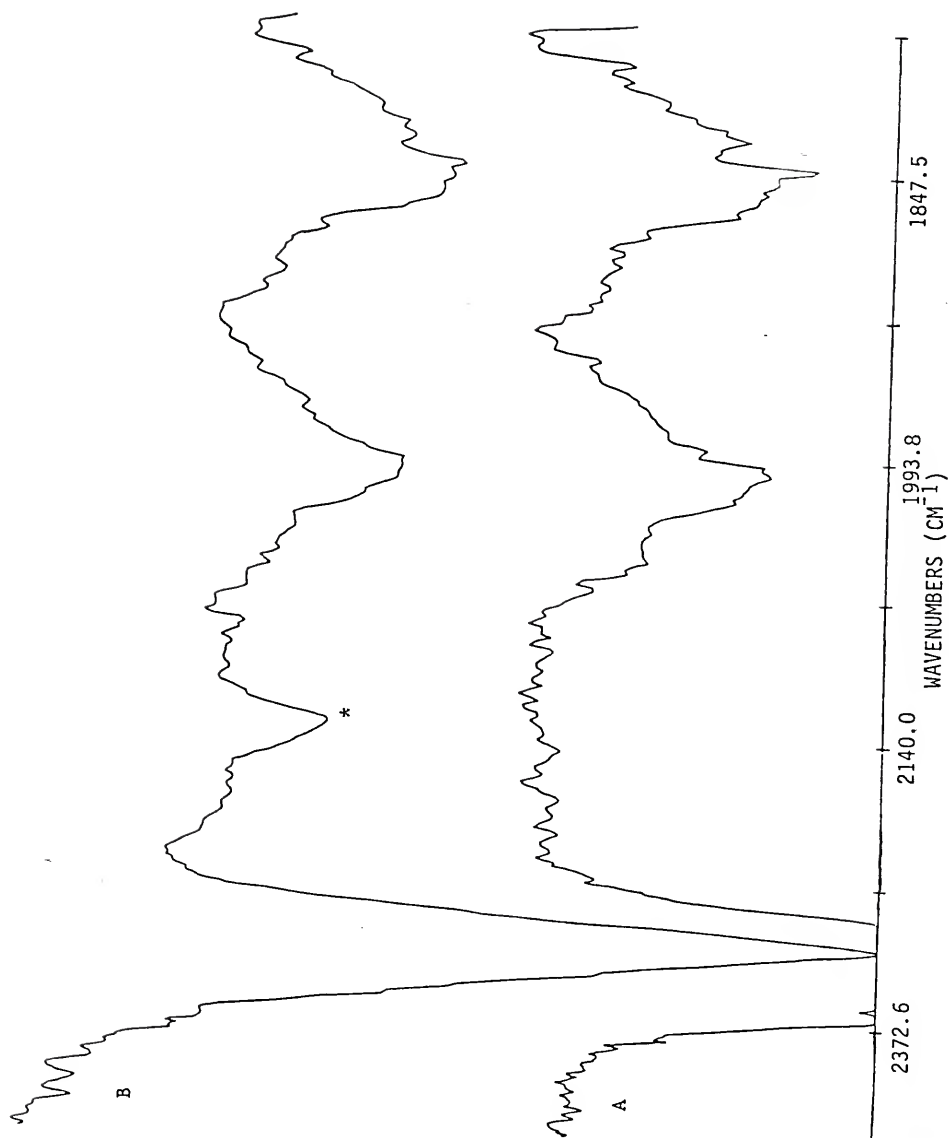
considers the average W-W distance in the Keggin ion is on the order of 3.4 A, whereas, the Rh-Rh bond is typically 2.7-2.8 A. Therefore, a deformation in the cage structure would result if two tungstens were replaced by two metal-metal bonded rhodiums which would be reflected in the IR. Additionally, the FABS results show no peaks above 5200 which is evidence against a "Rh_2W_{10}" configuration. The W^{183} NMR spectra will be more definative with the NMR results for $[(C_8H_{17})_3CH_3N]_8[GeW_{11}O_{39}]$.

Heteropolyanions are well known for their ability to accept multiple electrons without a major structural change and in most cases this is a reversible process. In mixed valent, HPAs the charge is somewhat delocalized throughout the tungstate framework. Usually, the energy between states is small enough that the intervalence charge transfer can occur by optical excitation giving rise to magnificantly colored compounds, heteropoly blues. Reduced anions have been classified as class II compounds according to the classification scheme of Robin and Day.[233] As a support, heteropolyanions can stabilize a variety of unusual oxidation states, such as Ni^{4+}, Re^{6+} and Td Co^{3+}. It was thought the heteropolytungstates under investigation might stablize a higher oxidation state of rhodium, such as the +4 state. Such a species would be interesting if it were stablized by the oxidatively resistant lacunary ligand. At best, there are a handful of isolable Rh^{4+} compounds. Recently, $RhO_2 \cdot 2H_2O$ was prepared by the ozonolysis of $Rh_2O_3 \cdot 5H_2O$.[234] This preparation was repeated. First

$$2Rh^{3+} \longrightarrow 2Rh^{4+} + 2e^- \qquad \varepsilon^0 \quad -1.43$$
$$O_3 + 2H^+ + 2e^- \longrightarrow O_2 + H_2O \qquad +2.07$$
$$\overline{O_3 + 2Rh^{3+} + 2H^+ \longrightarrow O_2 + 2Rh^{4+} + H_2O} \qquad +0.64 \text{ volts}$$
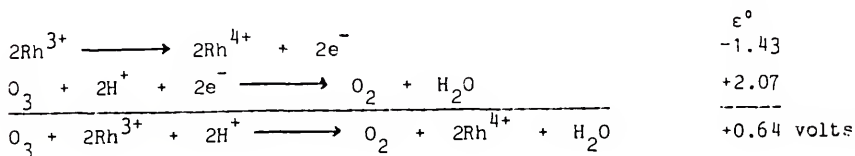
$Rh_2O_3 \cdot 5H_2O$ was precipitated from an aqueous $RhCl_3$ solution with KOH. The $Rh_2O_3 \cdot 5H_2O$ was then slurried in water and ozone bubbled through the solution for three hours. The light brown solid changed to a green-brown and a room temperature ESR was observed (g ~ 2.07). Unfortunately, the RhO_2 was quite insoluble (not even aqua regia would dissolve it) and of no synthetic utility. So, ozonolysis of the RhHPA was attempted directly since the polyoxoanion framework should be stable to O_3. Two grams of the tetrabutylammonium salt was slurried in 100 mL H_2O and O_3 bubbled through the solution for 8 hours. The solution was colorless and the RhHPA was a green-brown color. A room temperature ESR was observed (Figure 5-23) with a g ~ 2.06 and at liquid nitrogen temperatures the anisotropic spectrum was resolved (Figure 5-24). The spectrum is reminiscent of the spectra reported for Rh^{4+}. The question is, what is the nature of the Rh^{4+} coordination site? First, it should be noted that when rhodium(II) acetate is reacted with ozone the trinuclear rhodium(II) acetate $[Rh_3O(O_2CCH_3)_6(H_2O)_3]^+$ is found.[235] Other oxidants, such as Cl_2 or Ce^{4+}, produce oxidation products of unknown constitution. In the RhHPA case, it would be reasonable to assume the metal-metal bondis broken and a mononuclear Rh^{4+} species is formed. The isolation of a Rh^{4+} species bound to a heteropolytungstate would lend credence to the proposal that lacunary ligands can provide unusual stability to reactive metal centers.

To further explore the redox properties of the Rh_2^{4+} heteropolytungstate, cyclic voltammetry was conducted in acetonitrile solutions. The cyclic voltammograms (CV) for the

Figure 5-23. X-band ESR of Rh(IV)HPA powder (293 °K), g ~ 2.06.

200 G
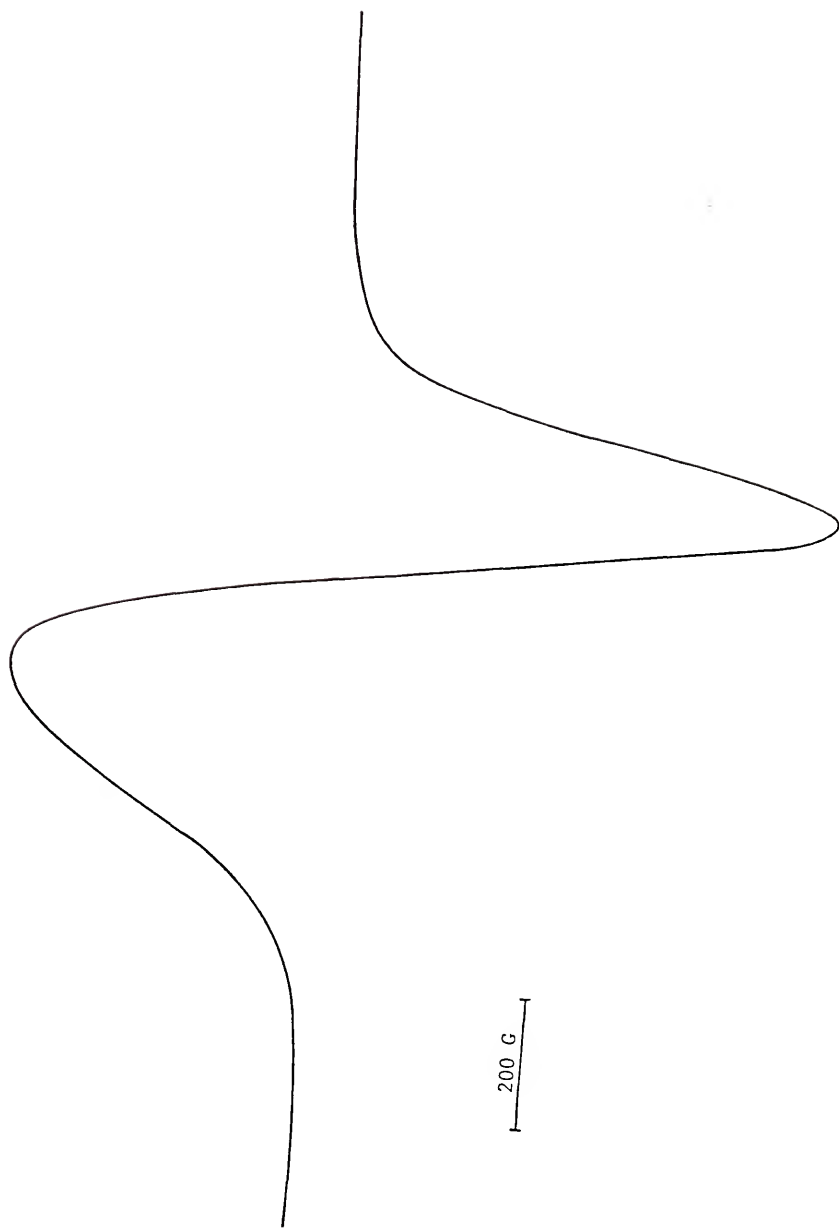
Figure 5-24. X-band ESR of Rh(IV)HPA powder (100 °K), $g_1 \sim 2.19$, $g_2 \sim 2.19$ and $g_3 \sim 1.97$.

g_2

g_3 →

← g_1

200 G
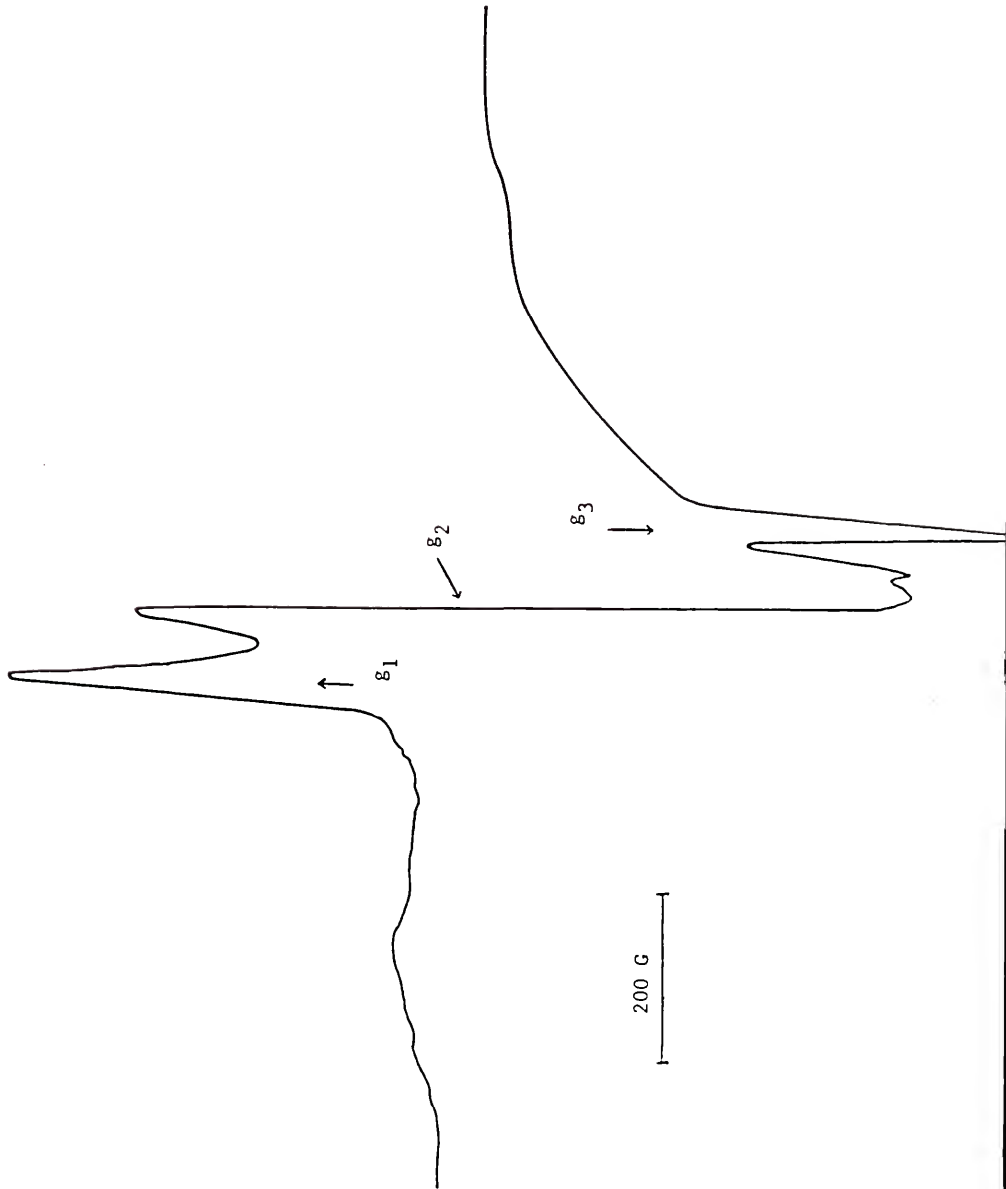
trioctylmethylammonium salt of $[GeW_{11}O_{39}]^{8-}$ and

$[GeRh_2W_{10+x}O_{38+x}]^{(6-2x)-}$ are shown in Figures 5-25 and Figure

5-26. Heteropolyainions are generally characterized by

multielectron waves, a positive potentials and a series of one

electron waves at the more negative potentials. Both the CV for

the lacunary ligand and the Rh complexed anion show a quasi

reversible wave and an irreversible peak at a very positive

potential. The calculated halfwave potential for the lacunary

ligand $E_{1/2} \sim +1.33$ volts (vs. NHE) and for the RhHPA

$E_{1/2} \sim +1.52$ volts (vs. NHE). The lower $E_{1/2}$ for the ligand can be

rationalized simply based on electrostatics since the ligand has a

much higher negative charge (-8 vs. -6 or less). Owing to these

large reduction peaks associated with the tungsten, it is unlikely

that any reductions associated with the rhodium will be observed.

Rhodium(II) acetate in acetonitrile shows a reversible wave at

+1.38 volts (vs. NHE) and if the Rh_2^{4+} moiety present in the RhHPA

has similar redox properties any half wave potentials would be in

the region of the cation oxidations. At the more negative

potentials, there are a series of anodic and cathodic waves which

are summarized below (in Table 5-8).

In general, for the RhHPA there is a shift to more negative

potentials compared to the lacunary ligand and the appearence of

additional waves at reducing potentials indicate that this anion

may be a very good oxidant.

To further attest to the redox capabilities of the RhHPA, a

series of photochemical experiments were conducted in order to

evaluate the oxidizing ability of this potential catalyst.

Figure 5-25. Cyclic Voltammogram for $[GeW_{11}O_{39}]^{8-}$ in acetonitrile from +1.7 to -1.7 volts, 0.1 M $(C_4H_9)_4NBF_4$, X = 100 mv/cm, Y = 100 mv/cm, 1 mA, 100 mv/sec.
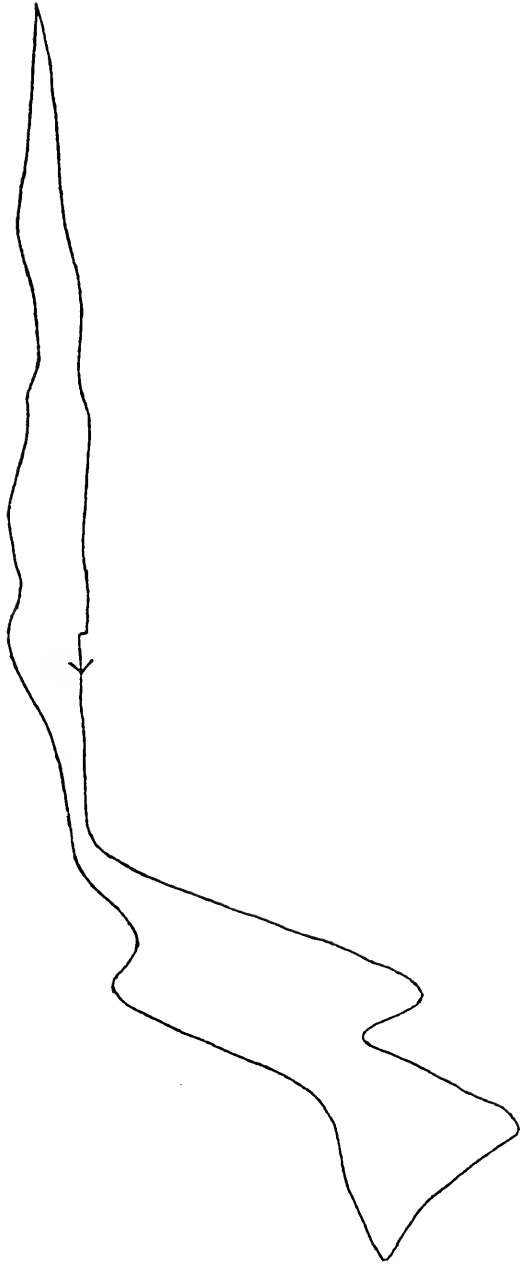
Figure 5-26. Cyclic Voltammogram for $[GeRh_2W_{10+x}O_{38+x}]^{(6-2x)-}$ in acetonitrile from +1.7 to -1.7 volts, 0.1 M $(C_4H_9)_4NBF_4$, X = 100 mv/cm, Y = 100 mv/cm, 1 mA, 100 mv/sec.
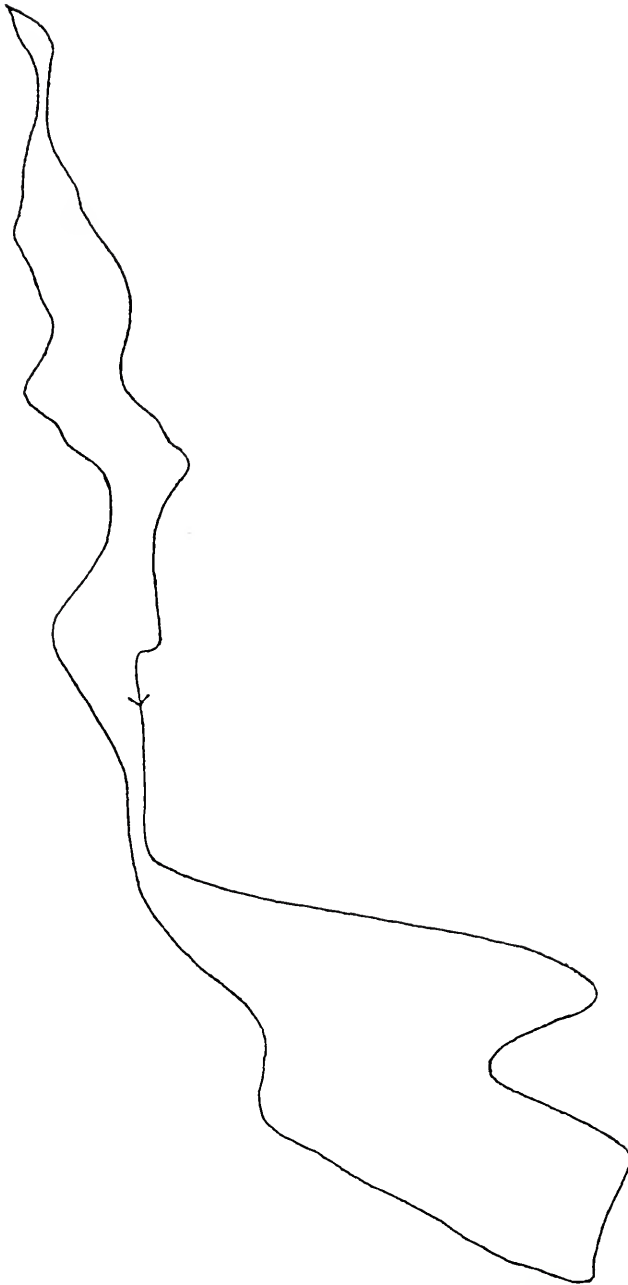
Table 5-8

HPA Cylic Voltametry Results

	Quasi reversible ($E_{1/2}$)	anodic	cathodic
$[GeW_{11}O_{39}]^{8-}$	+1.33	+1.17	+0.18
		+0.11	-0.14
		-0.33	-0.46
		-0.69	-0.94
$[GeRh_2W_{10+x}O_{38+x}]^{(6-2x)-}$	+1.52	+1.13	+0.14
		-0.29	-0.35
		-0.41	-0.50
		-0.69	-0.76
		-0.88	-0.93
		-1.05	-1.11

Employing a quartz shielded Havnia medium pressure mercury lamp as the light source, a p-xylene solution of the RhHPA was irradiated in a pyrex pressure bottle under argon for twelve hours and no color change was observed. Therefore, visible light would not initiate the reduction of the heteropolytungstate. When the same solution was irradiated in a quartz reaction vessel, the solution rapidly changed to a blue color. Upon exposure to air, the solution instantly changed to an orange-yellow color. Irradiating the sample again first produced a green color then a blue. This may suggest the green Rh_2^{4+} is oxidizing to a yellow $2Rh^{3+}$ with cleavage of the metal metal bond since the green color is no longer

air stable. During this reaction, GC analysis showed two unidentified oxidation products. Similar behavior is noted in both toluene and acetonitrile. The fact that this RhHPA can catalyze the photochemical oxidation of organic substrates is not unusual but it does encourage futher investigation into its oxidizing capabilities.

Oxidations with Molecular Oxygen

Oxidations with dioxygen or autoxidations can be spontaneous but more often they are catalyzed by metals. Liquid phase oxidations proceed by free radical chain reactions which can be controled by metal complexes. There are two types of metal catalyzed oxidations, namely homolytic and heterolytic.[236] The former being characterized by one electron changes and free radical intermediates. The later is characterized by two electron changes which usually involves coordination of the substrate to the metal center. Oxygen, which is potentially a four electron acceptor, interacts with transition metals in varied and complex ways making the homolytic or heterolytic nature of a reaction difficult to control. Some factors which govern the nature of an oxidation include the choice of metal, ligand system, solvent, temperature and substrate. Ideally the metal complex would have oxidatively resistant ligands, open coordination sites and available multiple oxidation states. The rhodium(II) heteropolytungstate fulfills all these requirements in that the polyoxoanion ligand is resistent to oxidation, the terminal ligands on the Rh_2^{4+} are quite labile allowing for coordination of substrate and the redox behavior of the RhHPA has previously been shown to be very active.

The RhHPA was screened for its ability to catalyze the oxidation of various substrates with dioxygen. Triphenlyphosphine is a fairly easily oxidized substrate and the RhHPA was found to catalyze this reaction, as shown below. Many metal complexes

$$2PPh_3 \quad + \quad O_2 \quad \xrightarrow[60°,\ DMF]{RhHPA} \quad 2Ph_3PO$$
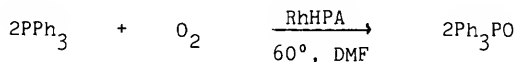
catalyze the oxygenation of phosphines[237] including rhodium complexes such as $Rh(PPh_3)_3Cl$ which has also been shown to be an effective catalyst for the oxidation of cyclohexene.[237,238] There is evidence that the cyclohexene reaction proceeds by a free radical chain mechanism. The autoxidation of cyclohexene generally affords a mixture of products including cyclohexenylperoxide, 2-cyclohexen-1-one, 2-cyclohexen-1-ol and cyclohexene oxide as shown below.
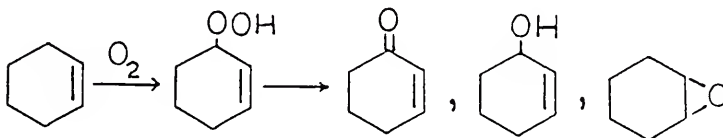
$Rh(PPh_3)_3Cl$ produced approximately a 60:40 ratio of allylic ketone to allylic alcohol.[239] This reaction appears to proceed by first formation of an alkyl peroxo species followed by peroxide decomposition to the observed products. The peroxide decomposition can be described by a Haber-Weiss type mechanism shown below

$$ROOH \quad + \quad Rh(III) \quad \longrightarrow \quad ROO\cdot \quad + \quad H^+ \quad + \quad Rh(II)$$

$$ROOH \quad + \quad Rh(II) \quad \longrightarrow \quad RO\cdot \quad + \quad OH^- \quad + \quad Rh(III)$$

or alternatively,

$$2ROOH + Rh(III) \longrightarrow 2ROO\cdot + 2H^+ + Rh(I)$$

$$2ROOH + Rh(I) \longrightarrow 2RO\cdot + 2OH^- + Rh(III)$$
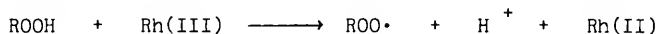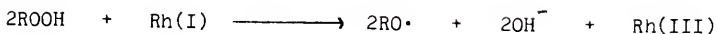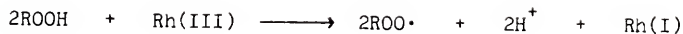
In contrast to this reaction the selective oxidations of cyclohexene with t-butlyperoxide catalyzed by rhodium(II) acetate, $Rh_2(O_2CCH_3)_4$ and μ_3-oxotrirhodium(III) acetate, $[Rh_3O(O_2CCH_3)_6(H_2O)_6]^+$, were recently reported to proceed via non radical chain pathways.[240,241] At 25 °C in acetic acid, the $Rh_2(O_2CCH_3)_4$/tBHP system was as much as 90% selective for the α,β-unsaturated carbonyl product. Using molecular oxygen as the oxidant the $Rh_2(O_2CCH_3)_4$ was only 73% selective for the enone. The RhHPA, $[GeRh_2W_{10+x}O_{38+x}]^{(6-2x)-}$ is similar to the rhodium(II) acetate in that it contains the Rh_2^{4+} moiety complexed to an oxidatively resistent lacunary anion. Since $Rh_2(O_2CCH_3)_4$ has unusual catalytic properties it is of interest to probe the stability and activity of the Rh_2^{4+} in the HPA coordination sphere.

The RhHPA in acetonitrile at 50 °C was found to catalyze the oxidation of cyclohexene to 2-cyclohexene-1-one with O_2 (40 psig) and with a selectivity from 70-95% depending upon the reaction conditions. In the absence of trace peroxides, free radical scavengers such as substituted phenols and N-phenyl-1-naphthylamine inhibited the oxidation attesting to the free radical nature of the reaction. However, in the presence of peroxides, radical traps had

no effect on the activity or selectivity of the reaction, suggesting a radical but not chain process. In the pages that follow, the attempts to characterize this system as well as the extension of this catalyst to other substrates will be described.

General features

The RhHPA did not catlyze the oxidation of cyclohexene to any measurable extent at room temperature or atmospheric pressure. The typical reaction conditions employed were 50 °C and 40 psig O_2. The reaction appears to be independent of oxygen pressure, for example, no increase in activity is observed between reactions run under 40 psig and 70 psig O_2. The primary oxidation product is the allylic ketone with small amounts (< 20%) of the allylic alcohol. Water is also continuously produced in the reaction but was not quantified. The production of allylic ketone vs. time is plotted in Figure 5-27. As can be seen from this curve, there is an induction period which varies in length depending upon the experimental conditions. Upon dissolution of the RhHPA in CH_3CN, the color changes from green to red-orange, the result of exchange of water for CH_3CN. This process has little if any effect on the induction period as confirmed by allowing an HPA solution to incubate for two hours prior to addition of the substrate and then observing no change in the induction period compared to that of a freshly prepared solution. It is more likely that these early stages of the reaction involve formation of a steady state concentration of a peroxy species, most likely cyclohexenyl peroxide, since in reactions where trace peroxides were present initially no induction period was observed. Following the

Figure 5-27.   Product 2-cyclohexen-1-one for RhHPA catalyzed
               oxidation of 5 mL cyclohexene in 50 mL acetonitrile
               (50 °C, 40 psig O_2).
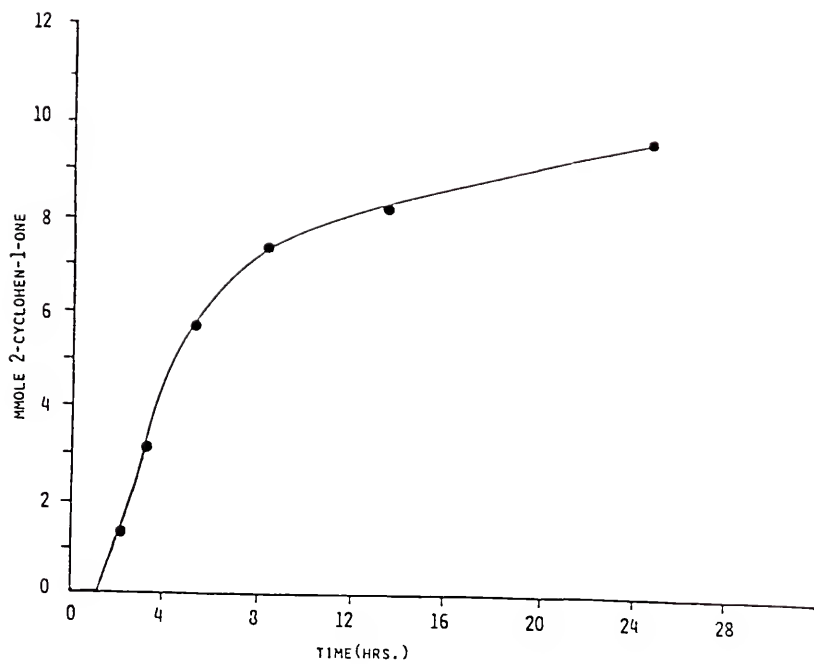
induction period, the allylic ketone is produced continuously for up to approximately 10 to 12 hours then the activity falls off (see Figure 5-27). The catalyst never really dies but is transformed to a less active and less selective form. This catalyst can be recovered and reused in subsequent oxidations but with the reduced activity corresponding to the later stages of the reaction. It appears that for every mole of enone produced approximately one mole of O_2 is consumed (Figure 5-28). In other words, only one oxygen atom of O_2 is incorporated into the allylic ketone. The other oxygen atom probably ends up as water as one might expect in a peroxide decomposition. The reaction appears to be first order in RhHPA and first order in olefin substrate. However, as the olefin concentration is increased the selectivity decreases. This data is summarized in Table 5-9. Products were first observed after 5 hours for the reaction with 0.021 mmole RhHPA and all other exhibited products after 3 hours.

Solvents

Nitrile solvents were found to be the only solvents in which the RhHPA would catalyze the oxidation of cyclic olefins. In acetonitrile, under 40 psig of oxygen and 50 °C, 100 moles of 2-cyclohexen-1-one are produced from cyclohexene per mole of RhHPA (moles RhHPA calculated using the most abundant molecular ion mass from FABMS results) in a 24 hour period.

For a series of nitrile solvents, the induction period increases and the catalyst activity decreased in the following order, $CH_3CN > CH_3CH_2CN > C_6H_6CN$. The importance of the nitrile solvents in the RhHPA/O_2 oxidations is twofold. First of all the

Figure 5-28. mmoles of O_2 and 2-cyclohexen-1-one vs. time. RhHPA/CH_3CN, 50 °C, 60 psig O_2.
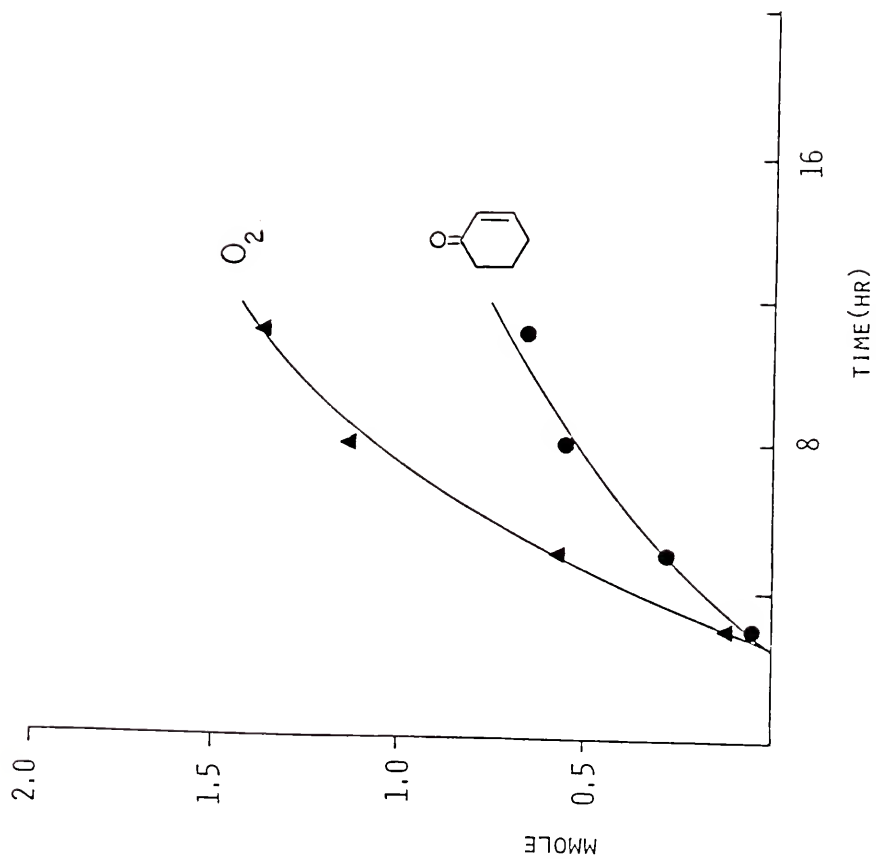
Table 5-9[a]

RhHPA Oxidation of Cyclohexene

mmole RhHPA	mmole enone (after 5 hours)	%enone	turnovers
0.021	0.4	94	19.0
0.063	2.8	93	44.4
0.015	3.8	94	36.2
0.105[b]	4.8	95	45.7
0.105[c]	6.3	76	62.8
0.147	4.3	96	29.3

a. 40 psig O_2, in 50 °C, 50 mL of CH_3CN, 5 mL of cyclohexene
b. 7 mL of cyclohexne
c. 9 mL of cyclohexene

nitriles are weakly solvating, apparently this lability is essential for the reaction to proceed. In strong donor solvents such as pyridine, no oxidation occurs presumably because the pyridine is bound tighter eliminating possible substrate coordination sites. On the other hand, solvents such as toluene do not displace the waters on the coordination sphere. Secondly, the nitriles somehow facilitate the production of alkylperoxides. This effect has been noted before in the production of alkylperoxides.[242] Additionally, acetonitrile may be directly involved in the oxidation in the form of a peroxyimidic acid which can be generated with H_2O_2 as follows,

$$RCN \quad + \quad H_2O_2 \quad \xrightarrow{\overset{OH^-}{\quad\quad}} \quad \overset{NH}{RCOOH}$$

Peroxymidic acids have been generated from both acetonitrile[243] and benzonitrile[244] in this manner. Such a reagent has been empolyed in the epoxidation of cyclooctene.[245]

As memtioned previously, water is continuously produced in the reaction. Therefore, it was desirable to know if water influences the reaction pathway. Water scavengers, such as dimethoxypropane, have no effect on the reaction but in the presence of 4A molecular sieves the reaction is accelerated as shown in Figure 5-29. There is also a decrease in the induction period. A slight loss in selectivity (88% vs. 95% without sieves) was noted. The fact that DMP has no effect on the catalyst activity leads one to suspect the Bronsted or Lewis acid properties of the sieves may have a role in the reaction. The results for a series of acids and bases a shown in Table 5-10. The adipic and benzoic acid were chosen because

Table 5-10

Effects of Additives

additive	induction period (hours)	enone (mmole)	% product
adipic acid	< 9.5	6.6	70
benzoic acid	< 10.0	3.7	70
2,6-lutiene	< 10.0	- 2.9	72
Na_2CO_3	< 2.0	9.8	89
$SnCl_4$	no reaction		

Figure 5-29. Plot of mmoles 2-cyclohexene-1-one product vs. time,
             RhHPA/CH$_3$CN, 50 °C, 40 psig O$_2$,   with 4A molecular
             sieves,   without sieves.
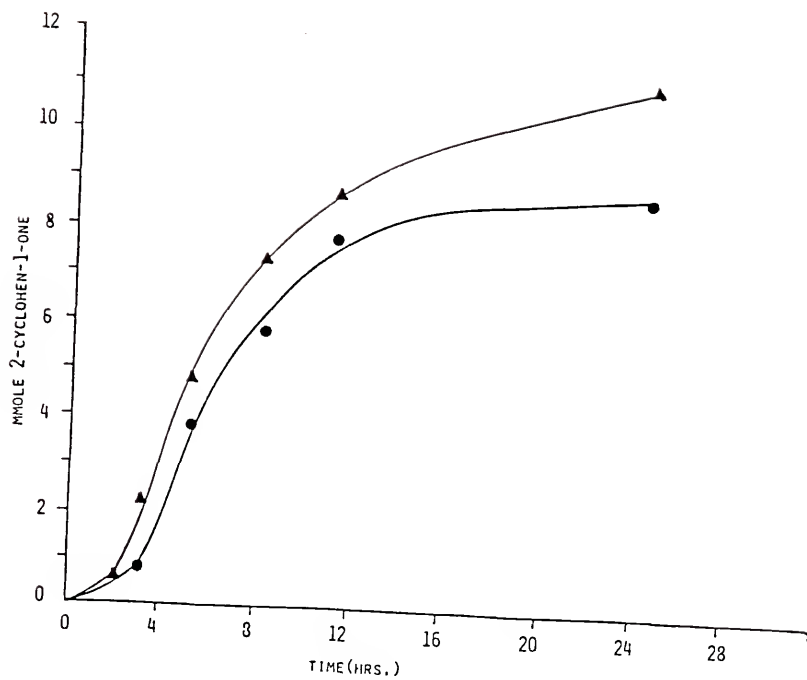
they could be formed as products. The carboxylic acid drastically increased the induction period and decreased both the activity and selectivity. The addition of cabonate ion decreases the induction period and improves the activity. Therefore, it would appear acid has an inhibitory effect. In this regard, lutidene is an anomoly because one might expect it to act as a proton spunge. Based on steric considerations, lutidene should not bind to the Rh_2^{4+} but there may be a weak interaction. This would be consistent with the fact that no catalytic activity is observed in peridene solvent whereas a dilute peridene solution may have some activity. A Lewis acid, such as stannic chloride, completely inhibits the reaction. This suggests the $CNCl_4$ is interacting with Rh preventing O_2 activation and formation of alkyl peroxides. Therefore, a series of co-catylists were investigated in an effort to get a mechanistic handle on the O_2 activation process. It was thought that the addition of a copper catalyst might promote formation of peroxide or acitvate the olefins as in the Rh/Cu 1-hexene oxidation (vide infra). However, in the presence of Cu(I) or Cu(II) salts, the reaction was completely inhibited even copper metal inhibited the reaction which warrented the use of a stainless steel pressure head. It is possible that the copper ions can displace the Rh_2^{4+} from the tungstate, generating a catalytically inactive species.

Deactivated catalyst

When the catalytic reaction is evaporated to dryness, a red-brown oil is recovered and unlike its catalytic precursor it does not turn green upon standing. The infrared spectra for this HPA, after reaction with cyclohexene and cyclohexenal peroxide, are shown in Figures 4-30 and 4-31 respectively. The tungstate

Figure 5-30.   FT-IR of deactivated RhHPA catalyst with reaction with cyclohexene.
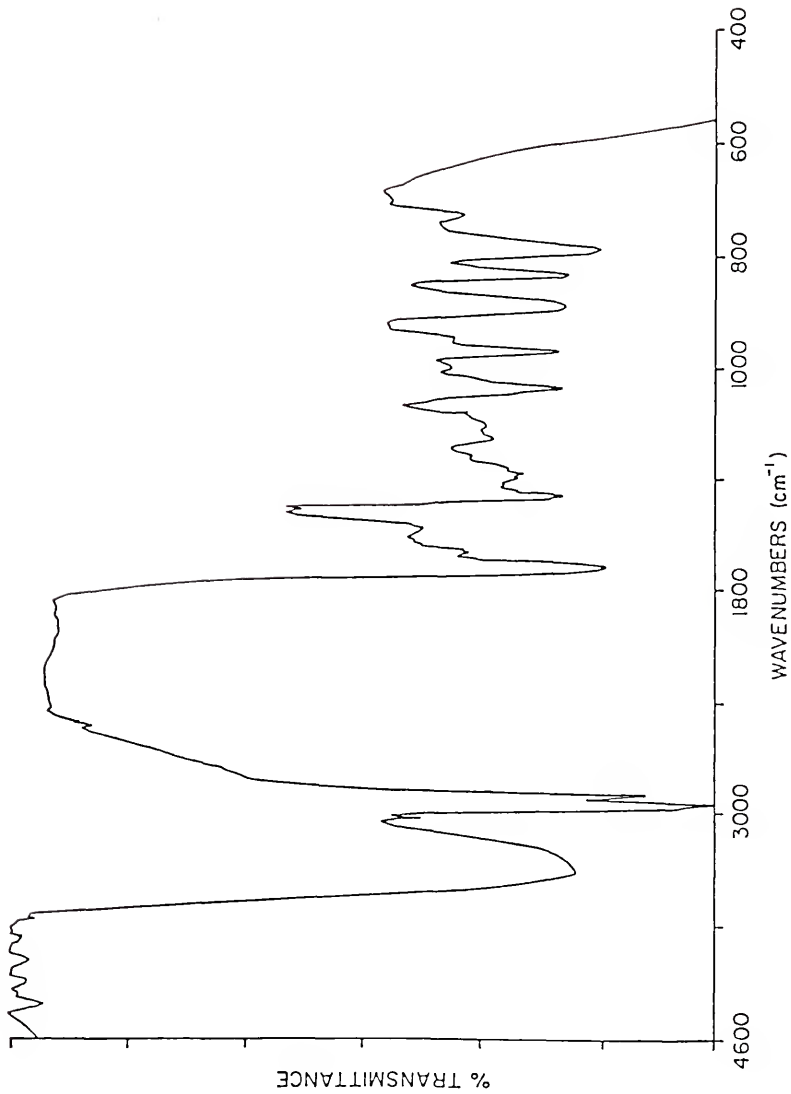
Figure 5-31.   FT-IR of deactivated RhHPA catalyst with reaction with cyclohexenol peroxide.

% TRANSMITTANCE vs WAVENUMBERS (cm⁻¹)
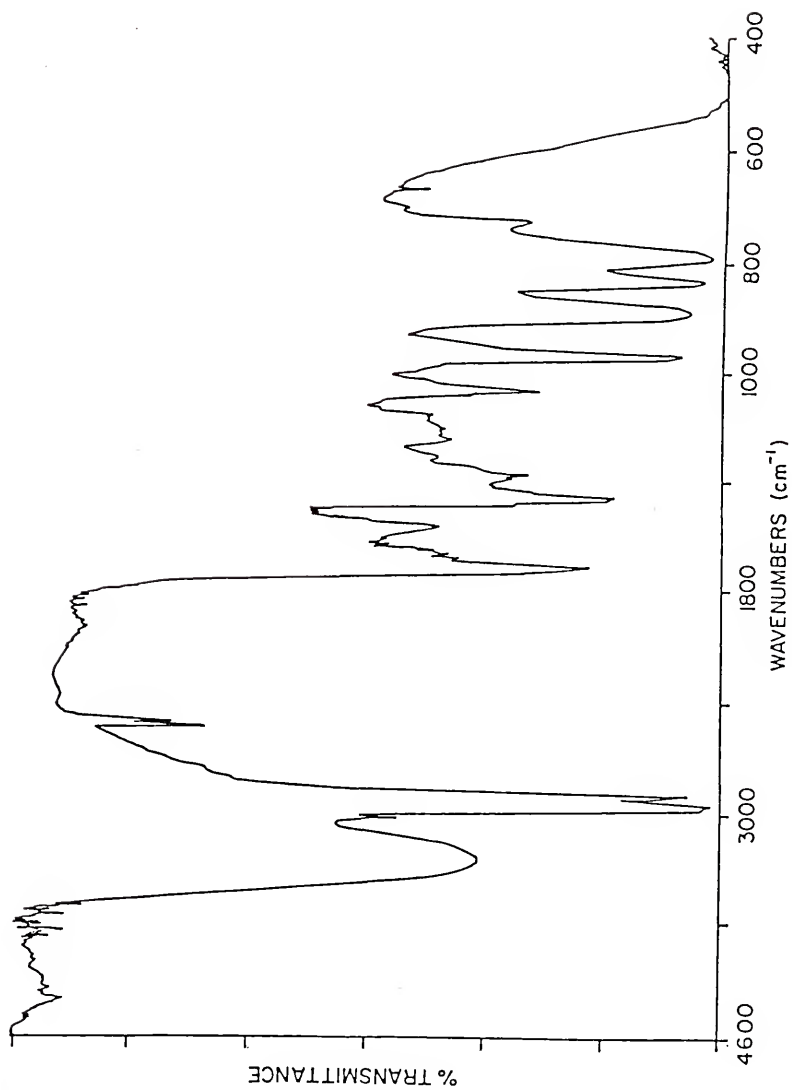
framework appears to have remained intact as evidenced by no change in the metal oxygen streaching frequencies. There is a new band at 1717 cm^{-1} which would be consistant with a carboxylate functionality. It is possible that carboxilic acids are generated as minor products and can chelate the rhodiums, inhibiting catalytic activity. However, C^{13} NMR of this catalyst showed no evidence of a carboxilate species and washing the catalyst with hydrochloric acid had no effect on the IR spectra.

The red-brown color is typical of Rh(III). Exposing the deactivated catalyst to hydrozene vapors, turns the catalyst green but after the vapors disapate, the oil reverts back to the red-brown color. The electronic spectrum of this HPA is masked by the large W$\leftarrow$O CT band. It would appear that the Rh metal-metal bond has been broken to generate a monomeric Rh(III) species. Further characterization by W^{183} NMR may confirm this.

This red-brown HPA can be dried and reused as a catalyst for the oxidation of cyclohexene. However, it is less active and less selective (88%) which would be consistant with the reactivity of other Rh(III) autoxidation catalyst.

Oxidations with Alkylperoxides

In the RhHPA catalyzed oxidation of cyclic olefins with dioxygen, the production of alkyl peroxides is implicated during the induction period. This is indicated by the fact that in the presence of trace peroxides there is no induction period and peroxides were detected in active catalytic solutions iodometrically. In the presence of tertbutylhydroperoxide (2.5 mmoles) at 50 °C under argon, the RhHPA (0.1 mmoles) catalyzed

the oxidation of cyclohexene to 2-cyclohexen-1-one (3.82 mmoles in 24 hours). This is compared to $Rh_2(O_2CCH_3)_4$ (0.05 mmoles) and tBHP (10 mmoles) in acetic acid at 25 °C which produced 2.84 mmoles of the allylic ketone over three days. Unlike the oxidations with dioxygen, the presence of trace peroxides precludes the need for a nitrile solvent. The RhHPA (0.1 mmoles) and tBHP (2.5 mmoles) at 40 °C in toluene oxidizes cyclohexene to primarily (93%) the allylic ketone. There is, however, substantial oxidation of the solvent to benzaldehyde.

Of more relevence to the cyclohexene oxidations is the decomposition of cyclohexenyl peroxide. Under argon at 50 °C, cyclohexenyl peroxide is selectively decomposed to 2-cyclohexen-1-one in the presence of the RhHPA in acetonitrile. Under these conditions, no other measurable products were observed. In the presence of oxygen, 120 turnovers were observed in 24 hours with no induction period. If under similar conditions, 2,6-dimethylphenol was present in the solution there was only a slight loss in activity (79 turnovers in 24 hours). This is contrast to solutions where trace peroxides were removed and substituted phenols completely inhibit the reaction. This suggests the peroxide decomposition proceeds by a nonradical chain pathway. The slight retardation of the catalyst activity in the presence of radical scavengers can be attributed to deactivation of the Rh_2^{4+} catalyst and generation of a Rh^{3+} autoxidation catalyst (vide infra).

In the presence of iodosylbenzene, the RhHPA will oxidize cyclohexene to 2-cyclohexene-1-ol and trace quantities of cyclohexene oxide.

Mechanism

Since the catalytic solutions containing peroxides are active even in the presence of radical traps, a Haber-Weiss mechanism can be ruled out. A mechanism more consistant with the general features of this reaction is shown in Figure 5-32. The Rh_2^{4+} may initially activate molecular oxygen and generate free peroxide. The Rh(III) could coordinate an olefin. A possible side reaction could then be β-hydride elimination to yield cyclohexadiene which in fact has been identified as a trace product. The coordinated olefin could be oxidized to yield an alkyl radical which could then react with O_2 and abstract a hydrogen from solvent or substrate to give cyclohexenol peroxide. The formation of alkyl radicals would be inhibited by radical traps. It should be pointed out that, both Rh(III) and Rh(II) are known to coordinate olefins. However if Rh(II) oxidized the olefin, the resulting Rh(I) would be unstable in the tungstate framework. It should also be pointed out that a 3+-3+ would not be metal-metal bonded and 3+-2+ complex would be unstable. This is consistant with the deactivated catalyst being a Rh(III) species, resulting from disruption of the metal-metal bond during oxidation. The peroxide decomposition is not effected by radical scavengers, therefore, a conserted mechanism is proposed to account for formation of primarily the allylic acid. Decomposition of the peroxide to the enol followed by oxidation to the ketone is ruled out since the RhHPA was observed not to oxidize the alcohol.

Figure 5-32. Proposed mechanism for the RhHPA catalyzed oxidation of cyclohexene.
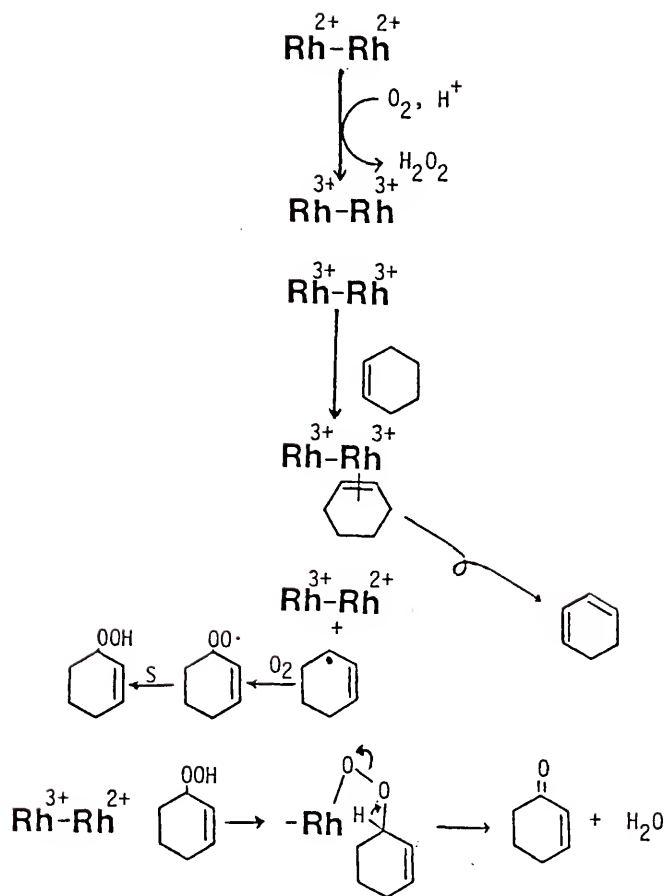
1-hexene Oxidation

Mimoun recently reported that rhodium trichloride in the presence of a copper or iron cocatalyst selectivity oxidizes (>98%) termenal olefins to methyl ketones in protic media.[246,247] Some of the general features of this reaction include a dependence on alcohol solvents for the initial reduction of Rh(II), inclusion of 98% of the oxygen atoms in the 2-ketone products, a first order dependence on both Rh(III) and olefin, a zero order dependence on oxygen pressure and a need for three equivalents of chloride ion for maximum activity. Further investigations of this unique system by Drago have resulted in a proposed mechanism consistent with the experimental results.[248,249] The active catalyst is now characterized as a rhodium(III) chloride complex produced as shown below. In an effort to understand the role of Cu^{2+} in this system,

$$RhCl_3 \quad + \quad Cu^{2+} \quad + \quad \tfrac{1}{2}(CH_3)_2CHOH \quad \longrightarrow$$

$$RhCl_2^+ \quad + \quad CuCl(s) \quad + \quad \tfrac{1}{2}(CH_3)_2CO \quad + \quad H^+$$
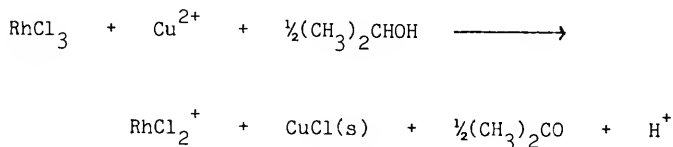
the oxidation of 1-hexene was studied in both the presence and absence of Cu^{2+}. The rhodium only system was far less active than the Rh(III)/Cu(II) system and only one oxygen atom of O_2 is incorporated into the ketone product. Additionally, water is continuously produced unlike the Rh(III)/Cu(II) system and maybe a factor in the catalyst deactivation. The following catalytic pathway was proposed for the $RhCl_3$ catalyzed oxidation of olefins.

H^+

H_2O → $RhCl_3$

$CH_3CHR'OH$

$Rh^{3+}OH$

H^+

$Rh^{3+} - O - \overset{R'}{\underset{CH_3}{CH}}$

CH_3CRO

OH

H^+

H_2O_2

H^+

$CH_3CR'O$

Rh
$\overset{|}{HC} - \overset{O}{C} - H$
H   R

Rh^+

H^+

RhOOH
$CH_2 = CHR$

H^+

O_2

RhOOH

$CH_2 = CHR$
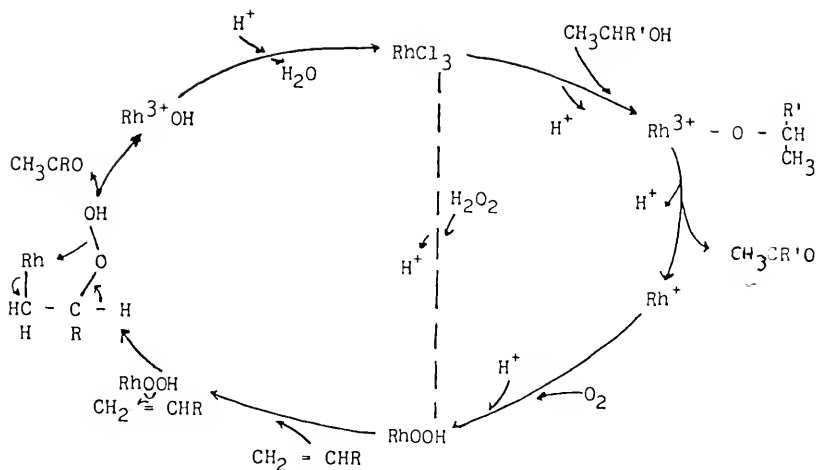
In contrast to the Rh(III)/Cu(II) system, the solvent is
continuously oxidized which yields the following reaction
stoichiometry.

$$RCH = CH_2 + O_2 + (CH_3)_2CHOH \xrightarrow{RhCl_3}$$
$$\underset{O}{R}CCH_3 + (CH_3)CO + H_2O$$
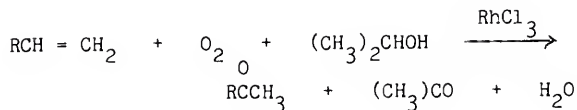
These results helped to establish the role of Cu^{2+} in the
mixed metal system. The importance of Cu^{2+} is twofold, (1) the
stoichmetric unsatruation of $RhCl_3$ in the initiation step as shown
above the reduction of O_2 to peroxide which is quickly captured by
the Rh(III) catalytic cycles shown in Figure 5-33. Mechanism A is
similar to that proposed for the Rh only oxidations except the
Cu^+/Cu^{2+} couple is involved in the unsaturation and reoxidation of
the Rh catalyst. Alernatively, in mechanism B, Cu^+ catalyzes the
addition of the olefin to the rhodium peroxy species.

Figure 5-33.   Proposed mechanism for the Rh(III)/Cu(II) catalyzed oxidation of terminal olefins with molecular oxygen.

As was previously mentioned, heteropolyanions have been employed as a cooxidants in the Pd catalyzed Wacker oxidations, replacing the corrosive $CuCl_2$. In a similar way, $CuH_2SiW_{12}O_{40}$, $CuHPW_{12}O_{40}$ and $CuHPMo_{12}O_{40}$ have recently been used in place of the $Cu(ClO_4)_2$ in the Mimoun Rh/Cu system.[250] The oxidation of 1-octene by $RhCl_3$ and $CuH_2SiW_{12}O_{40}$ was comparable to the Mimoun system in both activity and selectivity (>98%). In this system, it is speculated that the role of the CuHPA, as a counter ion, is to stericaly modify the Rh catalyst but not participate in any redox chemistry.

In light of these results, the RhHPA was investigated as a catalyst for the oxidation of 1-hexene in 2-propanol. Placing the trioctylmethylammonium RhHPA salt in 2-propanol resulted in a green solution with gradual formation of a white precipitate. At 55 °C, 40 psig O_2, and approximately an equimolar concentration of $CuCl_2$, this solution oxidizes 1-hexene to 2-hexanone with formation of nearly an equal amount of acetone. The continuous production of acetone is similar to the $RhCl_3$ only system, where as the Rh/Cu system shows only the initial production of acetone. When the RhHPA is used without a Cu^{2+} cocatalyst, 1-hexene is oxidized to 2-hexanone and the solvent is also oxidized to acetone. The RhHPA only system is far less active (3.6 turnover vs. 17.9 turnovers in 24 hours) and less selective the $RhHPA/CuCl_2$ system. In comparison with rhodium(II) acetate under identical conditions, no measurable activity was observed. On the other hand, $Rh_2(O_2CCH_3)_4/CuCl_2$ oxidized 1-hexene to 2-hexanone with 17 turnovers in only 19 hours. Trace amounts of acetone were observed, similar to

Mimoun's Rh/Cu system. One might speculate as to why the RhHPA and $Rh_2(O_2CCH_3)_4$ display such different reactivity. The carboxylate dimer has only tow coordination sites available, namely the axial positions. Since these sites are at opposite ends, the only synergestic interaction would be an electonic transinfluence across the metal-metal bond. The RhHPA on the other hand may have numerous coordination sites available depending upon the lability of the aquo ligands. Recall that the role of Cu^{2+} in the Rh(III) oxidation was thought to involve unsaturation and reoxidation of the Rh as well as the possibility of catatlyzing the addition of the olefin to the Rh. The RhHPA may activate molecular oxygen accounting for the continuous oxidation of solvent even in the presence of Copper(II).

The nature of the active catalytic species in the RhHPA oxidations is uncertain since it would appear that the HPA decomposes upon dissolution in 2-propanol. However, the behavior of this catalyst is unlike either $RhCl_3$ or $Rh_2(O_2CCH_3)_4$ and warrents further investigation.

In summary, dirhodium(II) heteropolytungstate has been prepared which may be the first example of homonuclear metal-metal bonded heteroatoms substituted into the tungstate framework. This complex may be viewed as a Rh_2^{4+} coordinated to the oxydatively resistant tungstate ligand. From this standpoint, the reactivity and stability of the RhHPA may be compare with other rhodium(II) dimers, such as $Rh_2(O_2CCH_3)_4$. The RhHPA was discovered to be a selective oxidation catalyst, especially for the alyllic oxidation of cyclic olefins. A sample of the RhHPA may produce 160 turnovers

in 24 hours whereas rhodiumacetate(II) producedonly 19 turnovers
under identical conditions. Although in both these compounds
rupture of the metal-metal bond occurs, resulting a Rh(III) species
which leads to autoxidation, the lacunary anion is more stable.
This may manifest itself in the RhHPA being a superior catalyst.

CHAPTER VI
CONCLUSION

As mentioned previously the binding and activation of molecular oxygen is of extreme importance to the scientific community. There is a continuous effort among researchers to develop new ways to produce and utilize O_2. The path to such discoveries most often involves the study of transition metal complexes and their reactivity with small molecules. The preceding chapters have related a number of exciting developments in this area. The O_2 and CO carriers described in Chapters II and III are significant not only from their application in gas separations but also because of their relevances to biological systems and potentials as catalysts. In particular, the anionic complex containing zeolites and metal complex containing membranes are considered propiertary development in the case of gas separation. These novel systems at the very least have the possibility to provide substantial improvements to the current state of the art production of O_2 and oxygen enriched air.

In the course of studying the interaction of O_2 with these metal complexes, the natural extension of this work was to exploit the reactivity of metal-O_2 complexes in order to affect a variety of chemical transformations. The discovery that the RhHPA, described in Chapter V, could activate molecular O_2 and oxidize organic substates selectively is quite significant. The

275

implications are that because of the unique oxidatively resistent HPA lacunary ligand, catalysts more stable and active than complexes similar to those in Chapters II and III may be developed. The results for the RhHPA catalyzed oxidations attest to this possibility.

REFERENCES

1. Werner, A.; Mylius, A. Z Anorg Chem. 1898, 16, 745.

2. Drago, R. S.; Corden, B. B. Acc. Chem. Res. 1980, 13, 353.

3. Niederhoffer, E. C.; Timmons, J. H.; Martell, A. E. Chem. Rev. 1984, 84, 137.

4. Gubelmann, M. H.; Williams, A. F. Struct. Bonding 1984, 55, 1.

5. Jones, R. D.; Summerville, D. A.; Basolo, F. Chem. Rev. 1978, 79, 139.

6. Tsumaki, T. Bull. Chem. Soc. Jpn. 1938, 13, 252.

7. Adduci, A. J. Chemtech 1976, 6, 575.

8. Bollote, B.; Aymes, D. J.; Paris, M. R. Bull. Soc. Chim. Fr. 1972, 141.

9. Collman, J. P. Acc. Chem. Res. 1977, 10, 265.

10. Herron, N.; Simmer, L. L.; Grzybowski, J. J.; Olszanski, D. J.; Jackels, S. C.; Callahan, R. W.; Cameron, J. H.; Christoph, G. G.; Busch, D. H. J. Am. Chem. Soc. 1983, 105, 6585.

11. Martell, A. E.; Calvin, M. "Chemistry of the Metal Chelate Compounds"; Prentice-Hall, Englewood Cliffs, N.J., 1952.

12. Collman, J. P.; Brauman, J. I.; Suslick, K. S. J. Am. Chem. Soc. 1975, 97, 7185.

13. Collman, J. P.; Suslick, K. S. Pure Appl. Chem. 1978, 50, 951.

14. Collman, J. P.; Gagne, R. R.; Kouba, J.; Ljusberg-Wahren, H. J. Am. Chem, Soc. 1974, 96, 6800.

15. Collman, J. P.; Reed, C. A. J. Am. Chem. Soc. 1973, 95, 2048.

16. Drago, R. S.; Gaul, J. H. Inorg. Chem. 1979, 18, 2019.

17. Misono, A.; Koda, S.; Uchida, Y. Bull. Chem. Soc. Jpn. 1969, 42, 3470.

18. Chauvin, Y.; Commereux, D.; Dawans, F. Prog. Polym. Sci. 1977, 5, 95.

19. Tsuchida, E.; Nishida, H. Adv. Polymer Sci. 1977, 24, 1.

20. Drago, R. S.; Gaul, J. H. J. Chem. Soc., Chem. Comm., 1979, 746.

21. Drago, R. S.; Gaul, J. H.; Zombeck, A.; Straub, D. K. J. Am. Chem. Soc. 1980, 102, 1033.

22. Drago, R. S.; Cannady, J. P.; Leslie, K. A. J. Am. Chem. Soc. 1980, 102, 6014.

23. Tsuchida, E. J. Macromol. Sci., Chem. 1979, A13, 545.

24. Wohrle, D.; Bohlen, H.; Aringer, C.; Pohl, D. Makromol. Chem. 1984, 185, 669 and references therein.

25. Nelson, D. A. "Separation of Gas Mixtures by Selective Extraction" Report No. GRI-80/0071, Battele Pacific Northwest Laboratories, Richland, WA, 1981.

26. Leal, O.; Anderson, D. L.; Bowman, R. G.; Basolo, F.; Burwell, Jr., R. L. J. Am. Chem. Soc. 1975, 97, 5125.

27. Tashkova, K.; Andreev, A. Inorg. Chim. Acta 1984, 84, 31.

28. Drago, R. S.; Pribich, D. C. Inorg. Chem. 1985, 24, 1983.

29. Yatsimirshii, K. B.; Yakubovich, T. N.; Bratushko, Y. I.; Kotlyar, S. S.; Yanishpol'skii, V. V.; Tertykh, V. A. Dokl, Akad. Nauk. SSSR 1985, 280, 83.

30. Pribich, D. C. Ph.D. Dissertation, University of Florida, 1985.

31. Keller, II, G. E. ACS Symposium Series No. 223, 1983.

32. Lunsford, J. H. Catal. Rev., Sci. Eng. 1975, 12, 137.

33. Howe, R. F.; Lunsford, J. H. J. Phys. Chem. 1975, 79, 1836.

34. Howe, R. F.; Lunsford, J. H. J. Am. Chem. Soc. 1975, 97, 5156.

35. Schoonheydt, R. A.; Pelgrims, J. J. Chem. Soc., Dalton Trans. 1981, 914.

36. Kellerman, R.; Hutta, P. J.; Klier, K. J. Am. Chem. Soc. 1974, 96, 5946.

37. Gustafson, L.; Lin, M.; Lunsford, J. H. J. Phys. Chem. 1980, 84, 3211.

38. Mizuno, K.; Imamura, S.; Lunsford, J. H. Inorg. Chem. 1984, 23, 3510.

39. Imamura, S.; Lunsford, J. H. Langmuir 1985, 1, 326.

40. Adamson, A. W. J. Am. Chem. Soc. 1951, 23, 5710.

41. Brown, L. D.; Raymond, K. W. J. Chem. Soc., Chem. Comm. 1974, 470.

42. Brown, L. D.; Raymond, K. W. Inorg. Chem. 1975, 14, 2595.

43. Carter, S. J.; Foxman, B. M.; Stuhl, L. S. J. Am. Chem. Soc. 1984, 106, 4265.

44. White, D. A.; Solodar, A. J.; Baizer, M. M. Inorg. Chem. 1972, 11, 2160.

45. Carter, S. J.; Foxman, B. M.; Stuhl, L. S. Inorg. Chem. 1986, 25, 2888.

46. Halpern, J.; Maker, J. P. J. Am. Chem. Soc. 1965, 87, 5361.

47. Purcell, K. F.; Yeh, S. M.; Eck, J. S. Inorg. Chem. 1977, 16, 1708.

48. Haase, D. J.; Walker, D. G. Chem. Eng. Prog. 1974, 70, 74.

49. Walker, D. G. Chem. Tech. 1975, 5, 308.

50. Calderazzo, F.; Cotton, F. A. Inorg. Chem. 1962, 1, 30.

51. Vaska, L. Science 1966, 152, 769.

52. Brenner, L. S.; Balch, A. L. J. Am. Chem. Soc. 1978, 100, 6099.

53. Ercolani, C; Monacelli, F.; Pennesi, G.; Rossi, G.; Anonini, E.; Ascenzi, P.; Brunori, M. J. Chem. Soc., Dalton Trans. 1981, 1120.

54. Collman, J. P.; Brauman, J. I.; Iverson, B. L.; Sessler, J. L.; Morris, J. M.; Gibson, Q. H. J. Am. Chem. Soc. 1983, 105, 3052 and references therein.

55. Nelson, D. A.; Hallen, R. T.; Lilga, M. A. "Separation of Gas Mixtures by Supported Complexes" Report No. PNL-4701, Battele Pacific Northwest Laboratories, Richland, WA, 1985.

56. Kim, S. J.; Takizawa, T. Chem. Soc., Chem. Comm. 1974, 356.

57. Kim, S. J.; Takizawa, T. Makromolec. Chem. 1974, 175, 125.

58. Kim, S. J.; Takizawa, T. Makromolec. Chem. 1975, 176, 891.

59. Lyke, S. E.; Moore, R. H. " Chemical Production from Industrial Byproduct Gases" Report No. PNL-3753, Battele Pacific Northwest Laboratories, Richland, WA, 1981.

60. Rabo, J. A.; Franscis, J. N.; Angell, C. L. U.S. Patent No. 4,019,879 1977.

61. Hirai, H.; Komiyama, M.; Wada, K. Chem, Lett. 1982, 1025.

62. Hirai, H.; Wada, K.; Komiyama, M. Bull. Chem. Soc. Jpn. 1986, 59, 1043.

63. Hirai, H.; Wada, K.; Komiyama, M. Chem. Lett. 1983, 361.

64. Hirai, H.; Komiyama, M.; Hara, S. Makromolec. Chem., Rapid Comm. 1981, 2, 495.

65. Hirai, J.; Hara, S.; Komiyama, M. Bull. Chem. Soc. Jpn. 1986, 59, 109.

66. Hirai, J.; Hara, S.; Komiyama, M. Bull. Chem. Soc. Jpn. 1986, 59, 1051.

67. Bruce, M. L. J. Organomet. Chem. 1972, 44, 209.

68. Pasquali, M.; Floriani, C. "Copper Coordination Chemistry: Biochemical and Inorganic Perspectives"; Ademine Press, New York, 1983, pg. 311.

69. Pasquali, M.; Floriani, C.; Gaetani-Manfredotti, A.; Guastini, C. J. Chem. Soc., Chem. Comm. 1972, 197.

70. Pasquli, M.; Marini, G.; Floriani, C.; Gaetani-Manfredotti, A.; Guastini, C. Inorg. Chem. 1980, 19, 2525.

71. Churchill, M. R.; DeBoer, B. G.; Rotella, F. J.; Abu Salah, O. M.; Bruce, M. I. Inorg. Chem. 1975, 14, 2051.

72. Savell, T. N.; Malachowski, M. R. Inorg. Chem. 1983, 22, 1883.

73. Karlin, K. D.; Haka, M. S.; Cruse, R. W.; Gultueh, Y. J. Am. Chem. Soc. 1985, 107, 5828.

74. Nelson, S. M.; Lavery, A.; Drew, M. G. B. J. Chem. Soc., Dalton Trans. 1986, 911.

75. Pasquali, M.; Floriani, C.; Gaetani-Manfredotti, A. Inorg. Chem. 1980, 19, 1191.

76. Keller, R. N.; Wycoff, H. D. Inorg. Syn. 1946, 2, 1.

77. Watt, G. W.; Javora, P. H. J. Inorg. Nucl. Chem. 1974, 36, 1745.

78. Zarembowitch, J.; Malek, R. Spectrochimica Acta, 1983, 39A 43.

79. Bell, A.; Walton, A.; Edwards, D. A.; Poulter, M. A. Inorg. Chim. Acta, 1985, 104, 171.

80. Dvorak, J.; Horyna, J. Czech Patent No. 140,572, 1971.

81. Pasquali, M.; Floriani, C.; Gaetani-Manfredotti, A. Inorg. Chem. 1981, 20, 3382.

82. Greek, B. F. Chem. Eng. News 1986, 64, 15.

83. Mitchell, J. K. Philadelphia J. Med. Sci. 1831, 13, 36.

84. Graham, T. Phil. Mag. 1866, 32, 401.

85. vonWroblewski, S. Wied. Annal. Phys. 1879, 8, 29.

86. Shakespear, G. A. Adv. Commun. Aeronaut. Report No. T.1164, 1918.

87. Shakespear, G. A.; Daynes, H. A. Proc. R. Soc. London 1920, 97, 273.

88. Stern, S. A.; Walawender, Jr., W. P. Sep. Sci. 1969, 4, 129.

89. Baker, R. W.; Blume, I. Chemtech. 1986, 16, 222.

90. Egli, S.; Ruf, A.; Buck, A. Swiss Chem. 1984, 6, 89.

91. Londsdale, H. K. J. Membr. Sci. 1982, 10, 81.

92. Pusch, W.; Walch, A. Angew. Chem., Int. Ed. Engl. 1982, 21, 660.

93. Stern, S. A.; Frisch, H. L. Ann. Rev. Mater. Sci. 1981, 11, 523.

94. Stern, S. A. "Membrane Separation Processes"; Elsevier, New York, 1976, pg. 295.

95. Weller, S. W.; Steimer, W. A. U.S. Patent No. 2,540,151, 1951.

96. Blackner, R. H.; Hedman, J. W. U.S. Patent No. 3,976,451, 1976.

97. Hedman, J. W. U.S. Patent No. 3,979,190, 1976.

98. Blackmer, R. H.; Hedman, J. W. U.S. Patent No. 4,174,955, 1979.

99. Itoh, Y; Asakawa, S. U.S. Patent No. 4,537,606, 1985.

100. Service manual for a OECO model OE-4A High-Humidity Membrane Oxygen Enricher, 1982.

101. Chem. Week July 25, 1984, 36.

102. Burnett, L. J.; Riley, R. L. "Gas Separation Membranes: Technology and Applications"; Fluid Systems Technical Report, San Diego, CA, 1977.

103. Henis, J. M. S.; Tripodi, M. K. U.S. Patent No. 4,230,463, 1980.

104. Henis, J. M. S.; Tripodi, M. K. J. Membrane Sci. 1981, 8, 233.

105. Burnmaster, B. M.; Carter, D. C. Paper presented at AICHE meeting, Houston, TX, 1983.

106. Haggin, J. Chem. Eng. News 1985, 63, 26.

107. Schultz, J. S.; Soddard, J. D.; Suchdeo, S. R. AICHE J. 1974, 20, 417.

108. Smith, D. R.; Lander, R. J.; Quinn, J. A. Rec. Dev. Sep. Sci. 1977, 3, 225.

109. Way, J. D.; Noble, R. D.; Flynn, T. M.; Sloan, E. D. J. Membrane Sci. 1982, 12, 239.

110. Kimura, S. G.; Matson, S. L.; Ward, III, W. J. Rec. Dev. Sep. Sci. 1979, 5, 11.

111. Hughes, R. D; Steigelmann, E. F. U.S. Patent No. 3,864,418, 1975.

112. Steigelmann, E. F. U.S. Patent No. 4,015,955, 1977.

113. Steigelmann, E. F.; Hughes, R. D. U.S. Patent No. 4,239,506, 1982.

114. Kimura, S. G.; Ward, III, W. J.; Matson, S. L. U.S. Patent No. 4,318,714, 1982.

115. Scholander, P. F. Science 1960, 131, 585.

116. Wittenberg, J. B. J. Biol. Chem. 1966, 241, 104.

117. Roman, I. C.; Baker, R. W. U.S. Patent No. 4,542,010, 1985.

118. Drago, R. S.; Balkus, Jr. K. J. Inorg. Chem. 1986, 25, 718.

119. Nishide, H; Ohyanagi, M.; Okada, O.; Tsuchida, E. Macromol. 1986, 19, 494.

120. Sterzel, H. J.; Sanner, A. Ger. Offen. DE No. 3,407,149, 1985, C.A. 104:110951j.

121. Nishide, H.; Kuwahara, M.; Ohyanagi, M.; Funada, Y.; Kawakami, H.; Tsuchida, E. Chem. Lett. 1986, 43.

122. Private communication Mark Barnes, University of Florida, 1986.

123. Felder, R. M.; Huvard, G. S. Methods Exp. Phys. 1980, 16C.

124. Paterson, C. M. J. Appl. Polym. Sci. 1968, 12, 2649.

125. Yasuda, H.; Rosengren, K. J. J. Appl. Polym. Sci. 1970, 14, 2839.

126. Salame, M. J. Polym. Sci. 1973, 41, 1.

127. Stannett, V. T. Polym. Eng. Sci. 1978, 18, 1129.

128. Kawakami, Y.; Karasawa, H.; Kamiya, H.; Aoki, T.; Yamashita, Y. Polym. J. 1986, 18, 237.

129. Carre, A.; Gamet, D.; Schultz, J.; Schreiber, H. P. J. Macromol. Sci., Chem. 1986, A23, 1.

130. Chainey, M.; Wilkinson, M. C.; Hearn, J. J. Polym. Sci. 1985, 23, 2947.

131. Briscoe, B. J.; Smith, A. C. J. Macromol. Sci., Phys. 1983, B22, 53.

132. Yan Amweongen, G. J. Rubber Chem. Tech. 1955, 25, 821.

133. Kemp, D. R.; Paul, D. R. J. Poly. Sci. 1973, 41, 79.

134. Kemp, D. R.; Paul, D. R. J. Poly. Sci., Phys. 1974, 12, 485.

135. Hoffmann, Jr., H. T. U.S. Patent No. 3,957,559, 1976.

136. Gutierrez, M. H.; Ford, W. T. J. Polym. Sci. Part A Polym. Chem. 1986, 24, 655.

137. Sanetra, R.; Kolaiz, B. N.; Wlochowicz, A. Polym. 1985, 26, 181.

138. Duda, J. L. Pure Appl. Chem. 1985, 57, 1681.

139. Rudnick, J.; Taylor, P. L.; Litt, M.; Hopfinger, A. J. J. Poly. Sci., Phys. Ed. 1979, 17, 311.

140. Lipator, Y. S. Russ. Chem. Rev. 1978, 47, 186.

141. Oleinik, E. F. Pure Appl. Chem. 1981, 53, 1567.

142. Mashelkar, R. A.; Kulkarni, M. G. Pure Appl. Chem. 1983, 55, 737.

143. Tsuchida, E.; Nishide, H.; Takane, M.; Yoshioka, H.; Wang, S. J. Inorg. Biochem. 1985, 25, 43.

144. Collman, J. D.; Brauman, J. I.; Doxsee, K. M.; Hallert, T. R.; Hayes, S. E.; Suslick, K. S. J. Am. Chem. Soc. 1978, 100, 2761.

145. Buchachenko, A. L. Russ. Chem. Rev. 1985, 54, 117.

146. Rabek, J. F.; Sanetra, J.; Ranby, B. Macromolec. 1986, 19, 1674.

147. Pope, M. T. "Heteropoly and Isopoly Oxometalates"; Springer-Verlag; New York, 1983.

148. Tsigdinos, G. A. Topics Curr. Chem. 1978, 76, 1.

149. Weakly, T. J. R. Struct. Bonding 1974, 18, 131.

150. Day, V. W.; Klemperer, W. G. Science 1985, 228, 533.

151. Keggin, J. F. Proc. Roy. Soc. A 1934, 144, 75.

152. Baker, L. C. W.; Simmons Baker, V. E.; Eriks, K.; Pope, M. T.; Shibata, M.; Rollins, O. W.; Fang, J. H.; Koh, L. L. J. Am. Chem. Soc. 1966, 88, 2329.

153. Weakley, T. J. R.; Malik, S. A. J. Inorg. Nucl. Chem. 1967, 29, 2935.

154. Tourne, C. M.; Tourne, G. F. Bull. Soc. Chim. Fr. 1969, 1124.

155. Tourne, C. M.; Tourne, G. F.; Malik, S. A.; Weakley, T. J. R. J. Inorg. Nucl. Chem. 1970, 32, 3875.

156. Weakley, T. J. R. J. Chem. Soc., Dalton Trans. 1973, 341.

157. Zonnevijlle, F.; Tourne, C. M. ; Tourne, G. F. Inorg. Chem. 1982, 21, 2742.

158. Zonnevijlle, F.; Tourne, C. M.; Tourne, G. F. Inorg. Chem. 1982, 21, 2751.

159. Schanten, A.; Cros, G. Polyhedron 1982, 1, 283.

160. Ortega, F.; Pope, M. T. Inorg. Chem. 1984, 23, 3292.

161. Cotton, F. A. "Advanced Inorganic Chemistry" 4th Ed., John Wiley and Sons, N.Y., 1980.

162. Ho, R. K. C.; Klemperer, W. G. J. Am. Chem. Soc. 1978, 100, 6772.

163. Knoth, W. H. J. Am. Chem. Soc. 1979, 101, 759.

164. Knoth, W. H. J. Am. Chem. Soc. 1979, 101, 2211.

165. Besecker, C. J.; Klemperer, W. G. J. Am. Chem. Soc. 1980, 102, 7598.

166. Besecker, C. J.; Klemperer, W. G.; Day, V. W. J. Am. Chem. Soc. 1982, 104, 6158.

167. Domaille, P. J.; Knoth, W. H. Inorg. Chem. 1983, 22, 818.

168. Besecker, C. J.; Day, V. W.; Klemperer, W. G.; Thompson, M. R. J. Am. Chem. Soc. 1984, 106, 4125.

169. Besecker, C. J.; Day, V. W.; Klemperer, W. G.; Thompson, M. R. Inorg. Chem. 1985, 24, 44.

170. Day, V. W.; Klemperer, W. G.; Maltbie, D. J. Organomet. 1985, 4, 104.

171. Day, V. W.; Earley, C. W.; Klemperer, W. G.; Maltibie, D. J. J. Am. Chem. Soc. 1985, 107, 8261.

172. Finke, R. G.; Droege, M. W. J. A. Chem. Soc. 1984, 106, 7274.

173. Knoth, W. H.; Harlow, R. L. J. Am. Chem. Soc. 1981, 103, 4265.

174. Barcza, L.; Pope, M. T. J. Phys. Chem. 1973, 77, 1975.

175. Nomiya, K.; Kobauashi, R.; Miwa, M.; Hori, T. Polyhedron 1984, 3, 1071.

176. Moffat, J. B. J. Molec. Catal. 1984, 26, 385.

177. Hayashi, H.; Moffat, J. B. J. Catal. 1982, 77, 473.

178. Hayashi, H.; Moffat, J. B. J. Catal. 1983, 81, 61.

179. Hayashi, H.; Moffat, J. B. J. Catal. 1983, 83, 192.

180. McMonagle, J. B.; Moffat, J. B. J. Catal. 1985, 91, 132.

181. Akimato, M.; Tsuchida, Y.; Sato, K.; Echigoya, E. J. Catal. 1981, 72, 83.

182. Akimato, M.; Shima, K.; Ikeda, H.; Echigoya, E. J. Catal. 1984, 86, 173.

183. Akimato, M.; Ikeda, H.; Okabe, A.; Echigoya, E. J. Catal. 1984, 89, 196.

184. Konishi, Y.; Sokata, K.; Misono, M.; Yoneda, Y. J. Catal. 1982, 77, 169.

185. Ai, M. J. Catal. 1981, 71, 88.

186. Ai, M. "Proceedings, Climax 4th International Conferences on the Chemistry and Uses of Molybdinum, Colorado, 1982" p. 306.

187. Kozhevnikov, I, V.; Matveev, K. I. Russ. Chem. Rev. 1982, 31, 1075.

188. Ogawa, H.; Fujinami, H.; Taya, K.; Teratoni, S. J. Chem. Soc. Chem. Comm. 1981, 1274.

189. Agawa, H.; Fujinami, H.; Taya, K.; Teratoni, S. Bull. Chem. Soc. Jpn. 1984, 57, 1908.

190. Hill, C. L.: Bouchard, D. A. J. Am. Chem. Soc. 1985, 107, 5148 and references therein.

191. Renneke, R. F.; Hill, C. L. J. Am. Chem. Soc. 1986, 108, 3528.

192. Baker, L. C. W.; Figis, J. S. J. Am. Chem. Soc. 1970, 92, 3794.

193. Zonnevijlle, F.; Tourne, G. F. Inorg. Chem. 1983, 22, 1198.

194. Katsoulis, D. E.; Pope, M. T. J. Am. Chem. Soc. 1984, 106, 2737.

195. Hill, C. J.; Brown, Jr., R. B. J. Am. Chem. Soc. 1986, 108, 536.

196. Saltzman, H.; Sharefkin, J. G. "Organic Synthesis"; Wiley, New York, 1973 Collect. Vol. 5, p. 658.

197. Rempel, G. A.; Legzdins, P.; Smith, H.; Wilkinson, G.; Ucko, D. A. Inorg. Synth. 1972, 13, 90.

198. Pope, M. T.; Katsoulis, D. E.; Harmalker, S. P. from the proceedings of the JSPS-NSF, US-Japan seminar entitled "The Catalytic Activity of Polyoxoanions", 1985, pg. 99.

199. Groves, J. T.: Nemo, T. E. J. Am. Chem. Soc. 1983, 105, 5786.

200. Traylor, T. G.; Marsters, Jr., J. C.; Nakans, T.; Dunlap, B. E. J. Am. Chem. Soc. 1985, 107, 5537 and references therein.

201. Che, C. M.; Chung, W. C. J. Chem. Soc., Chem. Comm 1986, 386.

202. Srinivasan, K.; Michaud, P.; Kochi, J. K. J. Am. Chem. Soc. 1984, 108, 2309.

203. Franklin, C. C.; VanAtta, R. B.; Tai, A. F.; Valentine, J. S. J. Am. Chem. Soc. 1984, 106, 814.

204. Van Atta, R. B.; Franklin, C. C.; Valentine, J. S. Inorg. Chem. 1984, 23, 4121.

205. Marcu, G. H.; Ciogolas, I. Rev. Roum. Chem. 1979, 24, 1049.

206. Boyar, E. B.; Robinson, S. D. Coord. Chem. Rev. 1983, 50, 109.

207. Fanning, J, C.; Drago, R. S. J. Am. Chem. Soc. 1968, 90, 3987.

208. Rocchiccioli, C.; Thouvenot, R. J. Chem. Res. Synop. 1977, 46 and references therein.

209. Acerete, R.; Hammer, C. F.; Baker, L. C. W. J. Am. Chem. Soc. 1979, 101, 267.

210. Acerete, R.; Harmalker, S.; Hammer, C. F.; Pope, M. T., Baker, L. C. W. J. Chem. Soc., Chem. Comm. 1979, 777.

211. Gansow, O. A.; Ho, R. K. C.; Klemperer, W. G. J. Organomet Chem. 1980, 187, C27.

212. Lefebvre, J.; Chauveau, F.; Doppelt, P.; Brevard, C. J. Am. Chem. Soc. 1981, 103, 4589.

213. Finke, R. G.; Droege, M.; Hutchinson, J. R.; Gansow, O. A. J. Am. Chem. Soc. 1981, 103, 1587.

214. Acerete, R.; Hammer, C. F.; Baker, L. C. W. J. Am. Chem. Soc. 1982, 104, 15384.

215. Kazansky, L. P.; Fedotor, M. A. J. Chem. Soc., Chem. Comm. 1983, 417.

216. Finke, R. G.; Droege, M. W. Inorg, Chem. 1983, 22, 1006.

217. Knoth, W. H.; Domaille, P. J.; Roe, D. C. Inorg. Chem. 1983, 22, 198.

218. Brevard, C.; Schimpf, R.; Tourne, G.; Tourne, C. M. J. Am. Chem. Soc. 1983, 105, 7059.

219. Domaille, P. J. J. Am. Chem. Soc. 1984, 106, 7677.

220. Knoth, W. H.; Domaille, P. J.; Farlee, R. D. Organomet 1985, 4, 62.

221. Maksimovskaya, R. I.; Busteva, K. G. Polyhedron 1985, 4, 1559.

222. Maksinmovskaya, R. I.; Fedotov, M. A.; Maksomov, G. M. Russ. J. Inorg. Chem. 1985, 30, 514.

223. Finke, R. G.; Rapko, B.; Dommaille, P. J. Organomet. 1986, 5, 175.

224. Finke, R. G.; Rapko, B.; Saxton, R. J.; Domaille, P. J. J. Am. Chem. Soc. 1986, 108, 2947.

225. Minelli, M.; Enemark, J. H.; Brownlee, R. T. C.; O'Connor, M. J.; Wedd, A. G. Coord. Chem. Rev. 1985, 68, 169.

226. Teze, A.; Herve, G. Inorg. Nucl. Chem. 1977, 39, 999.

227. Finke, R. G.; Droege, M. W.; Cook, C. J.; Suslick, K. S. J. Am. Chem. Soc. 1984, 106, 5750.

228. Suslick, K. S.; Cook, C. J.; Rapko, B.; Droege, M. W.; Finke, R. G. Inorg. Chem. 1986, 25, 241.

229. Johnson, S A.; Hunt, H. R.; Neuman, H. M. Inorg, Chem. 1963, 2, 960.

230. Kitchens, J.; Bear, J. L. J. Inorg. Nucl. Chem. 1969, 31, 2415.

231. Drago, R. S.; Long, J. R.; Cosmano, R. Inorg. Chem. 1981, 20, 2920.

232. Bilgrien, C.: Drago, R. S.; Vogel, G. C.; Stahlbush, J. Inorg. Chem. in press.

233. Robin, M. B.; Day, P. Adv. Inorg. Chem. Radiochem. 1967, 10, 247.

234. Sidorov, A. A.; Komozin, P. W.; Miroshinichenko, J. V.; Pichkov, V. N.; Sinitsyn, N. M.; Babaeva, V. P. Russ. J. Inorg. Chem. 1984, 29, 722.

235. Uemura, S.; Spencer, A.; Wilkinson, G. J. Chem. Soc., Dalton Trans. 1973, 2565.

236. Sheldon, R. A; Kochi, J. K. "Metal-Catalyzed Oxidations of Organic Compounds"; Academic Press, New York, 1981.

237. Lyons, J. E. "Aspects of Homogeneous Catalysis", Vol. 3, D. Reidel, Dordrecht, Holland, 1977, pg. 29.

238. Krukov, V. P.; Pasky, J. Z.; Lavingne, J. B. J. Am. Chem. Soc. 1968, 90, 4743.

239. Fusi, A.; Ugo, F.; Fox, F.; Pasini, A.; Cenini, S. J. Organomet. Chem. 1971, 26, 417.

240. Uemura, S.; Patil, S. R. Chem Lett. 1982, 1743.

241. Uemura, S.; Patil, S. R. Tet. Lett. 1982, 23, 4353.

242. Tanaka, K.; Imamura, J. Chem. Lett. 1974, 1347.

243. Payne, G. B.; Deming, P. H.; Williams, P. H. J. Org. Chem. 1961, 26, 659.

244. Payne, G. B. Tetahedron 1962, 18, 763.

245. Bach, R. D.; Knight, J. W. Org. Syn. 1981, 60, 63.

246. Mimoun, H.; Machirant, M. M. P.; Seree de Roch, I. J. Am. Chem. Soc. 1978, 100, 5437.

247. Ingersheim, I.; Mimoun, H. Nouv. J. Chem. 1980, 4, 161.

248. Nyberg, E. D.; Pribich, D. C.; Drago, R. S. J. Am. Chem. Soc. 1983, 105, 3538.

249. Drago, R. S.; Zuzich, A.; Nyberg, E. D. J. Am. Chem. Soc. 1983, 107, 2898.

250. Urabe, K.; Izumi, Y. from the proceedings of the JSPS-NSF, US-Japan semiar entitled "The Catalytic Activity of Polyoxoanions", 1985, pg. 121.

APPENDIX

Membrane	l (mm)	time (hr)	P_{O_2} (mmHg)	P_{N_2} (mmHg)	Flux (mmHg/hr)	Enrichment $\%O_2$
PS	0.371 ± .073	0	<.21	<.78	--	--
		11	14.85	43.15	4.73	5.130
		24	29.06	67.94	3.79	9.554
		34	38.81	81.19	3.35	11.940
		45	52.99	116.01	3.62	10.738
				2nd Cycle		
		0	<.21	<.79	4.58	10.087
		12	17.10	37.90	4.39	9.964
		20.5	27.87	62.13	4.39	10.109
		25	32.98	73.02	4.24	10.109
		36	42.55	96.45	3.86	9.612
PS	0.542 ± .124	0	<.21	<.79	--	--
		5	5.53	15.47	4.20	5.356
		12	10.84	30.16	3.42	5.449
		22.5	17.40	45.60	2.80	6.635
		29	21.09	59.91	2.79	5.038
PS	0.50 ± .000	0	<.21	<.79	--	--
		2.5	--	--	6.80	--
		5.5	7.96	21.04	5.27	6.447
		9	11.16	26.84	4.22	8.380
		25	23.08	42.92	2.64	13.968
		30	25.67	52.33	2.60	11.916
		37	28.63	61.37	2.43	10.809
		48	35.55	71.45	2.23	12.224
PS	0.164 ± .050	0	<.21	<.79	--	--
		2.5	16.49	48.51	26.00	4.373
		5.5	28.37	81.63	20.00	4.795
		9	39.18	111.82	16.28	4.947
		25	90.15	269.85	14.40	4.043
				2nd Cycle		
		0	<.21	<.79	--	--
		5	15.93	43.07	11.80	5.977
		11.5	27.43	70.57	8.52	6.995
		23	49.14	139.86	8.22	5.002
PS	0.150 ± .052	0	<.21	<.79	--	--
		2	5.70	14.30	10.00	7.486
		5	8.29	21.71	6.00	6.637
		10	12.80	34.20	4.70	6.242
		24	24.80	58.20	3.46	8.882
		30.5	34.60	81.40	3.80	8.832
		36	--	--	11.39	--

290

PS	0.250 ± .052	0	<.21	<.79	--	--
		4	4.86	15.18	5.00	3.078
		7	8.27	19.73	4.00	8.523
		11	12.13	28.87	3.73	8.582
		24	20.24	42.76	2.62	11.123
		28.5	23.47	47.53	2.49	12.053
		36	29.63	61.37	2.52	11.560
		48	48.68	111.32	3.33	9.424

2nd Cycle

		0	<.21	<.79	--	--
		7.5	8.68	22.31	4.13	7.012
		23	33.65	95.34	5.61	5.089

3rd Cycle

		0	<.21	<.79	--	--
		7.5	4.47	15.52	2.67	1.368
		27	29.71	76.29	3.92	7.026

PS	0.110 ± .028	0	<.21	<.79	--	--
		4	11.47	25.53	9.25	10.003
		7	15.44	32.56	6.85	11.162
		11	21.26	44.74	6.00	11.204
		24	31.85	64.15	4.00	12.176
		28.5	36.06	70.94	3.75	12.700
		36	43.15	82.85	3.50	13.246
		48	50.90	99.09	3.12	12.935

2nd Cycle

		0	<.21	<.79	--	--
		7.5	10.37	24.63	4.67	8.620
		23	27.08	49.91	3.34	14.173

3rd Cycle

		0	<.21	<.79	--	--
		5	8.47	20.52	5.80	8.229
		27	30.40	57.59	3.26	13.550

PS	0.131 ± .048	0	<.21	<.79	--	--
		2	8.11	20.89	14.50	6.945
		4	11.54	26.46	9.50	9.360
		6	15.07	31.93	7.83	11.060
		10	20.03	39.97	6.00	12.375
		14	24.61	45.39	5.00	14.158
		24	34.11	64.89	4.12	13.457
		30	37.58	68.42	3.53	14.454
		36	41.14	77.86	3.30	13.571
		48	50.71	97.29	3.08	13.259

			2nd Cycle			
		0	<.21	<.79	--	--
		2	4.30	11.70	8.00	5.890
		4	6.11	16.89	5.75	5.551
		6	8.69	20.31	4.83	8.963
		11	25.08	53.92	7.18	10.746
		24	94.07	264.93	14.96	5.204
		48	131.39	415.61	11.39	3.021
PS	0.192 ± .028	0	<.21	<.79	--	--
		2	5.90	19.10	12.50	2.584
		4	10.49	29.51	10.00	5.225
		6	17.48	45.51	10.50	6.756
		10	32.09	88.91	12.10	5.521
			2nd Cycle			
		0	<.21	<.79	--	--
		2	7.25	19.75	13.50	5.855
		4	--	--	13.00	--
PS	0.989 ± .160	0	<.21	<.79	--	--
		4	5.97	16.03	5.50	6.149
		10	11.72	31.28	4.30	6.257
		24	19.08	46.92	2.75	7.911
		34	30.07	59.93	2.65	12.413
		48	37.06	82.94	2.50	9.886
PS	1.567 ± .30	0	<.21	<.79	--	--
		8	8.72	23.28	2.75	6.246
		21	12.40	40.60	2.29	9.035
		24	20.40	42.60	2.21	11.364
		34.5	29.07	52.93	2.09	14.449
PS	0.238 ± .051	0	<.21	<.79	--	--
		4	5.51	19.49	6.25	1.034
		10	10.39	37.61	4.80	0.649
		24	24.70	89.30	4.75	0.607
		29	36.06	126.94	5.62	1.124
		48	81.48	280.52	7.54	1.507
PS	1.540 ± .120	0	<.21	<.79	--	--
		4	4.88	12.12	5.50	1.174
		10	8.86	29.14	3.80	2.320
		24	18.08	49.92	2.83	5.588
		33.5	25.02	59.98	2.54	8.431
PS/[P]-CH$_2$Cl						
	2.07 ± .023	0	<.21	<.79	--	--
	(7.63 % by wt)	4	6.44	22.56	7.25	1.232
		8	10.10	32.90	5.38	2.439
		21	20.00	44.00	3.52	6.039
		24	22.90	57.10	3.33	7.600
		32	29.70	67.30	3.03	9.661
		47	36.90	82.10	2.53	10.072

		2nd Cycle		
0	<.21	<.79	--	--
4	4.58	15.42	5.00	1.900
9	6.55	23.45	3.33	0.836
24	14.08	37.92	2.17	6.080
32	17.20	47.80	2.03	5.402

PS/[P]-CH$_2$Cl
1.36 ± .230
(13.3 % by wt)

0	<.21	<.79	--	--
4	4.64	17.36	5.50	0.069
10	8.09	26.91	3.50	2.106
25	16.86	46.14	2.52	5.766
34	25.09	55.91	2.38	9.974
48	30.95	72.05	2.15	9.053

		2nd Cycle		
0	<.21	<.79	--	--
5	3.53	12.47	3.20	1.093
9	6.13	19.87	2.89	2.572
24	17.76	46.24	2.67	6.757
33	30.59	73.41	3.15	8.411
46	33.96	80.04	2.48	8.793

PS/[P]-CH$_2$Cl
0.910 ± .074
(10.15 % by wt)

0	<.21	<.79	--	--
4	7.50	22.50	7.50	4.003
10	12.03	24.97	3.70	11.503
24	44.97	113.03	6.58	7.460
34	69.01	189.99	7.62	5.643
49	97.44	282.56	7.75	4.642

		2nd Cycle		
0	<.21	<.79	--	--
8	9.78	29.22	4.90	4.073
24	20.15	51.85	3.00	6.988
33	30.64	61.36	2.79	12.300
47	36.78	80.22	2.49	10.438

PS/[P]-CH$_2$Cl
1.055 ± .053
(19.77 % by wt)

0	<.21	<.79	--	--
4	--	--	3.75	--
9.5	9.69	25.31	3.68	6.688
24	23.11	56.89	3.33	7.885
29	30.05	67.95	3.38	9.663
35	27.22	81.78	3.11	3.974
48.5	29.16	96.84	2.60	2.141

PS/[P]-DPT

0.970 ± .116	0	<.21	<.79	--	--
(9.91 % by wt)	4	5.24	13.76	4.25	6.560
	12.5	12.09	31.91	3.52	6.477
	24.5	18.61	50.39	2.81	5.970
	31	22.55	63.45	2.77	5.223
	35	26.36	72.64	2.83	5.627
	50	34.49	92.51	2.54	6.158

2nd Cycle

	0	<.21	<.79	--	--
	6.5	7.30	19.70	4.15	6.052
	21.5	19.71	54.29	3.44	5.638
	24.5	21.91	61.09	3.39	5.402
	30.5	30.98	85.02	3.80	5.706
	46.5	50.69	141.31	4.13	5.399

PS/[P]-DPT

0.200 ± .078	0	<.21	<.79	--	--
(29.4 % by wt)	4	12.29	27.71	10.00	9.728
	6.5	16.32	35.68	8.00	10.3.77
	18	28.62	57.38	4.78	12.278
	24	35.37	68.63	4.33	13.008
	29	38.29	77.71	4.00	12.009
	43	49.70	100.30	3.49	12.135

2nd Cycle

	0	<.21	<.79	--	--
	2	--	--	8.00	--
	5	8.76	20.24	5.80	9.198
	10	15.90	34.10	5.00	10.807
	23.5	27.86	55.14	3.53	12.572
	33.5	40.14	79.86	3.58	12.451
	46.5	54.57	113.43	3.61	11.481

PS/[P]-DPT

0.507 ± .114	0	<.21	<.79	--	--
(26.0 % by wt)	3	4.29	14.71	6.30	1.600
	7	9.25	25.75	5.00	5.428
	19	24.70	49.30	3.89	12.396
	24	32.95	64.05	4.00	12.975
	32	43.65	107.35	4.72	7.907
	43.5	66.36	178.64	5.63	6.086

2nd Cycle

	0	<.21	<.79	--	--
	3	15.12	44.88	20.00	4.193
	6	25.75	78.25	17.33	3.763
	12	42.47	131.53	14.50	3.411
	23	67.16	213.84	12.22	2.902

PS/[P]-DPT (22.0 % by wt)

0.654 ± .113	0	<.21	<.79	--	--
	6	9.01	21.99	5.20	8.066
	19.5	19.93	44.07	3.28	10.141
	25	27.96	66.04	3.76	8.748
	32	36.56	88.44	3.90	8.244
	43.5	55.34	139.66	4.48	7.382

2nd Cycle

	0	<.21	<.79	--	--
	2.5	3.94	12.06	6.40	3.658
	5.5	5.97	22.03	5.09	0.326
	13	12.97	38.03	3.92	4.637
	24	33.07	95.93	5.37	4.637

3rd Cycle

	0	<.21	<.79	--	--
	4	6.91	23.09	7.50	2.027
	8.5	12.64	45.36	6.94	2.125
	12	26.13	62.87	6.92	3.251
	24	31.54	100.46	5.50	2.896
	28.5	68.80	232.20	10.56	1.856

PS/[P]-DPT

0.207 ± .078	0	<.21	<.79	--	--
(16.7 % by wt)	2.5	3.77	13.23	6.80	1.162
	5	8.30	29.70	7.60	0.840
	9	15.54	50.46	7.33	2.545
	20	21.96	67.04	4.45	3.680

PS/[P]-DPT

0.645 ± .11	0	<.21	<.79	--	--
(20.7 % by wt)	3	11.73	27.27	13.00	9.081
	7	19.76	39.24	8.43	12.495
	12	24.65	51.35	6.33	11.430
	24	35.59	72.41	4.50	11.956
	29	40.05	79.95	4.13	12.375
	36	46.16	91.84	3.83	12.452
	53	59.35	123.65	3.45	11.429

2nd Cycle

	0	<.21	<.79	--	--
	4	10.08	36.91	11.75	4.625
	7	18.72	50.27	9.85	6.135
	24	43.15	109.84	6.37	7.207
	31	52.45	130.54	5.90	7.666
	43	66.48	170.51	5.51	7.052

PS/[P]-DPT

0.457 ± .065 (29.35 % by wt)				
0	<.21	<.79	--	--
3	7.31	21.69	9.67	4.193
6	12.49	35.50	8.00	5.035
11.5	19.59	55.41	6.52	5.117
24	39.52	114.48	6.41	4.664
29	51.19	150.80	6.96	4.345
36	66.48	204.51	7.53	3.534
53	97.05	312.95	7.73	2.671

2nd Cycle

0	<.21	<.79	--	--
3	14.37	51.62	22.00	0.783
6	30.92	108.07	23.17	1.247

PS/[P]-CoSDPT

0.261 ± .144 (44 % by wt)				
0	<.21	<.79	--	--
3	7.44	20.56	9.33	5.564
6	11.02	25.98	6.17	8.791
11	17.53	36.47	4.91	11.456
24	40.47	105.52	6.08	6.725
30.5	64.80	180.19	8.03	5.450
35	73.08	231.91	8.71	2.963

PS/[P]-CoSDPT

0.357 ± .065 (18.6 % by wt)				
0	<.21	<.79	--	--
4	7.17	21.83	7.25	4.717
7.5	12.13	27.87	5.33	9.329
11	14.53	35.47	4.54	8.056
23	27.94	60.06	3.82	10.752
28	34.20	73.80	3.85	10.668

PS/[P]-CoSDPT

0.867 ± .049 (12.6 % by wt)				
0	<.21	<.79	--	--
2	3.49	12.51	8.00	0.855
4	5.88	20.12	6.50	1.608
6.5	9.62	28.38	5.85	4.322
11	15.08	46.92	5.63	3.322
24	41.65	123.35	6.87	4.242
30	56.90	172.10	7.63	3.846

2nd Cycle

0	<.21	<.79	--	--
3.5	6.62	23.38	8.57	1.064
6	12.39	40.61	8.83	2.380
13	29.47	89.53	9.15	3.768
24	--	--	11.08	--

PS/[P]-CoSDPT

0.677 ± .044	0	<.21	<.79	--	--
(17.2 % by wt)	1.75	7.23	17.17	14.28	7.934
	3.75	10.72	24.28	9.33	9.619
	5.75	13.94	29.06	7.48	11.418
	10	19.43	39.57	5.90	11.928
	13	21.28	44.72	5.07	11.250
	25	31.33	60.67	3.69	13.060
	29	34.62	63.38	3.38	14.362
	48	46.65	89.35	2.83	13.300

			2nd Cycle		
	0	<.21	<.79	--	--
	2	3.62	11.38	7.50	3.091
	4	6.39	15.61	5.50	8.049
	6	8.44	19.56	4.67	9.120
	9.5	11.60	25.40	3.89	10.352
	13	15.75	29.25	3.46	14.001
	24	26.32	49.68	3.17	13.640
	29	34.03	63.97	3.38	13.727
	34.5	39.35	79.65	3.45	12.071
	48	54.64	119.36	3.63	10.404

PS/[P]-CoSDPT

0.856 ± .051	0	<.21	<.79	--	--
(13.8 % by wt)	2	7.80	25.20	16.50	2.648
	4	10.93	35.07	11.50	2.759
	6.5	14.22	44.78	9.07	3.104
	11	17.70	56.30	6.73	2.917
	23.5	32.56	93.44	5.36	4.843
	29.5	41.31	117.69	5.39	4.981

			2nd Cycle		
	0	<.21	<.79	--	--
	3.5	9.03	28.97	10.86	2.760
	6	11.77	36.23	8.00	3.531
	13	19.78	58.22	6.00	4.355
	24	40.84	113.16	6.42	5.552

PS/[P]-CoSDPT

0.562 ± .115	0	<.21	<.79	--	--
(37 % by wt)	1.5	7.08	22.92	18.00	2.590
	4	16.68	41.32	13.75	7.766
	7.5	22.44	50.56	9.33	9.739
	19.5	30.87	67.13	4.87	10.496
	25	37.01	78.99	4.52	10.902
	33	42.71	89.29	3.91	11.353
	43	50.01	102.99	3.49	11.689

PS/[P]-CoSDPT

0.687 ± .124	0	<.21	<.79	--	--
(16.4 % by wt)	5	10.56	25.44	7.20	8.339
	18	23.77	47.23	3.94	12.478
	24	29.78	62.22	3.83	11.367
	29.5	32.97	66.03	3.35	12.306
	42	40.27	77.73	2.81	13.126

2nd Cycle

	0	<.21	<.79	--	--
	8	9.14	19.86	3.62	10.509
	24	21.91	40.09	2.58	14.342
	33.5	31.67	62.33	2.81	12.694
	47	38.64	74.36	2.40	13.196

3rd Cycle

	0	<.21	<.79	--	--
	6	7.01	17.99	4.17	7.022
	11	12.63	26.37	3.54	11.380
	25	26.72	54.28	3.24	11.982
	35	37.45	79.55	3.34	11.010
	48	50.21	112.79	3.39	9.805

4th Cycle

	0	<.21	<.79	--	--
	5	8.45	23.55	6.40	5.415
	10	18.00	44.00	6.20	8.029
	23	36.63	95.37	5.74	6.754
	35	52.16	138.84	5.46	6.307

PS/[P]-CoSDPT

0.70 ± .250	0	<.21	<.79	--	--
(9.49 % by wt)	4	--	--	5.75	--
	8	1.05	31.95	4.12	0.504
	24	28.99	31.01	2.50	7.486
	28	33.26	38.74	2.57	7.494
	32	37.40	41.60	2.47	6.089
	45	49.80	51.20	2.24	7.051

PS/[P]-CoSDPT

0.80 ± .210	0	2.10	7.90	--	--
(19.08 % by wt)	9	14.48	36.52	4.46	7.391
	24	25.85	55.15	2.96	10.912

PS/[P]-CoBr$_2$SDPT

0.675 ± .085	0	<.21	<.79	--	--
(21.7 % by wt)	2	7.38	20.62	14.00	5.347
	4	10.85	27.15	9.50	7.560
	6	14.32	32.68	7.83	9.460
	11	20.58	45.42	6.00	10.191
	14.5	24.10	52.90	5.31	10.304
	24	35.74	76.26	4.67	10.911
	29	40.47	90.53	4.52	9.897
	48	68.88	152.52	4.60	8.016

			2nd Cycle		
	0	<.21	<.79	--	--
	2	4.77	16.23	10.50	1.737
	4	7.95	22.05	7.50	5.523
	6	10.41	28.59	6.50	5.690
	10	16.34	40.66	5.70	7.667
	14	21.58	50.42	5.14	8.983
	24	36.25	82.75	4.96	9.465
	29	40.46	98.54	4.79	8.108
	36	51.22	122.78	4.83	8.434
	47	63.91	157.09	4.70	7.920

PS/[P]-CoBr$_2$SDPT
0.671 ± .047
(6.76 % by wt)

	0	<.21	<.79	--	--
	2	4.98	15.02	10.00	3.914
	4	8.48	20.52	7.25	8.255
	6	10.77	26.23	6.17	8.114
	11	17.33	36.67	4.91	11.090
	14.5	20.30	41.70	4.27	11.743
	24	31.51	59.49	3.79	13.621
	29	42.14	86.86	4.45	11.665
	35	54.77	119.23	4.97	10.478
	48	77.14	168.86	5.12	10.359

			2nd Cycle		
	0	<.21	<.79	--	--
	2	2.73	9.27	6.00	2.964
	4	4.79	15.21	5.00	2.964
	6	7.02	20.98	4.67	4.071
	10	12.99	37.01	5.00	4.986
	14	29.08	65.92	6.78	9.616
	23.5	61.77	147.23	8.89	8.556

PS/[P]-CoBr$_2$SDPT
0.514 ± .077
(11 % by wt)

	0	<.21	<.79	--	--
	2	1.02	1.98	1.50	13.173
	4	2.56	6.44	2.25	7.431
	6	5.18	10.82	2.67	11.358
	16	13.41	23.59	2.31	15.241
	25	20.34	33.66	2.16	16.664
	30	23.48	43.42	2.23	14.043

PS/[P]-CoBr$_2$SDPT
0.723 ± .136
(14.5 % by wt)

	0	<.21	<.79	--	--
	2	7.56	21.44	14.50	5.084
	4	11.53	27.47	9.75	8.574
	6	15.39	32.61	8.00	11.068
	11.5	21.29	44.71	5.74	11.262
	15	24.93	49.07	4.93	12.694
	24	34.37	68.63	4.29	12.374
	28	38.39	77.61	4.14	12.101
	38	50.41	106.59	4.13	11.085
	47.5	63.16	140.84	4.29	9.962

			2nd Cycle		
	0	<.21	<.79	--	--
	2	5.22	15.78	10.50	3.876
	4	8.48	21.52	7.50	7.276
	7.5	16.83	41.17	7.73	8.019
	10.5	25.33	63.67	8.47	7.463
	24	58.27	149.73	8.67	7.015

PS/[P]-CoBr$_2$SDPT
0.528 ± .072
(7.40 % by wt)

	0	<.21	<.79	--	--
	0	<.21	<.79	--	--
	2	4.46	9.54	7.00	10.857
	4	8.70	15.30	6.00	15.263
	6	11.15	21.85	5.50	12.782
	12	16.58	32.42	4.08	12.842
	18	19.30	34.70	3.00	14.749
	24	24.28	45.72	2.92	13.680
	29	28.46	51.54	2.75	14.573
	35	34.22	59.78	2.68	15.410

			2nd Cycle		
	0	<.21	<.79	--	--
	3	1.88	4.12	2.00	12.260
	6	4.83	9.77	2.33	13.517
	14	11.88	18.12	2.14	18.594
	24	19.71	31.29	2.12	17.644
	30.5	24.48	40.52	2.13	16.661
	48	39.84	69.16	2.27	15.555

PS/[P]-CoBr$_2$SDPT
0.747 ± .074
(12.62 % by wt)

	0	<.21	<.79	--	--
	0	<.21	<.79	--	--
	2	2.22	7.78	5.00	1.216
	4	4.40	13.60	4.50	3.420
	6	7.28	21.72	4.83	4.114
	9	11.57	28.43	4.44	7.923
	12	16.14	39.86	4.67	7.831
	24	45.39	111.61	6.54	7.910
	29	57.68	152.32	7.24	6.467
	35	73.99	204.01	7.94	5.615
	47	94.95	280.05	7.98	4.432

			2nd Cycle		
	0	<.21	<.79	--	--
	2	2.36	7.64	5.00	2.638
	4	4.42	14.58	4.75	2.280
	6	5.96	19.04	4.17	2.827
	10	9.43	27.57	3.70	4.498
	13	11.27	31.73	3.31	5.214
	24	28.09	76.91	4.37	5.754
	30	35.63	106.37	4.73	4.094

PS/[P]-CoBr$_2$SDPT

0.640 ± .051	0	<.21	<.79	--	--
(20.20 % by wt)	2	5.80	17.20	11.50	4.229
	4	10.04	24.96	8.25	7.687
	6	13.20	34.80	8.00	6.508
	10.5	26.93	70.07	9.24	6.769
	13	33.08	88.92	9.38	6.117
	24	62.01	168.99	9.62	5.846

		2nd Cycle			
	0	<.21	<.79	--	--
	2	4.15	20.19	9.00	2.069
	4	6.80	20.19	6.75	4.222
	6	9.57	26.43	6.00	5.573
	10	15.05	36.92	5.00	5.153
	13	15.15	44.85	4.61	4.256
	24	26.88	76.12	4.29	5.098
	29	34.43	93.59	4.41	5.902

PS/[P]-CoBr$_2$SDPT

0.207 ± .06	0	<.21	<.79	--	--
(6.6 % by wt)	5	6.59	15.41	4.40	8.948
	18.5	15.22	35.78	2.76	8.851

		2nd Cycle			
	0	<.21	<.79	--	--
	5.5	6.45	44.55	3.63	11.248

PS/[P]-CoBr$_2$SDPT

1.17 ± .110	0	<.21	<.79	--	--
(18.0 % by wt)	6	8.98	31.02	6.67	1.444
	20	22.98	48.02	3.55	11.368
	24	26.48	57.52	3.50	10.531
	33	30.90	69.10	3.03	9.000
	46	39.20	103.80	3.11	6.431

PS/[P]-CoBr$_2$SDPT

0.742 ± .120	0	6.51	24.49	--	--
(1.87 % by wt)	11	25.73	74.27	9.09	6.851
	13	30.78	75.22	8.15	11.359
	16	31.05	82.95	7.12	8.571
	22	34.86	91.14	5.73	8.848
	37	47.70	124.30	4.65	8.317
	61	59.36	143.64	3.33	9.725

PS/[P]-Co3FSDPT

0.544 ± .051	0	<.21	<.79	--	--
(6.30 % by wt)	2	3.16	10.84	7.00	1.574
	4	6.61	19.39	6.50	4.414
	6	10.83	23.17	5.67	10.863
	11	16.10	34.90	4.63	10.565
	29	31.31	57.69	3.07	14.184
	48	47.82	100.18	3.08	11.313

		2nd Cycle		
0	<.21	<.79	--	--
2	--	--	4.50	--
4	3.78	10.22	3.50	6.026
6	5.69	15.31	3.50	6.026
24	25.50	56.50	3.42	10.102
29	32.03	63.97	3.31	12.366
48	65.68	155.32	4.60	8.872

PS/[P]-Co3FSDPT
0.359 ± .050
(24.6 % by wt)

0	<.21	<.79	--	--
2	3.69	9.31	6.50	7.425
4	7.42	16.58	6.00	9.912
11	17.04	29.96	4.27	15.249
24	29.47	45.53	3.12	17.202

		2nd Cycle		
0	<.21	<.79	--	--
2	3.68	4.32	4.00	24.985
4	4.67	9.33	3.50	12.323
7	6.37	15.63	3.14	7.945
12	10.50	21.50	2.67	11.828
24	25.56	48.44	3.08	13.536

PS/[P]-Co3FSDPT
0.506 ± .075
(16.47 % by wt)

0	<.21	<.79	--	--
2.5	6.54	15.46	8.80	8.740
4	9.95	18.05	7.00	14.541
7	12.50	28.50	5.85	9.491
12	17.88	38.12	4.67	10.925
24	29.55	62.45	3.83	11.119

PS/[P]-Co3FSDPT
0.475 ± .077
(14.7 % by wt)

0	<.21	<.79	--	--
2	4.86	14.14	9.50	4.600
4	10.81	19.19	7.50	15.023
6	15.49	29.51	7.50	13.427
11	36.81	74.19	10.09	12.160
29	88.75	252.25	11.76	5.026

PS/[P]-Co3FSDPT
0.518 ± .040
(6.8 % by wt)

0	<.21	<.79	--	--
2	6.61	20.39	13.50	3.462
4	12.29	31.71	11.00	6.944
6	15.38	38.62	9.00	7.473
15	25.74	57.26	5.53	10.017
24	35.15	75.85	4.62	10.663
34	40.62	91.38	3.88	9.771
49	52.27	112.73	3.36	10.677

		2nd Cycle		
0	<.21	<.79	--	--
2	--	--	8.50	--
5.5	6.72	23.28	5.45	1.393
10	11.47	33.53	4.50	4.492
24	25.63	83.37	4.54	2.517

PS/[P]-Co3FSDPT
0.625 ± .085
(6.42 % by wt)

0	<.21	<.79	--	--
2	4.72	14.28	9.50	3.840
4	8.91	23.09	8.00	6.840
6	12.02	28.98	6.83	8.304
15	20.94	42.06	4.20	12.232
26	27.85	56.15	3.23	12.151
34	33.95	67.05	2.97	12.611
49	47.04	91.96	2.84	12.843

		2nd Cycle		
0	<.21	<.79	--	--
2	2.35	8.65	5.50	0.415
5.5	6.28	13.72	3.63	10.412
10	14.39	19.61	3.40	21.333
24	21.54	31.46	2.21	19.645

PS/[SG] 0.518 ± .040
(26.2 % by wt)

0	<.21	<.79	--	--
2	3.02	7.98	5.50	6.425
4	7.10	15.90	5.75	9.847
6	9.48	21.52	5.17	9.586
10	13.64	29.36	4.30	10.728
13	16.93	34.07	3.92	12.205
24	26.07	49.93	3.17	13.300
30	33.99	67.01	3.37	12.657
35	40.78	83.22	3.54	11.884
48	57.54	129.46	3.89	9.770

		2nd Cycle		
0	<.21	<.79	--	--
2	1.80	4.20	3.00	8.993
4	3.63	8.37	3.00	9.247
6	6.38	18.62	4.17	4.529
10.5	10.79	25.21	3.43	8.972
14	13.87	31.13	3.21	9.829
24.5	23.20	43.80	2.73	13.623
35	31.22	55.78	2.48	14.894
50	47.26	97.74	2.90	11.594

PS/[SG] 0.100
(14.0 % by wt)

0	<.21	<.79	--	--
12.5	12.30	30.70	3.44	7.618
21	20.68	51.32	3.43	7.727
25.5	24.36	63.64	3.45	6.684
38	105.72	385.28	12.92	6.531

PS/[SG]	0.171 ± .047	0	<.21	<.79	--	--
	(6.2 % by wt)	13	14.86	27.14	3.23	14.377
		20.5	26.20	55.80	4.00	10.955
		25	33.88	82.12	4.64	8.209
PS/[SG]	0.580 ± .101	0	<.21	<.79	--	--
	(36.6 % by wt)	2	7.75	24.24	16.00	3.254
		4	13.19	39.81	13.25	3.886
		6	17.14	50.86	11.33	4.202
		10	32.02	81.98	11.40	7.087
		13.5	40.05	113.95	11.41	5.004
		24	70.25	199.75	11.25	5.019
				2nd Cycle		
		0	<.21	<.79	--	--
		2	5.42	18.58	12.00	1.585
		4	7.42	22.58	7.50	3.724
		6	9.01	27.99	6.17	3.348
		10	14.11	37.89	5.20	6.138
		24	26.35	66.65	3.87	7.330
		30.5	33.93	87.07	3.96	7.041
		37	45.75	108.25	4.16	8.449
		47	57.63	142.37	4.36	7.111
PS/[SG]	0.514 ± .036	0	<.21	<.79	--	--
	(44.7 % by wt)	2	4.42	14.58	9.15	2.240
		6	8.76	26.24	5.83	4.039
		9.5	13.42	34.58	5.05	6.951
		12.5	15.93	46.07	4.48	7.451
		24	29.69	85.31	4.79	4.818
PS/[SG]	0.647 ± .083	0	<.21	<.79	--	--
	(26.2 % by wt)	2	2.27	7.73	5.00	1.748
		4	4.56	12.44	4.25	5.856
		6	5.54	18.46	4.00	2.090
		10	8.38	23.62	3.20	5.201
		24	21.64	56.36	3.25	6.742
		29	28.73	74.27	3.55	6.899
		36	37.63	97.37	3.75	6.874
		48	51.92	135.08	3.89	6.763
				2nd Cycle		
		0	<.21	<.79	--	--
		2	1.40	4.60	3.00	2.407
		4	2.85	8.15	2.75	4.905
		6	4.13	13.87	3.00	1.942
		9	7.55	20.45	3.11	5.971
		12	9.85	27.15	3.08	6.628
PS/[SG]	0.225 ± .045	0	<.21	<.79	--	--
	(13.0 % by wt)	12	16.30	35.70	4.33	10.289
		25	28.25	57.75	3.44	11.851
		30	32.94	60.06	3.10	14.415
		46	42.66	83.34	2.74	12.854

		2nd Cycle			
	0	<.21	<.79	--	--
	6	10.57	28.43	6.50	6.099
	12	18.74	45.26	5.33	8.288
	24	34.08	88.92	5.12	6.710
	29	47.67	150.33	6.83	3.078
PS/[SG] 1.450 ± .050	0	<.21	<.79	--	--
(24.14 % by wt)	4	3.79	13.21	4.25	1.296
	10	7.62	27.38	3.50	0.760
	24	18.93	53.07	3.00	5.288
	28	20.63	60.37	2.89	4.466
	33.5	25.82	69.18	2.83	6.176
	46.5	35.36	86.64	2.62	7.986
		2nd Cycle			
	0	<.21	<.79	--	--
	6	5.49	18.51	4.00	1.868
	13	9.65	31.35	3.15	2.539
	25.5	17.79	50.21	2.67	5.163
	31	26.07	59.93	2.77	9.134
	36	26.71	68.29	2.64	7.112
	50	32.32	86.68	2.38	6.163
PS/[SG] 1.19 ± .086	0	<.21	<.79	--	--
(28.10 % by wt)	12	16.31	41.69	4.83	7.128
	21	26.11	60.89	4.14	9.006
	35	35.09	86.91	3.48	7.766
	40.5	42.87	95.13	3.41	10.062
PS/[SG] 1.340 ± .09	0	<.21	<.79	--	--
(15.4 % by wt)	11	--	--	2.54	--
	23	14.14	45.86	2.61	2.559
	29	17.89	61.11	2.72	1.645
	34	23.07	68.93	2.01	4.073
	48	28.78	90.22	2.48	3.187
		2nd Cycle			
	0	<.21	<.79	--	--
	12	8.48	28.52	3.08	1.931
	24	14.92	50.08	2.71	1.953
	32	20.71	64.29	2.66	3.371
	47	29.55	83.45	2.40	5.152
		3rd Cycle			
	0	<.21	<.79	--	--
	9	5.95	18.05	3.43	3.800
	18	10.46	35.54	2.56	1.751
	24.5	15.43	48.57	2.61	3.111
	30	20.17	58.83	2.63	4.531
	43.5	27.37	81.63	2.51	4.107

		4th Cycle		
0	<.21	<.79	--	--
9	6.62	24.38	3.44	0.369
21	15.46	48.54	3.05	3.159
27.5	21.68	63.32	3.09	4.506
32.5	22.45	76.55	3.01	1.912
51	43.52	137.48	3.55	3.043

PS/[SG]-CoSDPT
0.807 ± .070
(10.0 % by wt)

0	<.21	<.79	--	--
1.5	2.81	9.19	8.00	2.470
3	5.81	15.19	7.00	6.659
5	8.20	22.80	6.20	5.393
8	12.35	28.65	5.12	9.138
13	18.85	46.15	5.00	7.997
24	26.48	52.52	3.29	12.525
29	34.34	74.66	3.76	10.507
34	40.97	90.03	3.85	10.274
47.75	58.75	135.25	4.06	9.283

		2nd Cycle		
0	<.21	<.79	--	--
2	3.11	10.89	7.00	1.249
4	5.23	15.77	5.25	3.909
6	6.60	20.40	4.50	3.462
10	9.16	26.84	3.60	4.433
13.5	11.60	31.40	3.18	5.992
24	20.28	44.72	2.71	10.207
29	25.55	55.45	2.79	10.546
34	30.67	68.33	2.91	9.980
48.5	44.62	105.38	3.09	8.745

PS/[SG]-CoSDPT
0.533 ± .097
(19.9 % by wt)

0	<.21	<.79	--	--
2	6.19	14.81	10.50	8.469
4	10.15	22.85	8.25	9.765
6	13.88	30.12	7.33	10.554
8	16.63	36.37	6.63	10.382
11	19.83	43.17	5.73	10.483
24	31.37	65.63	4.04	11.337
30	37.35	79.65	3.90	10.926
37	42.42	91.58	3.62	10.657
47.5	49.15	106.85	3.28	10.508

		2nd Cycle		
0	<.21	<.79	--	--
2	3.01	8.99	6.00	4.117
4	5.52	14.48	5.00	6.612
6	8.96	19.04	4.67	10.993
12	15.47	35.53	4.25	9.328
24	17.66	36.34	3.86	11.709
31	35.17	74.83	3.55	10.972
38	40.78	89.22	3.42	10.371
49	51.81	117.19	3.45	9.659

PS/[SG]-CoSDPT

0.358 ± .062	0	<.21	<.79	--	--
(18.7 % by wt)	2	3.41	11.59	7.50	1.773
	4	5.22	17.78	5.75	1.718
	6	7.43	23.57	5.17	2.966
	11	11.35	32.65	4.40	4.802
	24	27.62	65.38	3.87	8.703

2nd Cycle

	0	<.21	<.79	--	--
	2	1.11	3.89	2.50	1.216
	4.5	2.99	10.01	2.89	2.046
	6	4.99	16.01	3.50	2.714
	10	6.65	21.35	2.80	2.769
	13	9.10	23.90	2.54	6.564
	24	16.18	38.82	2.29	8.415

PS/[SG]-CoSDPT

0.384 ± .037	0	<.21	<.79	--	--
(16.1 % by wt)	2	5.25	18.75	12.00	0.887
	4	8.07	24.93	8.25	3.454
	6	12.50	32.50	7.50	6.772
	11	17.73	45.27	5.73	7.142
	24	32.24	80.76	4.71	7.526

2nd Cycle

	0	<.21	<.79	--	--
	2	2.33	8.67	5.50	0.207
	4.5	5.16	17.84	5.11	1.421
	6	8.40	26.60	5.83	2.996
	10	11.89	33.11	4.50	5.421
	13	17.49	47.51	5.00	5.905
	24	36.82	95.18	5.50	6.897

PS/[SG]-CoSDPT

1.478 ± .245	0	<.21	<.79	--	--
(7.31 % by wt)	2	12.98	34.02	23.50	6.630
	4	20.65	53.35	18.50	6.912
	6	28.59	74.41	17.17	6.759
	10	46.21	125.79	17.20	5.868
	24	90.02	273.98	15.17	3.731

2nd Cycle

	0	<.21	<.79	--	--
	2	4.97	9.03	7.00	14.548
	4	7.17	16.83	6.00	8.867
	6	10.61	23.39	5.67	10.215
	9	15.43	30.57	5.11	12.540
	13	25.97	54.03	6.15	11.457
	23	--	--	12.17	--

		3rd Cycle			
	0	<.21	<.79	--	--
	2	3.48	8.52	6.00	7.980
	4	7.80	16.20	6.00	11.486
	6	12.37	24.63	6.17	12.427
	11	21.31	47.69	6.27	9.880
	24	49.46	124.54	7.25	7.425

PS/[SG]-CoSDPT

0.571 ± .082	0	<.21	<.79	--	--
(6.56 % by wt)	2	4.75	12.25	8.50	6.929
	4.5	10.37	19.63	6.67	13.553
	6	13.07	24.93	6.33	13.380
	12	21.62	44.38	5.50	11.762
	24	44.18	98.82	5.96	9.896

		2nd Cycle			
	0	<.21	<.79	--	--
	2	4.08	8.92	6.50	10.406

PS/[SG]-CoSDPT

0.456 ± .063	0	<.21	<.79	--	--
(3.97 % by wt only)	2	4.51	14.49	9.502.720	
(on upper surface)	4	8.64	20.36	7.25	8.805
	6	11.68	24.32	6.00	11.442
	10	16.74	30.26	4.70	14.618
	24	26.77	46.23	3.04	15.679
	30	31.07	56.93	2.93	14.310
	38	36.50	64.50	2.66	15.140
	47.5	44.33	78.67	2.59	15.045

		2nd Cycle			
	0	<.21	<.79	--	--
	2	1.22	2.78	2.00	9.500
	4	2.76	8.24	2.75	4.076
	6	5.95	12.05	3.00	12.075
	12	10.24	20.76	2.58	12.037
	24	28.03	56.97	3.54	11.972
	29	37.89	79.11	4.03	11.387

PS/[SG]-CoSDPT

0.614 ± .077	0	<.21	<.79	--	--
(4.6 % by wt)	2	5.56	14.44	10.00	6.802
	4	9.87	21.13	8.00	9.833
	6	12.40	27.60	6.67	9.984
	10.5	17.18	35.82	5.05	11.414
	14	20.78	43.22	4.57	11.459
	24	33.69	69.31	4.29	11.710
	29	45.26	98.73	4.96	10.434
	36	60.58	151.42	5.89	7.575

PS/[SG]-CoSDPT

0.912 ± .034	0	<.21	<.79	--	--
(13.1 % by wt)	2	7.55	20.45	14.00	5.971
	4	12.38	31.62	11.00	7.134
	9	19.58	48.42	7.55	7.801
	11.5	23.78	54.22	6.78	9.490
	24	40.29	92.71	5.54	9.297

2nd Cycle

0	<.21	<.79	--	--
2	5.76	16.24	11.00	5.182
4	8.41	22.59	7.75	6.129
6	11.51	25.49	6.17	10.126
10	14.68	33.32	4.80	9.595
13	16.02	20.98	4.46	6.617
24	29.97	73.03	4.29	8.102
28	36.64	89.36	4.50	8.077
34	49.05	111.95	4.73	9.465
48.5	63.98	172.02	4.86	6.112

PS/[SG]-CoSDPT

0.492 ± .028	0	<.21	<.79	--	--
(2 % by wt)	2	5.83	12.17	10.00	8.170
	4	10.20	22.80	8.25	9.903
	6	14.15	20.85	7.33	11.141
	12	21.35	42.65	5.33	12.350
	15	24.28	48.72	4.87	12.264
	24	30.59	63.41	3.92	11.545
	29	34.83	72.17	3.69	11.549
	35	41.35	84.65	3.60	11.816
	48	50.77	109.23	3.33	10.730

2nd Cycle

0	<.21	<.79	--	--
2	4.67	11.33	8.00	8.170
4	11.48	26.52	9.50	9.220
6	16.70	43.30	10.00	6.827

PS/[SG]-CoSDPT

0.647 ± .051	0	<.21	<.79	--	--
(16.5 % by wt)	2	--	--	5.00	--
	4	3.45	10.55	3.50	3.366
	6	5.20	16.80	3.67	2.625
	10	9.38	22.62	3.20	8.313
	24	19.22	37.78	2.37	12.720
	30	24.59	44.41	2.30	14.638
	37	26.92	44.08	1.92	16.913
	52	45.45	88.55	2.58	12.920

	2nd Cycle			
0	<.21	<.79	--	--
2	--	--	6.50	--
4	4.31	12.69	4.25	4.336
6	5.43	15.57	3.50	4.849
10	8.45	20.55	2.90	8.124
24	19.89	38.11	2.42	13.287
31	25.61	49.39	2.42	13.153
44	42.67	86.33	2.92	12.077

PS/[Na-Y]
0.507 ± .095
(22.06 % by wt)

0	<.21	<.79	--	--
2	7.65	15.35	11.50	12.259
4	15.83	36.17	13.00	9.441
6	23.50	57.50	13.50	8.022
10	43.29	117.71	16.10	5.886
24	--	--	15.79	--

PS/[Na-Y]
0.464 ± .063
(13.8 % by wt)

0	<.21	<.79	--	--
2	4.23	8.77	6.50	11.575
4	7.35	16.65	6.00	9.627
6	10.80	23.20	5.67	10.774
12	21.34	44.66	5.50	11.331
24	40.08	90.92	5.46	9.596

	2nd Cycle			
0	<.21	<.79	--	--
2	2.11	5.89	4.00	5.415
4	5.12	12.88	4.50	7.431
6	8.96	20.04	4.83	9.906
10	16.87	37.13	5.40	10.246
24	45.95	107.05	6.37	9.031

PS/[Na-Y]
0.741 ± .138
(15.9 % by wt)

0	<.21	<.79	--	--
2	7.86	21.14	14.50	6.106
4	15.27	34.73	12.50	9.546
6	25.39	62.61	14.67	7.850

PS/[Na-Y]
0.639 ± .050
(24.16 % by wt)

0	<.21	<.79	--	--
2	3.60	9.40	6.50	6.665
4	6.39	14.61	5.25	9.409
6	9.02	19.98	4.83	10.116
12	15.22	30.78	3.83	12.094
24	25.98	48.02	3.08	14.101
30.5	30.53	56.47	2.85	12.090
36	37.13	72.87	3.05	12.754
48	54.56	111.44	3.46	11.867

			2nd Cycle		
	0	<.21	<.79	--	--
	2	1.96	7.04	4.50	0.760
	4	3.20	10.80	3.50	1.846
	6	5.42	15.58	3.50	4.813
	11	9.13	22 87	2.91	7.529
	24	20.13	41.87	2.58	11.461

PS/[Na-Y]

0.787 ± .150	0	<.21	<.79	--	--
(11.50 % by wt)	2	3.72	13.28	8.50	0.894
	4	7.82	17.18	6.25	10.225
	6	9.89	24.11	5.67	8.092
	11	16.35	35.65	4.73	10.450
	24	29.50	62.50	3.83	11.069
	30	36.08	76.92	3.77	10.936
	38	43.36	91.64	3.55	11.118
	48	53.58	118.42	3.58	10.149

			2nd Cycle		
	0	<.21	<.79	--	--
	2	3.88	12.12	8.00	3.230
	4	5.75	16.25	5.50	5.147
	6	8.51	23.49	5.33	5.605
	10	14.18	34.82	4.90	7.941
	24	32.32	68.68	4.21	11.001

PS/[Na-Y]

0.760 ± .097	0	<.21	<.79	--	--
(10.8 % by wt)	2	5.77	19.23	12.50	2.067
	6	12.36	28.64	6.83	9.157
	10	14.87	39.13	5.40	6.544
	24	28.51	59.49	3.67	11.400
	32	38.29	72.71	3.47	13.500
	44.5	47.08	91.92	3.12	12.876

			2nd Cycle		
	0	<.21	<.79	--	--
	3	6.69	18.31	8.30	5.776
	6	9.55	28.45	6.33	4.120
	9	14.27	30.73	5.00	10.707
	12	16.92	35.08	4.33	11.546
	24	28.98	58.11	3.62	12.212
	35	40.24	87.76	3.66	10.438
	48	56.24	122.76	3.73	10.419

PS/[Na-Y]

0.368 ± .048	0	<.21	<.79	--	--
(15.5 % by wt)	5	8.11	27.89	7.20	1.542
	21	19.45	55.55	3.57	4.930
	31	28.62	85.38	3.68	4.103
	43.5	46.29	132.71	4.11	4.863

		2nd Cycle			
	0	<.21	<.79	--	--
	3	5.49	17.51	7.62	2.875
	5	9.36	30.64	8.00	2.413
	11	21.51	64.49	7.82	4.012
PS/Co(bipy)(terpy)-Y					
0.809 ± .137	0	<.21	<.79	--	--
(19.8 % by wt)	3.5	14.80	36.20	14.57	8.027
	7	20.80	51.20	10.28	7.885
	17.5	31.73	66.27	5.60	11.377
	24	37.98	79.02	4.87	11.465
	29	42.28	86.72	4.45	11.774
	43.5	50.75	106.25	3.61	11.323
		2nd Cycle			
	0	<.21	<.79	--	--
	3	6.97	19.03	8.67	5.817
	8.5	13.23	31.77	5.29	8.394
	24	28.32	53.68	3.42	13.541
	34	39.85	77.15	3.44	13.056
	46	52.80	111.20	3.56	11.196
		3rd Cycle			
	0	<.21	<.79	--	--
	3	5.32	19.68	8.33	0.274
	5	10.48	34.52	9.00	2.298
	11	18.30	51.70	6.36	5.145
	29	33.19	92.81	4.34	5.341
PS/Co(bipy)(terpy)-Y					
0.600 ± .085	0	<.21	<.79	--	--
	2	--	--	5.50	--
	4	3.61	13.39	4.25	0.268
	6	5.88	17.12	3.83	4.659
	11	9.34	25.66	3.18	5.624
	24	19.97	41.03	2.54	11.736
	30	24.47	46.53	2.37	13.466
	36	27.39	49.61	2.14	14.568
	48	34.85	61.15	2.00	15.303
PS/(Co(bipy)(terpy)-Y					
0.413 ± .09	0	<.21	<.79	--	--
(30.5 % by wt)	2	5.93	18.07	12.00	3.705
	4	9.12	24.88	8.50	5.834
	6	12.62	31.38	7.33	7.670
	11	19.32	43.68	5.73	9.663
	24	34.67	74.33	4.54	10.807

		2nd Cycle			
	0	<.21	<.79	--	--
	2	3.86	14.14	9.00	0.464
	4	5.39	18.61	6.00	1.457
	6	9.13	25.87	5.83	5.081
	11	13.16	30.84	4.00	8.913
	24	23.51	34.49	2.42	19.537

PS/Co(NaCN)-Y-3

0.944 ± .109	0	<.21	<.79	--	--
(12.5 % by wt)	2	2.79	9.21	6.00	2.280
	4	6.97	16.03	5.75	9.318
	6	9.55	19.45	4.83	11.924
	10	14.66	39.34	4.40	12.315
	14	18.18	34.82	3.78	13.293
	24	44.26	96.74	5.87	10.392
	29	58.87	145.13	7.03	7.857

		2nd Cycle			
	0	<.21	<.79	--	--
	2	2.64	9.36	6.00	1.013
	4	5.32	14.68	5.00	5.624
	11	11.93	27.07	3.54	9.588
	24	56.89	143.11	8.33	7.444

PS/Co(NaCN)-Y-3

1.006 ± .066	0	<.21	<.79	--	--
(12.44 % by wt)	2	5.12	12.88	9.00	2.744
	4	9.54	21.46	7.75	9.784
	6	12.86	29.14	7.00	9.627
	10	17.88	40.12	5.80	9.828
	14	22.67	49.33	5.14	10.482
	24	31.96	68.04	4.17	10.959
	29	37.12	76.88	3.93	11.560
	48	56.26	124.76	3.77	10.086

		2nd Cycle			
	0	<.21	<.79	--	--
	2.5	4.33	13.67	7.20	3.040
	5	8.01	19.99	5.60	7.600
	11	20.79	48.21	6.27	9.142
	24	55.49	137.51	8.04	7.754

PS/Co(NaCN)-Y-3

0.882 ± .073	0	<.21	<.79	--	--
(15.6 % by wt)	2	4.43	15.57	10.00	1.140
	4	8.39	21.61	7.50	7.017
	6	11.52	27.48	6.50	8.590
	14	20.34	44.66	4.64	10.490
	24	26.87	60.13	3.62	10.070

	2nd Cycle			
0	<.21	<.79	--	--
2	--	--	5.00	--
4	4.20	14.80	4.75	1.120
6	5.05	18.95	4.00	0.032
12	10.61	27.39	3.16	6.960
24	21.01	42.99	2.67	11.827

	3rd Cycle			
0	<.21	<.79	--	--
2	--	--	5.50	--
4	3.78	12.22	4.00	2.660
6	5.81	17.19	3.83	4.265

BIOGRAPHICAL SKETCH

Kenneth J. Balkus, Jr., was born November 3, 1960, in Denver, Colorado. In 1978, he graduated with high honors from St. John's High School in Shrewsbury, Massachusetts. From there, he enrolled in Worchester Polytechnic Institute in Worchester, Massachusetts, and in 1982, earned a B.S. in chemistry with distinction. While at W.P.I., he conducted research in the area of inorganic chemistry under the tutelage of Dr. Nicholas Kildahl. He presented papers based on this work, at both the Eastern College's Science Conference and the ACS local meeting. In 1982, he entered the Ph.D. program at the University of Florida, Gainesville, and joined the research group of Dr. Russell Drago. During his stay at Florida, he presented papers at 3 Florida Catalysis conferences and at both the ACS local and national meetings. He received the 1986 Florida section student speaker award and was a finalist for the 1986 ACS Sherwin-Williams Award. After earning his Ph.D. in inorganic chemistry, he assumed a postdoctoral position in the research group of Dr. Bradford Wayland at the University of Pennsylvania, Philadelphia.
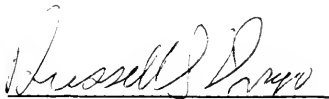
Kenneth is co-author of the following publications:

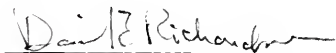Kildahl, N. K.; Balkus, Jr., J. K.: Flynn, M. J. Inorg. Chem. 1983, 22, 589.

Drago, R. S.; Balkus, Jr., K. J. Inorg. Chem. 1986, 25, 716.

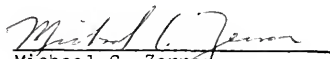Drago, R. S.; Balkus, Jr., K. J. U.S. Patent Appl. No. 746,675.

I certify that I have read this study and that in my opinion it conforms to acceptable standards of scholarly presentation and is fully adequate, in scope and quality, as a dissertation for the degree of Doctor of Philosophy.

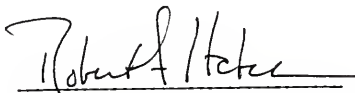Russell S. Drago
Graduate Research Professor
of Chemistry

I certify that I have read this study and that in my opinion it conforms to acceptable standards of scholarly presentation and is fully adequate, in scope and quality, as a dissertation for the degree of Doctor of Philosophy.

David E. Richardson
Assistant Professor of
Chemistry

I certify that I have read this study and that in my opinion it conforms to acceptable standards of scholarly presentation and is fully adequate, in scope and quality, as a dissertation for the degree of Doctor of Philosophy.

Robert C. Stoufer
Associate Professor of
Chemistry

I certify that I have read this study and that in my opinion it conforms to acceptable standards of scholarly presentation and is fully adequate, in scope and quality, as a dissertation for the degree of Doctor of Philosophy.

Michael C. Zerner
Professor of Chemistry

I certify that I have read this study and that in my opinion it conforms to acceptable standards of scholarly presentation and is fully adequate, in scope and quality, as a dissertation for the degree of Doctor of Philosophy.

Robert A. Hatch
Associate Professor of
History

This dissertation was submitted to the Graduate Faculty of the Department of Chemistry in the College of Liberal Arts and Sciences and to the Graduate School and was accepted as partial fulfillment of the requirements for the degree of Doctor of Philosophy.

December, 1986

Dean, Graduate School